Universidade do Minho
Escola de Ciências da Saúde

Maria Alexandra Oliveira da Silva

New insight into translation during yeast programmed cell death

Novas perspetivas sobre o processo de tradução na morte celular programada em levedura

Fevereiro de 2012

New insight into translation during yeast programmed cell death
Maria Alexandra Oliveira da Silva
UMinho | 2012

Universidade do Minho
Escola de Ciências da Saúde

Maria Alexandra Oliveira da Silva

New insight into translation during yeast programmed cell death

Novas perspetivas sobre o processo de tradução na morte celular programada em levedura

Tese de Doutoramento em Ciências da Saúde

Trabalho realizado sobre a orientação da
Professora Doutora Paula Cristina da Costa Alves Monteiro Ludovico
e co-orientação da
Doutora Elsa Clara Carvalho Logarinho Santos

Fevereiro de 2012

DECLARAÇÃO

Nome: Maria Alexandra Oliveira da Silva
Endereço electrónico: xanasilva@ecsaude.uminho.pt
Telefone: +351 939595423
Número do Bilhete de Identidade: 11887124

Título da dissertação: New insight into translation during yeast programmed cell death

Orientadora:
Professora Doutora Paula Cristina da Costa Alves Monteiro Ludovico

Co-orientadora:
Professora Doutora Elsa Clara Carvalho Logarinho Santos

Ano de conclusão: 2012
Designação Ramo de Conhecimento do Doutoramento:
Ciências da Saúde – Ciências da Saúde

Universidade do Minho, 20 de Fevereiro de 2012

Assinatura: _____

The work presented in this thesis was mainly done within the Microbiology and Infection Research Domain in the Life and Health Sciences Research Institute (ICVS), School of Health Sciences, University of Minho. Part of the work was also done in the Apoptosis Research Centre of the Children's Hospital of Eastern Ontario, Ottawa, Ontario, Canada and in the Department of Biology and CESAM, University of Aveiro, Portugal. The financial support was given by Fundação para a Ciência e Tecnologia by means of a project PTDC/BIA-MIC/114116/2009 and also by a grant, SFRH/BD/33125/2007.

AGRADECIMENTOS

No fim do percurso há que olhar para trás e agradecer a todos aqueles que, à sua maneira, nos guiaram e acompanharam na viagem.

Começo por agradecer à Professora Doutora Paula Ludovico pela excelente orientação ao longo destes anos, pelo constante apoio e incentivo, preciosos concelhos, criticas e sugestões e principalmente pelo rigor demonstrado… Obrigada por se mostrar sempre disponível para me ajudar a atingir os meus objetivos. Obrigada Paula! Foi uma viagem muito enriquecedora, pessoal e profissionalmente…

À Doutora Elsa Logarinho, gostaria de expressar o meu reconhecimento por todo o auxílio durante estes anos, e pela útil partilha do seu conhecimento.

Ao Professor Fernando Rodrigues, pelo apoio e pelas longas discussões científicas que tanto me ajudaram durante todos estes anos.

Ao ICVS, na pessoa da Professora Cecília Leão, queria agradecer a oportunidade e o privilégio de trabalhar neste instituto bem como o incondicional apoio na transposição de todos os obstáculos inerente ao meu trabalho.

I would like to acknowledge Professor Martin Holcik, for his valuable inputs and most of all, for his constant support during my stay in Ottawa, and also to all the people in his group, especially Alura Riley, for helping me with my experiments but more importantly with the cold. It was a real pleasure working with you all!!!

Ao Professor Manuel Santos, pela total disponibilidade demonstrada para me receber no seu laboratório e pelas discussões científicas ao longo destes anos que tanto contribuíram para o sucesso deste trabalho. Laura Carreto, João Paredes, Tatiana Costa, Ana Rita Bezerra, João Simões e Marisa Simões, obrigada por me fazerem sentir em casa e pela ajuda no laboratório…

À Fundação para a Ciência e Tecnologia pelo financiamento que permitiu a realização deste trabalho.

Aos MIRD, antigos ou recentes colegas, por todos os momentos partilhados, pela disponibilidade, ajuda e amizade. Obrigada amigos! No entanto, tenho que destacar duas pessoas a quem tenho que agradecer por terem feito este percurso sempre a meu lado. Foi uma honra Belém e Bruno. Obrigada pelas nossas conversas, cientificas ou não. Mais que colegas de bancada foram e serão sempre grandes amigos…

Ao Fernando, a quem, além de agradecer o incondicional apoio, compreensão e companhia nas longas noites e fins-de-semana de clausura no laboratório, tenho que pedir desculpa pelo tempo e espaço que esta viagem nos possa ter roubado. Sem ti este percurso não faria sentido!

Por último, quero agradecer a toda a minha família, principalmente aos meus pais, irmã e cunhado, por todo o apoio e incentivo ao longo não só destes 4 anos mas de toda a minha vida. Peço desculpa por todos os momentos de ausência…. Tudo o que consegui alcançar até hoje foi graças a vocês. Muito obrigada!

ABSTRACT

Global mRNA translation impairment has been described during the course of apoptosis in both mammalian and yeast. Nevertheless, the molecular pathways modulating translation during different scenarios of yeast apoptosis are still largely unexplored. Here we show by polysome profile analysis an impairment in cap-dependent translation initiation, correlated with alterations in translation machinery, such as the decrease in eIF4A levels and the phosphorylation of eIF2α by Gcn2 protein kinase upon acetic acid treatment. Gcn2p proved to play a preponderant role for the progression of the acetic acid-induced apoptosis, not only through the repression of cap-dependent translation initiation, but also by the induction of a cell cycle arrest in G0/G1 phase. Despite the observed impairment of cap-dependent translation initiation, some mRNAs, such as *AIF1* and eIF4G, were translated during acetic acid treatment. eIF4G harbors an IRES in the 5' untranslated region (5'UTR) of the mRNA allowing its translation by a cap-independent IRES-mediated translation, being also crucial for an efficient IRES-mediated translation of other mRNAs. The inhibition of the cap-dependent translation initiation associated with the observation of *AIF1* and eIF4G efficient translation during acetic acid treatment made us question the possibility of an alternative IRES-mediated translation occur during acetic acid treatment.

Furthermore, the translation machinery alterations proved to be dependent of the yeast caspase like protease, metacaspase, which induced also the specific fragmentation of the glycolytic enzyme glyceraldehyde 3-phosphate dehydrogenase (GAPDH). Although metacaspase role in the induction of the apoptosis is well established, its specific substrates were still unknown. The fact that GAPDH is specifically cleaved by metacaspase, suggests a role of this enzyme in the apoptotic process. In mammalian cells, GAPDH interacts with some virus and cellular mRNAs repressing their internal ribosome entry site (IRES)-mediated translation. GAPDH cleavage by caspase-1 during apoptosis suggests a regulation of its function by derepression of the IRES-mediated translation.

Upon the inhibition of translation initiation during acetic acid treatment, eEF1A, a translation elongation factor responsible for the delivery of aminoacyl-tRNAs to the ribosomes, appears to play a function unrelated to translation

elongation. A proteomic analysis combined with a proteinase K assay showed that upon acetic acid treatment, eEF1A is fragmented and the eEF1A N-terminal fragments are present in mitochondria where they appear to play a pro-apoptotic role. Apart from its role in translation this protein is also an actin-binding protein being responsible for the actin cytoskeleton organization. This re-localization to mitochondria reduces its binding to actin leading to actin cytoskeleton alterations which proved to be conserved from yeast to mammalian cells.

Our previously reported proteomic analysis in the same apoptotic conditions revealed an increased expression of heat shock protein 90 (HSP90) isoforms. We herein demonstrate by microarray analysis of polysomal mRNAs combined with the HSP90 isoforms 5' untranslated region (5'UTR) expression in monocistronic reporter plasmids harboring an hairpin, that HSP90 isoforms are translated by a cap-independent mechanism mediated by (IRES) elements. Moreover, genetic abrogation of HSP90 isoforms indicate divergent roles for HSP90 isoforms, Hsc82 acts as a pro-survival and Hsp82 as a pro-death molecule, upon the acetic acid treatment. In fact, the deletion of *HSC82* leads to a severe necrotic cell death, in spite of an apoptotic cell death, upon acetic acid treatment. These undisclosed functions of yeast HSP90 isoforms were confirmed through pharmacological inhibition of HSP90 activity, using 17-allylaminogeldanamycin (17AGG), and by the overexpression of each HSP90 isoform during acetic acid. These results suggest that the efficiency of HSP90 isoforms mRNA translation is an important component of the cellular response to acetic acid. In summary, the results presented in the scope of this thesis contributed to the understanding of the translation mechanisms regulating yeast cell death processes.

RESUMO

A inibição global da tradução foi descrita no decurso da apoptose tanto em leveduras como em mamíferos No entanto, as vias moleculares que modulam a tradução em diferentes cenários de morte celular programada (MCP) em levedura são ainda desconhecidas. Neste trabalho demonstramos, através de perfis polissomais, uma inibição da iniciação da tradução dependente da estrutura cap, correlacionada com alterações na maquinaria de tradução, tais como a redução dos níveis de eIF4A e a fosforilação do eIF2α mediada pela cinase Gcn2p, durante o tratamento com ácido acético. Gcn2p provou desempenhar um papel relevante na progressão da morte induzida por ácido acético não só pela repressão da iniciação da tradução dependente de cap mas também através da indução de um bloqueio do ciclo celular na fase G0/G1. Apesar da diminuição da iniciação da tradução dependente de cap, alguns mRNAs, tais como o *AIF1* e o eIF4G, são traduzidos durante o tratamento com ácido acético. eIF4G possui um *internal ribosome entry site* (IRES) na região 5' não traduzida (5'UTR) do mRNA o que permite a sua tradução independente de cap, sendo também fundamental para a tradução eficiente de outros mRNAs regulados por IRES. A inibição da iniciação da tradução dependente de cap associada à observação da tradução de *AIF1* e eIF4G levanta a possibilidade da ocorrência de uma tradução alternativa mediada por IRES durante o tratamento com ácido acético. Para além disso, as alterações na maquinaria de tradução observadas durante o tratamento com ácido acético parecem ser dependentes da ação da caspase de leveduras, a metacaspase, que provou ser ainda responsável pela clivagem específica da enzima glicolítica gliceraldeído-3-fosfato desidrogenase (GAPDH). Embora a importância da metacaspase na execução da apoptose esteja bem estabelecida, os substratos desta protease são ainda desconhecidos. O fato da GAPDH ser especificamente clivada pela metacaspase, sugere um papel desta enzima no processo apoptótico. Em mamíferos, a GAPDH interage com alguns mRNAs celulares e de vírus inibindo a sua tradução mediada por IRES. A clivagem da GAPDH pela caspase-1 durante a apoptose sugere uma regulação da sua função na tradução e a desrepressão da tradução mediada por IRES. Após a inibição da iniciação da tradução durante o

tratamento com ácido acético, o fator de elongação da tradução eEF1A, responsável pela entrega dos aminoacil-tRNAs nos ribossomas, parece desempenhar uma função independente do processo de tradução. Uma análise proteómica em conjunto com um ensaio de proteinase K mostraram que, após o tratamento das células com ácido acético, o eEF1A é fragmentado e os fragmentos N-terminais de eEF1A são detetados na matriz mitocondrial onde parecem desempenhar um papel pró-apoptótico. Para além da sua participação no processo de tradução esta proteína está também associada à actina sendo responsável pela organização do citoesqueleto de actina. A relocalização para a mitocôndria reduz a sua ligação à actina induzindo alterações no citoesqueleto de actina que provaram ser conservados tanto em levedura como em mamíferos.

Anteriormente, uma análise proteómica, nas mesmas condições apoptóticas, revelou um aumento dos níveis das isoformas da proteína de choque térmico 90 (HSP90). A análise de microarrays dos mRNAs presentes em frações polissomais complementada com a expressão dos 5'UTR das isoformas da HSP90 em plasmídeos monocistrónicos contendo um gancho no 5'UTR, demonstrou a presença de IRES no 5'UTR das HSP90 mediando a sua tradução independente de cap. A deleção genética das isoformas das Hsp90 sugere que estas desempenham funções divergentes durante o tratamento com ácido acético, Hsc82p atua como uma molécula de sobrevivência e Hsp82p como uma molécula pró-apoptótica. Além disso, a deleção da *HSC82* conduz a uma drástica morte celular necrótica durante o tratamento com ácido acético, sugerindo que estas isoformas são cruciais para o balanço e equilíbrio entre a apoptose e a necrose. Estas novas funções das isoformas da HSP90 foram confirmadas através da inibição farmacológica da atividade das HSP90, utilizando 17-allylaminogeldanamycin (17AGG), e da sobreexpressão de cada isoforma em células tratadas com ácido acético. Estes resultados sugerem que a eficiência de tradução do mRNA das isoformas da HSP90 é um componente importante da resposta celular ao ácido acético. Em resumo, os resultados apresentados no âmbito desta tese contribuíram para o aumento do conhecimento dos mecanismos de tradução que regulação processo apoptótico em levedura.

TABLE OF CONTENTS

LIST OF TABLES AND FIGURES

ABBREVIATIONS

17AGG: 17-allylaminogeldanamycin

5'UTR: 5' untranslated region

AA-tRNA: aminoacyl-tRNA

AIF: Apoptosis-inducing factor

APAF-1: Apoptotic protease activating factor 1

c.f.u.: Colony forming units

cDNA: Complementary deoxyribonucleic acid

CHX: Cycloheximide

CO_2: Carbon dioxide

CSNO: S-nitrosocysteine

DAPI: 4,6-diamino-2-phenyl-indole dihydrochloride

DMEM: Dulbecco's modified Eagle's medium

DNA: Deoxyribonucleic acid

DTT: Dithiothreitol

EDTA: Ethylenediaminetetraacetic acid

eEF1A: Translation elongation factor 1A

eIF2α: Translation initiation factor 2 alpha

eIF4E: Translation initiation factor 4E

eIF4G: Translation initiation factor 4G

FBS: Fetal bovine serum

GAAC: General amino acids control

GADPH: Glyceraldehyde-3-phosphate dehydrogenase

GFP: Green fluorescent protein

H_2O_2: Hydrogen peroxide

HEPES: 4-(2-hydroxyethyl)-1-piperazineethanesulfonic acid

HSP90: Heat shock protein 90

IAP: Inhibitor of apoptosis protein

IPTG: Isopropyl-1-thio-β-D-galactopyranoside

IRES: Internal ribosome entry site

ITAF: IRES trans acting factor

L-NAME: Nω–nitro-L-arginine methyl ester

Min: minutes

MLS: Mitochondrial localization sequence

mRNA: Messenger ribonucleic acid

NO: Nitric oxide

PBS: Phosphate buffered saline

PCD: Programmed cell death

PCR: Polymerase chain reaction

PI: Propidium iodide

PMSF: Phenylmethanesulfonylfluoride

RFU: Relative fluorescence units

RNA: Ribonucleic acid

RNAi: RNA interference

ROS: Reactive oxygen species

RT-PCR: Reverse transcription polymerase chain reaction

SC: Synthetic complete

SDS-PAGE: Sodium dodecyl sulphate – Polyacrilamide gel electrophoresis

siRNA: small interfering RNA

STS: Staurosporine

TCA: Trichloroacetic acid

TNF: Tumor necrosis factor

TOR: Target of rapamycin

TUNEL: Terminal dUTP nick-end labeling

XIAP: X-linked inhibitor of apoptosis protein

YCA1: Yeast metacaspase gene

YPD: Yeast rich medium

OBJECTIVES AND OUTLINE OF THE THESIS

In mammalian cells, posttranslational modifications and cleavage of translation factors by caspases during programmed cell death (PCD) lead to the impairment of cap-dependent translation. Nevertheless, a selective internal ribosome entry site (IRES) mediated translation is activated regulating the expression of PCD regulators, both anti- and pro-apoptotic proteins.

In yeast, a conservation of the alternative translation mechanisms regulating PCD is far from being completely disclosed. Despite the report that the fragmentation of translation factors occurs in different scenarios of yeast PCD, the role of yeast metacaspase in alterations and the evaluation of alternative translation mechanisms controlling yeast PCD have never been addressed.

The work reported in this thesis aimed to get new insights on the yeast translation regulatory mechanisms activated during PCD and on the proteins translated by these mechanisms as well as their contribution for the PCD process.

With the intention to drive the reader through the main achievements, this thesis was organized in five chapters:

In **chapter 1**, a general introduction mainly centered on the knowledge of the PCD processes and the translation regulatory mechanisms of PCD will be given.

In **chapter 2**, a characterization of the translation process and translation regulators modulating acetic acid-induced PCD, will be done.

In **chapter 3**, insights on the conservation of molecular pathways targeted by proteases during yeast apoptosis will be exposed. Furthermore, results are presented suggesting a new pro-apoptotic function of translation elongation factor 1A (eEF1A) upon acetic acid-induced apoptosis.

In **chapter 4**, results will be presented indicating that heat shock protein 90 (HSP90) chaperones isoforms are translated by an IRES-mediated cap-independent mechanism during acetic acid treatment, playing antagonistic roles in yeast PCD.

Finally, **chapter 5** comprises an integrative discussion focused on the main contributions of the present work to the understanding of the yeast PCD processes, combined with future perspectives.

CHAPTER 1

General introduction

1.1 PROGRAMMED CELL DEATH (PCD)

The crucial role of cell death in the cellular homeostasis has been widely described [6-8], however, it was only recognized after the discovery that cell death in multicellular organisms is subjected to genetic control, and the demonstration that abnormalities in cell death regulation lead to the onset of several diseases, including neurodegenerative diseases and several forms of cancer [6, 9-12]. The first description of the programmed cell death (PCD) process and its role in cellular homeostasis was in the 1960s when an insect physiologist, Carrol M. Williams, and his group referred for the first time to PCD, meaning that cells followed a sequence of controlled (and thereby implicitly genetic) steps towards their own destruction [13]. In 1972, John Kerr and coworkers generalized the idea that cell death followed a specific pattern that included shrinkage of the cell, apparently little damage to the organelles, coalescence and margination of chromatin and fragmentation of the cell and the nucleus [14]. These observations suggested that the ritualistic nature of cell death implied an organized and conserved mechanism: cell death was an aspect of life like any other [14]. Further reports followed, describing two distinct types of PCD, apoptosis and necrosis, based on morphological and biochemical criteria [12, 13, 15-19]. Apoptosis is the best studied and described type of PCD. The term apoptosis emerged in the early 1970 [14], although the phenomenon of apoptosis had been described already in the late 1700s. The word, apoptosis, is derived from Greek roots meaning, "dropping off" e.g. falling of leaves. The genetics and molecular mechanisms of apoptosis were first characterized in the late 1980s and early 1990s in studies using the nematode worm *Caenorhabditis elegans*. Apoptosis during *C. elegans* development is extremely precise and predictable specific genes are activated to kill exactly 131 cells, leaving 959 in the adult worm [20-22]. In other words, apoptosis is an evolutionarily conserved, genetically regulated, cellular suicide mechanism that plays a crucial role in development and in the defence of homeostasis.

For many years necrosis was considered as an alternative to apoptotic programmed cell death [18, 23]. However, in the last decade, necrosis has becoming accepted as a form of active and controlled PCD [18, 23-28] that under pathophysiological conditions, amplifies and catalyzes the pathological process therefore activating an

inflammatory response [18, 23]. The morphology of necrotic cells is very distinct from that of cells undergoing apoptosis. Structural changes occur both at the cytoplasm and the nucleus [18, 19, 23-31], chromatin flocculates and plasma membrane integrity is compromised releasing the cytoplasmic contents into the extracellular space leading to inflammation [18]. Unlike in apoptosis, the chromatin is not packed into discrete membrane-bound particles, but it forms many unevenly textured and irregularly shaped clumps, a feature that is being used for differentiating between the two modes of cell death. The mitochondria undergo inner membrane swelling and disintegration. Polyribosomes are dissociated and dispersed throughout the cytoplasm, giving the cytoplasmic matrix a dense and granular appearance and swelling and fragmentation of the cisterns of rough endoplasmic reticulum and Golgi apparatus are frequently observed. Necrotic cell death can be mediated by passive as well as active mechanisms. However, the molecules involved in the active mechanisms are just starting to be identified [18, 23-28]. The involvement of the death domain receptors like tumour necrosis factor (TNF) receptor 1 (TNFR1), Fas/CD95 and TRAIL-R or toll like receptors (TLR) 3 and 4 in the activation of necrosis by a mechanism dependent on the kinase RIP1 has been described [25, 32-34].

During the apoptotic PCD, characteristic morphological alterations are also observed, such as cytoplasmic shrinkage, nuclear condensation and cytoplasmic blebbing. These initial changes are followed by fragmentation of the nuclear contents and subsequent encapsulation of these fragments into apoptotic bodies [12, 14, 15, 19, 30], which are quickly phagocytised and digested by neighbouring cells or macrophages [12, 14, 35, 36]. As no cytosolic contents are released into the intercellular medium during apoptosis, inflammation is not triggered [39].

Biochemically, apoptotic cells are characterized by the production of reactive oxygen species (ROS), reduction in the mitochondrial transmembrane potential, intracellular acidification, externalization of phosphatidylserine for the cytoplasmatic outer membrane, selective proteolysis of a subset of cellular proteins, and degradation of DNA into internucleosomal fragments [9, 12, 15, 37]. These

characteristic manifestations of apoptosis reflect the activation of an intrinsic cell death apparatus well conserved in eukaryotes [3, 12, 20-22, 26, 36, 38-41].

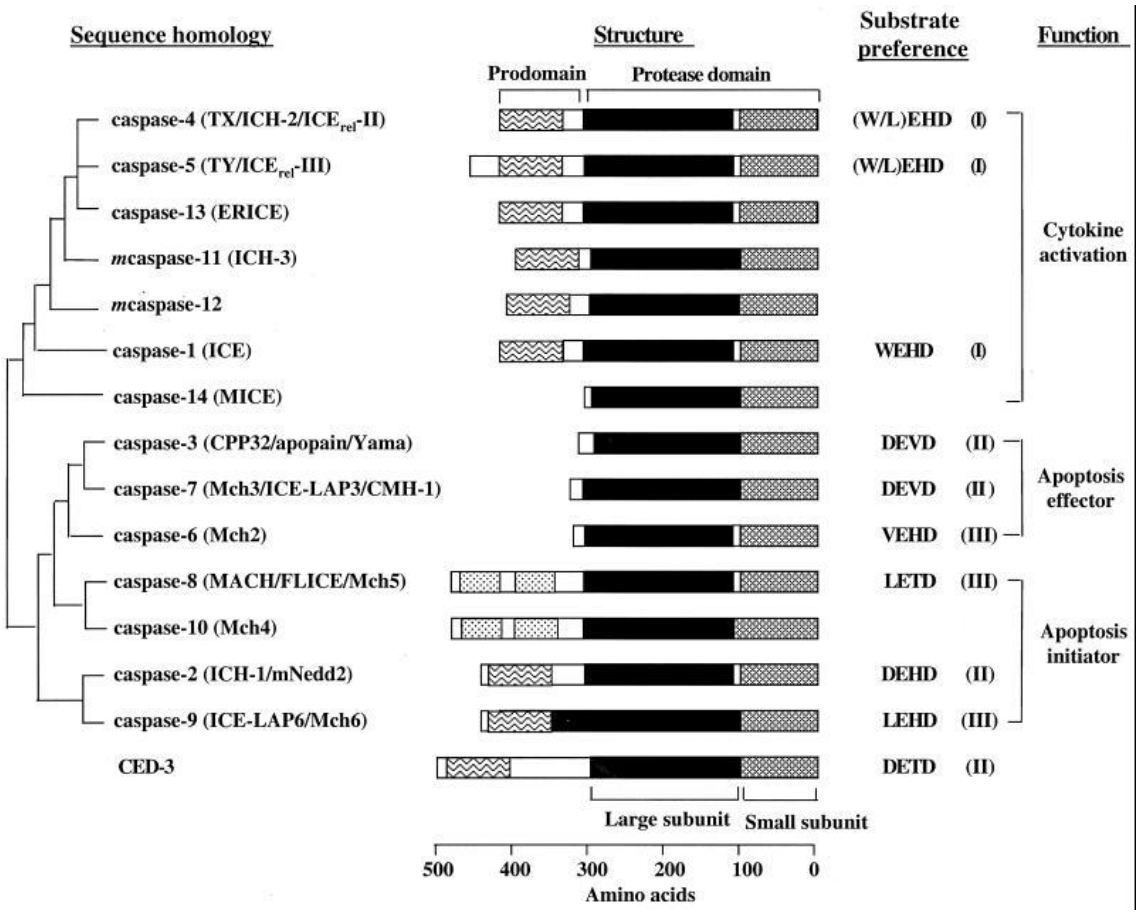

Figure 1 – Mammalian caspase family and *C. elegans* caspase CED-3. The structural and functional organization of caspases. From [1].

During apoptosis, a proteolytic system involving a family of proteases called caspases is activated [42-45]. Caspases are aspartate-specific cysteine proteases responsible for the cleavage of key enzymatic and structural substrates, resulting in the systematic and orderly disassembly of the dying cell [42-48]. These proteases were first implicated in apoptosis by genetic analysis in the nematode C. *elegans*, in which the deletion of a single gene, CED-3, resulted in the abrogation of PCD in the 131 cells normally undergoing apoptosis during the worm's development [21].

The mammalian caspase family of proteases consist of at least 14 mammalian members that can be divided, according to their structure and function, into initiator (pro-caspases 2, 8, 9 and 10) and effector (pro-caspases 3, 6 and 7) caspases (Figure 1). These proteases are constitutively expressed in almost all cell types as inactive proenzymes (zymogens) that become processed and activated in

response to a variety of pro-apoptotic stimuli [44]. Caspase activation involves proteolytic processing of the proenzyme at specific aspartate residues between the domains, resulting in removal of the prodomain as well as the linker region and formation of a heterodimer containing one large and one small subunit. The active caspase is a tetramer composed of two such heterodimers [44]. Initiator caspases are responsible for the activation of the effector pro-caspases which after activation carry on an apoptotic cascade culminating in the cellular disassembling. This cascade begins with autocatalytic activation of initiator caspase (caspase-2, -8, -9 and -10) that, in turn, transmit the signal by cleaving and thereby activating the

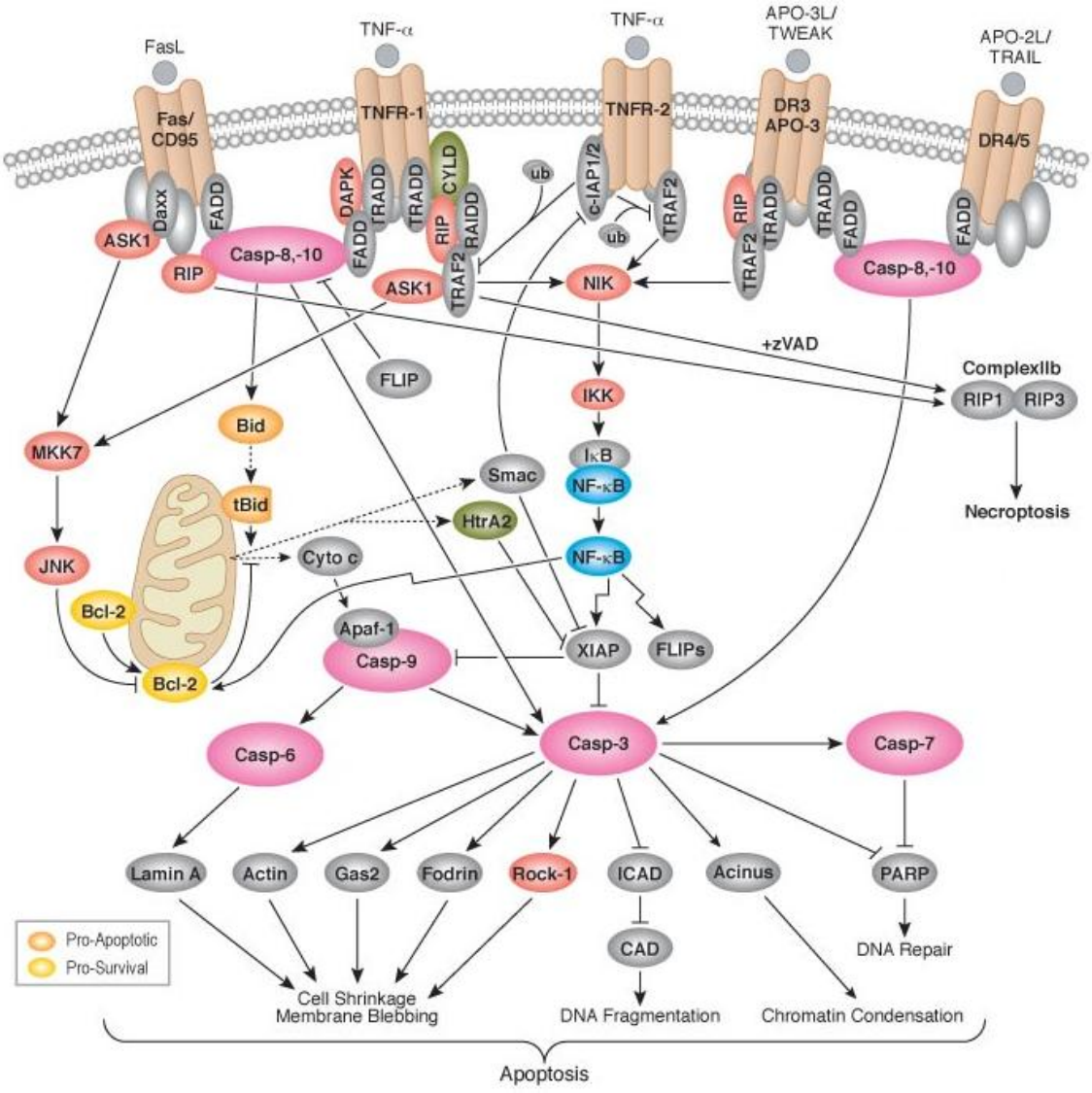

Figure 2 – Death receptor-signalling pathway and mitochondrial pathway of apoptosis. From Cell Signalling (http://www.cellsignal.com/reference/pathway/Death_Receptor.html).

downstream effector/executioners caspases such as caspase-3 [44].

Apoptosis is a highly regulated process, being controlled by tightly interconnected signalling pathways (Figure 2). Some of the pathways and events of the apoptotic program are conserved among species being considered fundamental events in the apoptotic process (Figure 2) [12, 13, 15, 38, 39, 49-51]. These include the action and regulation of the Bcl-2 family of proteins, cytochrome *c* release from mitochondria into the cytosol accompanied by mitochondrial dysfunction, and activation of caspases (Figure 2). There are two major signalling pathways of apoptosis, the death receptor pathway and the mitochondrial pathway [9, 51-54]. In the death-receptor signaling pathway, signal is provided by the interaction between the ligand and the death receptor. Death receptors, such as Fas/CD95 or TNFR1 belong to the tumor necrosis factor receptor (TNFR) superfamily, and the ligands belong to the tumor necrosis factor (TNF)/nerve growth factor family (Figure 2). Members of the death receptor family contain one to five cysteine-rich repeats in their extracellular domain and a death domain (DD) in their cytoplasmic tail. The DD is essential for initiating the apoptotic signal. Following ligation of death receptor by ligand, the death receptor oligomerizes and recruits adapter molecules and initiator caspases to a complex, the death-inducing signalling complex (DISC), which results in the activation of initiator caspases. Initiator caspases then cleave effector/executioner caspases (caspase-3, -6, and -7), which cleave a number of target substrates resulting in morphologic and biochemical characteristics of apoptosis (Figure 2). Apoptosis is a tightly regulated process. The most extensively studied and perhaps the most relevant regulators are Bcl-2 family proteins. This family includes anti-apoptotic proteins such as Bcl-2 and Bcl-XL, and pro-apoptotic proteins such as Bax and others [9, 55, 56].

These molecules either homodimerize or heterodimerize with molecules of opposing function (e.g. Bax may heterodimerize with Bcl-2 or Bcl-xL). The influence of this interaction in the apoptotic process appears to be dependent on the relative concentration of these molecules in heterodimers and the ratio between pro-apoptotic and antiapoptotic molecules. Though the regulatory role of Bcl-2 family proteins in mitochondrial pathway of apoptosis is well-established [9, 55, 56], their role in the regulation of death receptor signaling is controversial and may

be specific for each cell type. Despite the fact that these two pathways are distinct, death receptor signaling can activate the mitochondrial pathway via tBid [56]. Bid is a BH3-only protein exclusively cytosolic in living cells. Upon activation of cell surface death receptors, Bid is cleaved by active caspase-8 and the truncated Bid (tBid) translocates from cytosol to mitochondria inducing cytochrome *c* release through the binding to a mitochondria specific lipid, cardiolipin [56]. The ability to cleave and activate Bid may not be limited to caspase-8. Other caspases, such as caspase-3, as well as other proteases, have been shown to cleave and activate Bid. Mitochondria play a crucial role for the progression of the PCD processes [24, 39, 52, 55, 57]. A number of stimuli, including chemotherapeutic agents, UV radiation, stress molecules (ROS and reactive nitrogen species RNS), and growth factor withdrawal appear to mediate PCD via the mitochondrial pathway which can be independent from death-receptor pathway [57, 58].

Mitochondria are organelles comprised by the matrix surrounded by the inner membrane (IM), the intermembrane space and an outer membrane (OM). In the IM are enclosed several molecules, including ATP synthase, electron transport chain, and adenine nucleotide translocator (ANT). Under physiological conditions these molecules allow the respiratory chain to create an electrochemical gradient (membrane potential). The OM contains a voltage-dependent anion channel. The intermembrane space contains holocytochrome *c*, certain procaspases, adenylate kinase 2, EndoG, Diablo/Smac, and apoptosis-inducing factor (AIF). IM permeabilization leads to changes in mitochondrial membrane potentials while OM permeabilization results in the release of these molecules into the cytoplasm. The release of cytochrome *c* is one of the major steps in the mitochondrial pathway of apoptosis associated with the permeabilization of mitochondrial OM, promoting the formation of the apoptosome which activates caspase 9 leading to the activation of the executioner caspases to orchestrate apoptosis. The components of apoptosome are cytochrome *c*, an adapter molecule Apaf-1 (Apoptotic protease-activating factor) and procaspase-9. The binding of cytochrome *c* to Apaf-1 leads to its unfolding and exposure of its oligomerization domain which is stabilized in the presence of ATP or dATP. Caspase recruiting domain (CARD) in the oligomer binds to the CARD domains of procaspase-9 to activate caspase-9. Active caspase-9

then cleaves and activates executioner caspases, such as caspase-3, to induce apoptosis [57]. CAD (caspase-activated DNase) is responsible for the degradation of chromosomal DNA. Activation of CAD is initiated by the cleavage of ICAD (inhibitor of caspase-activated DNase) by effector caspases, such as caspase-3.

EndoG and AIF are released from mitochondria in response to various stimuli being translocated to the nucleus, where they have a role in DNA degradation. Unlike CAD, activation of EndoG and AIF is independent of caspase activation. It is possible that EndoG and AIF may participate in nuclear DNA degradation when caspase activation is limited by an apoptosis-like mechanism.

PCD is a highly regulated mechanisms under a complex and rigorous molecular control [26]. Although scientists have focused their research in the genetic alterations that regulate PCD, an increasing body of evidence is also emerging showing a tight regulation of the translation process and factors during the PCD process [5, 59, 60].

1.2 TRANSLATION CONTROL DURING PCD

Translation process is divided in three phases: initiation, elongation and termination [61]. Canonical cap-dependent translation initiation involves the binding of the mRNA 5'-m^{7}G cap-structure to the cap-binding protein eIF4E. eIF4G binds to eIF4E recruiting other proteins such as the eIF4A helicase, responsible for the unfold of the mRNAs 5' untranslated region (5'UTR) secondary structure, forming the cap-binding complex (eIF4F). After the assembly of the eIF4F complex with the mRNA, 40S ribosomal subunit is recruited originating the 43S complex comprised of the 40S ribosomal subunit, a ternary complex containing an initiator tRNA molecule (tRNAiMet), the initiation factor eIF3, which makes the connection between 40S and eIF4G, and the initiation factors eIF1 and eIF1A, which help the recognition of the start codon (Figure 3A). After the assembly, the 43S initiation complex scans along the 5'UTR searching for the initiation AUG codon where the 60S subunit binds to form an elongation-competent 80S ribosome. 5'- and 3'-ends of the mRNA interact during cap-dependent initiation in

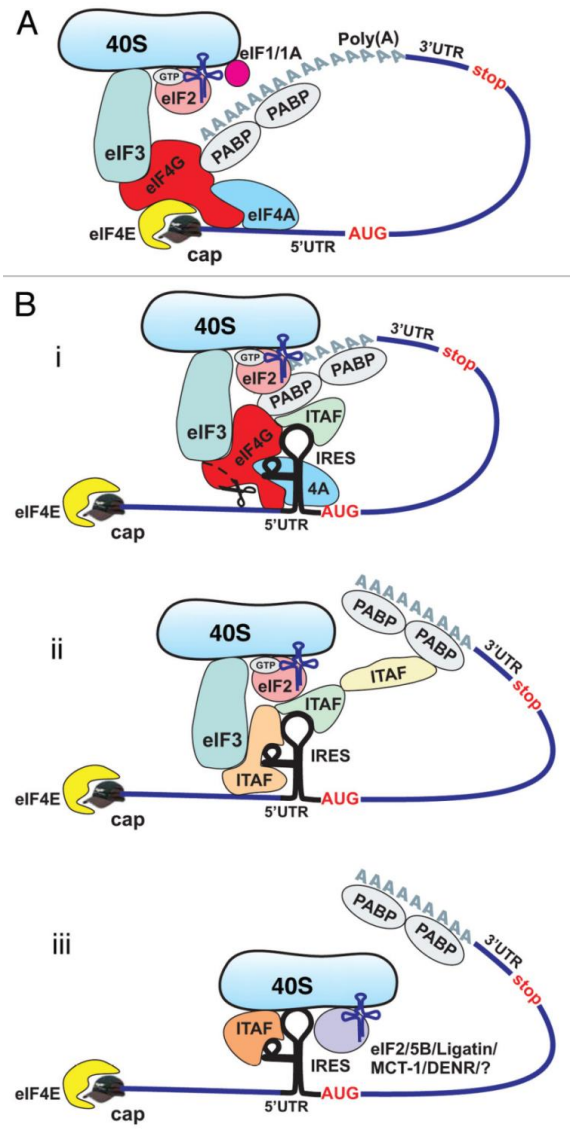

Figure 3 – Cap-dependent and IRES-mediated translation initiation mechanisms. (A) Cap-dependent translation. (B) IRES-mediated translation (i) using most of the canonical translation initiation factors and many ITAFs with the circularization of the mRNA, (ii) using a limited number of canonical factors and ITAFs and (iii) canonical factors are dispensable, but some ITAFs are required. From [5].

eukaryotes through the poly(A)-binding protein (PABP) interaction with eIF4G, leading to the circularization of the mRNA. For decades this cap-dependent initiation of translation was assumed as the only mechanism allowing the progression of cellular mRNAs translation [62, 63].

1.2.1 Cap-dependent translation impairment during PCD

Translation is the final step in the flow of the genetic information, therefore a regulation at this level allows for an immediate response to changes in physiological conditions, such as cellular stress or activation of PCD, that require immediate changes in protein levels. To answer that, diverse adaptation strategies, as regulation of global translation combined with selective translation, have evolved providing rapid and reversible regulation of protein expression.

Table 1 – Translation initiation factors alterations during PCD.

Translation initiation factor	Modification	References
eIF2α	Cleavage by caspase-3	[64, 65]
eIF2α	Ser^{51}Phosphorylation	[66-73]
eIF3 (p35), eIF3b, eIF3f, eIF3g, eIF3k	Cleavage by caspase-3 or inhibition of activity by interaction with other protein	[65, 74-77]
eIF4B	Cleavage by caspase-3	[65]
eIF4E	Cleavage by caspase-3	[78-80]
4E-BP1	Cleavage by caspase-3	[65, 81]
eIF4GI and eIF4GII	Fragmentation by caspase-3 and caspase-8	[59, 65, 73, 82-87]
DAP5/p97	Reduced levels or cleavage by caspase	[88-92]

Over the last years, several studies have demonstrated that during PCD, translation initiation factors, mainly translation initiation factor 4G (eIF4G) family members [59, 65, 73, 82-87], but also translation initiation factor 2α (eIF2α) [64, 65], 3 (eIF3) [65], 4B (eIF4B) [65], 4E (eIF4E) [78-80], DAP5/p97 [88-92]

and eIF4E binding proteins (4E-BP1) [65, 81], are targets of specific cleavage mediated by caspases in a variety of cell types and in response to different stimuli (Table 1). Moreover, post-translational modifications such as the phosphorylation of eIF2α mediated by haem-regulated inhibitor kinase (HRI), protein kinase RNA (PKR), PKR-like endoplasmic reticulum kinase (PERK) or general control non-derepressibe-2 (GCN2), lead to the reduction of the canonical cap-dependent translational initiation [66-73]. However, others mechanisms, such as the GCN4 translation by four upstream open reading frames (ORFs), firstly described in yeast, being induced by the phosphorylation of eIF2α as a response to amino-acid starvation [93, 94] and cap-independent internal ribosome entry site (IRES)-mediated translation, which selectively recruits mRNAs harbouring IRES in their 5' untranslated region (5'UTR), have shown to be activated in order to fulfil the cellular requirements.

1.2.2.1 IRES-mediated translation

IRES-mediated translation is a tightly controlled mechanism of translation of specific mRNAs regulated by their unique sequences in the 5'UTR, in conditions of global translation impairment such as stress and apoptosis. IRES are sequences with a high percentage of GC and several AUGs usually present in long 5' UTRs mRNAs but that can also be found in the mRNA coding sequence. These sequences form a complex secondary structure, which directly recruit ribosomes independently of the mRNA cap-structure and of the eIF4E [4]. However, no similarities between the structures or sequences of these cellular IRES were identified so far. Several canonical translation initiation factors may participate in the initiation of IRES-mediated translation. Different IRES-containing mRNAs have shown to require specific canonical translation initiation factors (Figure 3B) [4, 5, 95]. Furthermore, for an efficient IRES-mediated translation, auxiliary cellular proteins, known as IRES trans-acting factors (ITAFs), are also required [96]. These ITAFs can stimulate or inhibit the activity of IRES elements by affecting ribosome recruitment or modifying the structure of the IRES mRNA itself.

This alternative translation has proven to be an important regulatory mechanism for the organism homeostasis being associated both to survival or death of the cell.

1.2.2 Apoptotic regulators IRES-mediated translation during PCD

During the last decade, IRES sequences have been reported in the mRNA of proteins with important roles in cell growth, differentiation and regulation of PCD [4]. Example of this mechanism is the translation of several mammalian apoptotic regulators, both inhibitors and inducers of apoptosis (Figure 3).

Mammalian anti-apoptotic proteins, such as c-IAP1 [97], HIAP2 [98, 99] and the well described X-chromosome-linked inhibitor of apoptosis (XIAP) [99-108] are translated by an IRES-mediated mechanism blocking the apoptotic process through direct binding and inhibition of caspases activity. The contribution

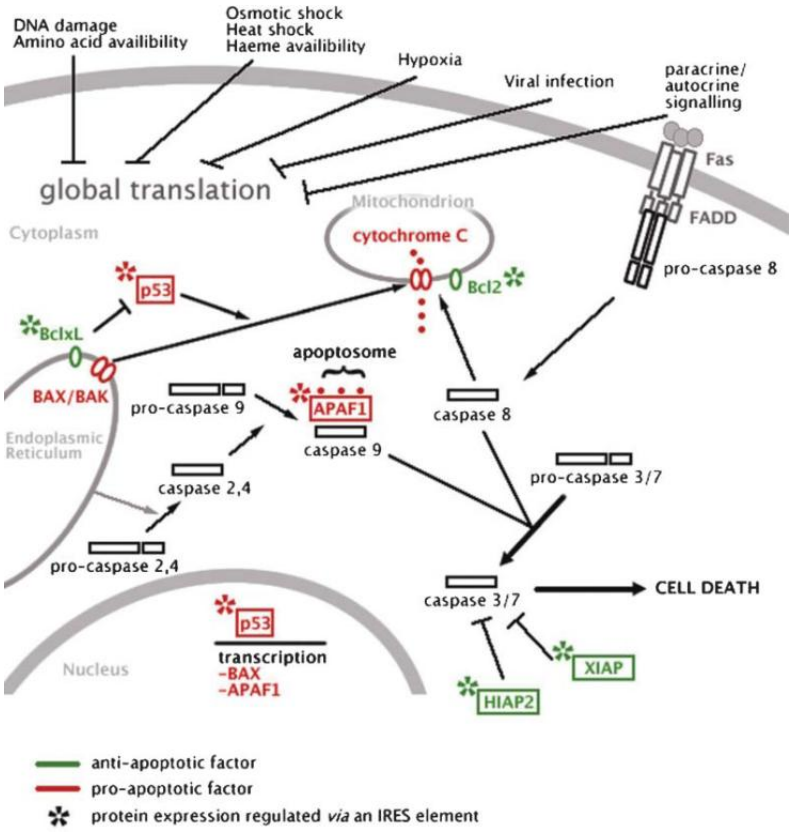

Figure 4 – IRES-mediated translation initiation regulates the expression of key apoptotic players, both pro-apoptotic and anti-apoptotic factors. From [4]

of pro-apoptotic proteins such as Apaf-1 [109-111], c-myc [112-117], DAP5 [91, 118] and p53 [119-121] for PCD is also regulated by IRES, leading to the activation of the apoptotic cascade. The balance between the relative levels of these apoptotic regulators will determine the cells fate, survival or cell death (Figure 3).

Table 2 – IRES-containing mRNAs with a role in the modulation of PCD.

IRES-containing PCD regulator	Function in PCD	References
Bcl-2	Anti-apoptotic protein	[122-124]
c-IAP1	Anti-apoptotic protein	[97]
HIAP2	Anti-apoptotic protein	[98, 99]
HSP70	Anti-apoptotic protein	[125-127]
OCT4B-190	Anti-apoptotic protein	[128]
Sp1	Anti-apoptotic protein	[129]
XIAP	Anti-apoptotic protein	[99-106, 130-133]
Apaf-1	Pro-apoptotic protein	[109-111]
CDK1	Pro-apoptotic protein	[123]
c-myc	Pro-apoptotic protein	[112-117]
DAP5	Pro-apoptotic protein	[91, 118]
p53	Pro-apoptotic protein	[119-121]

A role of glyceraldehyde-3-phosphate dehydrogenase (GAPDH), a glycolytic enzyme, in the repression of p53 translation by direct binding to the p53 3'UTR has been described [134]. In mammalian cells, this enzyme is a known inhibitor of virus and mammalian mRNAs IRES-mediated translation [119, 134-138]. Hence, GAPDH is responsible for the inhibition/repression of cap-independent IRES-mediated translation in higher eukaryotes as a protective mechanism against opportunistic viral infections and apoptosis. Its specific cleavage by caspase-1 during apoptosis [139] might lead to the unblock of p53 IRES-mediated translation and ultimately to the apoptotic cell death.

Therefore, IRES-mediated translation is an important piece of the intricate puzzle that controls PCD and a deregulation of this process may lead cellular alterations.

1.3 HSP90 CHAPERONES AND PCD

HSP90 chaperones are highly conserved constitutively abundant proteins with crucial roles in protein folding/refolding as well as in the general response to stress and PCD [140-143]. Although HSP70 chaperones proved to be translated by IRES-mediated translation [125], and despite the overlapping functions of HSP70 and HSP90 [2, 144-149], a regulation of HSP90 chaperones translation at this level was never addressed. Prominent members of mammalian HSP90 family are the cytoplasmic chaperones Hsp90α and Hsp90β [141, 142]. Hsp90β is expressed constitutively to a higher level than Hsp90α, which is generally stress-inducible [141]. Unlike to other eukaryotic HSPs [150], the nucleotide sequence of HSP90 chaperones include several introns and exons, mainly in the 5' and 3'UTRs

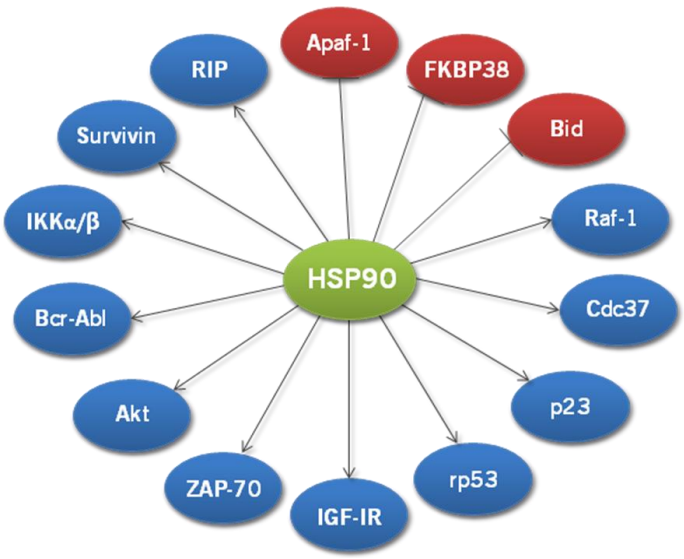

Figure 5 – HSP90 client proteins have a crucial role in PCD. Proteins marked in blue are anti-apoptotic proteins which stability is regulated by HSP90. Proteins marked in red are involved in the progression of PCD and are repressed by interaction with HSP90.

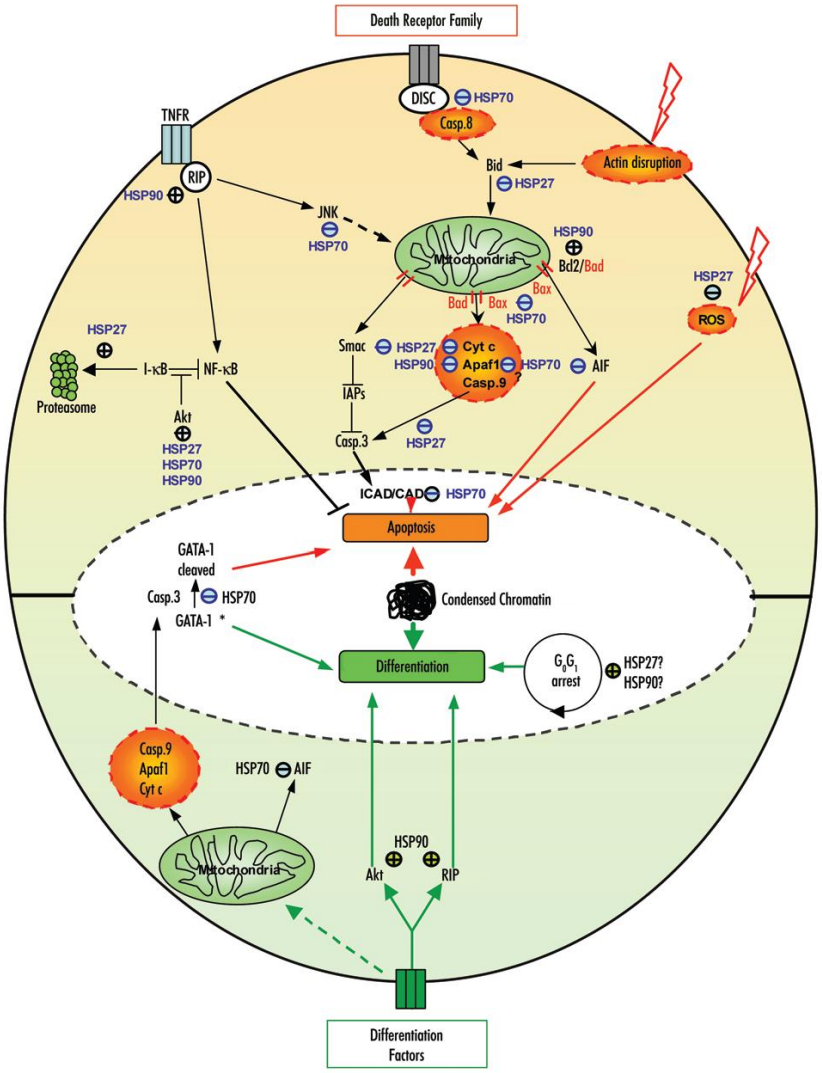

Figure 6 – Modulation of apoptosis by HSP90 through interaction with client proteins. From [2].

[151, 152]. The differences in the amino acid sequence and the differential patterns of expression of Hsp90α and Hsp90β isoforms raises the possibility of their interaction with distinct client proteins, being involved in different cellular functions. However, most of the studies do not differentiate the functions of HSP90α and HSP90β. Despite this obstacle for the elucidation of HSP90 isoforms cellular functions, recent studies suggest that some functions of the HSP90β are not overlapped by HSP90α [153, 154]. During oxidative stress induced by ascorbate/menadione, in mammalian cells only the HSP90β is cleaved leading to the reduction of the levels of its client proteins Bcr-Abl, RIP and Akt [153, 154].

Their function influences the activity and stability of a wide range of client proteins such as key regulators in cellular growth, differentiation and cell death pathways [155]. Hsp90 chaperones are responsible for the stability of anti-apoptotic proteins, such as: Survivin, IGF-IR, Cdc37, Zap-70, BcR-Abl, IKKα/β, rp53, Bcl-2 and AKT [143, 153, 156-166] and in the repression of pro-apoptotic proteins such as Apaf-1, Bid and FKBP38 [167-171] (Figure 5). In fact, the regulation of the Fas- and Tumor-necrosis factor receptor 1 necrotic process by mammalian HSP90 chaperones through the interaction with its client protein RIP1 has also been described [25, 172, 173]. Modulation of the HSP90 expression leads to cellular alterations. The overexpression of HSP90 induces cell survival and their depletion by siRNA or inhibition using geldanamycin triggers apoptosis [32, 160, 165, 172, 174-180]. The fact that Apaf-1 translation is tightly regulated by IRES and its contribution for the PCD process in under control of HSP90, is a good evidence that PCD is a complex process under the control of different sequential mechanisms and molecules and the smallest alteration in this process may lead to carcinogenesis.

Since HSP90 chaperones are powerful inhibitors of apoptosis, a modulation of their cellular levels affects the cellular homeostasis. In fact, HSP90 are the only chaperones targeted in cancer therapy, namely in anti-Acute Myeloid Leukemia (AML) treatment to sensitize tumor cells to chemotherapy-induced death through the use of HSP90 specific inhibitor geldanamycin [159, 181-185], [184, 186, 187]. However, the outcome of these treatments is below expectations, probably due to an undifferentiated inhibition of all the HSP90 isoforms therefore affecting the function of different client proteins in distinct molecular pathways [188].

1.4 Yeast PCD

For decades, the apoptotic process was assumed to occur only in multicellular organisms as a protective mechanism of rapid removal of unwanted or damaged cells that could otherwise inflame the surrounding cells with their cytoplasmic contents. This perception changed in 1997, when Madeo and coworkers showed that the yeast *Saccharomyces cerevisiae* also undergoes PCD

with typical apoptotic markers such as externalization of phosphatidylserine to the leaflet of the outer plasma membrane, degradation of DNA, condensation of chromatin, and production of reactive oxygen species (ROS) [189]. Several reports followed showing the occurrence of this process induced by diverse exogenous stimuli like H_2O_2 [190] and acetic acid [191], the two most extensively studied apoptotic stimuli in yeast [3, 189, 191, 192], or by endogenous stimuli such as

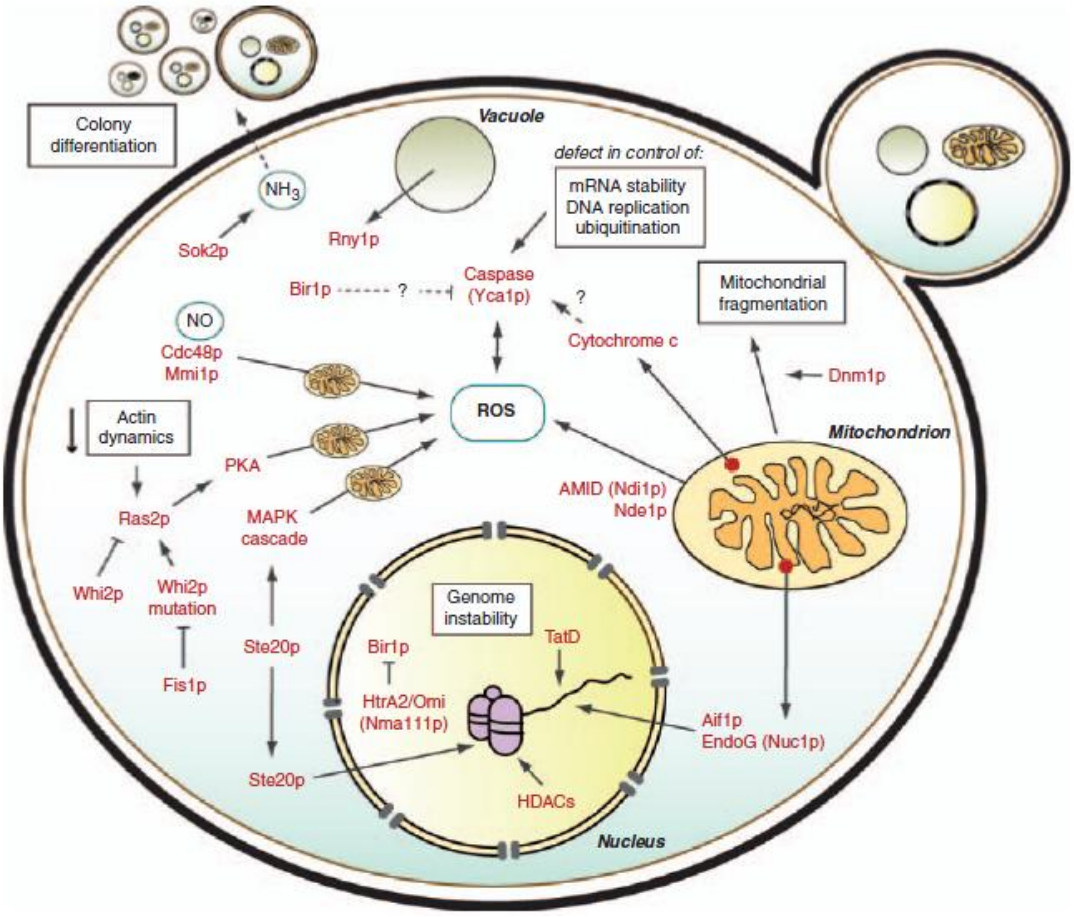

Figure 7 – Proteins and pathways regulating yeast apoptosis. From [3]

mating pheromones [193, 194] and aging [195, 196]. This was the starting point for the study of an old process in a new unicellular eukaryotic model. Scientist focused their attention on the molecular pathways and regulators controlling the apoptotic process searching for conserved mechanisms from yeast to mammalian cells. In fact, throughout this decade, the knowledge on the yeast apoptotic regulatory mechanisms had a massive development. Yeast apoptosis proved to be mediated by several orthologues of mammalian apoptotic regulators, both anti-apoptotic proteins such as Bir1p (XIAPp) [197] and Cdc48p (VCP) [189] and pro-

apoptotic proteins as Aif1p (AIF) [41], Nuc1p (endoG) [198], and Nma111p (HtrA2/Omi) [197] (Figure 7). Furthermore, a conservation of the molecular pathways involved in the regulation of the apoptotic process was also observed (Figure 7). The activation of an yeast caspase like protease, metacaspase [40], the mitochondrial membrane depolarization [199], release of cytochrome *c* from mitochondria to cytoplasm [199], mitochondrial fission and fusion [200, 201] and actin cytoskeleton alterations [202-204] support the conservation of the main apoptotic hallmarks of PCD from yeast to mammalian cells (Figure 7).

Over a decade ago, a family of proteases presenting structural similarities to caspases was identified in protists, fungi and plants [205]. These proteases were named metacaspases and classified, according to the presence or absence of a N-terminal prodomain containing a proline-rich repeat motif, as type I or type II, respectively. In spite of the structural similarity with the remotely related caspases, a large body of accumulating evidence shows that all metacaspases are highly specific for P1-Arg and P1-Lys substrates [206].

Yeast cells have a single gene, *YCA1,* encoding a type I metacaspase that was first implicated in the execution of oxidative stress induced cell death [40] but that is estimated to participate in approximately 40% of the described yeast apoptotic scenarios [207]. Nevertheless, non-death functions have also been assigned to yeast metacaspase such as cell cycle regulation [208] and protein catabolism [209]. Although the mechanisms regulating this multifunctional protein, metacaspase, still remain elusive, it is known that metacaspases activity is regulated through S-nitrosation and thus dependent on the endogenous levels of nitric oxide (NO) [210]. S-nitrosation of one metacaspase Cys residue keeps it inactive. However, a second catalytic Cys residue, highly conserved in all known metacaspases but absent in all members of caspases, can rescue metacaspase activity in the presence of high NO levels [210]. Accordingly, in yeast H_2O_2-induced apoptotic conditions [40, 190], a cell death process dependent on metacaspase activity and NO generation, metacaspase activity and cell death are abolished in the presence of L-NAME, an inhibitor of NO synthesis [211, 212].

One of the major mechanistic challenges for understanding the role of metacaspases in cell survival and death is still the identification of their natural

substrates. Until recently, the only protein known to be cleaved by metacaspases in vivo was the evolutionarily conserved TSN (Tudor *staphylococcal* nuclease) [213] found in all eukaryotes except in budding yeast [213]. Thus, although in yeast, metacaspase is essential for apoptosis execution upon a wide range of either physiological or external stimuli [40, 214], the substrates and therefore the specific molecular pathways targeted/regulated by this protease are still unknown.

1.4.1 Acetic acid and H_2O_2: the paradigmatic inducers of yeast PCD

Over the last decade, diverse stimuli have been associated to the induction of yeast apoptosis. Among those stimuli, acetic acid and H_2O_2, are the most studied and were used in most of the experiments presented in this thesis.

Although acetic acid is used as an external apoptotic stimulus, this compound is an end product of yeast alcoholic fermentation and could be considered as a natural physiological apoptotic stimulus. In the course of acetic acid apoptotic process, mitochondria appear to play a preponderant role. Acetic acid treatment leads to the production of ROS in mitochondria, induction of the mitocondrial membrane depolarization [199], release of cytochrome *c* to cytoplasm [199], translocation of Aif1p from mitochondria to the nucleus [41], leading to DNA fragmentation, culminating with the mitochondria fission and fusion [200]. Moreover, during acetic acid-induced apoptosis, a severe intracellular amino acid starvation occurs, leading to the inhibition of the target of rapamycin (TOR) and of protein phosphatases Pph21p and Pph22p, downstream mediators of TOR signaling [215], derepressing Gcn2p kinase and therefore leading to a cell cycle arrest in G0/G1 phase [215]. Proteomic analysis of acetic acid-treated cells also revealed a decrease in the levels of several translation factors, namely eIF4A, eEF1A, eEF2 and eEF3A [215]. Furthermore, an extensive degradation of ribosomal RNAs occurs during acetic acid-induced apoptosis [216]. These data together with the literature regarding the translation regulation of apoptosis in mammalian cells, strongly suggests a regulation of translation process during acetic acid induced-apoptosis. Despite the described degradation of mitochondria and ribosomal RNA during acetic acid treatment, a recent report demonstrated that

autophagy is not involved in the modulation of acetic acid-induced apoptosis [201]. Curiously, it is suggested that the yeast metacaspase, performs a role in the acetic acid-induced apoptosis, unrelated to its caspase activity [217].

During H_2O_2-induced apoptosis, a different apoptotic cascade appears to be activated, in which metacaspase plays a key role [40, 214, 218, 219], having high levels of activity [40]. Metacaspase participation in acetic acid-induced apoptosis is not as essential as in H_2O_2-induced apoptosis [217]. Moreover, alterations in the translation process also proved to contribute for the H_2O_2-induced apoptosis, such as the extensive degradation of ribosomal RNAs [216] and the decrease of global translation mediated by the phosphorylation of eIF2α through Gcn2p kinase (the amino acid control kinase) [220].

Although the knowledge in the yeast apoptotic cell death has been greatly improved during the last years, establishing yeast as a good model for the study of PCD, the participation/conservation of some apoptotic mechanisms, such as the IRES-mediated translation, from yeast to mammalian was never addressed.

Nevertheless, similar to what occurs in mammalian cells, the occurrence of a PCD with typical necrotic features, such as the increase in cell volume (oncosis), swelling of organelles, DNA degradation and plasma membrane disruption with the loss of intracellular contents, has also been described in yeast [221]. Moreover, the nuclear release of yeast HMGB1 (Nhp6Ap) was considered a molecular marker of necrosis in yeast [222]. The balance between the occurrence of apoptotic or necrotic cell death upon acetic acid or H_2O_2 treatment was previously reported to be determined, for the same period of treatment, by concentration, higher concentrations will lead to necrosis, while lower concentrations to apoptosis [190, 191]. This balance is important for the cellular homeostasis, therefore a methodical study of the mechanisms controlling this balance is of utmost importance.

In yeast, it has been reported that the inhibition of yeast HSP90, by radicicol, leads to the inhibition of tunicamycin-induced necrosis [223]. Yeast HSP90 family of chaperones, as well as their mammalian counterparts, are responsible for the protein folding/refolding, influencing the activity and stability of a wide range of client proteins that function as key regulators in PCD [142, 224]. These data

suggest a conservation of the molecular regulators of necrosis from yeast to mammalian cells. Nonetheless, no homologue of RIP1 in yeast is known, but other serine/threonine kinase, Slt2p, interacts with HSP90 [225, 226] and may have a role in the regulation of necrotic cell death.

1.4.2 Translation control in yeast PCD

In yeast, few reports showed the involvement of translation control in PCD. A recent study in *S. cerevisiae* revealed that oxidative stress, by exposure to H_2O_2, causes a dose-dependent inhibition of translation through Gcn2 kinase (the amino acid control kinase) phosphorylation of eIF2, but that some mRNAs are still translated after oxidative stress [220]. Interestingly, our published results, using yeast *S. cerevisiae* as model, also showed that under acetic acid induced PCD, the

Table 3 – Yeast mRNAs capable of being IRES mediated translated.

IRES-containg mRNAs	Function in yeast cell	References
BOI1	Protein implicated in polar invasive growth	[227]
FLO8	Transcription factor required for flocculation, also related to invasive growth	[227]
GIC1	Protein involved in initiation of budding and cellular polarization	[227]
GPR1	Golgi matrix protein involved in the structural organization of the cis-Golgi	[227]
HAP4	Transcriptional activator and global regulator of respiratory gene expression	[228]
L-A	Double-stranded RNA (dsRNA) virus of the yeast *S. cerevisiae*	[229]
MSN1	Transcriptional activator involved in invasive growth	[227]
NCE102	Protein of unknown function involved in invasive growth	[227]
TIF4632	Translation initiation factor eIF4G, subunit of the mRNA cap-binding protein complex (eIF4F)	[227]
URE2	Transcriptional regulator involved in nitrogen catabolism repression	[230-233]
YAP1	Transcription factor required for oxidative stress tolerance	[234]
YMR181c	Protein of unknown function involved in invasive growth	[227]

expression of some translation factors such as eIF4A, eEF1A, eEF2 and eEF3A is diminished [215], but the levels of several other proteins, such as the HSP90 chaperones were increased [215]. These data, strongly suggests the existence of

an alternative IRES-mediated cap-independent mechanism regulating the translation of specific mRNAs upon the apoptotic stimulus, similar to what is described in mammalian cells [4, 5, 95, 235]. In yeast, IRES were mainly reported in transcriptional regulators involved in the response to yeast stress stimulus such as transcription factor *FLO8* required for invasive growth [227], transcription factor *YAP1* [234] and transcriptional activators *HAP4* [228] and *MSN1* [227], involved in the response to oxidative stress and transcriptional repressor of genes involved in nitrogen catabolism *URE2* [230] (Table 3). Moreover, during yeast nutrient starvation an eIF4G-dependent IRES-mediated cap-independent translation of several genes is required for invasive growth as a response to stress [227] (Table 3). However, the role of IRES in the regulation of yeast PCD phenomena has never been addressed.

The identification of the yeast apoptotic regulators capable of putative IRES-mediated translation during PCD would allow an integrated view of the signaling pathways that control the yeast life and cell death decisions.

This chapter attempts to summarize the relevant findings on the translation control of mammalian cells apoptotic processes and the information relative to a conservation of this regulation from yeast to mammalian cells. However, several questions concerning the control of the translation process and its contribution for the yeast apoptotic process remain to be answered. On the next chapters, results will be presented in an attempt to get new insights on the yeast translation regulation of apoptosis, through the study of translation machinery alterations, mRNAs capable of overcoming global translation impairment during apoptosis, as well as their role in the PCD processes, hopping to contribute for the continuous knowledge of the molecular regulatory mechanism controlling cell death.

CHAPTER 2

Global translation impairment during acetic acid-induced apoptosis in *Saccharomyces cerevisiae*

Silva, A., Sampaio-Marques, B., Holcik, M., Santos, M.A. and Ludovico, P.

Part of the results described in this chapter were published as follow:

Sampaio-Marques, B., Felgueiras, C., Silva, A., Rodrigues, F. and Ludovico, P. Yeast chronological lifespan and proteotoxic stress: is autophagy good or bad? Biochemical Society transactions 2011, 39:1466-1470.

Silva, A., Sampaio-Marques, B., Carreto, L., Holcik, M., Santos, M.A. and Ludovico, P. HSP90 chaperones: translationally regulated endogenous modulators of yeast acetic acid-induced cell death. Manuscript in preparation.

The results described in this chapter were presented in the following national or international congresses:

National congresses:

- XVIII Jornadas de Biologia de Leveduras Prof. Nicolau van Uden. Lisboa, Portugal. (2010) "Translation modulation during acetic acid-induced apoptosis in yeast". (Oral communication).
- Microbiotec 09. Vilamoura, Portugal. (2009). "Acetic acid-induced apoptosis in *Saccharomyces cerevisiae* involves global translation impairment". (Poster presentation).

International congress:

- 7th IMYA – International Meeting on Yeast Apoptosis. Graz, Austria. (2009). "Global translation impairment during acetic acid-induced apoptosis in *Saccharomyces cerevisiae*". (Poster presentation).

2.1 ABSTRACT

The decrease of global mRNA translation efficiency during the progression of apoptosis in mammalian cells is a well recognized event [95]. In yeast a correlation between these two processes has also been observed, but the molecular basis of this regulation was never deeply explored. Our previous report revealed a downregulation of translation factors eIF4A, eEF1A, eEF2 and eEF3A levels during yeast acetic acid-induced apoptosis [215], suggesting an impairment of translation during the apoptotic process. In order to better understand the cascade of events leading to translation alterations upon acetic acid treatment, a thorough study of the translation process and of the changes induced by abrogation of one of its key described regulator, Gcn2p kinase [236-238], during acetic acid-induced apoptosis was studied. Polysome profiling kinetic analysis showed a premature dose-dependent reduction of cap-dependent translation initiation correlated with the phosphorylation of eIF2α by Gcn2p kinase, and a later inhibition of translation elongation. Furthermore, Gcn2p kinase proved to be a crucial player in acetic acid-induced apoptosis, due to the more resistant phenotype displayed by *GCN2* deleted cells and the severe reduction of eIF2α phosphorylation. Nevertheless, RT-PCR analysis of polysomal fractions revealed that some mRNAs, such as the pro-apoptotic factor *AIF1*, are translated under these conditions, suggesting the activation of an alternative translation process. Altogether, these results demonstrate that translation regulation is an important component of the cellular response to acetic acid-induced apoptosis.

2.2 INTRODUCTION

Although apoptosis is a phenotypical well characterized programmed cell death (PCD) process, the complete uncover of the molecular pathways underneath this phenomenon is a continuous challenge. The involvement of the translation process in the regulation of apoptosis is a still emerging concept [95, 96, 239-243]. In mammalian cells, global cap-dependent translation proved to be reduced during the progression of apoptosis [95] due to mRNA 5' decapping and specific fragmentation of translation factors, mainly the translation initiation factor 4G (eIF4G) family members [59], mediated by caspases. Besides caspases, other pro-apoptotic proteins were associated to the regulation of translation factors during apoptosis, such as the apoptosis-inducing factor AIF, which binds to the eIF3g during the apoptotic stimulus blocking translation [76]. Post-translational modifications of translation initiation factors, such as, phosphorylation of subunit α of translation initiation factor 2 (eIF2α) were also described [59]. However, the involvement of translational control in yeast PCD is still scarce. The deletion of *LSM4* gene, involved in yeast mRNA decay, inhibits mRNA decapping leading to an increase in mRNA stability and ultimately triggering a caspase-dependent apoptotic process [244-246]. Furthermore, an extensive degradation of ribosomal RNAs is observed during H_2O_2- and acetic acid-induced apoptosis and a decrease of global translation due to the phosphorylation of eIF2α by Gcn2p kinase (the amino acid control kinase) also occurs during oxidative stress [220]. In fact, Gcn2p appears to play a crucial role in the regulation of distinct cellular processes. Apart from its role in the regulation of translation initiation through eIF2α phosphorylation, this kinase has been related to the control of cell cycle, through a DNA damage checkpoint between G1 and S phase [247, 248], being also involved in the TOR-mediated activation of autophagy [249]. Previously, we have shown by proteomic analysis that during acetic acid-induced apoptosis, a severe intracellular amino acid starvation occurs [215] and the levels of translation initiation factor 4A (Tif1/2p) and translation elongation factors 1A (Tef1/2p), 2 (Eft1/2p) and 3A (Yef3p) were decreased [215] suggesting an impairment of translation during yeast apoptosis regulation. Herein we show the occurrence of translation alterations

during the execution of acetic acid-induced apoptosis and disclose the involvement of the known translation regulator, Gcn2p kinase, in this process.

2.3 MATERIALS AND METHODS

Strains, media and treatments

Saccharomyces cerevisiae strain BY4742 (*MATα his3*Δ1 *leu2*Δ0 *lys2*Δ0 *ura3*Δ0) and its isogenic derivatives Δ*tif1,* Δ*eft1,* Δ*gcn2* and Δ*aif1* (EUROSCARF, Frankfurt, Germany) were used. For acetic acid treatment, *S. cerevisiae* cells were grown until the middle exponential phase in liquid YPD medium containing glucose (2%, w/v), yeast extract (0.5%, w/v) and peptone (1%, w/v) at 26ºC (150 r.p.m.). Cells were initially harvested, ressuspended in fresh medium (pH 3.0) and incubated at 26ºC for 1h. Afterwards, cells were ressuspended (10^8 cells/mL) in fresh medium (pH 3.0) followed by the addition of 180, 195, 210 or 225 mM of acetic acid and incubated during 15, 30, 60, 120 and 200 min at 26ºC with stirring (150 r.p.m.), with or without the presence of 2.5 mM chloroquine, 1.1 μM rapamycin and 2% threalose (in this condition glucose in not added to the YPD medium). After the 200 min treatment, approximately 300 cells were spread on YPD agar plates and viability was determined by counting colony forming units after 2 days of incubation at 26ºC [199]. Cells were also harvested for further studies described below.

Protein synthesis analysis

Protein synthesis was analysed in cells exposed to 195 mM of acetic acid during 15 min. Cultures were labelled with 85 μM L-[^{35}S] methionine during the last 5 min of the acetic acid treatment, and 100 μg/mL cycloheximide (CHX) was just added before harvesting the cells. Total protein extracts were resolved by sodium dodecyl sulfate polyacrylamide gel electrophoresis (SDS-PAGE), as described below, and either the gels were stained with Coomassie blue or protein extracts were detected by enhanced chemiluminescence.

Polysome profile analysis

Yeast cells were grown to middle exponential phase and treated with acetic acid as described above. Five minutes before cells being harvested, CHX was added to a final concentration of 100 μg/mL, cells were collected, washed with cold phosphate-buffered saline (PBS) and disrupted using lysis buffer [20 mM Tris (pH 8.0), 140 mM KCl, 1.5 mM MgCl2, 0.5 mM DTT, 1 mM PMSF, 100 μg/mL CHX] and glass beads (Sigma). 40 units A_{280nm} were loaded onto 11 mL 15 - 50 % sucrose gradients containing 20 mM Tris-HCl at pH 8.0, 140 mM KCl, 5 mM MgCl2, 0.5 mM DTT, 100 μg/mL CHX and 500 μg/mL heparin. Gradients were centrifuged using a SW41 rotor (Beckman-Coulter) at 35000 rpm for 2 hours and 45 min at 4ºC. Polysomal profiles were visualized by monitoring RNA absorbance at 254nm using a Bio-Rad Biologic LP system adapted for this use. Monosomal and polysomal fractions of the gradient were collected into tubes containing 8M guanidine-HCl, ethanol was added to a final concentration of 50% and fractions were stored at – 80 ºC.

Polysomal RNA preparation

Polysomal mRNA was precipitated with ethanol 85%, extracted using phenol: chloroform and precipitated, first with 1.5 M lithium chloride (LiCl) for removing any residual heparin, and then with 100% ethanol plus 110 mM sodium acetate, pH 5.3.

RT-PCR analysis

Total RNA was isolated from monosomal and polysomal fractions. For quantitative reverse transcription polymerase chain reaction (RT-PCR), reverse transcription of RNA to cDNA was carried out using the First-Strand cDNA synthesis kit (GE Biosciences). The quantitative PCR was performed on a Stratagene Mx3005PTM real-time thermocycler using EVAGreen (Bio-Rad) and gene-specific primers as described in Table 4.

Relative expression levels were determined using the standard curve method. Controls lacking reverse transcriptase (RT) demonstrated no significant genomic DNA amplification.

Table 4 - List of primers for quantification of mRNA expression by RT-PCR and their efficiency (Eff).

Gene	Primer sequence	Eff (%)
AIF1	F: GATACGGCTGCCAGCTTTGAT R: TGAGCCAGTTGCAAGAACCAA	96.5
BIR1	F: CGTCCGATTTTTCACCATCA R: CATGCAAACTGCGTGTGAGA	99.3
CLN3	F: GCCCCTTTGGAAGCTTTCATT R: TGGCACCCAATTTGATCTCG	98.4
TIF4632	F: TCCGAGGAGACATTAGAGTCCG R: ACCGAACCTTCAAGAGTTGCC	99.1
ACT1	F: GATCATTGCTCCTCCAGAA R: ACTTGTGGTGAACGATAGAT	98.2
TDH2	F: CCGCTGAAGGTAAGTTGA R: CGAAGATGGAAGAGTTAGAGT	95.1
PDA1	F: TGACGAACAAGTTGAATTAGC R: TCTTAGGGTTGGAGTTTCTG	94.8
TUB2	F: TACCACATCCATTGCTGAG R: CACCTTCTTCCATACCTTCA	93.2

Assessment of intracellular reactive oxygen species

Free intracellular reactive oxygen species (ROS) were detected with dihydrorhodamine 123 (DHR123) (Molecular Probes). DHR123 was added from a 1 mg/mL stock solution in ethanol to $5x10^6$ cells/mL suspended in PBS, reaching a final concentration of 15 μg/mL. Cells were incubated for 90 min at 30°C in the dark, washed in PBS and analyzed by flow cytometry. Flow cytometric assays were performed on a BD LSR II™ (Becton Dickinson, NJ, USA) using BD FACSDiva Software 6.0 (Becton Dickinson, NJ, USA). Twenty thousand cells per sample were analyzed using the FlowJo software (Tree Star, Ashland, OR, USA). Data express the percentage of DHR123-positive cells compared to the total number of counted cells.

Immunoblot analysis

For detection of protein levels in total cellular extracts, untreated or acetic acid-treated cells (195 Mm) were collected and disrupted using glass beads in lysis buffer [1% v/v Triton X-100, 120 mM NaCl, 50 mM Tris-HCl pH 7.4, 2 mM EDTA, 10% v/v Glycerol, 1 mM PMSF and Complete Mini protease inhibitor

cocktail (Roche, Mannheim, Germany)]. From total protein extracts, 40 μg (100 μg for the protein synthesis analysis assay) were resolved on a 12% SDS-PAGE gel and transferred to a nitrocellulose membrane (Amersham) over 90 min at 100 V. Membranes were then probed with polyclonal rabbit Ser51 phosphorylated eIF2α (Sui2p) antibody (1:2000, Upstate), polyclonal rabbit anti-eIF2α (1:2000, Cell Signaling Technology), polyclonal rat anti-eIF4G (Tif4631/Tif4632p) (1:1000, kindly provided by Michael Altmann), polyclonal rabbit anti-eEF2 (Eft1/2p) (1:15 000), polyclonal rabbit anti-eEF1A (Tef1/2p) (1:15 000, both antibodies were kindly supplied by Prof. T.G. Kinzy), polyclonal rabbit anti-eIF4A (Tif1/2p) (1:15 000, kindly supplied by Prof. M. Montero-Lomelí) and polyclonal goat anti-actin (1:5000, kindly provided by Prof. Campbell Gourlay). Horseradish peroxidase (HRP)-conjugated anti-rabbit, anti-rat and anti-goat IgG secondary antibody were used, at a dilution of 1:5000 and detected by enhanced chemiluminescence.

Cell cycle analysis

Cell-cycle analysis was performed in wild-type and Δ*gcn2* untreated and 195 mM acetic acid-treated cells after 200 min of treatment. Cells were harvested, washed and fixed with ethanol (70% v/v) at 4ºC. Following, cells were sonicated, treated with RNase for 1 h at 50ºC in sodium citrate buffer (50 mM sodium citrate, pH 7.5), and subsequently incubated with proteinase K (0.02 mg per 10^7 cells). Cellular DNA was then stained overnight at 4ºC with SYBR Green 10000X (Molecular Probes), diluted tenfold in Tris-EDTA (pH 8.0). Samples were then diluted 1:4 in sodium citrate buffer, sonicated and analyzed by flow cytometry as described in [215]. Determination of cells in each phase of the cell cycle was performed offline using MODFIT LT 3.2 software (Verity Software House, Topsham, ME).

Vacuolar membrane staining

FM 4-64 (*N*-(3-Triethylammoniumpropyl)-4-(6-(4-(Diethylamino)phenyl)hexatrienyl) Pyridinium Dibromide, Molecular Probes Inc., Eugene, OR) staining was performed as described [250]. Prior to staining, wild-type and Δ*gcn2* cells expressing GFP-Atg8 (pRS416-GFP-Atg8 plasmid was kindly

provided by F. Reggiori) were cultured overnight in YPD medium, harvested during mid-logarithmic phase, pre-incubated for 1h in YPD (pH 3.0) and treated for 200 min in YPD (pH 3.0) with 195 mM of acetic acid. For FM 4-64 staining, cells were harvested and ressuspended in fresh YPD medium. FM 4-64 was added to 25 μM from a stock solution of 16 mM in DMSO. The cells were then incubated with shaking for 10-15 min at 30ºC. After this preliminary labelling step, the cells were harvested at 700 g for 3 min at room temperature, ressuspended in fresh YPD medium and incubated with shaking for 60 min. Afterwards, the cells were harvested, ressuspended in fresh YPD medium, placed on standard slides, and visualized by epifluorescence microscopy with an Olympus BX61 microscope equipped with a high-resolution DP70 digital camera and with an Olympus UPlanSApo 100X/oil objective, with a numerical aperture of 1.40.

Preparation of protein extracts for 2-D gel electrophoresis (2-DE)

For preparation of total cellular extracts, untreated and acetic acid-treated wild-type and Δ*gcn2* cells (195 and 270 mM) were collected and disrupted using glass beads in lysis buffer [1% v/v Triton X-100, 120 mM NaCl, 50 mM Tris-HCl pH 7.4, 2 mM EDTA, 10% v/v Glycerol, 1 mM PMSF and Complete Mini protease inhibitor cocktail (Roche, Mannheim, Germany)]. Protein concentrations were determined with a commercially available kit (RotiNanoquant, C. Roth, Karlsruhe, Germany) and protein aliquots (100 μg, 600 μg) stored at -20ºC. To verify the reproducibility, three independent samples from total cellular extract were obtained for each of the three conditions (control and 195 and 270 mM acetic acid-treated cells) and each sample separated within four 2-DE gels.

2-DE

For 2-DE the protein pellet was ressuspended in urea buffer (8 M urea, 2 M thiourea, 1% [w/v] CHAPS, 20 mM DTT, 0.8% [v/v] carrier ampholytes and Complete Mini protease inhibitor cocktail). The protein separation was done as previously described [164]. Briefly, the protein solution was adjusted with urea buffer to a final volume of 350 μL and in-gel rehydration was performed over night. Isoelectric focusing (IEF) was carried out in IPG strips (pH 3–10, non linear, 18

cm; GE Healthcare, Uppsala, Sweden) with the Multiphor II system (GE Healthcare) under paraffin oil for 55 kVh. SDS-PAGE was done overnight in polyacrylamide gels (12.5% T, 2.6% C) with the Ettan DALT II system (GE Healthcare) at 1-2 W per gel and at 12ºC. The gels were silver stained and analyzed with the 2-DE image analysis software Melanie 3.0 (GeneBio, Geneva, Switzerland). The apparent isoelectric points (pI) and molecular masses (Mr) of the proteins were calculated with Melanie 3.0 (GeneBio) using identified proteins with known parameters as a reference. An expression change was considered significant if the intensity of the corresponding single spot differed reproducibly more than two-fold and was reproducible for all three experiments.

Identification of altered proteins by mass spectrometry

To identify low abundant proteins, the spots were excised from 2-D gels separated with 600 μg of protein, in-gel digested, and identified from the peptide fingerprints as described elsewhere [251]. Proteins were identified with the ProFound database, version 2005.02.14 (http://prowl.rockefeller.edu/prowl-cgi/profound.exe) using the following parameters: 20 p.p.m.; 1 missed cut; MH+; +C2H2O2@C (Complete), +O@M (Partial). The identification of a protein was accepted if the peptides (mass tolerance 20 p.p.m.) covered at least 30% of the complete sequence. Sequence coverage below 20% was only accepted if at least three main peaks of the mass spectrum matched with the sequence and the number of weak-intensity peaks was clearly reduced. If the protein spot was detected at a lower molecular mass than expected, which indicates processing or fragmentation, the spot-specific peptides in the mass spectrum were also analyzed to confirm which parts of the corresponding protein sequence matched with these peptides. If the mass spectrum of the spot lacked peptides observed for the complete protein it was indicated as a protein fragment. Therefore, both the spot position observed by 2-DE and the specific peptides in the corresponding mass spectrum were analyzed to indicate a putative protein fragment.

Statistical analysis

Arithmetic means of ROS pruduction and cell survival rates are presented with standard deviation with a 95% confidence value. Statistical analysis was carried out using independent samples *t*-test analysis. A p-value <0.05 was assumed to denote a significant difference.

2.4 RESULTS

2.4.1 Global translation impairment triggered by acetic acid

Our previous work on the proteomic profile of acetic acid apoptosing cells has shown that translation is severely affected, indicating a failure of the protein synthesis machinery in these conditions [215]. To further elucidate the regulation of protein synthesis, the translation alterations occurring during acetic acid treatment were assessed. Although acetic acid-induced apoptosis is a paradigmatic scenario to study yeast cell death [41, 191, 199, 215, 252], a scale-up condition of acetic acid treatment for the induction of apoptosis in approximately 50% of the wild-type exponential *S. cerevisiae* cells was optimized. This scale-up allowed to collect high amounts of total cellular extracts and to isolate enough RNA to perform polysome profile studies and to evaluate the role of translation in this process. Results showed that 195 mM of acetic acid induces about 50% of apoptotic cell death upon 200 min treatment and this was the concentration selected for the studies herein described (Figure 8A). In a first approach to evaluate the rate of translation process during acetic acid treatment, the incorporation of L-^{35}[S] methionine in the yeast cells was analyzed. After 15 min of acetic acid treatment, and even though the same amount of protein was loaded, as shown by Coomassie blue staining (Figure 8B), no protein synthesis was detected by chemiluminescence in total protein extracts of treated cells. This result suggests that L-^{35}[S] methionine was unable to enter the cells (Figure 8B) and supports our previously published data suggesting the blockage of amino acid uptake in acetic acid treated cells, leading to a severe cellular amino acid starvation [215]. Thus, translation alterations during acetic acid-induced apoptosis were assessed. For such purpose, the polysomal profile of wild-type cells treated with two different acetic acid

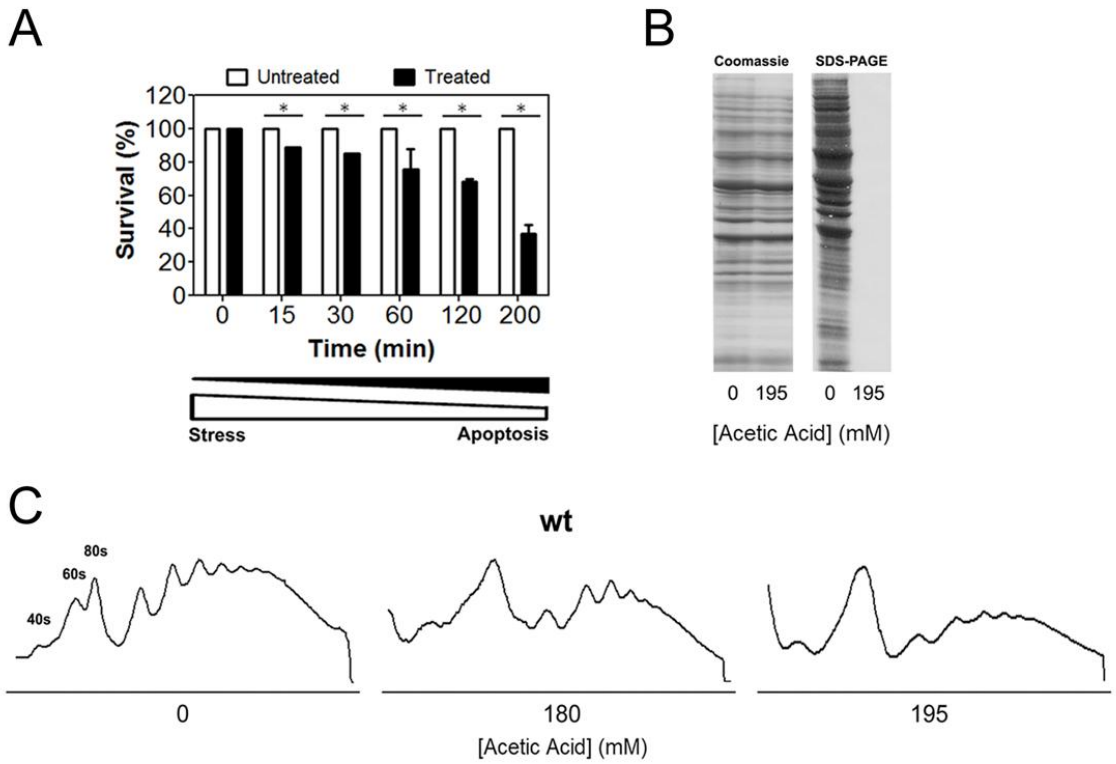

Figure 8 - Global translation impairment during acetic acid-induced apoptosis. (A) Kinetic analysis of the survival rate of wild-type *S. cerevisiae* cells untreated and treated with 195 mM of acetic acid. (B) Protein synthesis analysis of wild-type *S. cerevisiae* cells in the absence or presence of 195 mM of acetic acid during 15 min. Cultures were pulse-labelled with [^{35}S] methionine during the final 5 min of the acetic acid treatment, and protein levels were analysed by SDS-PAGE. (C) Polysome profile of yeast cells treated with the indicated concentrations of acetic acid for 15 min. The peaks containing the small ribosomal subunit (40S), the large ribosomal subunit (60S), and both subunits (80S) are indicated.

concentrations (180 and 195 mM) was obtained. This analysis revealed an impairment of global translation in acetic acid treated cells, as reflected by the decrease of the polysomal fraction (corresponding to the polypeptide chains that are being actively assembled) and the increase of the monosomal fraction (corresponding to the small, large and both ribosomal subunits, 40s, 60s and 80s, respectively) (Figure 8C). This effect was shown to be dependent on the acetic acid concentration tested as cells treated with the highest concentration (195 mM) displayed a pronounced decrease of the polysomal fraction (Figure 8C). The impact of acetic acid on translation efficiency was further addressed by a kinetic analysis

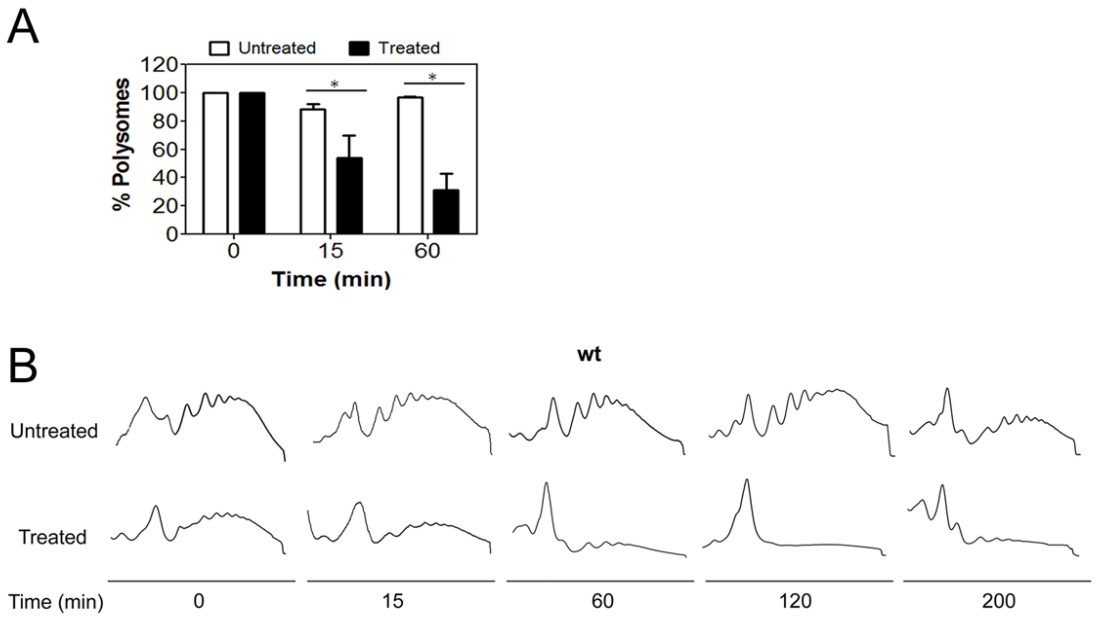

Figure 9 – Translation impairment increases throughout the 200 min of acetic acid treatment. (A) Statistic analysis of the percentage of total mRNA present in the polysomal fractions in the absence or presence of 195 mM of acetic acid during 0, 15 and 60 min. (B) Kinetic analysis of the polysomal profile of wild-type cells treated with or without 195 mM of acetic acid reveals a gradual and non transient translation impairment.

of polysome profile in association with the kinetic analysis of cell viability throughout the 200 min of treatment with 195 mM acetic acid (Figure 8A, 9). The acetic acid concentration selected (195mM) induced a progressive decline of survival along the treatment time course, compatible with a first response to the imposed stress and a later activation of the apoptotic cell death. At 200 min of acetic acid treatment, a heterogeneous population where 40% of cells are still coping with stress but 60% have lost the proliferative capacity is observed (Figure 8A). The analysis of polysome profile showed a decrease in the percentage of polysomes in acetic acid treated cells after 15 min that was aggravated at 60 min (Figure 9A). The impairment of translation was also confirmed by the observation of a decrease in the polysomal fraction and an increase in the monosomal fraction of acetic acid treated cells that was maintained and exacerbated throughout the 200 min of acetic acid treatment (Figure 9B).

These results showing that acetic acid affects both the initiation and the elongation steps of translation leading to a drastic reduction of the translation process efficiency raised three important questions: the cells are not able to recover from the acid stress imposed, translation control is an important event during the process of acetic acid-induced apoptosis, or both.

2.4.2 Translation impairment induced by acetic acid is mediated by alterations in translation machinery

The observation of global translation impairment upon acetic acid-induced apoptosis prompted us to investigate the cascade of events leading to this alteration. Thus, we decided to perform a kinetic analysis of the protein levels of the translation initiation factors 4A (eIF4A/Tif1/2p) and 4G (eIF4G/Tif4631/2p)

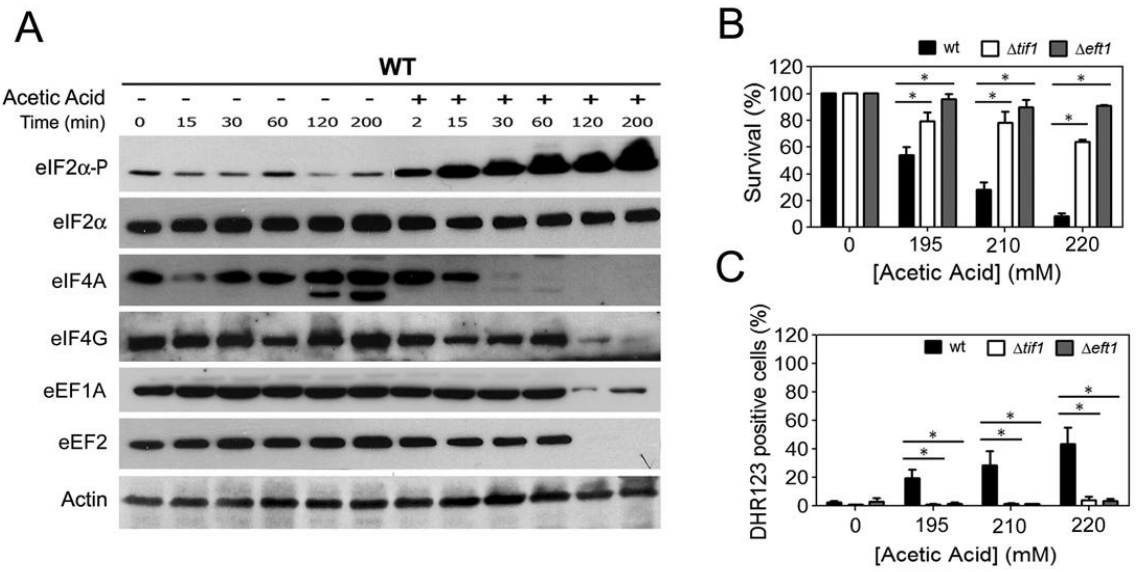

Figure 10 - Global translation impairment during acetic acid-induced apoptosis is mediated by translation factors downregulation and post-translational modifications. (A) Immunoblot kinetic analysis of eIF2α (Sui2p) phosphorylation and translation initiation factors eIF2α (Sui2p), eIF4A (Tif1/2p) and eIF4G (Tif4631/2p) and translation elongation factors eEF1A (Tef1/2p) and eEF2 (Eft1/2p) levels in wild-type *S. cerevisiae* cells upon treatment with or without (untreated) 195 mM of acetic acid. Actin was used as loading control. (B) Survival assay of wild-type, *TIF1* and *EFT1* deleted strains upon acetic acid treatment. (C) Percentage of wild-type, Δ*tif1* and Δ*eft1* cells exhibiting high levels of intracellular ROS detected by FACS measurements of the dihydrorhodamine 123 fluorescence. *p≤0.05 versus control, *t*-test, $n=3$.

and of the elongation factors 1A (eEF1A/Tef1/2p) and 2 (eEF2/Eft1/2p), previously shown in our proteomic analysis to be decreased upon acetic acid challenge [215]. The phosphorylation status of the translation initiation factor 2α (eIF2α/Sui2p) was also determined due to its well-known role on translation regulation [236, 253-256]. Immunoblot analysis revealed that just after 15 min of acetic acid treatment, the previously shown impairment of translation was correlated to alterations in translation initiation (Figure 10A). An increase in the levels of phosphorylated eIF2α and a decrease in the levels of eIF4A (Figure 10A), suggested an impairment in the assembly of the translation initiation complex, crucial for the cap-dependent translation initiation [237], leading to a translation initiation impairment at early points of acetic acid treatment. The decrease in the levels of the elongation factors eEF1A and eEF2 and of the initiation factor eIF4G (a subunit of the mRNA cap-binding protein complex [237] was observed only at 120 min (Figure 10A). The concurred decrease of these translation factors at the same time point suggests that the drastic impairment of translation elongation only occurs after about 120 min (Figure 10A). These findings, together with the knowledge that eIF4G plays a role in yeast and mammalian internal ribosome entry site (IRES)-mediated translation [59, 82, 90, 227, 257-259] and that eEF1A increases the efficiency of the yeast IRES-mediated translation [232], raises the hypothesis that a minor selective translation mediated by cap-independent mechanisms might occur during acetic acid treatment.

In order to assess the relevance of the above described translation factors for the modulation of the apoptotic process induced by acetic acid a survival assay with the respective deleted strains was performed. Deletion of *SUI2* (eIF2α) and *TIF4631/2* (eIF4G) genes lead to unviable strains and a reliable *TEF1/2* (eEF1A) deleted strain is not available thus, we evaluated the resistance of *TIF1* (eIF4A) and *EFT1* (eEF2) deleted strains to acetic acid treatment (Figure 10B). Despite the fact that during acetic acid-induced apoptosis a decrease in the levels of both Tif1p and Eft1p is observed, the disruption of the respective genes leads to an increased resistance to acetic acid (Figure 10B). The deleted cells also displayed low reactive oxygen species (ROS) levels when compared to wild-type treated cells (Figure 10C). These results suggest that the alterations occurring in the translation process

during acetic acid treatment are also contributing to the apoptotic process. Thus, the control of the translation process upon acetic acid treatment appears to be crucial to determine the fate of the cells treated with acetic acid.

2.4.3 Gcn2p kinase modulates translation initiation impairment induced by acetic acid

Gcn2p is the only kinase described to be responsible for the phosphorylation of eIF2α in yeast [253, 256, 260, 261]. Due to the observed increased levels

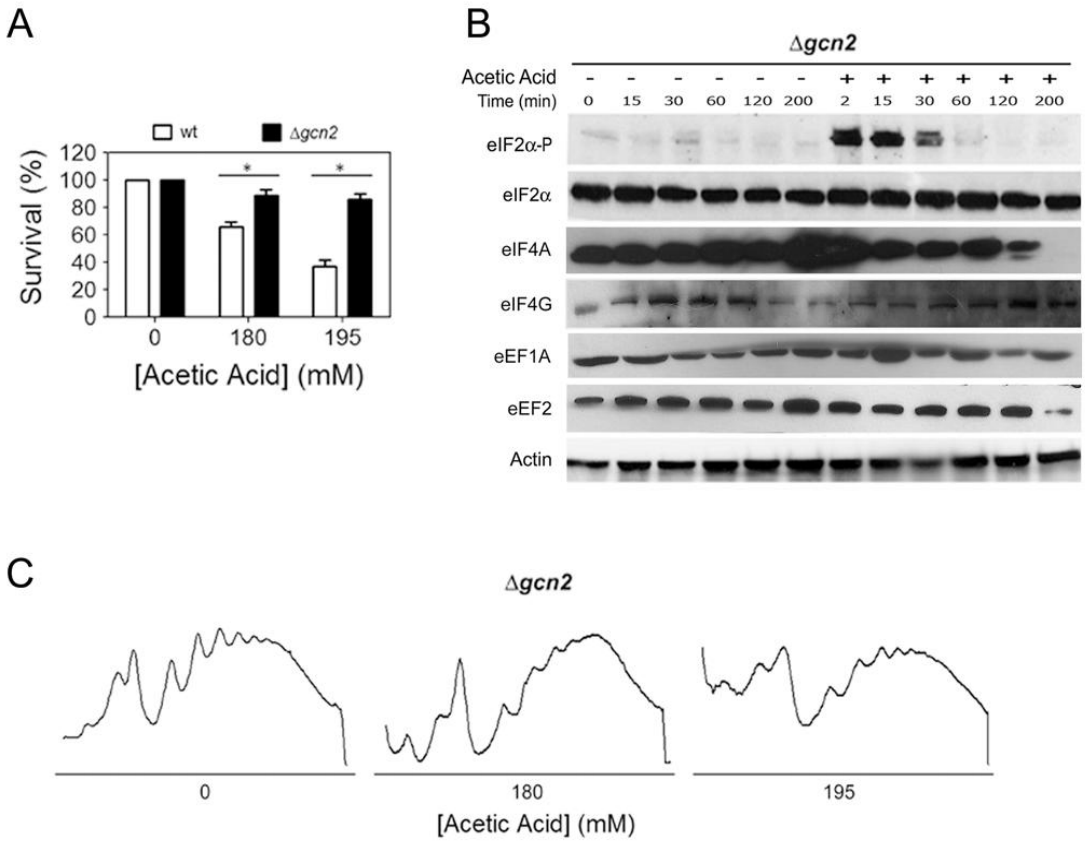

Figure 11 - Gcn2 kinase modulation of translation alterations during acetic acid-induced apoptosis. (A) Comparison of the survival rate of wild-type and Δ*gcn2 S. cerevisiae* cells upon treatment with the indicated concentrations of acetic acid; *p≤0.05 versus wild-type, *t*-test, *n*= 3. (B) Immunoblot kinetic analysis of eIF2α (Sui2p) phosphorylation levels, translation initiation factors eIF2α (Sui2p), eIF4A (Tif1p) and eIF4G (Tif4631/2p) and translation elongation factors eEF1A (Tef1/2p) and eEF2 (Eft1/2p) levels in Δ*gcn2 S. cerevisiae* cells upon treatment with or without (untreated) 195 mM of acetic acid. Actin was used as loading control. (C) Polysomal profile of *GCN2*-disrupted yeast cells treated with the indicated concentrations of acetic acid for 15 min.

of eIF2α phosphorylated (Figure 10A), we decided to study the role of Gcn2p in the regulation of translation during acetic acid treatment. Thus, the resistance of the respective deleted strain to acetic acid treatment was studied. A more resistant phenotype of the *GCN2* deleted cells was observed, when compared to the wild-type cells (Figure 11A), associated with a drastic decrease in the phosphorylation levels of eIF2α, observed by immunoblot analysis (Figure 11B). Nevertheless, phosphorylation of eIF2α was detected in the first time points of acetic acid treatment (Figure 11B) suggesting the presence of other undisclosed kinases capable of its phosphorylation. Abrogation of *GCN2* also elicited an efficient translation as reflected by the levels of translation factors eIF4A, eIF4G, eEF1A and eEF2 (Figure 11B) and by the polysomal profile analysis (Figure 11C). These findings showed that acetic acid treatment leads to an impairment of translation initiation mainly regulated by the phosphorylation of eIF2α under the control of Gcn2p kinase. Disruption of *GCN2* turns cells resistant to acetic acid, a phenotype associated with the recovery of translation competence. These data implicate the control of translation by Gcn2p in the progression of cell death induced by acetic acid.

Besides Gcn2p involvement in the regulation of protein synthesis, this kinase has also been described as a cell cycle regulator of cells exposed to ultraviolet (UV) irradiation through a Gcn2-dependent checkpoint which delays cells entry into S phase [247]. In fact, when we analyzed the cell cycle profile of wild-type cells after acetic acid treatment, an arrest in the G0/G1 phase was observed [215]. However, in the *GCN2* deleted strain this arrest in G0/G1 was alleviated (Figure 12A), suggesting that upon acetic acid treatment, the control of cell cycle related alterations, is under the regulation of Gcn2p kinase. Gcn2p is under control and repression by the target of rapamycin (TOR) pathway, responsible for the sensing of amino acid [237, 262-264], which was found to be inhibited during acetic acid-induced apoptotic cell death [191, 215, 218]. It is well known that amino acid starvation-induced inhibition of TOR leads to induction of autophagy [265-272] through Gcn2p-dependent activation of Atg8p and Atg4p autophagic components [249]. Since our previous data showed that acetic acid-induced a severe intracellular amino acid depletion [215], a role for autophagy in this cell death

process was addressed despite the recent report that autophagy is not involved in acetic acid-induced apoptosis [201]. Atg8p (homologous to the mammalian LC3 autophagic marker protein) is a phosphatidylethanolamine-conjugated ubiquitin-like protein required for the formation of autophagosomes and a key molecular component of the autophagic process [273]. The analysis of the mRNA expression levels of *ATG8* revealed a slight increase in *ATG8* mRNA levels in wild-type cells after 200 min of incubation, both untreated and acetic acid treated cells, when compared to *GCN2* disrupted cells (Figure 12B). To further assess the role of autophagy, wild-type and Δ*gcn2* cells were transformed with a plasmid expressing the Atg8p tagged with GFP and the cellular vacuoles were marked with a fluorescent dye which binds to the vacuolar membrane (FM 4-64). After acetic acid treatment we observed a discrete increase in the levels of GFP-Atg8p and its localization in the internal membrane of the vacuole in the wild-type-treated cells. In *GCN2* deleted cells GFP-Atg8p was not found in the vacuoles (Figure 12C) and a diffuse green fluorescence, corresponding to the GFP-Atg8p, was observed all over the cell (Figure 12C). These results indicate that, as previously reported [249], in *GCN2* deleted cells autophagy is abrogated. However, some activation is observed in wild-type treated cells. To further address the role of autophagy, a pharmacological modulation of the autophagic process during acetic acid-induced apoptosis was performed and the survival rate of wild-type and *GCN2* deleted cells was assessed. For the inhibition of the autophagic process we used chloroquine which raises the lysosomal/vacuole pH leading to the inhibition of lysosome/vacuole-autophagosome fusion and lysosomal/vacuole protein degradation [274-278]. The induction of autophagy was achieved through a TOR-dependent pathway, using rapamycin [265, 267-270, 272, 279], and by a TOR-independent pathway using trehalose [280-282]. In wild-type acetic acid-treated cells, the inhibition of the lysosome/vacuole-autophagosome fusion by chloroquine led to a more pronounced cell death (Figure 12D). This result corroborates the previous observed colocalization of GFP-Atg8p with the vacuoles (Figure 12C), and suggests that upon acetic acid stimulus, activation of autophagy might be an important stress response mechanism. The incubation of the cells with acetic acid and rapamycin produced no synergistic effect (Figure 12D), most probably due to

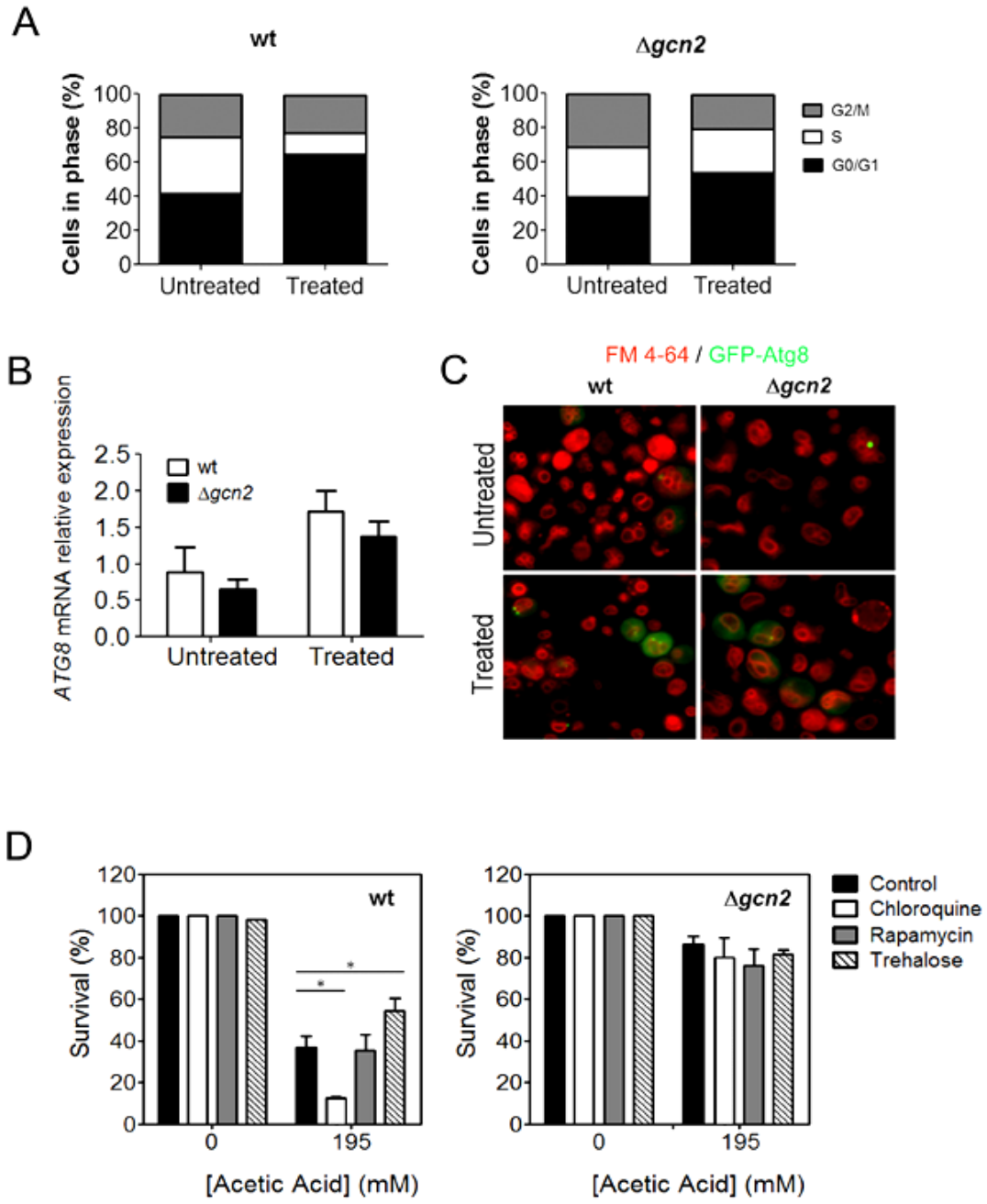

Figure 12 - The role of cell cycle and autophagy regulation by Gcn2p during acetic acid-induced apoptosis. (A) Analysis of the percentage of cells in each phase of the cell cycle in wild type and *GCN2* deleted cells untreated or upon 200 min of acetic acid treatment (195 mM). (B) Normalized relative expression levels of *ATG8* mRNA (*ACT1*, *TDH2*, *PDA1* and *TUB1* as internal references) in wild-type and Δ*gcn2* cells. (C) Image of wild-type and Δ*gcn2* cells harboring a plasmid expressing the GFP-Atg8 protein and colocalization with the vacuoles stained with a fluorescent dye (FM 4-64). (D) Comparison of the survival rate of wild-type and Δ*gcn2 S. cerevisiae* cells upon treatment with 195 mM acetic acid in the presence of 2.5 mM chloroquine, 1.1 μM rapamycin or 2% trehalose.*p≤0.05 versus wild-type, *t*-test, $n = 3$.

the repression of TOR pathway promoted by acetic acid [215]. Autophagy induction by a pathway independent of TOR, and therefore independent of Gcn2p kinase, increased survival (Figure 12D) suggesting that during acetic acid-induced apoptosis the activation of a TOR pathway-independent autophagy might play a protective role. Results showed that the manipulation of the autophagic process, even at a basal level, induces different responses in wild-type cells to acetic acid treatment (Figure 12D). The fact that the inhibition of autophagy increased cell death and induction of autophagy protected from cell death mediated by acetic acid was a good evidence of the involvement of autophagy in the cell's response to acetic acid treatment as a pro-survival mechanism. Nevertheless, *GCN2* disrupted cells, showing low levels of *ATG8* mRNA (Figure 12B), displayed an increased resistance to acetic acid treatment in the presence of both inhibitor and inducers of the autophagic process (Figure 12D). These data showed that Gcn2p role in acetic acid-induced apoptosis is related with the control/repression of cell cycle and cap-dependent translation initiation, and not with the regulation of the autophagic process, being an important player in the cellular response to acetic acid. In fact, the pro-survival effect of autophagy during acetic acid treatment appears to be under the control of other pathways besides TOR pathway.

2.4.4 Proteomic analysis of *AIF1* deleted cells revealed alterations in translation factors upon acetic acid treatment

In mammalian cells a regulation of translation initiation by the apoptosis-

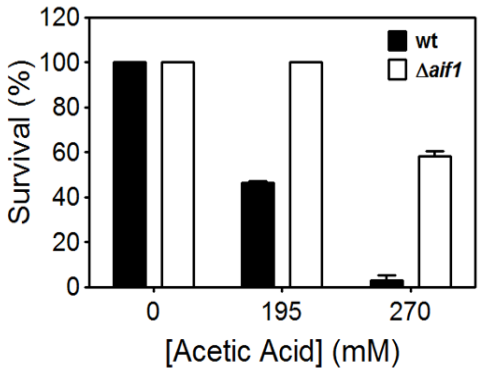

Figure 13 – Survival assay for the optimization of the ideal acetic acid concentration for the induction of about 50% of cell death in wild-type and *AIF1* deleted strain.

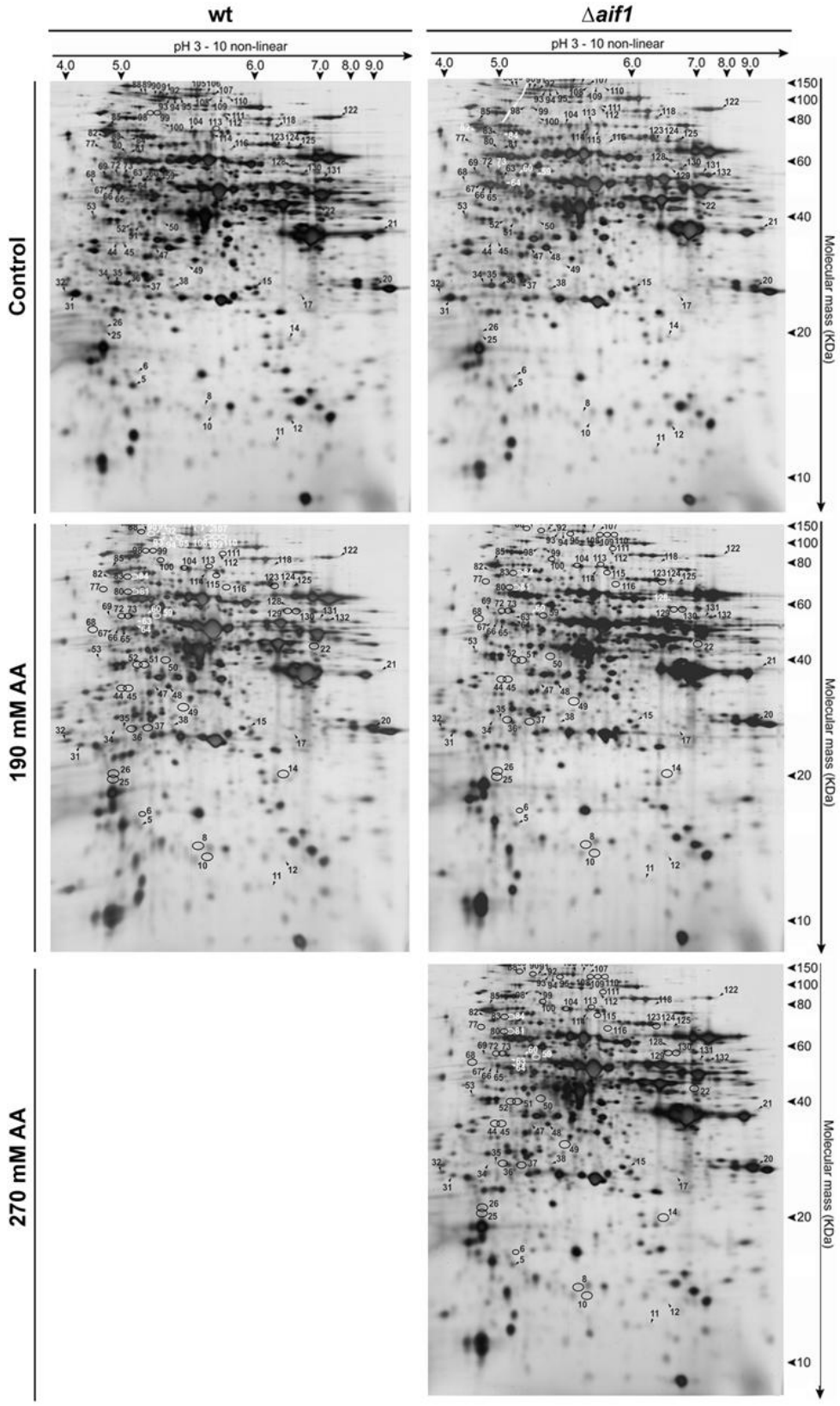

Figure 14 – Proteomic profile analysis of the acetic acid-induced Aif1p-independent apoptotic process. Representative silver-stained 2-D gel of total protein extracts wild-type and Δ*aif1* cells untreated and treated with 195 or 270 mM of acetic acid. Spots altered upon acetic acid treatment are represented by numbers (1 – 132).

inducing factor (AIF), homologous to yeast Aif1p, through interaction with subunit p44 of translation initiation factor 3 (eIF3g) has been described [76]. Since in yeast, Aif1p is a crucial player during acetic acid-induced apoptosis [41, 283-285], we decided to evaluate the proteomic profile of Δ*aif1* cells using two different concentrations of acetic acid capable of inducing about 50% of apoptotic cell death in wild-type (195 mM) and in the more resistant *AIF1* deleted cells (270 mM) (Figure 13). By comparing the total cellular proteome of untreated and acetic acid- treated cells both in wild-type and *AIF1* deleted cells, several spots were

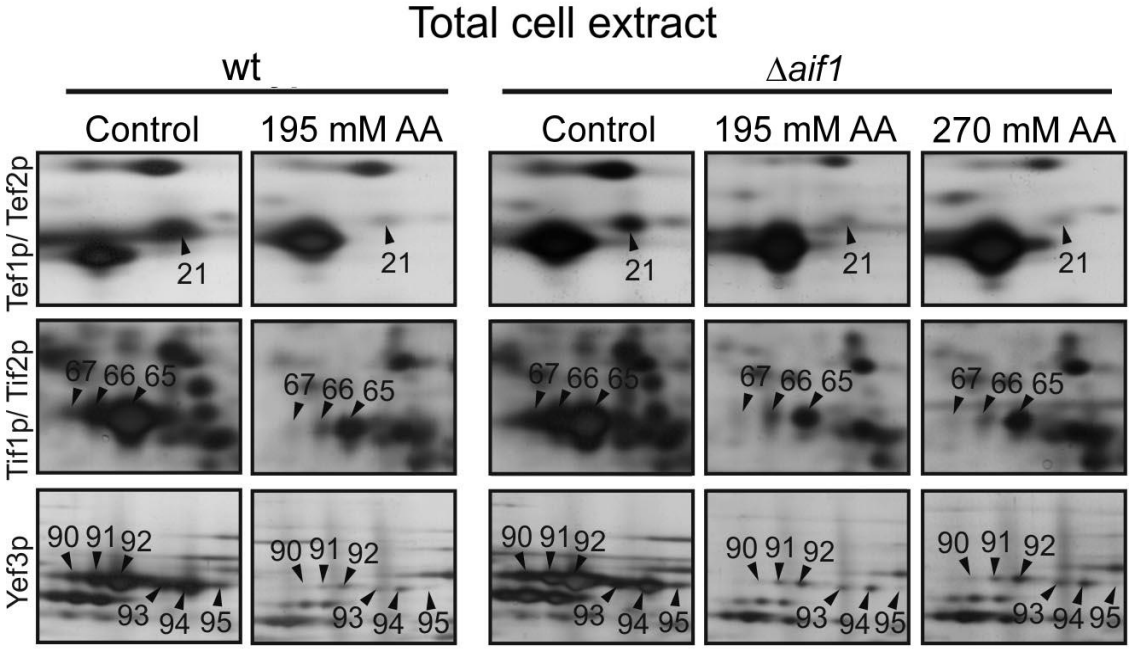

Figure 15 – Deletion of *AIF1* gene does not prevent alterations in translation machinery when cells are challenged with acetic acid. Enlarged 2-D gel parts represent altered proteins in total cellular extracts from wild-type and Δ*aif1* untreated and treated (195 mM and 270 mM acetic acid) yeast cells.

found affected (Figure 14). Among them 10 spots related with the translation process showed decreased intensity (Figure 15). Mass spectrometry analysis revealed that 1 spot corresponded to eEF1A (Tef1/2p), 3 spots to eIF4A (Tif1/2p) and 6 spots to eEF3A (Yef3p) (Figure 15), previously described as down-regulated in wild-type cells [215]. No differences in the levels of translation initiation and elongation factors were found comparing the proteomic profile of wild-type and

Δ*aif1* acetic acid treated cells. In fact, the treatment of *AIF1* deleted cells with 195mM or 270 mM of acetic acid, the later inducing 50% of cell death in Δ*aif1* cells (Figure 13), revealed a decrease in the levels of translation factors eIF4A, eEF1A and eEF3A in both conditions (Figure 15). Results showed that translation machinery alterations are maintained in the absence of *AIF1*, suggesting that these alterations are independent of *AIF1* and therefore Aif1p does not have a role in the regulation of translation during acetic acid treatment.

2.4.5 Evaluation of apoptotic regulators translation during acetic acid-induced apoptosis.

In mammalian cells, after an apoptotic stimulus, cap-dependent translation process is reduced [95, 243]. However, it has been reported that several apoptotic regulators, both inhibitors and inducers of apoptosis such as XIAP and Apaf-1, respectively [109, 132], are capable of being translated by an alternative mechanism, a selective cap-independent translation mechanism [95]. In yeast, cap-independent translation has also been described [227, 230], however, its occurrence in an apoptotic condition was never addressed. Based on the results described above and in the knowledge that the inhibition of translation elongation by cycloheximide prevents acetic acid-induced apoptosis [199], we hypothesized that although cap-dependent translation is impaired, an alternative translation might have a role in the apoptotic process. Therefore, we evaluated if in yeast, the translation of key apoptotic regulators, namely the pro-apoptotic protein Aif1p [41], crucial for the progression of acetic acid-induced apoptosis [41], and the anti-apoptotic protein Bir1p (homologous of mammalian IAP proteins [197], such as XIAP) where translated during acetic acid treatment. Monosomal and polysomal fractions of wild-type cells (Figure 16A) were analyzed by RT-PCR. The analysis of the percentage of *AIF1* mRNA present in each fraction of the polysomal profile revealed that despite of a small increase in the percentage of *AIF1* in the monosomal fraction of treated cells (Figure 16B), there was still a significant amount of *AIF1* mRNA in polysomal fractions upon 15 min (Figure 16B) and 30 min (data not shown) of incubation with acetic acid, when compared to polysomal fractions of untreated cells. The results indicated that *AIF1* mRNA translation is

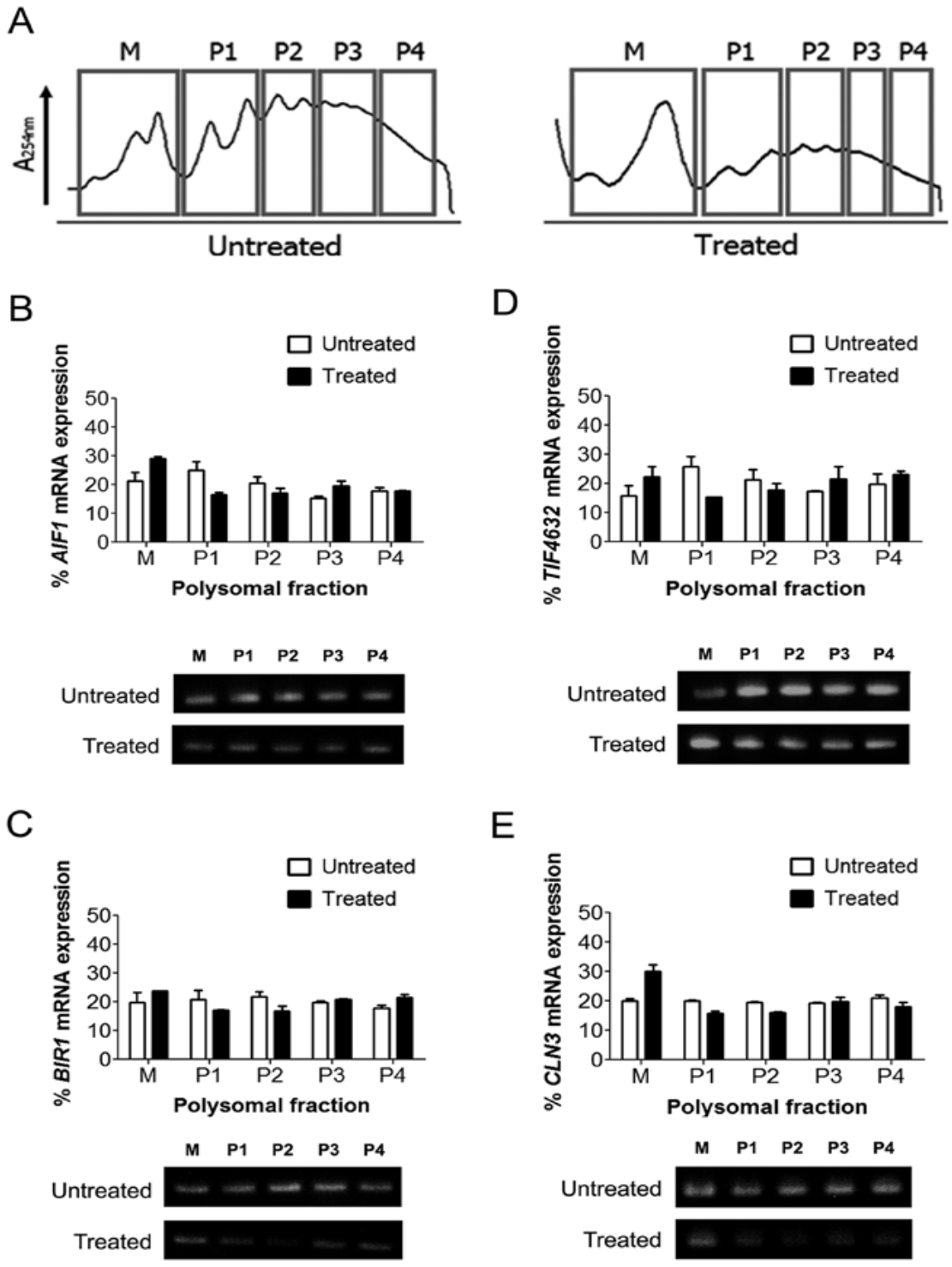

Figure 16 - RT-PCR analysis of apoptotic regulators mRNA levels by upon acetic acid treatment. (A) Illustration of the polysomal fractions from which mRNAs were extracted and analysed by RT-PCR (M, monosomal fraction; P1, P2, P3 and P4, polysomal fractions). Analysis of the percentage of (B) *AIF1*, (C) *BIR1*, (D) *TIF4632* and (E) *CLN3* mRNA absolute expression, by RT-PCR and DNA electrophoresis in agarose gel, in each of the polysomal profile fractions of untreated and acetic acid treated cells (195 mM) during 15 min.

occurring despite global translation impairment. As an opposite results almost no *BIR1* mRNA was observed in the polysomal fractions upon 15 (Figure 16C) and 30 min (data not shown) of acetic acid treatment. In fact, after acetic acid treatment, the percentage of *BIR1* mRNA (Figure 16C) was reduced in the polysomal fractions and increased in monosomal fraction, both at 15 (Figure 16C) and 30 min of incubation (data not shown), indicating that upon acetic acid treatment the translation of this apoptotic regulator was reduced. These results were confirmed by the analysis, as a negative control, of the percentage of *CLN3* mRNA in each fraction (Figure 16E). Cln3 is a G1 cyclin described as unable of being translated by a cap-independent mechanism [234], and as expected the percentage of *CLN3* mRNA in the polysomal fractions was also decreased in cells challenged with acetic acid (Figure 16E). eIF4G (*TIF4632*) was previously shown to be translated by an IRES-mediated cap-independent mechanism being also crucial for the efficient IRES-mediated translation of other mRNAs during nutrient starvation [227]. Therefore, the percentage of *TIF4632* (eIF4G) mRNA was also assessed in an attempt to uncover if during acetic acid treatment, a condition known to induce amino acid starvation [215], and translation impairment, eIF4G was also translated. Results showed that, similar to *AIF1* mRNA, *TIF4632* mRNA levels slightly increased in the monosomal fraction but were strongly present in the polysomal fractions (Figure 16D) proving its ability to be translated during acetic acid treatment and suggesting the activation of an IRES-mediated translation. These results suggest that in yeast, like in mammalian cells, a cap-independent translation mechanism may be mediating the translation of several mRNAs involved in the modulation of the apoptotic process.

2.5 DISCUSSION

Over the past few years, the involvement of the translation process in the regulation of apoptosis has emerged as a crucial mechanism both in mammalian and yeast cells [4, 59, 60, 95, 215, 218, 220, 243, 286, 287]. Since translation is the final stage in the course of genetic information flow, regulation at this level leads to a direct response to changes in physiological conditions. During *S. cerevisiae* acetic acid-induced apoptosis, a general amino acid starvation occurs and a translation reduction might allow cells to conserve resources and to initiate a reconfiguration of gene expression. In fact, our results clearly demonstrate a gradual impairment of the translation process during acetic acid treatment. In an early stage, a decrease in the levels of translation initiation factor eIF4A and an increase in the phosphorylation levels of eIF2α mediated by Gcn2p occur, leading to the inhibition of cap-dependent translation initiation. However, only at later time points a decrease in the levels of translation initiation factor eIF4G and elongation factors eEF1A and eEF2 is observed. In fact, in yeast, the eIF4G, a translation factor known to harbor an IRES in the 5'UTR [227], and eEF1A have been described as crucial factors for an efficient IRES-mediated translation [227, 232]. These data strongly suggest that although cap-dependent translation is impaired during acetic acid treatment, an alternative translation mechanism may be activated, such as the IRES-mediated process. A similar regulation of translation process has been described during oxidative stress induced by H_2O_2 [220], but an alternative translation mechanism has never been suggested. The alternative cap-independent translation might be important in controlling the translation of proteins with a central role in the stress response to stress of cells struggling to survive and the apoptotic process of cells committed to death. Curiously, Gcn2 kinase appears to be a key mediator of the acetic acid-induced apoptosis, since deletion of *GCN2* gene reverts not only the previously described decrease in eIF4A, eEF1A and eEF2 levels, but also the eIF2α phosphorylation, leading to unblocked translation and to the abrogation of acetic acid-induced cell death. Besides Gcn2p role in the control of translation initiation, this kinase is also involved in the regulation of other processes, such as cell cycle [247] and autophagy [249]. Investigation of the

contribution of these processes for Gcn2 key participation in the acetic acid-induced apoptosis revealed that cell cycle arrest in G0/G1 phase upon acetic acid treatment [215] is mediated by Gcn2p.

Although we could not detect a marked autophagic response after 200 min of acetic acid treatment in the wild-type strain, a slight increase in the levels of *ATG8* mRNA detected by RT-PCR and Atg8p visualized by epifluorescence microscopy analysis of Atg8p-GFP localization with the cell vacuoles suggest that autophagy might be activated during acetic acid treatment. Furthermore, the pharmacological modulation of the autophagic process revealed that in acetic acid challenged cells autophagy acts as a pro-survival mechanism in response to the acid stress despite the diminished levels of *ATG8* after 200 min of acetic acid treatment. These data made us hypothesize that autophagy might be activated during yeast cells early response to stress decreasing during the course of acetic acid treatment due to the activation of the apoptotic cascade. However, the activation of autophagy during acetic acid treatment appears to be mediated by other autophagy regulators besides Gcn2p. Thus, these studies allowed the elucidation of Gcn2p function during acetic acid-induced apoptosis, showing the critical contribution of this kinase to the inhibition of cap-dependent translation initiation and cell cycle arrest, increasing the knowledge on the acetic acid apoptotic cascade.

In mammalian cells, the control of translation initiation by the apoptosis inducing factor 1 (AIF1), homologous of yeast Aif1p, has been described [76]. Aif1p is a crucial player of yeast acetic acid-induced apoptosis [41]. Thus, a role for this pro-apoptotic protein in translation machinery alterations during acetic acid treatment was address through proteomic analysis of *AIF1* deleted cells treated with acetic acid. The proteomic analysis of wild-type and *AIF1* deleted cells showed the same alterations in the levels of translation factors upon acetic acid treatment. A decrease in the levels of translation factors eIF4A, eEF1A and eEF3 in *AIF1* deleted cells was observed both in acetic acid-induced stress (195 mM) and cell death conditions (270 mM) proving that, in yeast, Aif1p is not involved in the control of translation initiation during apoptosis. In fact, it appears that it is the translation process that regulates Aif1p function in apoptosis. Polysomal fractions RT-PCR analysis shows that *AIF1* as well as eIF4G (*TIF4632*) mRNAs are

efficiently translated upon acetic acid treatment despite the observed impairment of cap-dependent translation suggesting the activation of an alternative cap-independent mechanism mediating *AIF1* and eIF4G mRNA translation, during acetic acid treatment.

Altogether, our data demonstrate the importance of translation control during acetic acid treatment at a concentration that induces a stress response in 40% of the cells and commits to death the remaining 60% of the cells upon 200 minutes of treatment. The translation alterations observed in this heterogeneous population strongly suggest that translation control is important both for the cell survival response and the cell death process. Furthermore, this study highlighted some of the translation regulatory mechanisms controlling acetic acid induced apoptosis. The early impairment of cap-dependent translation initiation, mediated by Gcn2p, and the later decrease in the levels of eIF4G, eEF1A and eEF2 strongly suggest the activation of an alternative IRES-mediated cap-independent translation during acetic acid treatment. This cap-independent translation appears to mediate the translation of *AIF1* and eIF4G (*TIF4632)* mRNAs during acetic acid treatment. *AIF1* is a pro-apoptotic factor and its translation during acetic acid treatment is clearly related to the cell death process. However, IRES-mediated translation of eIF4G has been related to nutrient starvation-induced stress conditions [227], therefore its translation during acetic acid treatment might be related with the cellular response to stress.

These results showed an intricate network of regulatory pathways in the course of the apoptotic process induced by acetic acid, thus opening new perspectives for future investigations. In this apoptotic scenario, translation process appears to be an important link for the different pathways.

CHAPTER 3

Metacaspase-mediated alterations in translation machinery during apoptosis

Silva, A., Almeida, B., Sampaio-Marques, B., Reis, M.I.R., Silva, T.L., Logarinho, E., Rodrigues, F., Ohlmeier, S., Gourlay, C.W., do Vale, A. and Ludovico, P.

Part of the results described in this chapter were published as follow:

Silva, A., Almeida, B., Sampaio-Marques, B., Reis, M.I.R., Ohlmeier, S., Rodrigues, F., do Vale, A. and Ludovico, P. Glyceraldehyde-3-phosphate dehydrogenase (GAPDH) is a specific substrate of yeast metacaspase. Biochim Biophys Acta 2011, 1813 (12):2044-2249.

The results described in this chapter were presented in the following congresses:

National congresses:

- XVII Jornadas de Biologia de Leveduras Prof. Nicolau van Uden. Braga, Portugal. (2009). "Involvement of eEF1A in acetic acid-induced apoptosis in yeast". (Oral communication)
- XVIII Jornadas de Biologia de Leveduras Prof. Nicolau van Uden. Lisboa, Portugal. (2010) "Translation modulation during acetic acid-induced apoptosis in yeast". (Oral communication)

International congresses:

- 6th IMYA - International Meeting on Yeast Apoptosis. Leuven, Belgium. (2008). "NO-mediated apoptosis in yeast". (Poster presentation. Oral communication by Paula Ludovico).
- 7th IMYA - International Meeting on Yeast Apoptosis. Graz, Austria. (2009). "GAPDH and aconitase are targets of proteolytic degradation during oxidative stress-induced apoptosis in *Saccharomyces cerevisiae".* (Oral communication by Paula Ludovico).

3.1 ABSTRACT

In mammalian cells, translation factors are substrates of caspases during the apoptotic process. In yeast, metacaspase (Yca1p), a caspase-like protease, is required for the execution of apoptosis upon a wide range of stimuli. However, the specific degradome of this protease has not been unraveled so far. In a search for conserved translation factors targeted as substrates by metacaspase, a degradome and deletion analysis were performed using two paradigmatic scenarios of yeast apoptosis, H_2O_2 and acetic acid. Degradome analysis revealed several spots corresponding to proteins fragments. However, only a small group of individualized spots were identified corresponding to the glycolytic enzyme, the glyceraldehyde-3-phosphate dehydrogenase (GAPDH) [219]. Nitric oxide (NO) signaling was shown to be required for metacaspase specific GAPDH cleavage [219].

In a search for possible mitochondrial substrates, mitochondrial proteomic analysis showed the cleavage and translocation of translation elongation factors 1A (eEF1A) and 2 (eEF2) to mitochondria. Furthermore, a proteinase K assay revealed that eEF1A N-terminal fragments are imported to mitochondrial matrix, performing a putative pro-apoptotic role, upon acetic acid-induced apoptosis [215]. Interaction between eEF1A and Dnm1p [288], a dynamin-related GTPase required for mitochondrial fission [289], has been previously reported [288]. Nevertheless, Dnm1 appears to play no role in the eEF1A mitochondrial localization. eEF1A is a yeast well described bona fide actin binding and bundling protein, and its translocation to mitochondria was correlated with a decrease of its binding to actin leading to alterations in the actin cytoskeleton [290]. Therefore, the role of mammalian eEF1A1 isoform and DRP1, a Dnm1p homolog, in the actin cytoskeleton organization and cell survival was also addressed in HeLa cells during staurosporine-induced apoptosis. These results unravel eEF1A as an important player in cell death process both in yeast and mammalian cells, in a way unrelated to its function in translation. Nevertheless, eEF1A cleavage upon acetic acid treatment proved not to be mediated by metacaspase. Despite that, the analysis of other translation factors levels during acetic acid-induced apoptosis in the absence of metacaspase, suggests a role for this protease in the activation of Gcn2 kinase-mediated phosphorylation of subunit α of translation initiation factor 2 (eIF2α) and

in the downregulation of the translation initiation factor 4A (eIF4A), observed during the apoptotic process. However, to assess if this regulation is mediated by direct interaction of Gcn2p and eIF4A with metacaspase or by interaction with its upstream regulators further studies are required. In conclusion, in this work, we demonstrate eEF1A and eEF2 cleavage and translocation to mitochondria, where they appear to play a role unrelated to translation. Moreover, we highlight GAPDH as a substrate of metacaspase, speculating its possible role in the regulation of translation, and reveal translation initiation factors eIF2α and eIF4A as downstream targets of the metacaspase cascade, in apoptotic conditions, consolidating the existence of conserved molecular pathways targeted during apoptosis from yeast to mammals.

3.2 INTRODUCTION

The apoptotic cascade is orchestrated by different "executioner" caspases which target specific substrates within the cell producing the biochemical and morphological alterations associated to apoptosis. Fragmentation of translation factors by caspases, namely translation initiation factor 2 subunit α (eIF2α), 3 (eIF3), 4B (eIF4B) and 4G (eIF4G) [59, 72, 83], as a mechanism of translational control during the apoptotic process is widely described in mammalian cells [59, 72, 83] [4, 66, 67, 95, 286, 287]. One of the strategies reported is the acquisition of distinct functions, unrelated with the translation process, of translation factors upon the induction of apoptosis. The translation elongation factor 1A (eEF1A) is committed to translation through the delivery of aminoacyl-tRNAs (AA-tRNAs) to ribosomes, but has also been implicated in several other processes, such as, nuclear export of proteins [291], cancer, aging and apoptosis [287, 288, 292-294]. Moreover, eEF1A plays an imperative role, conserved from yeast to mammalian cells, in the control of the actin cytoskeleton organization, by a direct C-terminal interaction with F-actin. A deregulation of eEF1A levels within the cell leads to severe actin cytoskeleton alterations [289, 295-300]. In *Trypanosoma brucei*, this translation factor was even associated to the import of tRNAs to the mitochondria [301, 302]. Nevertheless, the role of eEF1A in tRNA import to mitochondria in yeast and mammalian cells [303-305] was never addressed. In yeast, interaction between eEF1A, codified by *TEF1* and *TEF2* isoforms [306-308], and Dnm1p, a dynamin-related GTPase with a role in mitochondrial fission, has been established [288]. Despite the function of eEF1A isoforms in the translation process, these isoforms appear to acquire divergent functions in other processes, both in yeast and in mammalian cells [287, 309-313].

Glyceraldehyde-3-phosphate dehydrogenase (GAPDH) is a well-known glycolytic enzyme playing multiple functions and interacting with multiple partners independent of its role in energy metabolism [314-316]. In fact, a role of GAPDH in the repression of specific mammalian cells mRNAs translation, such as angiotensin II type 1 receptor (AT1R) [317] and p53 [134, 318], which was proven to harbor an internal ribosome entry site (IRES) sequence in the mRNA

[119-121], through binding to the 3' untranslated region (3'UTR) of the mRNAs [134, 317] has been suggested. The repression of virus translation by GAPDH, through interaction with IRES present in the virus mRNAs [135-138], has also been reported. The specific cleavage of GAPDH by caspase-1 during apoptosis [139], a process known to require IRES-mediated translation [4, 95, 243], suggests a tight regulation of GAPDH function in the repression of mRNAs translation during apoptosis.

Although in yeast, a member of a family of caspase-like proteases [40], metacaspase (Yca1p), has been reported as an apoptotic executor upon a wide range of either physiological or external stimuli [40, 214], the substrates targeted by this protease are still unknown. Yeast single metacaspase is a type I metacaspase with a prodomain, similar to that of inflammatory and pro-apoptotic initiator caspases [319], that is processed during its activation [40]. Conflicting data exists regarding the ability of yeast metacaspase to cleave typical mammalian caspase substrates [40]. However, yeast metacaspase was shown to cleave P1-Arg and P1-Lys substrates similarly to plant metacaspases [48, 320]. Metacaspases activity was also found to be regulated through S-nitrosation and thus dependent on the endogenous levels of nitric oxide (NO) [210]. Accordingly, during yeast H_2O_2-induced apoptotic conditions [189], a cell death process dependent on metacaspase activity [40] and NO generation [211, 212], metacaspase activity and cell death are abolished in the presence of L-NAME, an inhibitor of NO synthesis [211, 212]. In this context, the identification of yeast metacaspase specific substrates mediating translation alterations and of putative new functions performed by translation factors, unrelated to the translation process, during acetic acid treatment is crucial. This information is of utmost importance for the integrated understanding of translation process contribution to the acetic acid-induced apoptosis and to clarify if a conservation of the apoptotic targeted pathways occurs from yeast to mammalian.

3.3 MATERIALS AND METHODS

Strains, media and treatments

Saccharomyces cerevisiae strain BY4742 (*MAT*α *his3*Δ1 *leu2*Δ0 *lys2*Δ0 *ura3*Δ0) and its isogenic derivatives Δ*yca1* and Δ*dnm1* (EUROSCARF, Frankfurt, Germany) were used. Strain M198 (*MAT*a *leu2*-3,112 *his4*-713, *met2*-1, *ura3*-52, *trp1*-Δ1 Δ*tef1*::*LEU2*) (kindly provided by Prof. Sandbaken), corresponding to Δ*tef1* cells previously described in [35], was also used. For construction of the metacaspase-overexpressing strain, *YCA1* was amplified by PCR (primers 5'-ccgggaattcgatgtatccaggtagtggacgt-3' and 5'-ccg gggatccctacataataaattgcagatttacgtc-3'), using genomic DNA, isolated from BY4742 strain and cloned into the EcoRI and BamHI sites of pGREG546 (EUROSCARF, Frankfurt, Germany), in order to express a N-terminal GST fusion under the control of a galactose-inducible promoter, generating pGREG546*YCA1*. Strain Δ*yca1* was transformed with pGREG546*YCA1*, generating strain *YCA1*^{overexp}. Construction of p416 plasmids eEF1A and eEF1A fragments N6C458, N1C146 and N1C177

Table 5- List of primers for construction of p281 monocistronic plasmids.

Gene	Primer sequence
p416 *eEF1A N1C458*	F: GGCCGGATCCATGGGTAAAGAGAAGTCTGAC R: GGCCGTCGACTTACTTAGCAGCCTTTTGAGCAGC
p416 *eEF1A N6C458*	F: GGCCGGATCCTCTGACATTAACGTTGTCGTT R: GGCCGTCGACTTACTTAGCAGCCTTTTGAGCAGC
p416 *eEF1A N1C146*	F: GGCCGGATCCATGGGTAAAGAGAAGTCTGAC R: GGCCGTCGACTCTAACACCCAAGGTGAAAGC
p416 *eEF1A N1C177*	F: GGCCGGATCCATGGGTAAAGAGAAGTCTGAC R: GGCCGTCGACCTTGATAAAGTTGGAGGTTTC
pYX222 *eEF1A N1C458*	F: GCGGGATCCATGGGTAAAGAGAAGTCTCAC R: GCGGGATCCTTTCTTAGCAGCCTTTTGAGCAGCC
pYX222 *eEF1A N6C177*	F: GCGGGATCCTCTCACATTAACGTTGTCGTT R: GCGGGATCCCTTGATAAAGTTGGAGGTTTC

were amplified by PCR using the primers described in Table 5, digested and cloned into the BamHI and SalI sites of p416 which displays a galactose-inducible promoter. Wild-type cells were transformed with the plasmids. For construction of

pYX222 plasmids harboring the eEF1A gene or eEF1A N6C177 between a mitochondrial localization sequence (MLS) and a DsRed reporter gene eEF1A gene and N6C177 fragment were amplified by PCR using the primers described in Table 1, digested with BamHI, and cloned into pYX222 vector between the N-terminal MLS and the C-terminal DsRed (kindly provided by Dr. Stephan Jacobs). Δ*tef1* cells were transformed with the plasmids.

Wild-type cells expressing the p416 plasmids with the eEF1A fragments were grown until exponential growth phase (OD640nm=0.5) on synthetic complete (SC) medium containing glucose (2%, w/v), yeast nitrogen base (0.17%, w/v, Difco), 300 mg/L of L-leucine, 50 mg/L of L-histidine and 50 mg/L of L-lysine. Cells were washed, ressuspended in SC medium containing galactose (2%, w/v) and incubated at 26ºC with stirring (150 r.p.m.) to induce the eEF1A total protein and fragments expression. After 16 hours, 10^8 cells/mL were harvested and ressuspended in fresh SC medium with galactose (2%, w/v) (pH 3.0), treated with 210 or 225 mM of acetic acid and incubated for 200 min at 26ºC with stirring (150 r.p.m.).

For H_2O_2 treatment, yeast cells were grown until the early stationary growth phase in liquid YPD medium containing glucose (2%, w/v), yeast extract (0.5%, w/v) and peptone (1%, w/v), harvested and ressuspended (10^7 cells/mL) in fresh YPD medium followed by the addition of 0.5, 1, 1.5 and 2 mM H_2O_2 and incubation for 200 min at 26ºC with stirring (150 r.p.m.) in the dark, as previously described [211]. For acetic acid treatment, *S. cerevisiae* cells were grown until the middle exponential phase in liquid YPD medium, harvested, ressuspended in fresh medium (pH 3.0) and incubated at 26ºC for 1h. Then cells were ressuspended (10^8 cells/mL) in fresh medium (pH 3.0) followed by the addition of 180, 195, 210 or 225 mM of acetic acid and incubation during 0, 15, 30, 60, 120 and 200 min at 26ºC with stirring (150 r.p.m.). After H_2O_2 or acetic acid treatment, approximately 300 cells were spread on YPD agar plates and viability was determined by counting colony forming units after 2 days of incubation at 26ºC [199]. Cells were also harvested for protein extraction and immunoblot analysis as described below.

HeLa cells were cultured in DMEM medium (Invitrogen, Carlsbad, CA) supplemented with 10% fetal bovine serum (FBS), 1% glutamax, and 1% antibiotics mixture (Invitrogen) and grown at 37°C in a 5% CO_2 humidified chamber. eEF1A1 (NM_001402.5), eEF1A2 (NM_001958.2), and DNM1 (NM_005690.3) RNAi depletions were achieved using a pool of small interfering siRNAs (siRNAs) generated from nonconserved sequences (nucleotides 1383-2519, 327-1334, and 348-1757 from the start codon, respectively) with the BLOCK-iT Dicer RNAi kit accordingly to the manufacturer's instructions (Invitrogen). Cells (10^5 cells/well) were plated in DMEM medium with 5% FBS and without antibiotics, on six-well plates (Nunc, Naperville, IL) containing poly-L-lysine–coated glass coverslips. Two hours later, cells were transfected with siRNA-oligofectamine complexes prepared in Opti-MEM I medium (Invitrogen) according to the manufacturer's instructions and analyzed 24 or 48 h after transfection. Mock transfections were used as control. Afterwards, cells were treated with staurosporine for 18h (0.1 μM, Sigma, St. Louis, MO), and cell viability using the CellTiter-Blue® Cell Viability Assay (Promega, Madison, USA), immunofluorescence of eEF1A and actin, and apoptosis detection by TUNEL assay were assessed, as described below.

Metacaspase overexpression and activation

Strain *YCA1*^{overexp} was grown until exponential growth phase (OD640nm=0.5) on synthetic complete (SC) medium containing glucose (2%, w/v), yeast nitrogen base (0.17%, w/v, Difco), 300 mg/L of L-leucine, 50 mg/L of L-histidine and 50 mg/L of L-lysine. Cells were washed, ressuspended in SC medium containing galactose (2%, w/v) and incubated at 26ºC with stirring (150 r.p.m.) to induce metacaspase overexpression. After 16 hours, 10^7 cells/mL were harvested and ressuspended in fresh SC medium with galactose (2%, w/v), and metacaspase was activated by the addition of 2 mM of H_2O_2 [40] and incubation for 200 min at 26ºC with stirring (150 r.p.m.).

Preparation of protein extracts

For total protein extracts, untreated, H_2O_2- and acetic acid-treated cells were collected and disrupted using glass beads in lysis buffer [1% v/v Triton X-100, 120 mM NaCl, 50 mM Tris-HCl pH 7.4, 2 mM EDTA, 10% v/v Glycerol, 1 mM PMSF and Complete Mini protease inhibitor cocktail (Roche, Mannheim, Germany)] as described in [211, 215]. For mitochondrial protein extracts, yeast cells were harvested and cell wall was digested with zymolyase buffer [2 M Sorbitol-D, Phosphate buffer 1 M (pH 7.5), Zymolyase 20.000 U, 125 mM β-mercaptoethanol, 0.5 M EDTA] at 30ºC for 1 hour. Protoplasts were disrupted with lysis buffer [Sorbitol-D 0.5 M, Tris 20 mM, EDTA 1 mM, and 2.85 mM phenylmethanesulphonyl fluoride (PMSF)] using a Potter homogenizator. Mitochondria extracts were separated, washed by high speed centrifugation at 12000 r.p.m. for 15 min at 4ºC (Beckman Coulter, JA-25.50 Rotor) and ressuspended in sorbitol buffer [0.5 Sorbitol-D, 5 mM EDTA, 50 mM Tris]. HeLa cells were collected by centrifugation and disrupted using RIPA buffer [50 mM Tris-HCl pH 7.6, 150 mM NaCl, 1% NP-40, 1% Na-deoxycholate, 0.1% SDS]. Protein concentration was determined by Bradford method [321] and protein aliquots of yeast total extracts (1 mg, 40 μg), yeast mitochondrial extracts (600 μg, 100 μg and 40 μg) and HeLa cells total extracts (40 μg) were stored at -20ºC.

Digestome analysis

Digestome analysis was performed according to the methodology previously described in [322], with adaptations. Four hundred micrograms of total protein extracts obtained from untreated wild-type yeast cells or HeLa cells were resolved by sodium dodecyl sulfate polyacrylamide gel electrophoresis (SDS-PAGE) 12% (first dimension). After migration, the lanes were excised and treated as described in [322], soaked in digestion buffer [50 mM Tris-HCl, 150 mM NaCl and 10 mM DTT] with 5 mg of either active metacaspase-enriched extracts (obtained from H_2O_2-treated YCA1overexp cells) or inactive metacaspase-enriched extracts (obtained from H_2O_2-treated Δ*yca1* or untreated $YCA1^{overexp}$ cells), incubated overnight at 37ºC, washed with ultrapure water and incubated in loading buffer [50 mM Tris-HCl (pH 6.8), 2% SDS, 0.1% bromophenol blue, 10% glycerol,

2.5% β-mercaptoethanol] for 10 min at 95ºC. After cooling, lanes were subjected to a second dimension SDS-PAGE. Proteins in the gels were immunoblotted as described below or stained using Colloidal Blue Staining Kit (Invitrogen) for mass spectrometry identification.

2-DE

Three independent samples from mitochondrial extract were used to verify the reproducibility for each of the two conditions (control and 195 mM acetic acid-treated cells) and each sample separated within four 2-D gels. For 2-DE the protein pellet was ressuspended in urea buffer (8 M urea, 2 M thiourea, 1% [w/v] CHAPS, 20 mM DTT, 0.8% [v/v] carrier ampholytes and Complete Mini protease inhibitor cocktail). The protein separation was done as previously described [164]. Briefly, the protein solution was adjusted with urea buffer to a final volume of 350 μL and in-gel rehydration was performed over night. Isoelectric focusing (IEF) was carried out in IPG strips (pH 3–10, non linear, 18 cm; GE Healthcare, Uppsala, Sweden) with the Multiphor II system (GE Healthcare) under paraffin oil for 55 kVh. SDS-PAGE was done overnight in polyacrylamide gels (12.5% T, 2.6% C) with the Ettan DALT II system (GE Healthcare) at 1-2 W per gel and at 12ºC. The gels were silver stained and analyzed with the 2-DE image analysis software Melanie 3.0 (GeneBio, Geneva, Switzerland). The apparent isoelectric points (pI) and molecular masses (Mr) of the proteins were calculated with Melanie 3.0 (GeneBio) using identified proteins with known parameters as a reference. An expression change was considered significant if the intensity of the corresponding single spot differed reproducibly more than two-fold and was reproducible for all three experiments.

Identification of altered proteins by mass spectrometry

To identify low abundant proteins, the spots were excised from 2-D gels separated with 600 µg of protein, in-gel digested, and identified from the peptide fingerprints as described elsewhere [251]. Proteins were identified with the ProFound database, version 2005.02.14 (http://prowl.rockefeller.edu/prowl-cgi/profound.exe) using the following parameters: 20 ppm; 1 missed cut; MH+;

+C2H2O2@C (Complete), +O@M (Partial). The identification of a protein was accepted if the peptides (mass tolerance 20 ppm) covered at least 30% of the complete sequence. Sequence coverage below 20% was only accepted if at least three main peaks of the mass spectrum matched with the sequence and the number of weak-intensity peaks was clearly reduced. If the protein spot was detected at a lower molecular mass than expected, which indicates processing or fragmentation, the spot-specific peptides in the mass spectrum were also analyzed to confirm which parts of the corresponding protein sequence matched with these peptides. If the mass spectrum of the spot lacked peptides observed for the complete protein it was indicated as a protein fragment. Therefore, both the spot position observed by 2-DE and the specific peptides in the corresponding mass spectrum were analyzed to indicate a putative protein fragment.

Proteinase k assay

Three aliquots of 100 μg mitochondrial protein extracts of each sample were centrifuged at 13000 r.p.m. for 10 min at 4ºC. Supernatants were discarded and two aliquots pellets (1 and 2) of each sample were ressuspended in 500 μL of HS buffer [0.6 M Sorbitol-D, 20 mM HEPES-KOH, pH 7.4] and the other (3) was ressuspended in H buffer [20 mM HEPES-KOH, pH 7.4]. 5 μL of dH_2O was added to pellet 1 and 5 μL of 10 mg/mL proteinase K to pellets 2 and 3. Mitochondrial extracts were incubated for 25 min on ice and 5 μL of 0.2 M PMSF was added to each sample followed by 5 min incubation on ice. Samples were centrifuged at 13000 r.p.m. for 10 min at 4ºC, pellets were ressuspended in HS buffer, precipitated overnight in acetone, and centrifuged at 13000 r.p.m. for 30 min at 4ºC. Supernatants were discarded, pellets were dried, ressuspended in 30 μL of Laemmli buffer (BioRad) and immunoblotted as described in below.

Immunoprecipitation

Anti-actin antibody was added to 1 mg of total protein extracts from untreated and acetic acid treated yeast cells in a total volume of 500 μL and incubated for 4h at 4ºC on a shaker. Afterwards, 20 μL of washed protein A/G agarose beads (Pierce) were added to each sample and incubated overnight at 4ºC

on a shaker. Agarose beads were collected by centrifugation (3000 rpm, 1min, 4ºC), washed twice with 1 mL ice-cold lysis buffer [1% v/v Triton X-100, 120 mM NaCl, 50 mM Tris-HCl pH 7.4, 2 mM EDTA, 10% v/v Glycerol, 1 mM PMSF and Complete Mini protease inhibitor cocktail (Roche, Mannheim, Germany)] and with 1mL ice-cold wash buffer [0.1% v/v Triton X-100, 120 mM NaCl, 50 mM Tris-HCl pH 7.4, 2 mM EDTA and 10% v/v Glycerol]. Afterwards, agarose beads were eluted in 30 μL of Laemmli buffer (BioRad), boiled for 5 min to dissociate the immunocomplexes from the beads and collected by centrifugation (10000 r.p.m., 1min). The supernatant fraction was immunoblotted as described in below.

Immunoblotting

Yeast total and mitochondrial protein extracts, mitochondrial extracts from proteinase K assay, supernatants from actin immunoprecipitation and HeLa cells total extracts were resolved on a 12% SDS-PAGE gel and transferred to a nitrocellulose membrane (Amersham) over 90 min at 100 V. Total protein extracts of the digestome analysis were probed with a monoclonal mouse anti-GAPDH (MAB474, Chemicon) as described [211] and a polyclonal rabbit anti-S-nitroso-cysteine (CSNO) (N5411, Sigma-Aldrich) at a dilution of 1:500. Total protein extracts of H_2O_2- and acetic acid-treated cells were probed with polyclonal rabbit Ser51 phosphorylated eIF2α (Sui2) antibody (1:2000, Upstate), polyclonal rabbit anti-eIF2α (1:2000, Cell Signaling Technology), polyclonal rat anti-eIF4G (Tif4631/Tif4632p) (1:1000, kindly provided by Michael Altmann), polyclonal rabbit anti-eEF2 (Eft1/2p) (1:15000), polyclonal rabbit anti-eEF1A (Tef1/2p) (1:15000, both antibodies were kindly supplied by Prof. T.G. Kinzy), polyclonal rabbit anti-eIF4A (Tif1/2p) (1:15000, kindly supplied by Prof. M. Montero-Lomelí), polyclonal goat anti-actin (1:5000, kindly provided by Campbell Gourlay), monoclonal rabbit anti-aconitase antibody (1:1500, kindly provided by Lill, R.) and monoclonal mouse anti-porin antibody (1:5000, MAB474, Chemicon). Membranes of HeLa cells protein extracts were probed with polyclonal mouse anti-eEF1A (1:750, Santa Cruz Biotechnology, Inc) and polyclonal goat anti-actin (1:300, Santa Cruz Biotechnology, Inc). Horseradish peroxidase (HRP)-conjugated anti-rabbit, anti-rat, anti-goat and anti-mouse IgG secondary antibodies (Cell Signaling

Technology) were used, at a dilution of 1:5000 and detected using an enhanced chemiluminesce's kit (Pierce).

Assessment of intracellular reactive oxygen species (ROS)

Free intracellular ROS were detected with dihydrorhodamine 123 (DHR123) (Molecular Probes, Eugene, OR, USA). DHR123 was added from a 1 mg/mL stock solution in ethanol, to $5x10^6$ cells/mL suspended in PBS, reaching a final concentration of 15 μg/mL. Cells were incubated for 90 min at 30°C in the dark, washed in PBS and analyzed by flow cytometry. Flow cytometric assays were performed on a BD LSR II™ (Becton Dickinson, NJ, USA) using BD FACSDiva Software 6.0 (Becton Dickinson, NJ, USA). Twenty thousand cells per sample were analyzed using the FlowJo software (Tree Star, Ashland, OR, USA). Data express the percentage of DHR123-positive cells compared to the total number of counted cells.

TUNEL assay

DNA strand breaks were assessed by Terminal Deoxynucleotidyl Transferase-mediated dUTP Nick End Labeling (TUNEL) assay with the In situ Cell Death Detection Kit, POD (Roche Applied Science, Indianapolis, IN). Yeast cells were initially fixed with 3.7% formaldehyde followed by digestion of the cell walls with lyticase. After preparation of cytospins, the slides were rinsed with PBS, incubated in permeabilization solution (0.1%, v/v, Triton X-100 and 0.1%,w/v, sodium citrate) for 3 min on ice, rinsed twice with PBS, and incubated with 10 µL of TUNEL reaction mixture (terminal deoxynucleotidyl transferase and FITC-dUTP) for 60 min at 37ºC . Finally, the slides were rinsed three times with PBS and incubated with 40 μl of PI/RNase solution (PI 50 μg/mL and RNase 12.5 μg/mL) in Tris buffer (10 mM, pH 7.0) for 20 min at 37ºC in the dark. Coverslip was mounted with a drop of anti-fading agent Vectashield (Molecular Probes, Eugene, OR). HeLa cells DNA strand breaks were assessed according to the manufacturer's instructions. Cells were visualized with an Olympus PlanApo 60X/oil objective, with a numerical aperture of 1.42. For quantification of TUNEL-positive cells, at least

400 cells from three independent assays were counted. Data express the percentage of TUNEL-positive cells compared to the total number of counted cells.

Immunofluorescence

HeLa cells were fixed for 20 min in freshly prepared 2% paraformaldehyde (Sigma) in phosphate-buffered saline (PBS), permeabilized with 0.5% Triton X-100 in PBS for 5 min, washed in PBS and blocked with 10% FBS. Primary antibodies were used as follows: mouse anti-eEF1A (1:250, Cruz Biotechnology, Inc) and goat anti-actin (1:300, Cruz Biotechnology, Inc). Alexa Fluor 488, and 568 conjugated secondary antibodies were used at 1:1500 (Molecular Probes, Eugene, OR) and DNA was stained using 4,6-di-amino-2-phenyl-indole dihydrochloride (DAPI) (Sigma). Most images were acquired as Z-stacks with 0.2–0.3-μm spacing using a 60x 1.42 NA objective on an Olympus FluoView FV1000 confocal microscope.

Statistical analysis

Arithmetic means of free intracellular ROS, TUNEL staining and cell survival rates are presented with standard deviation with a 95% confidence value. Statistical analysis was carried out using independent samples *t*-test analysis. A p-value <0.05 was assumed to denote a significant difference.

3.4 RESULTS

To disclose if translation factors are specific substrates of yeast metacaspase in yeast apoptotic scenarios associated with an impairment of translation process, namely H_2O_2- [220] and acetic acid-induced apoptosis (chapter 2), a digestome analysis [322] and a mutagenesesis analysis of *YCA1* deleted cells were performed.

3.4.1 Metacaspase-mediated alterations during H_2O_2-induced apoptosis

3.4.1.1 Digestome analysis revealed GAPDH as a cleavage target of metacaspase

With the aim of disclosing translation factors as substrates of yeast metacaspase during H_2O_2-induced apoptosis a digestome analysis was performed. Although digestome analysis, an in vitro assay, does not mimic cellular physiological conditions, it represents a starting point in the search for putative specific substrates of proteases. In a first dimension SDS-PAGE, total protein extracts from untreated wild-type yeast cells were resolved. Upon protein separation, gel lanes were excised and incubated with active metacaspase-enriched extracts obtained from *YCA1*^{overexp} cells undergoing apoptosis induced by H_2O_2 treatment (a condition known to induce metacaspase activation [40]). After incubation, gel lanes were mounted on a second SDS-PAGE gel and proteins resolved a second time by molecular weight. Digestome analysis of total protein extracts revealed numerous spots below the diagonal, corresponding to putative protein fragments of metacaspase substrates cleaved during the incubation of the gel lane with active metacaspase-enriched extracts (Figure 17A) [219]. However, by mass spectrometry, we were only able to identify three of these spots Figure 17A, spot 1, 2 and 3), corresponding to peptide fragments of the isoforms 2 or 3 (Tdh2p/Tdh3p), but not of the isoform 1 (Tdh1p), of the glycolytic enzyme glyceraldehyde-3-phosphate dehydrogenase (GAPDH) (Figure 17B). Immunoblot of the digestome analysis using active metacaspase-enriched extracts with an anti-

GAPDH antibody showed three GAPDH fragments immediately below the diagonal (Figure 17A, spot 4, 5 and 6) [219]. Some of these labelled fragments are most likely the complementary GAPDH protein fragments of the peptides identified by

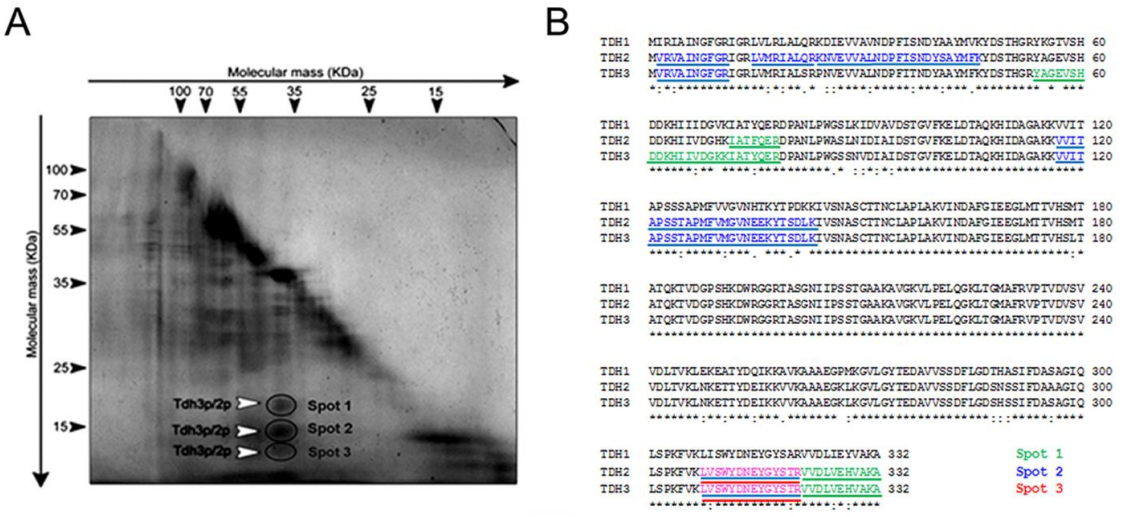

Figure 17 - GAPDH is cleaved by metacaspase-enriched protein extracts. (A) Total protein extracts from untreated wild-type cells subjected to SDS-PAGE, incubated with active metacaspase-enriched extracts (from H_2O_2-treated YCA1^{overexp} cells) and then subjected to a second SDS-PAGE. The gel was stained with Coomassie blue. Spots below diagonal (1, 2 and 3), corresponding to cleaved proteins, were excised and analysed by MALDI-TOF mass spectrometry. (B) Sequence of GAPDH isoforms Tdh1p (NP_012483.1), Tdh2p (NP_012542) and Tdh3p (NP_011708) retrieved from NCBI. Mass spectrometry analyses of the three spots identified peptides matches to Tdh2p and Tdh3p but not Tdh1p. Sequences of the detected peptides are indicated with different colours. Pink coloured peptide was identified both in spot 2 and 3.

mass spectrometry (Figure 17A, 10B, spots 3, 2 and 1, respectively). The question whether GAPDH cleavage observed was due to metacaspase or to other activated proteases was addressed. For such purpose, gel lanes were also incubated either with extracts from untreated *YCA1*^{overexp} cells or H_2O_2-treated *Δyca1* cells, two paradigmatic conditions of absence of metacaspase activity. Digestome analysis showed that the absence of metacaspase activity (Figure 18B, 18C) resulted in the appearance of a GAPDH fragment (spot 6) below the full-length GAPDH protein that is also present in the digestome obtained with H_2O_2-treated *YCA1*^{overexp} cells, indicating that this is a biological phenomenon independent of metacaspase

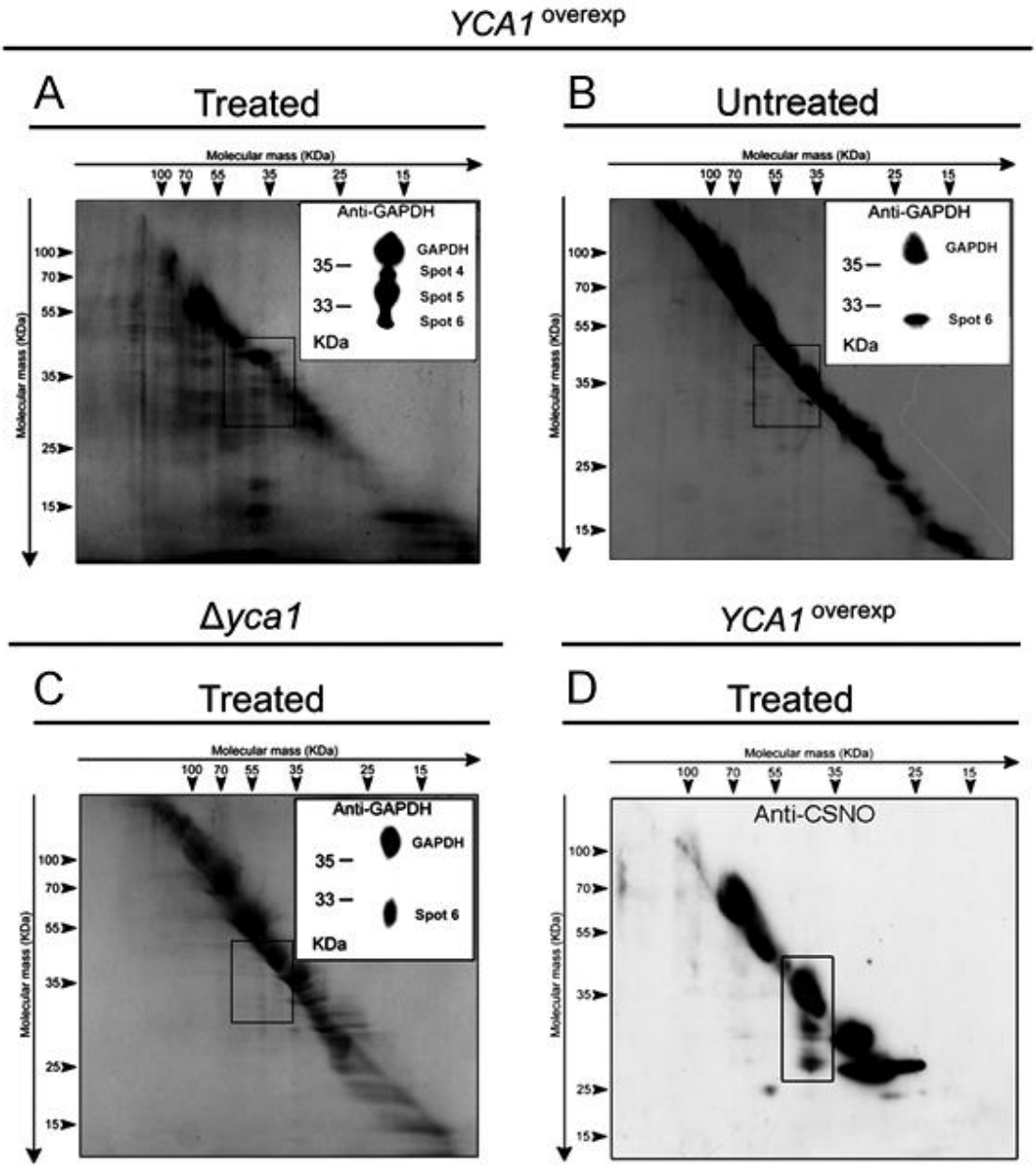

Figure 18 – Digestome analysis of protein extracts from wild-type untreated cells incubated with protein extracts from (A) H_2O_2-treated *YCA1*^{overexp} cells; (B) untreated *YCA1*^{overexp} cells and (C) H_2O_2-treated Δyca1 cells. Immunoblot analyses with a monoclonal anti-GAPDH antibody revealed spots 4, 5 and 6. Data are representative of at least three independent experiments. (D) Immunoblot analysis of diagonal gel represented in (A) with anti-S-nitroso-cysteine (CSNO) antibody.

activity. However, two other spots (spots 4 and 5) were detected in the digestome analysis under active metacaspase conditions (Figure 18A) and were not generated when active metacaspase was absent. These data suggest that GAPDH is cleaved

by metacaspase and that specific cleavage products only occur when metacaspase is active.

Our previous data have demonstrated that upon H_2O_2-induced apoptosis, yeast cells are able to synthesize nitric oxide (NO) leading to the S-nitrosation of GAPDH [211]. Therefore, we questioned if the metacaspase specific GAPDH cleavage and NO signalling are correlated. Immunoblot with an anti-CSNO antibody in the same experimental conditions revealed that the three GAPDH fragments were nitrosated (Figure 18D). Therefore, these results suggest the occurrence of an NO signalling for metacaspase-mediated GAPDH cleavage and demonstrate that the role of metacaspase in yeast H_2O_2-induced apoptosis involves the cleavage of the glycolytic enzyme GAPDH.

Since in mammalian cells the cleavage of GAPDH by caspase-1 has been described [139] and GAPDH sequence is highly conserved among species, we

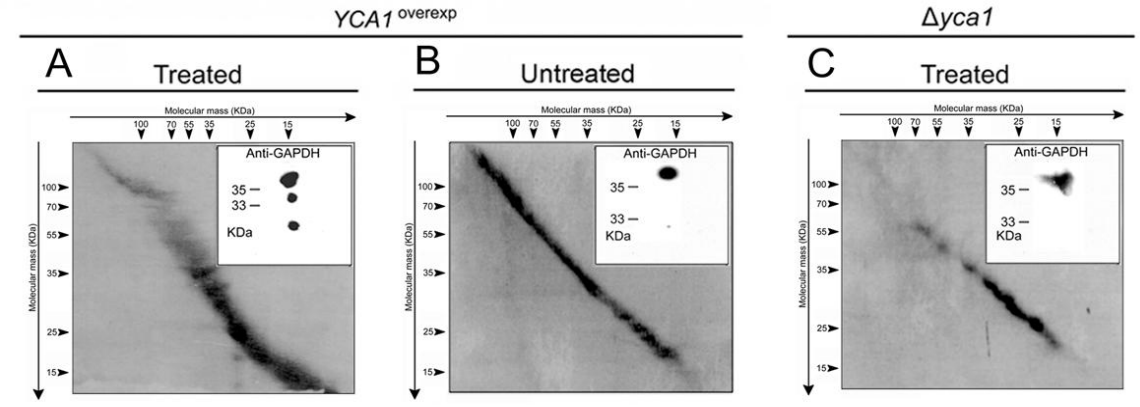

Figure 19 - Mammalian GAPDH is a cleavage target of metacaspase-enriched protein extracts. Coomassie-stained diagonal gels of total protein extracts from untreated HeLa cells incubated with protein extracts from (A) H_2O_2-treated *YCA1*^{overexp} cells; (B) untreated *YCA1*^{overexp} cells and (C) H_2O_2-treated Δyca1 cells, and respective immunoblot analysis with a monoclonal anti-GAPDH antibody. Data are representative of at least three independent experiments.

decided to evaluate a functional conservation of GAPDH cleavage sequences from yeast to mammalian cells. Digestome analysis of HeLa cells total protein extracts incubated with active metacaspase-enriched extracts was performed. As expected, metacaspase was able to cleave mammalian GAPDH (Figure 19A). Immunoblot analysis of the diagonal gels revealed two GAPDH spots immediately below the

diagonal (Figure 19A) although these fragments were distinct from the ones produced by incubation with yeast protein extracts, showing that these proteases have distinct cleavage target sites. Furthermore, diagonal gels of HeLa cells total protein extracts after incubation with extracts from untreated *YCA1*^{overexp} cells or H_2O_2-treated Δ*yca1* cells showed that the absence of metacaspase activity (Figure 19B, 19C) resulted in the lack of GAPDH fragments below the full-length GAPDH protein, indicating that mammalian GAPDH specific cleavage products only occur when metacaspase is active. Our results indicate that yeast metacaspase recognizes target sequences distinct from the ones recognized by caspases of higher eukaryotes corroborating previous results that attributed to metacaspase an arginine/lysine-specific endopeptidase activity in contrast to the cysteine-aspartic proteases of caspases [320]. Altogether, these results show that although metacaspases have a proteolytic activity distinct from caspases, their targeted molecular pathways upon an apoptotic stimulus display similarities and during apoptotic cell death both of them degrade metabolic enzymes. Despite these results, we were unable to address a role for metacaspase in the cleavage of translation factors, as described in mammalian cells, since we could not identify the other numerous spots observed below the diagonal in the digestome analysis. Nevertheless, in mammalian cells a regulation of internal ribosome entry site (IRES) mediated cap-independent translation of virus and mammalian mRNAs [135-138] and of mRNA stability by GAPDH [323] has been addressed. The conserved degradation of GAPDH in the course of the apoptotic cascade might be a regulatory mechanism for the activation of an IRES-mediated translation upon the apoptotic stimulus from yeast to mammalian cells.

3.4.1.2 In vivo metacaspase cleavage of GAPDH during H_2O_2-induced apoptosis

Several proteins shown to be specifically cleaved by in vitro methodologies, such as the digestome analysis, proved later not to be substrates of the caspases under in vivo apoptotic conditions. Thus, metacaspase specific GAPDH fragmentation was evaluated by immunoblot analysis of GAPDH levels, in total

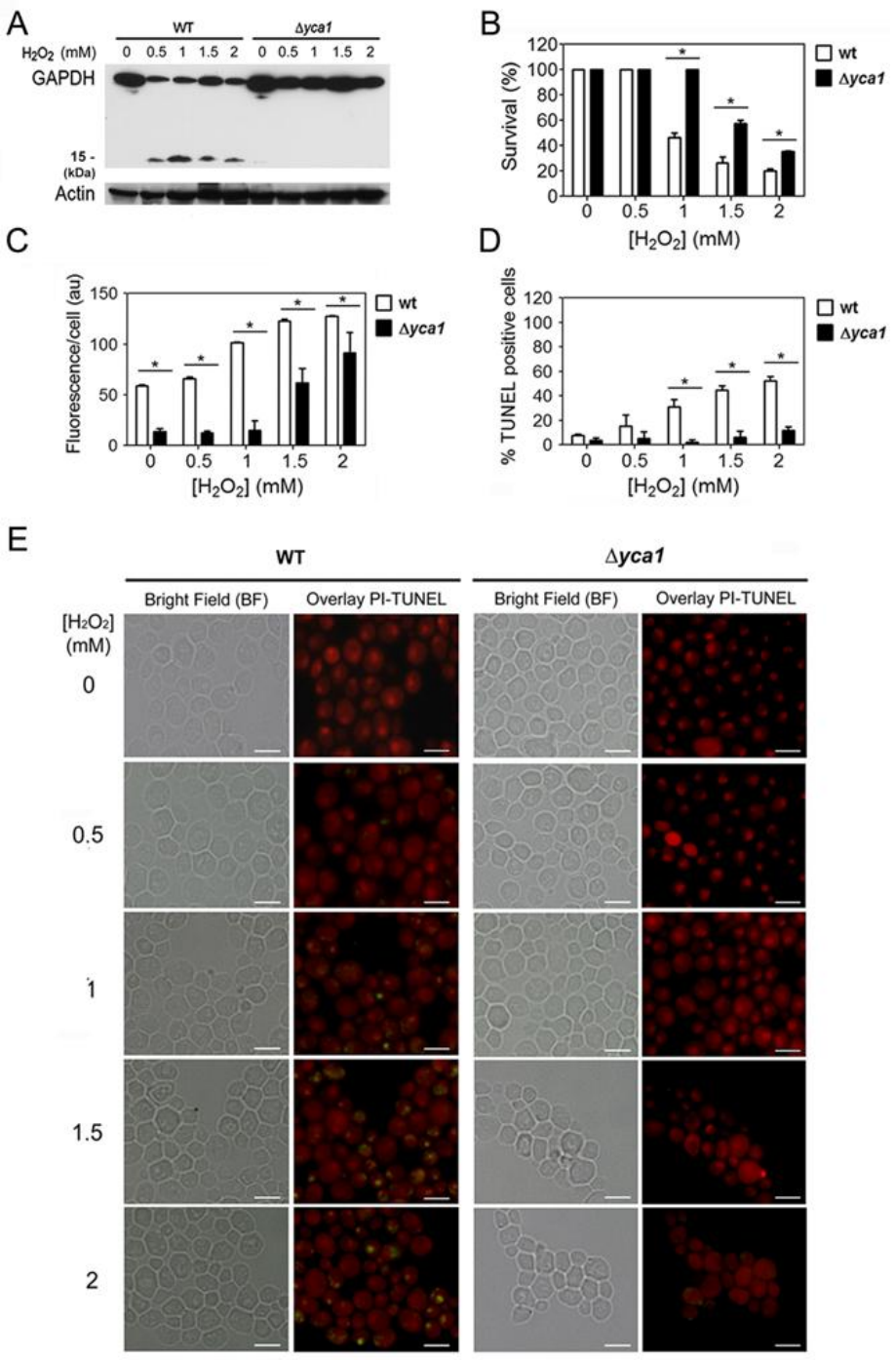

Figure 20 - GAPDH specific cleavage by metacaspase during H_2O_2-induced apoptosis. (A) Immunoblot analysis of GAPDH and actin protein levels in 40 μg of total protein extracts of H_2O_2-treated and untreated wild-type and Δ*yca1* cells. (B) Comparison of the survival rate of wild-type and Δ*yca1* cells upon H_2O_2 treatment. (C) Percentage of wild-type and Δ*yca1* cells exhibiting high levels of intracellular ROS detected by FACS measurements of the dihydrorhodamine 123 fluorescence. (D) Percentage of wild-type and Δ*yca1* cells displaying TUNEL positive phenotype. (E) Epifluorescence and bright field micrographs of untreated and H_2O_2-treated wild-type and Δ*yca1* cells displaying TUNEL reaction to visualize double-strand DNA breaks. Cells were co-stained with propidium iodide in order to facilitate nuclei visualization. Bar, 5 μm.

protein extracts from wild-type and Δ*yca1* cells challenged with H_2O_2 (Figure 20A). As expected, H_2O_2 (concentrations ranging from 0.5 mM to 2 mM) induced apoptotic cell death of wild-type cells (Figure 20B) as revealed by the high levels of reactive oxygen species (ROS) (Figure 20C) and the increasing percentage of cells displaying TUNEL positive phenotype (Figure 20D, 20E). In contrast, Δ*yca1* cells were more resistant to H_2O_2 and thus had increased survival (Figure 20B), TUNEL negative phenotype (Figure 20D, 20E) and lower percentage of cells with high ROS levels (Figure 20C). Moreover, apoptotic cell death of wild-type cells was accompanied by a clear reduction of the GAPDH levels that was not observed in Δ*yca1* cells (Figure 20A), suggesting the requirement of metacaspase for the occurrence of fragmentation of this protein in vivo. Simultaneously, it was possible to detect a GAPDH fragment with lower molecular weight (15kDa) (Figure 20A) compatible with one of the fragments observed by digestome analysis (Figure 20A). The absence of other fragments in the immunoblot analysis, as observed by in vitro digestome assay, suggests that the peptides liberated from the precursor protein, can be further processed, resulting in fragments that are released or degraded.

These results suggest that GAPDH is a specific target of metacaspase during H_2O_2-induced apoptosis. As demonstrated in mammalian cells [119, 134, 139], the fragmentation of GAPDH during apoptosis might be part of a mechanism of derepression/activation of an alternative cap-independent translation of specific mRNAs with a role in the yeast apoptotic process.

Altogether these data reinforce a link between translation control, metabolism and cell death. However, the role of metacaspase in translation machinery alterations during cell death remains elusive.

3.4.2 Metacaspase-mediated alterations during acetic acid-induced apoptosis

Since digestome analysis was unable to reveal metacaspase substrates related to the translation machinery, a different approach was followed. As opposed to the incubation of protein extracts with metacaspase, we analysed the

effect of the deletion of *YCA1* in the levels of translation factors affected during the acetic acid-induced apoptosis.

3.4.2.1 eEF1A as a modulator of cell death

eEF1A N-terminal metacaspase-independent fragmentation and re-localization to mitochondrial matrix upon acetic acid-induced apoptosis

In mammalian cells, the target of mitochondria by caspases has been described as part of the apoptotic cascade [322]. To identify potential metacaspase substrates in mitochondria during acetic acid-induced apoptosis, an apoptotic scenario in which mitochondria plays a prominent role [39, 41, 199-201, 324-328], a proteomic analysis, combined with mass spectrometry, of purified mitochondrial extracts from untreated and acetic acid treated cells was performed, showing that two spots corresponding to fragments of the translation elongation factor eEF1A (Tef1p/Tef2p) were present in mitochondria, upon acetic acid treatment (Figure 21A) [290]. These two eEF1A fragments were composed by the N-terminal sequences of the protein from amino acids 6-177 (Figure 21B, amino acid sequence highlighted at orange) and amino acids 6-146 (Figure 21B, amino acid sequence highlighted at orange and green), with a molecular weight of about 19 kDa [290]. To further validate the proteomic analysis eEF1A levels and cellular localization were assessed. Upon acetic acid treatment a decrease in the levels of eEF1A in cytoplasm was observed together with a re-localization of the total protein and eEF1A fragments (with molecular weight of about 19 kDa and 31 kDa) to mitochondria (Figure 21C). Moreover, to elucidate if the eEF1A fragments detected in the mitochondria upon the apoptotic stimulus were only interacting with mitochondria outer membrane or were able of enter the mitochondrial matrix, a proteinase K assay was performed. Mitochondrial extracts of untreated and acetic acid-treated cells were incubated with proteinase K in the presence or absence of sorbitol (osmotic protector of the mitochondrial membrane integrity). The digestion of the proteins interacting with the outer membrane was assessed through the incubation with proteinase K and sorbitol. Proteins of the outer membrane and intermembrane space were digested through the incubation with proteinase K in the absence of sorbitol. This assay revealed that upon the induction of apoptosis by

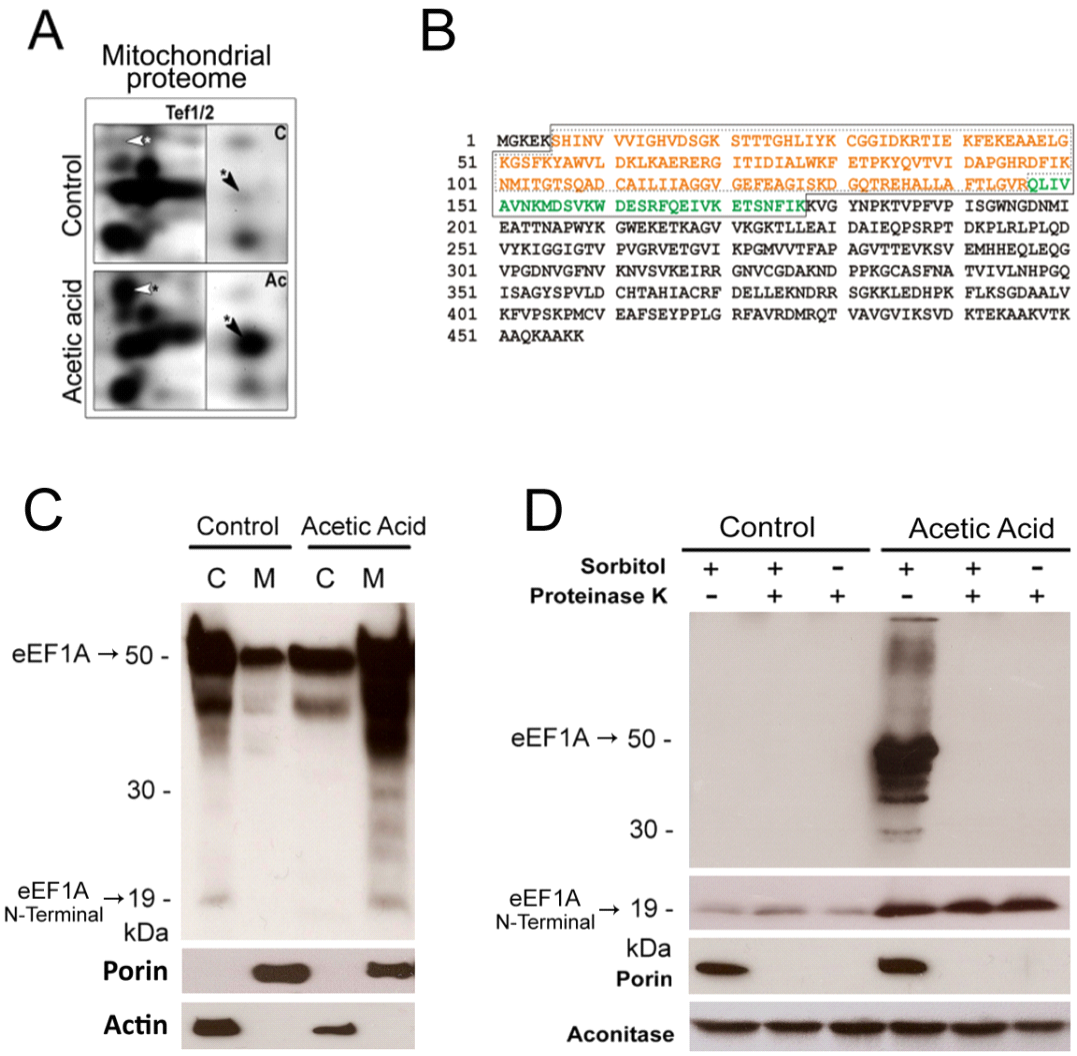

Figure 21 - Re-localization of eEF1A N-terminal fragments to mitochondria during acetic acid-induced apoptosis. (A) Comparison of protein levels in purified mitochondrial extracts of untreated and acetic acid-treated wild-type *S. cerevisiae* cells. Selected two-dimensional gel regions are shown enlarged. Putative protein fragments are marked with an asterisk. Arrows indicate the respective spots. (B) Peptide fingerprints of the two eEF1A fragments corresponding amino acids 5-146 and 6-177 to N-terminal sequences as identified in 2D gel electrophoresis of mitochondrial extracts from acetic acid treated cells. (C) Immunoblot analysis of eEF1A levels in cytoplasmic and mitochondrial extracts of untreated and acetic acid treated wild-type cells. (D) Immunoblot analysis of eEF1A levels after proteinase K assay of mitochondrial extracts from untreated and acetic acid treated cells.

acetic acid, an eEF1A fragment of 30 kDa and total eEF1A protein interact with the outer surface of the mitochondria being immediately removed after digestion with proteinase K in the presence of sorbitol (Figure 21D). However, the eEF1A N-

terminal fragment of 19kDa was detected in the mitochondrial matrix even after the incubation of mitochondrial protein extracts with proteinase K without sorbitol (Figure 21D). The fact that eEF1A was fragmented during acetic acid-induced apoptosis, but was not degraded, being re-localized to the mitochondria raised the hypothesis that beyond its role in translation and the other described functions, eEF1A plays a role in acetic acid-induced apoptosis. Despite this fact, immunoblot

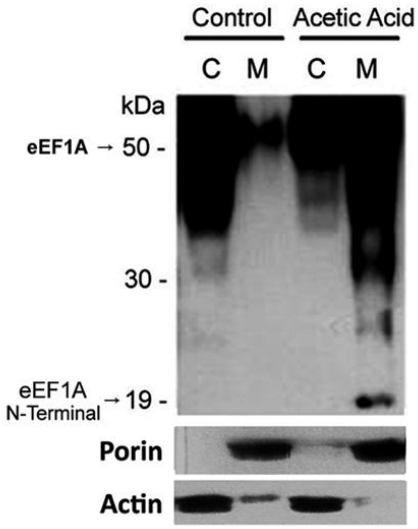

Figure 22 – eEF1A fragmentation during acetic acid treatment is independent of yeast metacaspase. Immunoblot analysis of eEF1A expression in cytoplasmic and mitochondrial extracts of untreated and acetic acid treated (195 mM) Δ*yca1* cells.

analysis of eEF1A levels in cytoplasmic and mitochondrial extracts of *YCA1* deleted cells showed that eEF1A cleavage upon the acetic acid stimulus was not mediated by metacaspase (Figure 22). Although an interaction between these two proteins has been described [209], eEF1A fragmentation and re-localization to mitochondria still occurs in *YCA1* disrupted cells (Figure 22).

Yeast eEF1A, as well as that of other organisms, is a bona fide actin binding and bundling protein [289, 295-299] with a crucial role in the regulation of actin cytoskeleton organization. Therefore, we addressed whether acetic acid treatment affects the eEF1A binding to actin and the possible implications to the actin cytoskeleton organization. Immunoprecipitation of actin from total protein extracts of acetic acid treated cells followed by immunoblot of eEF1A levels revealed that during acetic acid treatment the affinity of eEF1A to actin was diminished, and this

decrease was dependent on the acetic acid concentration (Figure 23A). The interaction of mitochondria with cytoskeleton elements regulating mitochondrial dynamics, namely mitochondria fusion and fission, has been described both in yeast and mammalian cells [329-331]. In fact, actin and Tef1p, but not Tef2p,

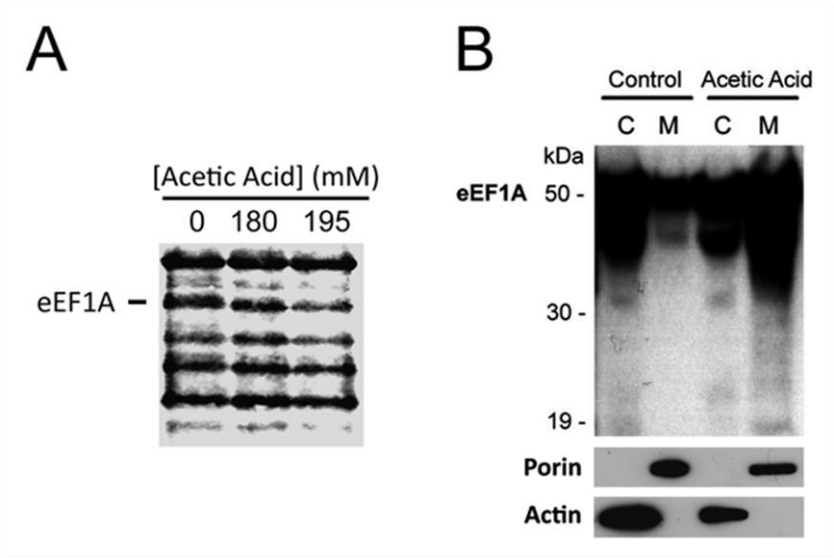

Figure 23 - Fragmentation and translocation of eEF1A to mitochondria reduces its affinity to actin and is independent of mitochondria dynamics. (A) Immunoprecipitation of actin from total protein extracts of untreated and acetic acid treated cells, followed by immunoblot analysis of eEF1A levels and binding to actin. (B) Immunoblot analysis of eEF1A levels in cytoplasmic and mitochondrial extracts of untreated and acetic acid treated Δ*yca1* cells.

interaction with the Dynamin-related GTPase, Dnm1p, involved in mitochondrial fission, has been previously shown [332]. Although Tef1p interacts with several mitochondrial proteins, the interaction with Dnm1p might be of importance for the execution of the apoptotic process, as Dnm1p has previously been linked to the promotion of mitochondria fragmentation/degradation and cell death upon acetic acid-induced apoptosis in yeast [200, 333]. Our results showed that during acetic acid treatment, eEF1A binding to actin decreased (Figure 23A) and eEF1A N-terminal fragments re-localized to mitochondrial matrix (Figure 21). Thus, we decided to evaluate the relevance of Dnm1p on the translocation of eEF1A fragments to mitochondria. With this purpose, we observed the levels of the eEF1A in cytoplasmic and mitochondrial extracts of untreated and acetic acid treated Δ*dnm1* cells. Immunoblot results exhibited the eEF1A fragments in mitochondria

extracts of *DNM1* deleted cells upon acetic acid-induced apoptosis (Figure 23B) excluding the possibility of the Dnm1p-mediated translocation of eEF1A to mitochondria. Nevertheless, Dnm1p is not the only regulator of the mitochondria fission/fusion process during acetic acid-induced apoptosis [200] and other proteins could be interacting with eEF1A, regulating this process.

A second mitochondrial proteomic analysis was performed under the same apoptotic conditions. This analysis revealed a new spot in mitochondria extracts upon acetic acid treatment, corresponding to the translation elongation factor 2 (eEF2/Eft1/2p) (Figure 24). Nevertheless, a thorough analysis of the function of this protein in mitochondria during acetic acid treatment and of a putative correlation with the eEF1A fragments in this process should be performed.

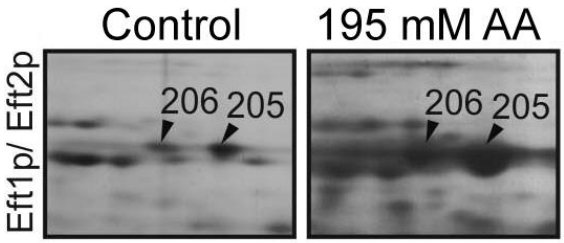

Figure 24 – Translocation of eEF2 fragment to mitochondria during acetic acid-induced apoptosis. Comparison of protein levels in purified mitochondrial extracts of untreated and acetic acid-treated (195 mM) wild-type *S. cerevisiae* cells. Selected regions of the two-dimensional gel are shown. Arrows indicate the respective spots.

These results suggest that upon acetic acid treatment the apoptotic cascade is activated, and after 120 min of incubation (Figure 10A) eEF1A is cleaved by a caspase-independent pathway and N-terminal fragments are re-localized to the mitochondrial matrix. The presence of eEF1A N-terminal fragments in mitochondria matrix during the apoptotic process allows us to hypothesize the involvement of eEF1A fragments in the mitochondrial apoptotic cascade. The fact that both eEF1A and eEF2 are found in mitochondria at later time points of the acetic acid treatment strongly suggest that this translocation and the function performed by these fragments in the mitochondria are related with the progression of the apoptotic process. Since in silico analysis suggests that the N-terminal fragments of eEF1A, re-localized to the mitochondrial matrix, are GTP-binding domains involved

in the delivery of the aminoacyl-tRNAs to ribosomes and eEF2 is involved in ribosomal translocation during protein synthesis [334], their re-localization to mitochondria might be a signalling for this translation factors participation in the translation of mitochondrial mRNAs with a role in apoptosis.

Moreover, given that eEF1A is an inhibitor of Gcn2p [294, 335], and this kinase plays a crucial role in the regulation of translation initiation during the acetic acid-induced apoptosis (Figure 10A, 11B), the cleavage of eEF1A might be a cellular mechanism to impair this inhibition.

The eEF1A N-terminal fragments act as pro-apoptotic molecules upon acetic acid treatment

Although the previous results ruled out eEF1A as a substrate of metacaspase during the acetic acid-induced apoptosis, we cannot reject the hypothesis that eEF1A N-terminal fragments are players in the apoptotic cascade. To understand the role of eEF1A N-terminal fragments in mitochondria during acetic acid-induced apoptosis, p416 plasmids harbouring eEF1A full gene and eEF1A truncated in N6C458, N1C146 or N1C177 were transformed in wild-type cells. Higher concentrations of acetic acid were used in order to achieve about 50% (210 mM) and 35% (225 mM) of cell death in the wild-type cells harbouring the empty plasmid vector (Figure 25). The expression of the eEF1A total protein (N1C458) did not affect the resistance of wild-type cells to acetic acid. However, expression of eEF1A protein truncated in the first 5 amino acids (N6C458) revealed a slight increase in the resistance to acetic acid, suggesting a role of the eEF1A 5 N-terminal amino acids in the signalling of the protein to mitochondria and therefore in its function during the apoptotic process. Survival assay also showed that the expression of the eEF1A N1C146 or N1C177 fragments enhanced the susceptibility of the cells to acetic acid-induced apoptosis (Figure 25). Furthermore, the N1C177 fragment appears to have a more pronounced effect in this phenotype (Figure 25). Nevertheless, the expression of the eEF1A fragments without the apoptotic stimulus was not able to induced cell death. eEF1A is involved in different functions such as translation elongation and actin cytoskeleton

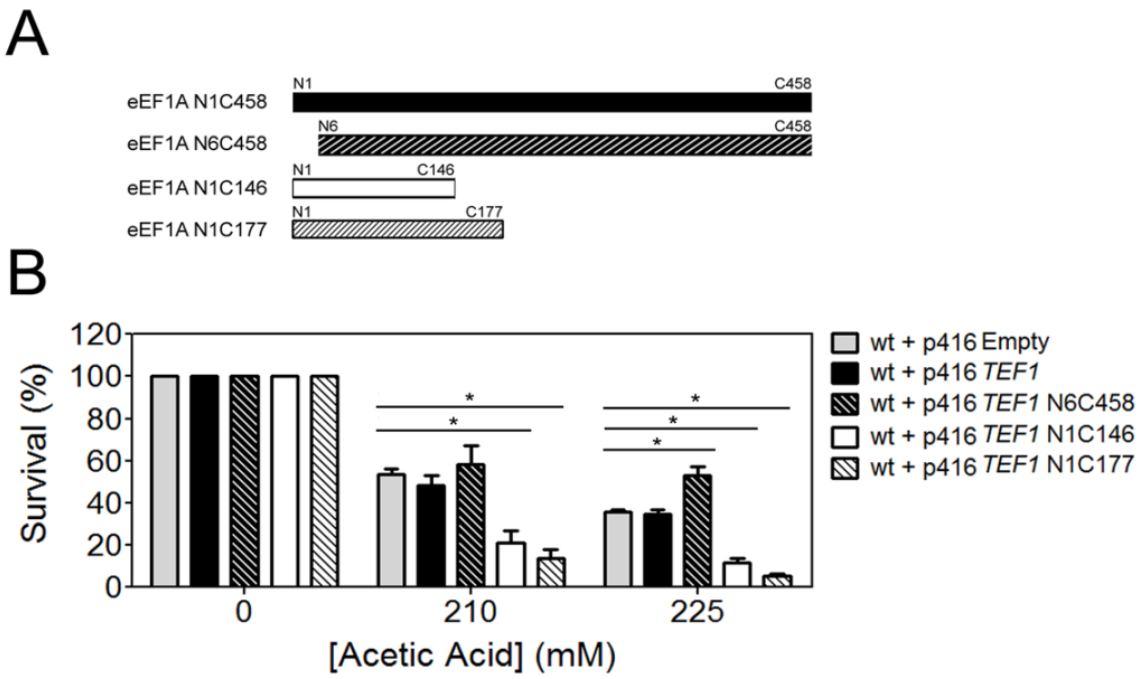

Figure 25 – eEF1A N-terminal fragments N1C146 and N1C177 play pro-death function in cells challenged with acetic acid. (A) Scheme of the eEF1A fragments inserted in the p416 plasmid. (B) Comparison of the survival rate of wild-type *S. cerevisiae* cells expressing eEF1A total protein, N6C458 fragment and N-terminal N1C146 or N1C177 fragments upon treatment with 210 and 225 mM acetic acid.

organization and its fragmentation affects these processes which might contributing to the induction of the apoptotic process. On the other and, eEF1A N-terminal fragments pro-apoptotic role may only be activated upon their translocation to mitochondria, which only occurs during the apoptotic process. Moreover, eEF1A N-terminal fragments are probably downstream players on the apoptotic cascade, therefore an interaction with the upstream regulators, upon the triggering of apoptosis, is necessary for their pro-apoptotic function. To disclose the mechanism beneath this phenotype, eEF1A isoform *TEF1* deleted cells, harbouring a pYX222 plasmid expressing eEF1A full gene (N1C458) or eEF1A N-terminal fragment N6C177 (the eEF1A fragment that induced a more pronounced apoptotic phenotype) in frame with a mitochondrial localization sequence (MLS) in the N-terminal and a DsRed reporter in the C-terminal were transformed in *TEF1* deleted cells (Figure 26A, 26B). The *TEF1* deleted cells expressing the pYX222 empty vector proved to be more resistant to acetic acid treatment (Figure 26) that wild-

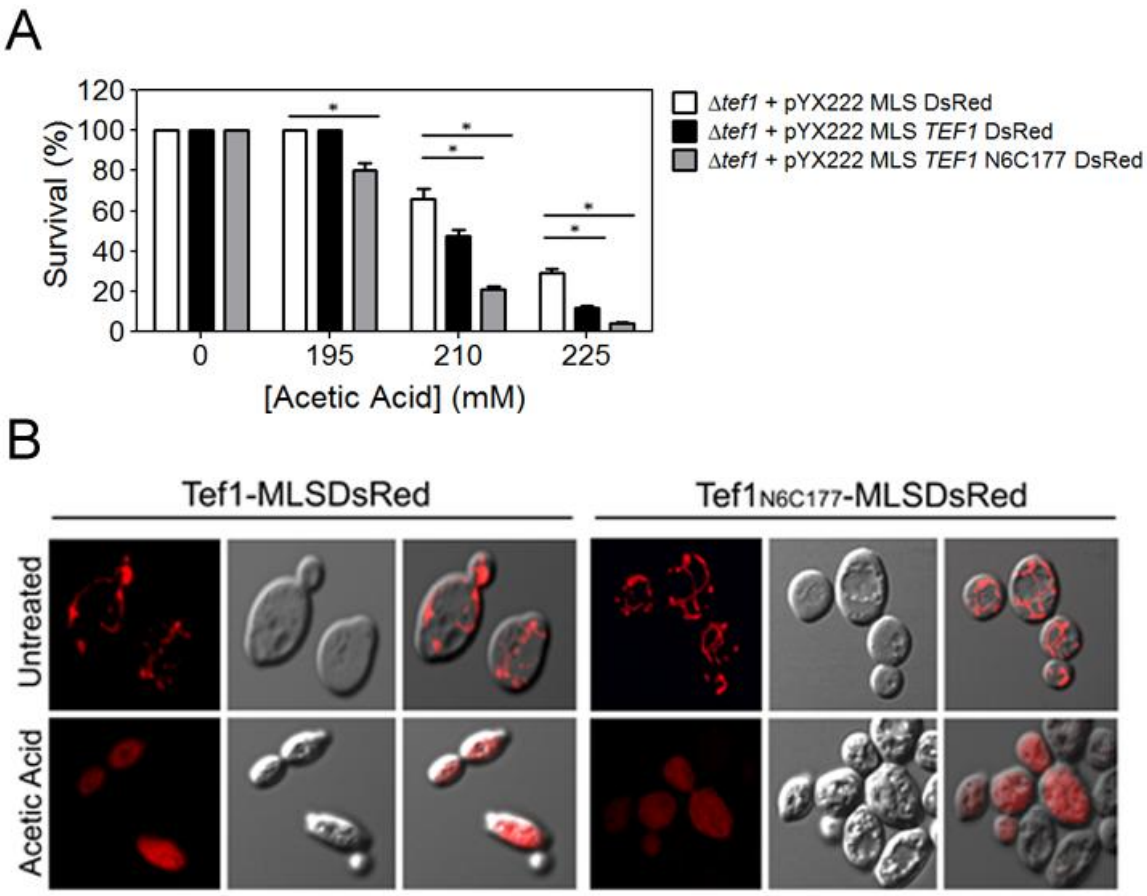

Figure 26 – The pro-apoptotic function of eEF1A N-terminal fragment in the mitochondria is only active upon the acetic acid apoptotic stimulus. (A) Comparison of the survival rate of Δ*tef1 S. cerevisiae* cells expressing eEF1A total protein and N-terminal N6C177 fragment with a mitochondria localization sequence (MLS) in the N-terminal and a DsRed reporter in the C-terminal, upon treatment with 195, 210 and 225 mM acetic acid. (B) Confocal micrographs of strains used in (A) treated with 210 mM acetic acid in order to confirm the mitochondrial localization of the eEF1A protein and the N-terminal fragment.

type cells (Figure 25), suggesting the involvement of eEF1A in the apoptotic process. The eEF1A total protein and N6C177 fragment translocation to mitochondria was confirmed by confocal microscopy visualization of the DsRed expression in mitochondria under physiological conditions (Figure 26B). Nonetheless, no alteration in the cell survival and mitochondria morphology was observed upon the expression of eEF1A N6C177 fragment in mitochondria under these conditions (Figure 26B), proving that expression and translocation of eEF1A N6C177 fragment to mitochondria by itself is not capable of inducing apoptosis,

therefore ruling out our first hypothesis. However, acetic acid triggers an apoptotic cascade that might promote the pro-death role of eEF1A protein (Figure 26A). Protection conferred by the deletion of *TEF1*, when compared to wild-type cells (Figure 25), was abrogated upon the expression of eEF1A total protein during acetic acid treatment (Figure 26B), excluding also the second hypothesis. An even higher susceptibility to cell death was observed in cells expressing the eEF1A N6C177 fragment in mitochondria matrix (Figure 26A), supporting our third hypothesis and revealing eEF1A N-terminal N6C177 fragment as a downstream player in the apoptotic cascade. Despite that, confocal microscopy, could not confirm the eEF1A fragments localization in the mitochondria upon acetic acid treatment (Figure 26B). The reason for the observed DsRed degradation could rely on the cleavage of eEF1A N-terminal sequences, as occurs in the eEF1A total protein upon the apoptotic stimulus or the well described fission and degradation of mitochondria during acetic acid-treatment [39, 200, 201, 336]. Thus, the elucidation of the specific function exerted by these fragments and at which step of the mitochondrial acetic acid-induced apoptotic cascade they play a part, namely during the production of reactive oxygen species (ROS), reduction of mitochondrial potential, depolarization of mitochondria outer membrane, translocation of Aif1p from mitochondria to the nucleus, release of cytochrome *c* to cytosol, or mitochondrial fragmentation/degradation [41, 199, 200, 326, 328], is of utmost importance for the disclose of acetic acid-induced apoptotic cascade of events.

siRNA-mediated eEF1A1 knockdown in HeLa cells leads to actin cytoskeleton alterations with increased susceptibility to apoptosis

Since previous results from our lab showed that the deletion of *TEF1,* but not *TEF2,* reverted the apoptotic phenotype induced by acetic acid in yeast and a decrease of the actin cytoskeleton alterations observed [290], we decided to evaluate if this phenomenon was evolutionarily conserved. Mammalian eEF1A isoforms, eEF1A1 and eEF1A2, are expressed mutually exclusive [337]. eEF1A2, is normally expressed only in muscles and neurons, being also related with tumor development in tissues that normally express only eEF1A1 [292, 309, 310, 312, 313, 338-340]. Both isoforms of eEF1A have been characterized to function in the protein elongation step of translation. However, eEF1A1, but not eEF1A2, has

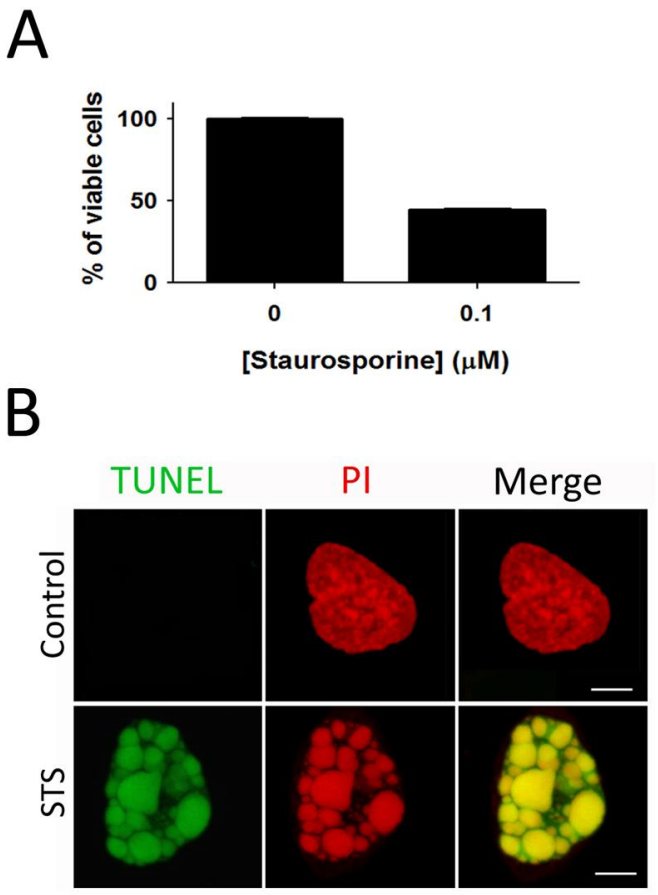

Figure 27 – Staurosporine (STS)-induced apoptotic cell death in HeLa cells. (A) Cell titer-blue cell viability assay of untreated and STS treated cells. (B) TUNEL assay of untreated and STS treated cells.

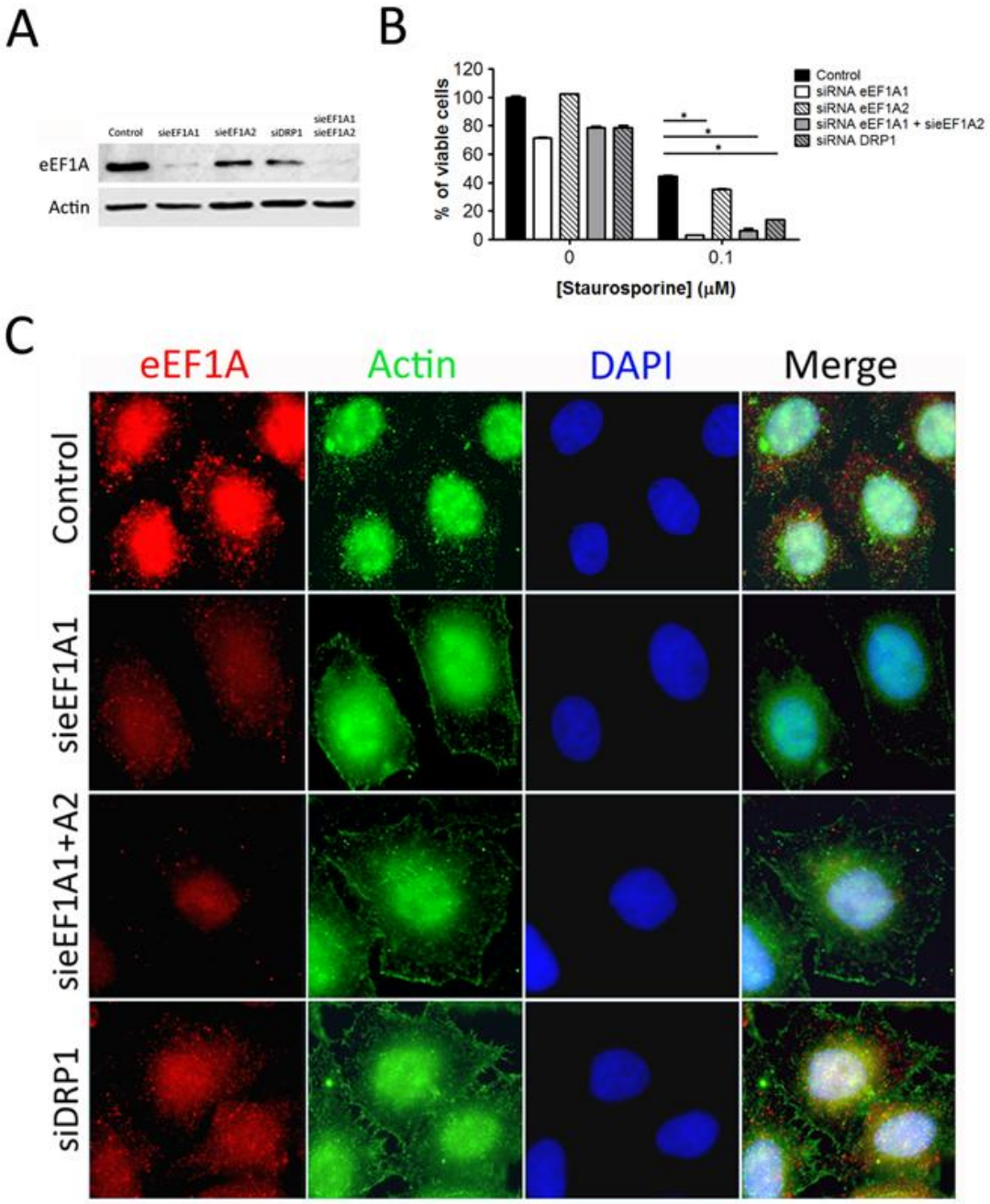

Figure 28 – eEF1A RNAi depletion in HeLa cells increases susceptibility to staurosporine-induced apoptosis with actin cytoskeleton alterations. (A) Confirmation of the depletion efficiencies of eEF1A isoforms by immunoblot analysis. (B) Survival assay of untreated and STS treated cells upon eEF1A1, eEF1A2 and DRP1 RNAi depletions for 48h. (C) Immunofluorescence of eEF1A and actin protein expression levels.

additional non-canonical roles in actin binding/bundling [341]. Therefore, relevance of eEF1A isoforms in the actin cytoskeleton organization during the induction of apoptotic cell death was determined in HeLa cells, an immortalized human cell line of epithelial cells from cervical carcinoma. Mitochondrial fission-mediated apoptotic cell death was induced in HeLa cells using staurosporine (STS) [342]. In order to confirm the induction of apoptosis by STS in about 50% of HeLa cells in our experimental conditions, viability and TUNEL assays were performed after eighteen hours of incubation with 0.1 μM of STS (Figure 27A, 27B). RNAi depletion of eEF1A1 and eEF1A2 isoforms and DRP1 (the mammalian homolog of yeast *DNM1*) was performed. Forty eight hours after transfection with the siRNAs, efficient repressions were ascertained as confirmed by immunoblot analysis of eEF1A levels (Figure 28A). Although silencing of eEF1A1 proved to be very efficient, the silencing of eEF1A2 produced almost no effect in eEF1A total levels (Figure 28A), suggesting that either eEF1A2 silencing was not efficient or eEF1A2 isoform levels in these cells are low as expected [309, 313]. The silencing of DRP1 affected the levels of eEF1A (Figure 28A) suggesting a regulation of eEF1A by DRP1. Furthermore, we evaluated the viability of RNAi cells exhibiting low/absent levels of eEF1A isoforms when treated with STS. In HeLa cells, the depletion of eEF1A1, but not of eEF1A2, increased the susceptibility to apoptotic cell death (Figure 28B), which could be explained by the fact that mRNA silencing is an immediate process leaving no time for cells to adapt to new conditions or because in mammalian cells these proteins perform a protective role upon the apoptotic stimulus. Furthermore, immunostaining of eEF1A and actin revealed actin cytoskeleton alterations in the absence of eEF1A1, the described actin binding/bundling protein in mammalian cells, (Figure 28C) and its complete destruction after STS treatment (data not shown). Therefore, similar to yeast, in mammalian cells eEF1A1, but not eEF1A2, is a crucial player in the regulation of actin cytoskeleton organization, playing also an important role in the apoptotic process. However, the suggested pro-apoptotic role of eEF1A in yeast is dissimilar from the protective role observed in mammalian cells. These antagonist roles are most likely due to the distinct apoptotic cell death pathways activated.

Nonetheless, these results demonstrate the relevance of eEF1A in the modulation of apoptosis both in yeast and mammalian cells.

3.4.2.2 The phosphorylation of eIF2α and the levels of IF4A are not affected in Δ*yca1* cells challenged with acetic acid

Despite the observed metacaspase-independent cleavage and mitochondrial re-localization of eEF1A during acetic acid induced-apoptosis, the role of yeast metacaspase in other translation factors alterations upon acetic acid treatment was evaluated. For this purpose, an immunoblot kinetic analysis of eIF2α phosphorylation levels and translation initiation factors eIF2α (Sui2p), eIF4A (Tif1p) and eIF4G (Tif4631/2p) and translation elongation factor eEF2 (Eft1/2p)

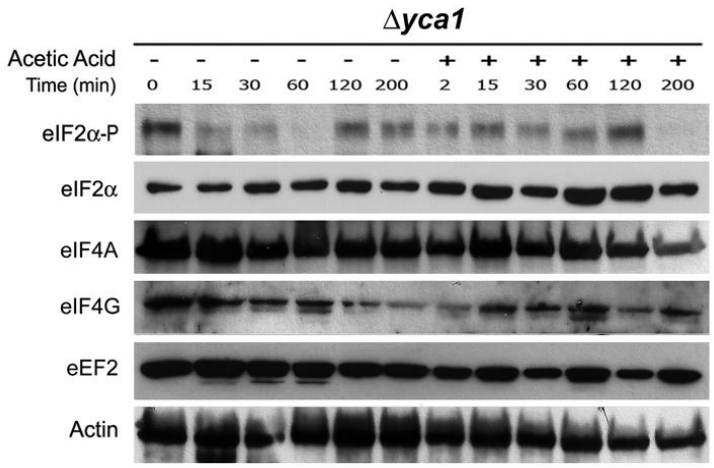

Figure 29 - Yeast metacaspase (Yca1p) involvement in translation regulation during acetic acid-induced apoptosis. Immunoblot kinetic analysis of eIF2α phosphorylation levels, translation initiation factors eIF2α (Sui2p), eIF4A (Tif1p) and eIF4G (Tif4631/2p) and translation elongation factor eEF2 (Eft1/2p) levels in Δ*yca1 S. cerevisiae* cells untreated or treated with 195 mM of acetic acid. Actin was used as loading control.

levels in *YCA1* deleted cells upon acetic acid treatment was performed (Figure 29A). This experiment revealed a decrease in the phosphorylation levels of eIF2α to a basal level upon acetic acid treatment (Figure 29), when compared to the wild-type cells (Figure 10A). Since in mammalian cells PERK kinase activation for the phosphorylation of eIF2α is caspase-dependent [59, 72], and in yeast, the

deletion of *YCA1* reduced the Gcn2p-mediated phosphorylation of eIF2α, a regulation of translation initiation through the control of Gcn2p kinase activity by metacaspase might be occurring. Moreover, the levels of eIF4A appeared almost unaltered when Δ*yca1* cells were challenged with acetic acid suggesting once more a regulation of translation machinery by metacaspase during the apoptotic process (Figure 29). Despite this observation, no eIF4A fragmentation was detected by immunoblot analysis. Therefore, we could not infer if eIF4A is a metacaspase substrate or if it is indirectly regulated by this protease. The levels of eEF4G and eEF2 were also less affected (Figure 29) that in wild-type cells. However, this effect was not as notorious as the one observed in the eIF4A. Altogether, these data showed that translation machinery is also a target of yeast metacaspase, directly or indirectly, in scenarios of apoptotic cell death highlighting a new putative link, which deserves further investigation, between translational control and cell death.

Altogether these results show the relevance of metacaspase in the regulation of the translation during the apoptotic process. The down-regulation of translation initiation factors levels upon the apoptotic stimulus combined with the specific cleavage of GAPDH, which might lead to the derepression of an IRES-mediated translation, by metacaspase, strongly suggests metacaspase as an apoptotic upstream regulator of the translation process during acetic acid-induced apoptosis.

3.5 DISCUSSION

In mammalian cells, the targeting of translation machinery by caspases during apoptosis [59, 72, 83] is well established. In yeast, metacaspase seems to be one of the executors of the apoptotic events [214] despite its enigmatic role. The routes to unravel metacaspase functions undoubtedly have to pass through the identification of its specific substrates and how substrates cleavage is involved in the apoptotic phenotype. Therefore, using different methodologies, digestome and mutagenesis analysis, we studied the targeting of translation machinery by metacaspase during different scenarios of yeast apoptosis. A relation between metacaspase and apoptosis has been previously established during acetic acid-induced apoptosis since a metacaspase-dependent decapping of mRNA leading to mRNA degradation has been reported [218, 244, 246]. Digestome analysis revealed the first yeast metacaspase substrate, the glycolytic enzyme GAPDH, a common apoptotic substrate from yeast to mammalian [219]. GAPDH is S-nitrosated during H_2O_2-induced apoptosis [211]. Since metacaspase activity is dependent on the NO intracellular levels [212] and we show that GAPDH fragments appear nitrosated, similarly to what occurs in higher eukaryotic cells, a NO signalling appears to be regulating metacaspase substrates targeting [45]. Nonetheless, we were unable to identify the other spots observed below the diagonal, corresponding to other putative metacaspase substrates, and to disclose a role of metacaspase in the cleavage of translation machinery by this methodology. However, in mammalian cells a relation between translation impairment and the activation of a GAPDH mediated apoptotic pathway has been established [343]. Furthermore, the specific binding of this glycolytic enzyme to IRES of virus RNAs leading to the inhibition of virus RNA cap-independent translation in mammalian cells and blocking the viral infection has been widely reported [135-138], as well as the binding to mammalian cells mRNAs, such as the pro-apoptotic molecule p53 and AT1R [136, 317, 323, 344], impairing their IRES-mediated translation. The translation of several apoptotic regulators, both pro-apoptotic [101] and anti-apoptotic [109], is regulated by IRES. The cleavage of GAPDH by caspase-1 [139] upon an apoptotic stimulus might prevent its interference in the cap-independent translation crucial for the development of the

apoptotic process [4, 95, 243]. Therefore, the activation of metacaspase during acetic acid treatment leading to the cleavage of GAPDH might be an upstream regulatory mechanism to trigger an alternative cap-independent translation process mediated by IRES which in physiological conditions is repressed by the binding of GAPDH to the mRNAs. The elucidation of mRNAs target of GAPDH binding in yeast and the relevance of these interactions for the efficient translation of these mRNAs and consequently their function is of utmost importance for the understanding of the regulatory mechanisms mediating apoptosis.

The targeting of mitochondrial proteins by caspases during apoptosis in mammalian cells [322] prompted us to investigate a conservation of this regulation during yeast apoptosis. Analysis of mitochondrial proteomic profile revealed eEF2 protein and two N-terminal fragments of eEF1A in the purified mitochondrial fractions [290] of acetic acid-treated cells despite the decreased of eEF1A and eEF2 levels in total cellular extracts [215]. These data strongly suggested a role of these translation elongation factors in the apoptotic process and further studies were performed. Despite the fact that both eEF1A total protein and N-terminal fragments were found in the mitochondrial extracts, only the N-terminal fragments proved to be imported to the mitochondrial matrix. Moreover, the expression of these N-terminal fragments results in an increased susceptibility to acetic acid treatment, strongly suggesting the pro-apoptotic role of these fragments. The mitochondrial localization of eEF1A fragments raises the possibility that eEF1A is a key player in the promotion of the well described acetic acid-induced mitochondrial alterations, namely in the release of apoptotic factors, such as cytochrome *c* [199] and Aif1p [41]. Moreover, eEF1A translocation to mitochondria may have multiple implications for the cell, besides its role in the process of translation elongation, eEF1A plays a role in several other housekeeping processes [287, 345], such as actin cytoskeleton organization [295, 296]. During acetic acid-induced apoptosis the binding of eEF1A to actin proved to be compromised, which might affect actin conformational stability and therefore the actin cytoskeleton organization, ultimately leading to the induction of apoptosis. In fact, the decrease in the cytosolic levels of eEF1A during acetic acid-induced apoptosis led to alterations in the actin cytoskeleton [290] even though the F-actin structures were unaffected

[346]. The mammalian eEF1A isoform eEF1A1 was also shown to have a crucial role in STS-induced apoptosis in HeLa cells. In contrast to yeast, silencing of eEF1A1 mRNA increases susceptibility of HeLa cells to the apoptotic stimulus, suggesting the performance of a pro-survival role by eEF1A1, indicating that this translation factor is also an important player in mammalian cell death processes. Nevertheless, further studies using different apoptotic stimuli are crucial for a better understanding of the eEF1A role in apoptosis. Conservation of the eEF1A1-regulated actin cytoskeleton organization is also maintained from yeast to mammalian. Epifluorescence microscopy analysis reveals that silencing of eEF1A1 leads to alterations in the actin cytoskeleton, which are more pronounced upon the STS-induced apoptosis. These results suggest a role for the translation factor eEF1A unrelated to the translation process during the course of the apoptotic process both in yeast and mammalian in which eEF1A most likely acts as a pro- or anti-apoptotic proteins depending on the apoptotic process triggered. Nevertheless, in yeast, this role proved not to be mediated by metacaspase, unlike the alterations observed in levels of other translation factors during yeast acetic acid-induced apoptosis. Although a direct interaction and cleavage of translation factors by metacaspase could not be proven, an indirect regulation of eIF4A levels and of eIF2α phosphorylation, suggests a regulation of Gcn2p kinase activity, by metacaspase during acetic acid-induced apoptosis.

The data obtained open new perspectives for the elucidation of the molecular cascade regulated by metacaspase activation. The specific cleavage of GAPDH, which in mammalian cells acts as a repressor of cap-independent translation, and the regulation of some translation factors levels, suggests a regulation of the translation process by this protease. Furthermore, the fragmentation of eEF1A and re-localization in mitochondria together with eEF2 suggest that during acetic acid-induced apoptosis, these factors are part of the apoptotic process leading to actin cytoskeleton alterations from yeast to mammalian cells.

CHAPTER 4

HSP90: translationally regulated modulators of cell death

Silva, A., Sampaio-Marques, B., Rodrigues, F., Holcik, M., Santos, M.A. and Ludovico, P.

Results described in this chapter will be published as follow:

Silva, A., Sampaio-Marques, B., Carreto, L., Rodrigues, F., Holcik, M., Santos, M.A. and Ludovico, P. HSP90 chaperones: translationally regulated endogenous modulators of yeast acetic acid-induced cell death. Manuscript in preparation.

The results described in this chapter were presented in the following national or international congresses:

International congresses:

- 8th IMYA – International Meeting on Yeast Apoptosis. Canterbury, Kent, UK. (2011).The role of HSP90 in yeast acetic acid-induced apoptosis. (Poster presentation).

National congresses:

- Microbiotec 11. Braga, Portugal. (2011). "HSP90: endogenous modulators of yeast acetic acid-induced apoptotic cell death". (Poster presentation).

4.1 ABSTRACT

Global mRNA translation impairment has been described during the course of apoptosis both in mammalian and yeast cells. Nevertheless, the molecular pathways modulating translation during different scenarios of apoptosis are still largely unexplored. Polysome profile analysis during yeast acetic acid-induced apoptosis revealed a global impairment of translation, correlated to the phosphorylation of eIF2α subunit by Gcn2 protein kinase (Chapter 2). Nevertheless, our previously reported proteomic analysis in the same apoptotic conditions revealed increased levels of heat shock protein 90 (HSP90) isoforms [215]. We herein demonstrate by microarray analysis of polysomal mRNAs combined with the HSP90 isoforms 5' untranslated region (5'UTR) expression in monocistronic reporter plasmids harboring an hairpin, that HSP90 isoforms are translated by a cap-independent mechanism mediated by internal ribosome entry site (IRES) elements in the 5'UTR of the mRNA. Genetic abrogation of HSP90 isoforms indicate divergent roles for HSP90 isoforms, Hsc82p acting as a pro-survival and Hsp82p as a pro-death molecule, in response to acetic acid treatment. Moreover, the deletion of *HSC82* leads to a severe necrotic cell death suggesting a role of these isoforms in the balance between apoptosis and necrosis, upon acetic acid treatment. These undisclosed functions of yeast HSP90 isoforms were confirmed through pharmacological inhibition of HSP90 activity, using 17-allylaminogeldanamycin (17AGG), and overexpression of each HSP90 isoform in acetic acid challenged cells. These results suggest that the efficiency of HSP90 isoforms mRNA translation is an important component of the cellular response to acetic acid. A role of HSP90 in the regulation of mammalian programmed cell death (PCD) has also been addressed, given the use of these proteins as attractive targets to cancer therapy. Our data show that different HSP90 isoforms are up-regulated depending on the drugs used to modulate the apoptotic cell death in the Acute Myeloid Leukaemia cell lines suggesting that, similar to yeast, in mammalian cells HSP90 isoforms play distinct functions.

4.2 INTRODUCTION

Programmed cell death (PCD) includes all types of cell death executed by regulated mechanisms and under rigorous molecular control, ranging from apoptosis to necrosis [27]. Nowadays, an increasing body of evidence is revealing the involvement of translation control in PCD processes [4, 76, 95, 243]. The specific fragmentation and/or alteration in the phosphorylation state of several translation factors during PCD [59, 286], prompts a selective cap-independent translation, mediated by internal ribosome-entry site (IRES) elements in the 5' untranslated region (5'UTR) of mRNAs, which directly recruit ribosomes independent of the interaction with the mRNA cap-structure [4, 109, 118, 347, 348]. Interestingly, in mammalian cells, IRES sequences were found in mRNAs of both inhibitors and inducers of PCD, such as XIAP and Apaf-1, respectively [101, 109]. In yeast, the knowledge on translational control of apoptosis is still scarce. During oxidative stress a reduction of global translation mediated by the phosphorylation of eIF2α by Gcn2 kinase (the amino acid control kinase) has been described [220]. Moreover, during yeast nutrient starvation an eIF4G-dependent IRES-mediated translation of several genes is required for an efficient response to stress [227]. IRES were reported in yeast transcriptional regulators such as transcription factors *FLO8* [227] and *YAP1* [234], transcriptional activators *HAP4* [228] and *MSN1* [227] and transcriptional repressor *URE2* [230] being involved in the response to yeast stress stimulus.

Heat shock protein 90 (HSP90) chaperones are a family of highly conserved proteins with crucial functions in protein folding/refolding [141, 144, 349] as well as in regulation of the balance between autophagy and proteasome activity [188, 350-355], with a role in cell proliferation, apoptosis and necrosis [32, 141, 143, 172-174, 185, 188, 223]. It has been described that the binding of HSP90 to Apaf-1, inhibits the formation of the apoptosome, and therefore the induction of apoptosis [140, 167]. Moreover, the interaction of HSP90 with the death domain kinase receptor interacting protein (RIP) was proved to be crucial for inhibition of tumor necrosis factor (TNF)-induced cell death [173]. HSP90 inhibitors, such as allylaminogeldanamycin (17AGG) and radicicol, proved to prevent necrosis induction by Fas- and tumor-necrosis factor receptor 1 in mammalian cells [172,

173] and by tunicamycin in yeast [223]. Besides the already described functions of HSP90 chaperones, in yeast, these isoforms also interact with a wide number of proteins [356], being required for pheromone signaling [357], mitochondrial proteins delivery [147, 357], transcriptional regulation [225, 226, 358, 359], and translational control, namely ribosome biogenesis [358], mRNA stability [358] and Gcn2 kinase maturation and regulation [360]. Nonetheless, despite the HSP90 chaperones crucial role in cell death, the translation of HSP90 mRNAs mediated by IRES was never addressed neither in yeast nor in mammalian cells.

Herein we show the occurrence of a translational rearrangement during the progression of acetic acid-induced apoptosis with the activation of a cap-independent IRES-mediated translation regulation of the HSP90 isoforms expression, among several others molecules, and their antagonistic role in this apoptotic process.

4.3 MATERIALS AND METHODS

Strains, media and treatments

S. cerevisiae strain BY4742 (*MAT*a *his3*Δ1 *leu2*Δ0 *lys2*Δ0 *ura3*Δ0) and its respective *HSC82* and *HSP82* genes knockouts (EUROSCARF, Frankfurt, Germany) were used. For acetic acid treatment, *S. cerevisiae* cells were grown until the middle exponential phase in liquid YPD medium containing glucose (2%, w/v), yeast extract (0.5%, w/v) and peptone (1%, w/v). Cells were initially harvested, ressuspended in fresh medium (pH 3.0) and incubated at 26ºC for 1h. Then cells were ressuspended (10^8 cells/mL) in fresh medium (pH 3.0) followed by the addition of 180 or 195 mM acetic acid and incubation during 15, 30, 60, 120 and 200 min at 26ºC with stirring (150 r.p.m.) with or without the presence of 10 and 100 μM of 17-allylaminogeldanamycin (17AGG). After the 200 min treatment, approximately 300 cells were spread on YPD agar plates and viability was determined by counting colony forming units after 2 days of incubation at 26ºC [199]. Cells were also harvested to further studies described below.

For construction of the Hsc82p- and Hsp82p-overexpressing strains, *HSC82* and *HSP82* were amplified by PCR (*HSC82* primers 5'-

GGATCCATGGCTGGTGAAACTT-3' and 5'-ATCGATTTAAAGATCTTCTTCAGA-3, *HSP82* primers 5'-GGATCCGGAAGCTTGATGACAGA-3' and 5'-ATCGATTTAAAGATCTTCTTCAGAA-3') using genomic DNA, isolated from *HSP82* and *HSC82* deleted cells, respectively, and cloned into the BamHI and ClaI sites of pUG35 (EUROSCARF, Frankfurt, Germany), which displays a MET25 promoter, generating pUG35*HSC82* and pUG35*HSP82*. Δ*hsc82* cells were transformed with pUG35*HSC82* and Δ*hsp82* cells with pUG35*HSP82*, generating strains *HSC82*^{overexp} and *HSP82*^{overexp}, respectively. *HSC82*^{overexp} and *HSP82*^{overexp} cells were grown until exponential growth phase (OD_{640nm}=0.5) on synthetic complete (SC) medium containing glucose (2%, w/v), yeast nitrogen base (0.17%, w/v, Difco), 300 mg/L of L-leucine, 50 mg/L of L-histidine and 50 mg/L of L-lysine at 26ºC with stirring (150 r.p.m.). Cells were washed, ressuspended in fresh SC medium (pH 3.0), treated with 160, 180 and 210 mM of acetic acid and incubated for 200 min at 26ºC with stirring (150 r.p.m.).

Table 6 - List of primers for construction of p281 monocistronic plasmids.

Gene	Primer sequences
HSC82 5'UTR	F: ATTGTTAAGATCTCCGCGGCTCGAGAGCTTTTAACCGTACTAGATAGTTTATA R: GGTAACGCCAGGGTTTTCCCAGTCGGATCCCATATTTCAGAATGATTCTATTTTTCT
HSP82 5'UTR	F: ATTGTTAAGATCTCCGCGGCTCGAGAGCTTAATCGGATTATTAACTCATACGCT R: GGTAACGCCAGGGTTTTCCCAGTCGGATCCCATATCTTTGCGTGTTTGTTTGTGCTT
TIF4632 5'UTR	F: ATTGTTAAGATCTCCGCGGCTCGAGATGTATTCGTTTCACTTGGCTCATTGTATATG R: GGTAACGCCAGGGTTTTCCCAGTCGGATCCCATAGTGCCTACAATTGATCTATTGTTC
CLN3 5'UTR	F: ATTGTTAAGATCTCCGCGGCTCGAGCACAATTTCTTTCTTGATTTTTTCTTCT R: GGTAACGCCAGGGTTTTCCCAGTCGGATCCCATCGTACAGAAAGCGTATCAAATCAGTG

For construction of p281*HSC82*, p281*HSP82*, p281*TIF4632* and p281*CLN3* plasmids, DNA encoding *HSC82*, *HSP82, TIF4632 and CLN3* 5'UTR was amplified by PCR using the primers described in Table 6, digested with BamHI and EcoRI, and cloned by homologous recombination into p281 vector at the 5'UTR of a β-galactosidase (LacZ) reporter gene with (p281h) or without a stable hairpin in the 5'UTR, and under the control of the GAL1/10 promoter [230, 361, 362]. Δ*hsc82* cells were transformed with p281 empty vector, p281h empty vector, p281h*HSC82* 5'UTR*,* p281h*TIF4632* or p281h*CLN3* plasmid and Δ*hsp82* cells p281 empty vector, p281h empty vector, p281h*HSP82* 5'UTR*,*

p281h*TIF4632 or* p281h*CLN3* plasmid. Cells were grown until exponential growth phase (OD_{640nm}=0.5) on synthetic complete (SC) medium containing glucose (2%, w/v), yeast nitrogen base (0.17%, w/v, Difco), 300 mg/L of L-leucine, 50 mg/L of L-histidine and 50 mg/L of L-lysine. Cells were washed, ressuspended in SC medium containing galactose (2%, w/v) and incubated at 26ºC or 37ºC with stirring (150 r.p.m.) for 18 hours.

Mammalian cells, namely, HL-60 and Jurkat cell lines, were cultured in DMEM medium (Invitrogen, Carlsbad, CA) supplemented with 10% fetal bovine serum (FBS), 1% glutamax, and 1% antibiotics mixture (Invitrogen) and grown at 37°C in a 5% CO_2 humidified chamber.

Polysome profile analysis

Yeast cells were grown to middle exponential phase and treated with acetic acid as described above. Five min before cells being harvested, cycloheximide (CHX) was added to a final concentration of 100 μg/mL to freeze protein synthesis elongation, cells were collected, washed twice and disrupted using lysis buffer [20 mM Tris at pH 8.0, 140 mM KCl, 1.5 mM $MgCl_2$, 0.5 mM DTT, 100 μg/mL CHX, 1 mg/mL heparin and 1% Triton X-100] and glass beads (Sigma). 40 units A_{280nm} were loaded onto 11 mL 15 - 50 % sucrose gradients containing 20 mM Tris-HCl at pH 8.0, 140 mM KCl, 5 mM $MgCl_2$, 0.5 mM DTT, 100 μg/mL CHX and 500 μg/mL heparin. Gradients were centrifuged using a SW41 rotor (Beckman-Coulter) at 35000 rpm for 2 hours and 45 min at 4ºC. Polysomal profiles were visualized by monitoring RNA absorbance at 254nm using a Bio-Rad Biologic LP system adapted for this use. Monosomal and polysomal fractions of the gradient were collected into tubes containing 8M guanidine-HCl and stored at – 80 ºC. In order to obtain sufficient quantity of mRNA for microarrays analysis, identical fractions were pooled into a single tube.

Polysomal RNA preparation

Polysomal mRNA was precipitated with ethanol 85%, extracted using phenol: chloroform and precipitated, first with 1.5 M lithium chloride (LiCl) for removing

any residual heparin, and then with 100% ethanol plus 110 mM sodium acetate, pH 5.3.

RT-PCR analysis

Total RNA isolated from both polysome profile fractions and mammalian cell lines reverse transcription to cDNA was carried out using the First-Strand cDNA synthesis kit (GE Biosciences). The quantitative PCR was performed on a CFX96 Touch real-time thermocycler (Bio-Rad) using SsoFast EvaGreen Supermix (Bio-Rad) and gene-specific primers as described in Table 7.

Table 7 - List of primers for quantification of mRNA expression by RT-PCR and their efficiency (Eff).

Gene	Primer sequences	Eff (%)
TIF4632	F: TCCGAGGAGACATTAGAGTCCG R: ACCGAACCTTCAAGAGTTGCC	99.1
HSC82	F: CCGGTGAATCTCTAAAGGCA R: ATCAATTGGGTCGGTCAAGA	96.3
HSP82	F: GAGTTGACGAAGGTGGTGCT R: ATGCAAAGGAAGTTGGTTCG	97.9
CLN3	F: GCCCCTTTGGAAGCTTTCATT R: TGGCACCCAATTTGATCTCG	98.4
TIF34	F: CCTCTAAACACCGCCGTAAT R: CAAACTTACCTTCGTTGGCA	99.7
CAF20	F: CTGTGCCAGTTGCTACCATT R: AACCAAGAATTGGCTTGTCC	99.4
CIT2	F: GGTCATGCTGTGCTAAGGAA R: AGTCAATACGCCAGGTGCTA	99.6
COX3	F: TTCCATTCAGCTATGAGTCCTG R: CGGTAGGTTGTACAGCTTCAAT	99.8
HSP104	F: AAGCGAGAAGTATGCGGTCT R: AAAGCCACCTTCATCGTACC	99.0
ACT1	F: GATCATTGCTCCTCCAGAA R: ACTTGTGGTGAACGATAGAT	98.2
TDH2	F: CCGCTGAAGGTAAGTTGA R: CGAAGATGGAAGAGTTAGAGT	95.1
PDA1	F: TGACGAACAAGTTGAATTAGC R: TCTTAGGGTTGGAGTTTCTG	94.8
TUB2	F: TACCACATCCATTGCTGAG R: CACCTTCTTCCATACCTTCA	93.2
HSP90AA1-1	F: GGCTTCAGCTAGTGGGGTCT R: TTCACCTCAGGCTCATGACA	95.3
HSP90AA1-2	F: GGTCCTGTGCGGTCACTTAG	99.8

	R: ATCAACTGGGCAATTTCTGC	
HSP90AB1	F: GTCTGGGTATCGGAAAGCAA R: CTGCCTGAAAGGCAAAAGTC	99.5
HSP90B1	F: GAAGGGGACTTGAGACTCACC R: TCCACATCAACTTCATCGTCA	98.6
HSP90N	F: TCTGGTGAATTTCCTGTTTCC R: GACATGGGGGACATCAGAAC	97.1

Relative expression levels were determined using the standard curve method. Controls lacking reverse transcriptase (RT) demonstrated no significant genomic DNA amplification.

Microarrays analysis

Reverse transcription, cDNA transcription, cRNA labelling with Cyanine 3-CTP and hybridization was carried out using the One-Color Microarray-Based Gene Expression Analysis (Low Input Quick Amp Labeling) kit (Agilent Technologies). Before hybridization, free dye was removed using RNeasy mini spin columns (Quiagen), and the efficiency of cRNA synthesis and dye incorporation (labelling efficiency in pmol Cy3/μg cRNA) was measured by spectrophotometry (NanoDrop 1000, Thermo Fisher Scientific). Each hybridization was carried out using 600 ng of Cyanine 3-labelled cRNAs and the Yeast Gene Expression Microarray (V2: G4813A, Agilent Technologies), for 17 hours at 65ºC, in an Agilent hybridization oven. Microarrays were scanned using the Agilent DNA Microarrays Scanner G2565AA and raw data was extracted using the Agilent feature extraction protocol GE1_105_Dec08 (PerkinElmer).

Data normalization and analysis

Using the normalized M values (log2 ratios) obtained, statistical differences were calculated using the *t*-test. Differentially expressed genes were identified for a False Discovery Rate below 0.001 (FDR < 0.001). Functional analysis of expression data obtained was done using Expander software. The data sets are were submitted to ArrayExpress (http://www.ebi.ac.uk/arrayexpress/).

Immunoblot

For immunoblot analysis, untreated or acetic acid-treated cells were collected and disrupted using glass beads in lysis buffer [1% v/v Triton X-100, 120 mM NaCl, 50 mM Tris-HCl pH 7.4, 2 mM EDTA, 10% v/v Glycerol, 1 mM PMSF and Complete Mini protease inhibitor cocktail (Roche, Mannheim, Germany)]. From total protein extracts, 40 μg were resolved on a 12% sodium dodecyl sulfate polyacrylamide gel electrophoresis (SDS-PAGE) and transferred to an nitrocellulose membrane (Amersham) over 90 min at 100 V. Membranes were then probed with polyclonal rabbit Ser51 phosphorylated eIF2α antibody (1:2000, Upstate), monoclonal rat anti-HSP90 (1:1000, Calbiochem) and polyclonal goat anti-actin (1:5000, kindly provided by Campbell Gourlay). Horseradish peroxidase (HRP)-conjugated anti-rabbit, anti-rat and anti-goat IgG secondary antibody were used, at a dilution of 1:5000 and detected by enhanced chemiluminescence.

β-galactosidase activity (LacZ)

LacZ activity was measured following the protocol described in the Clontech Yeast Protocols Handbook using O-nitrophenyl-β-D-galactopyranoside (ONPG) as a substrate. Cells were disrupted using glass beads in Z buffer [60 mM $Na_2HPO_4.7H_2O$, 40 mM $NaH_2PO_4.H_2O$, 10 mM KCl, 1 mM $MgSO_4.7H2O$, 0.27% (v/v) β-mercaptoethanol].

TUNEL assay

DNA strand breaks were assessed by a TUNEL assay with the In situ Cell Death Detection Kit, POD (Roche Applied Science, Indianapolis, IN). Yeast cells were initially fixed with 3.7% formaldehyde followed by digestion of the cell walls with lyticase. After preparation of cytospins, the slides were rinsed with PBS, incubated in permeabilization solution (0.1%, v/v, Triton X-100 and 0.1%,w/v, sodium citrate) for 3 min on ice, rinsed twice with PBS, and incubated with 10 μL of TUNEL reaction mixture (terminal deoxynucleotidyl transferase and FITC-dUTP) for 60 min at 37ºC . Finally, the slides were rinsed three times with PBS and a coverslip was mounted with a drop of anti-fading agent Vectashield (Molecular Probes, Eugene, OR) and with 2 μL of 50 μg/mL propidium iodide (PI, Molecular

Probes) solution in Tris buffer (10 mM, pH 7.0) with $MgCl_2$ (5 mM) and RNase (0.5 μg/mL). Cells were visualized with an Olympus PlanApo 60X/oil objective, with a numerical aperture of 1.42.

Statistical analysis

Arithmetic means of cell survival rates are presented with standard deviation with a 95% confidence value. Statistical analysis was carried out using independent samples *t*-test analysis. A p-value <0.05 was assumed to denote a significant difference.

4.4 RESULTS

4.4.1 Microarray analysis of mRNAs translated during acetic acid treatment

Data herein presented showing that the elongation factors and eIF4G levels were unaffected for a long period of the acetic acid treatment (Figure 10), together with our previous proteomic data revealing that some protein levels are increased under the same conditions [215], suggests that acetic acid treated cells and capable of cap-independent translation. Thus, microarray profiling of polysomal mRNAs of acetic acid treated cells was assessed (Figure 30). With this purpose, RNA was extracted from independent cultures, polysomal profile was performed and polysomal fractions (Figure 30A), corresponding to the fractions in which mRNAs are being actively translated, were collected for further RNA purification, reverse transcription, labeling using Cy3 and hybridized to Agilent Yeast Gene Expression Microarray (V2:G4813A). The data obtained were submitted to ArrayExpress. Data analysis revealed different translational profile at 0, 15 and 30 min (Figure 30B, 30C, 30D). A 2-fold cut-off value was used to analyse the translatomics by cross-time point's comparison. The mRNA profile of polysomal fractions revealed 323 mRNAs up-regulated genes (Figure 30BI - blue dots) and 132 down-regulated mRNAs (Figure 30BI – red dots) after 15 min of acetic acid treatment, corresponding to 5.1% and 2.1% of the total number of mRNAs analysed (6392 genes in the array), respectively. After 30 min of treatment the cluster of the mRNAs altered showed only 165 up-regulated mRNAs (Figure 30BII

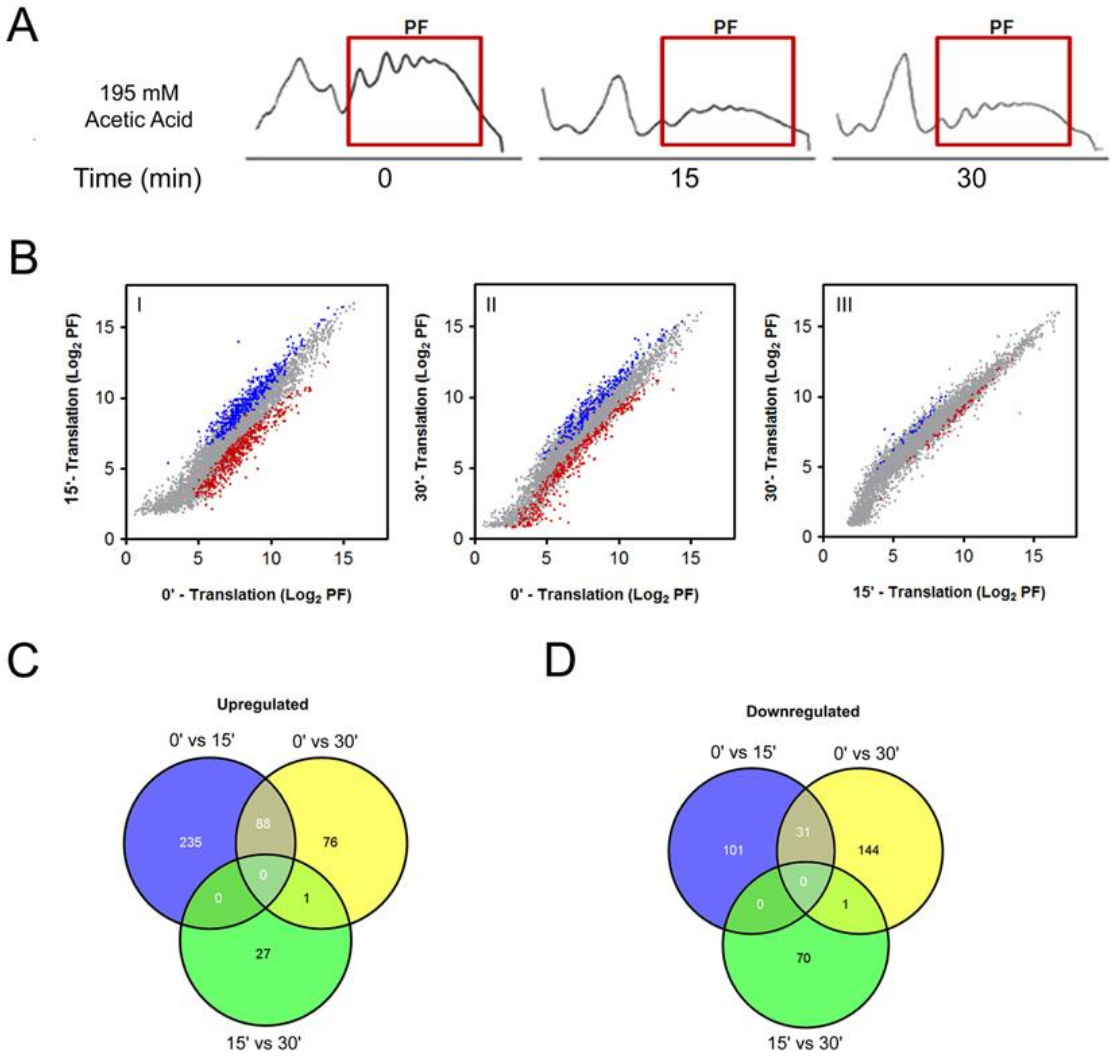

Figure 30 - Microarray analysis of mRNAs translated during acetic acid treatment. (A) Polysomal fractions (PF) of the polysomal profiles of yeast wild type cells untreated (0 min) or treated with acetic acid for 15 min and 30 min collected for microarray and RT-PCR analysis. (B) Graphical representations of the translational microarray data for mRNAs altered from 0 to 15 min (I), 0 to 30 min (II) and 15 to 30 min (III) of acetic acid treatment. The mRNAs in polysomal fractions at 15 min or 30 min of acetic acid treatment (log_2 PF) have been plotted against the mRNAs in polysomal fractions at 0 min of acetic acid treatment (control). Venn diagram of the (C) upregulated and (D) downregulated mRNAs at 15 min and 30 min of acetic acid treatment when compared with control. The data sets were submitted to ArrayExpress (http://www.ebi.ac.uk/arrayexpress/).

- blue dots) and 176 down-regulated mRNAs (Figure 30BII - red dots). These mRNAs correspond to 2.6% and 2.7% of the total number of genes mRNAs analysed, respectively. The clustering of the mRNAs altered from 15 to 30 min revealed 28 up-regulated mRNAs (Figure 30BIII - blue dots) and 71 down-regulated mRNAs (Figure 30BIII - red dots) corresponding to 0.65% and 1.11% of the total number of mRNAs analysed.

A Venn diagram for the up- and down-regulated mRNAs at 15 and 30 min of acetic acid treatment was obtained corroborating the dot plots presented. The Venn diagrams showed that from 15 to 30 min 88 mRNAs are maintained up-regulated and 31 down-regulated (Figure 30C and 30D). These results showed that up-regulation of some mRNAs is maintained from 15 to 30 min, but most of the altered mRNAs at each time point was different, suggesting the occurrence of a remodelling of the translational process during the period from 15 to 30 min of the acetic acid treatment. The data points to an active translation of specific mRNAs under conditions of cap-dependent translation impairment.

The acetic acid treatment induces a progressive decline of survival along the treatment time course (Figure 8A), compatible with a first response to the imposed stress and a later activation of the apoptotic cell death. Therefore, after 15 min of acetic acid treatment most of the up-regulated mRNAs are probably involved in the cells response to the acid stress. mRNAs up-regulated after 15 min of acetic acid treatment revealed several known apoptotic regulators such as the anti-apoptotic *CDC48* [189] and *SAP30* [363] and the pro-apoptotic *FIS1* [200], among other mRNAs such as the translation initiation factors eIF3 (*TIF34*), responsible for the ribosome scanning, and eIF4G (*TIF4632*), important for the IRES-mediated translation (Attachment II, Table 1). At this time point we could also detect *HSC82, ILV3*, *LYS7* and *THR1* which were also found upregulated in a proteomic analysis of acetic acid treated cells [215], and *CAF20*, a described inhibitor of cap-dependent translation [364] through the interaction with eIF4E (Attachment II, Table 1). However, at 30 min of acetic acid treatment about 20% of the cells have lost the proliferative capacity being committed to death. Thus, the up-regulated mRNAs at this time point may also be involved in the activation and progression of the apoptotic cascade. After 30 min of acetic acid treatment up-regulation of

CAP20, *CDC48*, *SAP30* and *HCS82* is maintained, as well as other mRNAs such as *DNM1*, involved in acetic acid-induced mitochondrial fission [200], and the *HSP82* chaperone, also found up-regulated in the proteomic analysis [215]

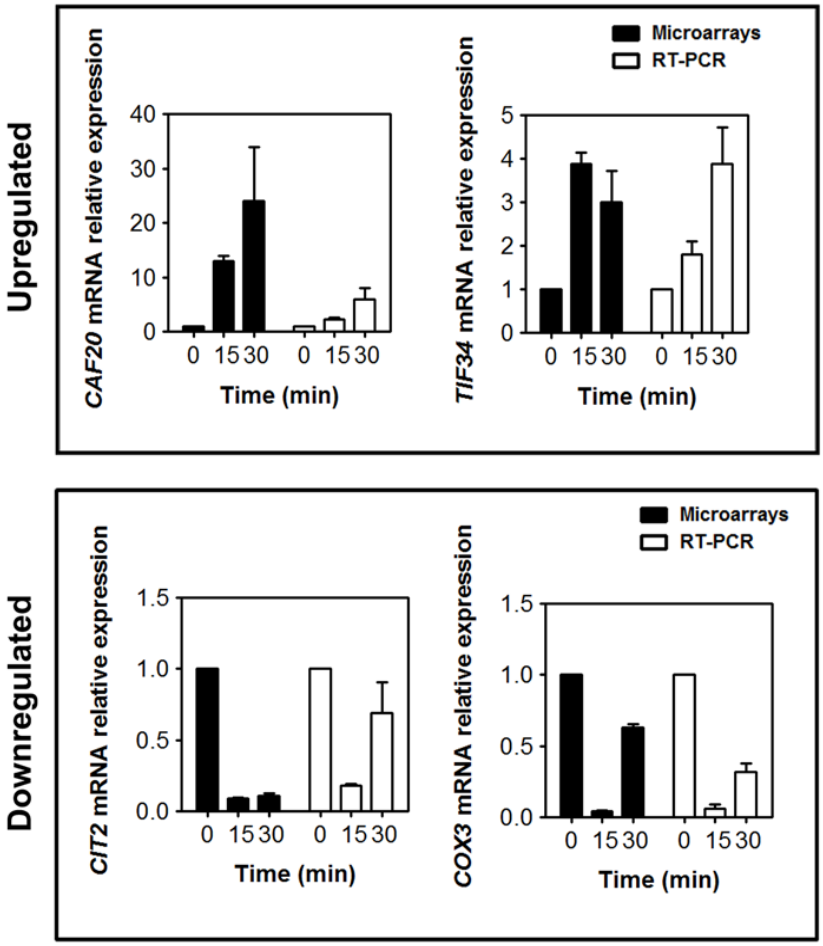

Figure 31 – Validation of microarray data by RT-PCR analysis of selected genes. Microarray and RT-PCR data are shown for up-regulated mRNAs *CAF20* and *TIF34* and down-regulated mRNAs *CIT2 and COX3* in polysomal fractions from yeast cells challenged with acetic acid for 0, 15 and 30 min. The values are expressed relative to untreated control cultures and are the means of triplicate microarray and RT-PCR determinations.

(Attachment II, Table 3). Since at 15 and 30 min of acetic acid treatment a heterologous population of cells mounting a response to the acid stress and cells activating the apoptotic cascade is present, it is expected that in the microarray analysis mRNAs involved in both process are found up-regulated under the regulation of a cap-independent translation.

The microarrays results were validated by RT-PCR analysis of mRNAs found altered in the polysomal fractions of the acetic acid treated cells using the same RNA samples. In fact, RT-PCR analysis confirmed the general tendency detected by microarray analysis (Figure 31). For this validation both mRNAs found up-regulated and down-regulated in the polysomal fractions at 15 and 30 min of acetic acid treatment were used. We were able to confirm the up-regulation of *TIF34* and *CAF20* mRNAs and the down-regulation of *COX3* and *CIT2* mRNAs *oth* at 15 and 30 min of incubation with acetic acid. Although some variation in the levels of each mRNA was observed from microarray to RT-PCR analysis, the tendency of the levels of each mRNA is maintained in both analyses (Figure 31).

4.4.2 Functional classification of mRNAs regulated during acetic acid treatment

Microarray results were also analysed and grouped into functional categories according to the Expander software TANGO tool and the *Saccharomyces* Genome Database GO Term Mapper (db.yeastgenome.org/cgi-bin/SGD/GO/goTermMapper).

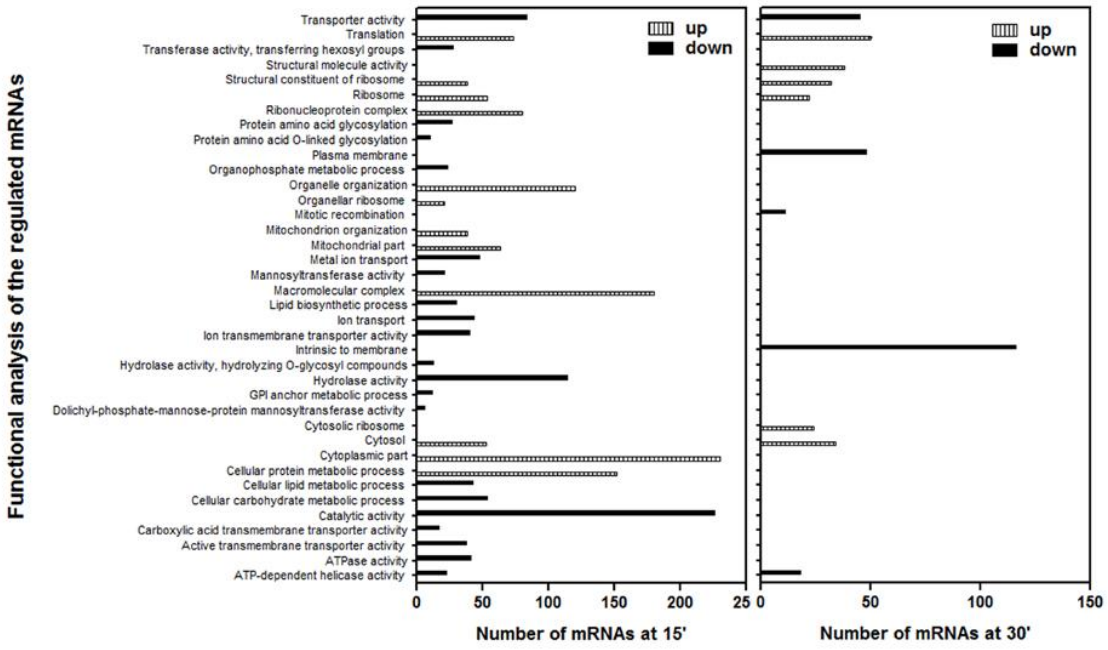

Figure 32 - Functional analysis of the regulated mRNAs in microarray analysis of yeast cells treated with acetic acid during 15 min (15') and 30 min (30').

Fifteen minutes of incubation with acetic acid induced the translation of mRNAs involved in different functional categories such as translation with the up-regulation

of the initiation factors eIF3, eIF4G, and the inhibitor of cap-dependent translation, *CAF20* [364] and several structural constituents of the ribosomes (Figure 32 and Attachment II, Table 1). On the other hand, several of the reduced mRNAs at 15 min participate in different metabolic processes such as transport, organophosphate, lipid and carbohydrate metabolism (Figure 32 and Attachment II, Table 2). However, functional categories analysis of the mRNAs whose expression was up-regulated at 30 min, revealed a shorter list of activated functions, exposing mainly cellular functions related to the ribosomal biogenesis and regulation of the translation process (Figure 32 and Attachment II, Table 4).

At 30 min of acetic acid treatment besides the up-regulation of *HSC82* mRNA, already detected at 15 min, *HSP82* mRNA was also increased, suggesting a role for HSP90 chaperones in acetic acid response. Heat shock protein 90 (HSP90) isoforms, HSC82 and HSP82 were both found up-regulated during acetic acid treatment suggesting a role for HSP90 chaperones in acetic acid-induced apoptosis which will be further investigated.

4.4.3 HSP90, IRES chaperones translated during acetic acid treatment

mRNAs encoding molecular chaperones HSP90, namely *HSC82* and *HSP82* were found up-regulated in the polysomal fractions of yeast cells challenged with acetic acid, both by microarrays analysis and by RT-PCR (Figure 33A). The *HSC82* mRNA levels at 15 min were higher than those from *HSP82*, about 4 fold, but at 30 min this effect was reverted and *HSP82* mRNA levels increased about 25 fold (Figure 33A). In fact, the percentage of *HSC82* and *HSP82* mRNA in monosomal and polysomal fractions was not altered upon 15 min or 30 min of acetic acid treatment (Figure 33C, 33D), demonstrating that although cap-dependent translation initiation was impaired (Figure 8, 9, 10), this did not affect HSP90 isoforms translation. The increased HSP90 isoforms mRNAs detected in polysomal fractions was shown to have an imprint in total cellular RNAs (Figure 33E) and protein levels (Figure 33F). The RT-PCR analysis of total cellular RNA, performed in acetic acid treated cells revealed an increase in the levels of both isoforms, *HSC82* and *HSP82*, dependent on the concentration of acetic acid tested (Figure 33E). Supporting the data obtained in polysomal fractions, *HSP82* displayed

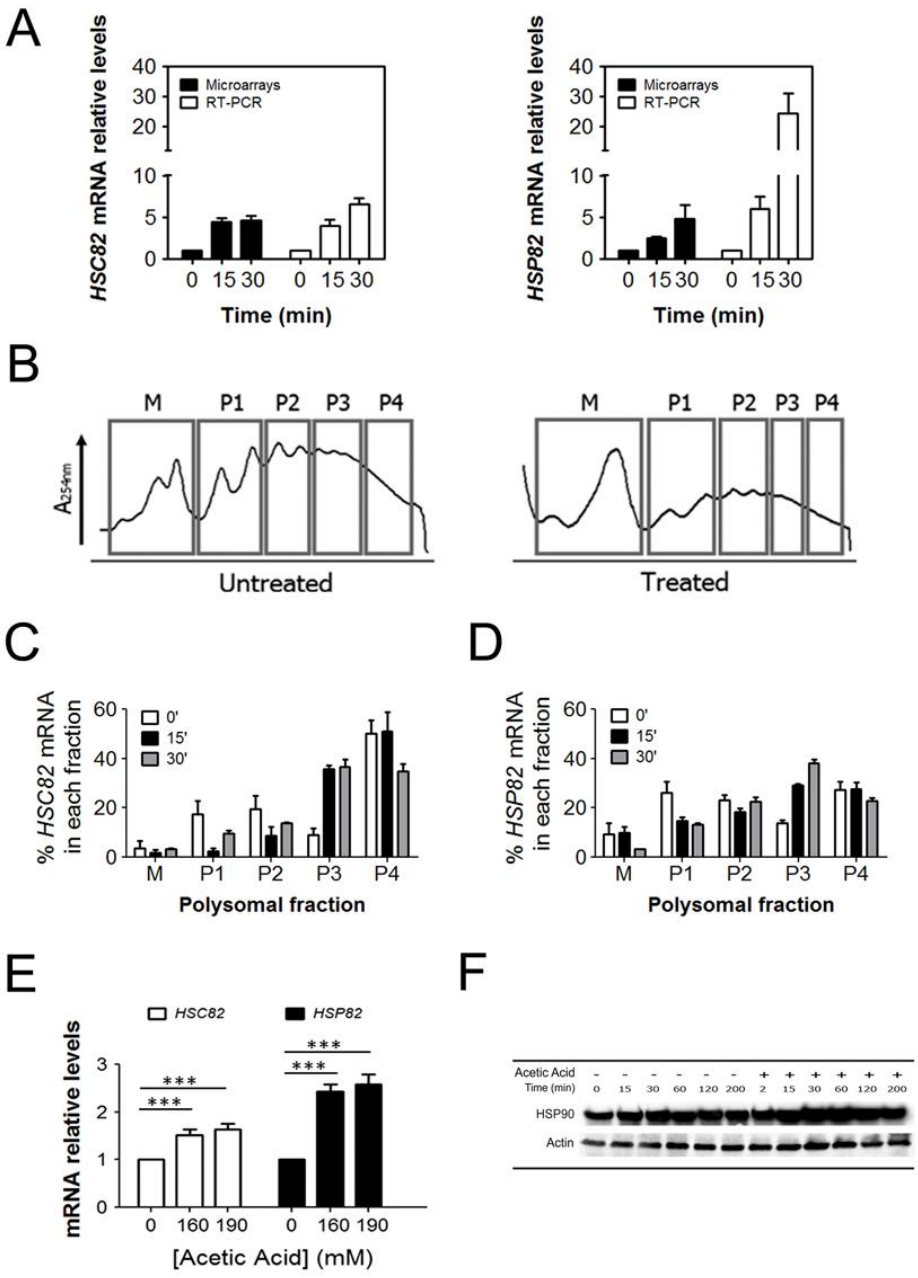

Figure 33 - HSP90 isoforms translation during acetic acid treatment. (A) Microarray and RT-PCR of *HSC82* and *HSP82* mRNAs levels in polysomal fractions from yeast cells challenged with acetic acid for 0, 15 and 30 min. The values are expressed relative to untreated cultures and are the means of triplicate microarray and RT-PCR determinations. (B) Illustration of the polysomal fractions from which mRNAs were extracted and analysed by RT-PCR (M, monosomal fraction; P1, P2, P3 and P4, polysomal fractions). RT-PCR of (C) *HSC82* and (D) *HSP82* mRNA expression in polysomal fractions demonstrate their translation upon 15 min treatment with acetic acid. (E) RT-PCR analysis of *HSC82* and *HSP82* expression in total mRNA of yeast cells after 200 min acetic acid treatment. (F) Immunoblot kinetic analysis of HSP90 in wild type cells after treatment with acetic acid.

higher relative mRNA levels when compared to *HSC82* (Figure 33E). Although immunoblot analysis did not allow the discrimination between Hsc82p and Hsp82p, the kinetics showed an increase of HSP90 isoforms levels in acetic acid-treated cells (Figure 33F). The levels of HSP90 progressively increased from 15 up to 60 min of acetic acid treatment after what a slight decrease was observed (Figure 33F).

These results showed that *HSC82* and *HSP82* mRNAs are translated during the acetic acid treatment, in spite of the cap-mediated translation impairment observed under these conditions (Figure 8, 9, 10), raising the question of whether or not these mRNAs could be translated by a cap-independent mechanism.

In mammalian cells, the presence of IRES in the 5'UTR of mammalian apoptotic regulators mediating their translation during an apoptotic stimulus has been described [4, 95-97, 99, 101, 108, 109, 111, 118, 243, 348, 365, 366]. In yeast, IRES are present in mRNAs of several transcriptional regulators controlling their contribution for an efficient stress response [227, 228, 230, 234]. However, the activation of this alternative translation mechanism has never been addressed in yeast apoptotic conditions. Thus, the increased mRNAs and protein levels of HSP90 isoforms observed during acetic acid treatment, despite the translation initiation impairment, led us to hypothesized that 5'UTR of HSP90 isoforms mRNA might enclose IRES sequence(s) mediating their efficient translation during acetic acid treatment.

To test whether the 5'UTR of HSP90 isoforms mRNA harbor IRES sequence(s) and are capable of internal translation initiation, the 5'UTR of *HSC82* and *HSP82* were inserted in-frame between the *GAL1* gene promoter and the mRNA of β-galactosidase (LacZ) reporter gene of monocistronic plasmids containing a stable hairpin structure, which abolishes cap-dependent translation (Figure 34) [230, 361]. These constructs were transformed in *HSC82* mutant cells or in *HSP82* mutant cells according to the 5'UTR in study. The determination of the LacZ reporter activity was assessed in cells after 18h of galactose induction at 26°C and at 37°C, the latter is a condition known to inactivate eIF4E activity and thus the cap-dependent translation [230]. As expected, constructs encoding LacZ mRNA with a 5'UTR derived from the *GAL1* gene (p281 empty) [230, 361]

showed a high translation efficiency at 26°C and a significant decrease upon incubation at 37°C in both strains (Figure 34). Insertion of a stable hairpin structure in the 5'UTR [230, 361] (p281h empty) resulted in a significant

Strain / Construct	Δ*hsc82* LacZ activity 26ºC	Δ*hsc82* LacZ activity 37ºC	Δ*hsp82* LacZ activity 26ºC	Δ*hsp82* LacZ activity 37ºC
GAL — LacZ	10341 (±2806)	2768 (±198)	9065 (±1546)	2215 (±253)
GAL — (hairpin) — LacZ	5 (±5)	3 (±1)	9 (±7)	5 (±4)
GAL — *TIF4632 5'UTR* — LacZ	313 (±80)	28 (±10)	261 (±126)	16 (±5)
GAL — *CLN3 5' UTR* — LacZ	7 (±2)	1 (±1)	5 (±3)	3 (±1)
GAL — *HSC82 5'UTR* — LacZ	302 (±32)	494 (±116)	-	-
GAL — *HSP82 5'UTR* — LacZ	-	-	3617 (±1051)	2283 (±381)

Figure 34 - HSP90 isoforms translation mediated by IRES. Expression of *HSC82*, *HSP82*, *TIF4642* and *CLN3* 5'UTR tagged with a β-galactosidase (LacZ) reporter gene in monocistronic plasmids under the control of the GAL1/10 promoter. LacZ activity (relative milliunits) was determined after 18 h induction of the cells in 2% galactose at the indicated temperature.

reduction of LacZ activity (Figure 34). Control plasmids harboring the *CLN3* 5'UTR, negative control [234], and *TIF4632* 5'UTR, positive control previously reported to harbor IRES in the 5'UTR [227], were constructed and transformed in both strains (Figure 34). *TIF4632* 5'UTR promoted an efficient translation as revealed by LacZ activity whereas *CLN3* 5'UTR did not display any IRES activity as demonstrated by the absence of LacZ activity (Figure 34).

The LacZ activity was significantly higher in cells expressing monocistronics plasmids under the control of *HSC82* 5'UTR or *HSP82* 5'UTR in the presence of a stable hairpin both at 26°C and 37°C (Figure 34). These results indicated that the *HSC82* 5'UTR and *HSP82* 5'UTR harbor IRES that allow a competent translation in conditions of cap-dependent translation impairment promoted either by the

presence of a stable hairpin or by the inhibition of eIF4E binding at the cap-structure at 37°C (Figure 34).

Altogether, these data reveal a new regulatory mechanism controlling translation during acetic acid treatment, a condition that we have previously shown to inhibit cap-dependent translation (Chapter 2). Furthermore, this IRES-mediated translation regulates HSP90 isoforms expression and most likely is involved in the regulation of the HSP90 increased mRNA levels observed during acetic acid treatment.

4.4.4 Modulation of HSP90 isoforms expression suggests a dual role of these chaperones in response to acetic acid

The data presented strongly suggests that Hsc82p and Hsp82p are translated by a cap-independent mechanism upon acetic acid treatment in conditions known to induce 50% of cell death [191, 215]. Thus, the contribution of these isoforms for the apoptotic process was studied. For such purpose, the susceptibility/resistance of *HSC82* and *HSP82* mutant cells to acetic acid treatment was determined. Deletion of *HSC82* resulted in an increased susceptibility while deletion of *HSP82* augmented the resistance to acetic acid treatment compared to wild-type cells (Figure 35A). These results indicate opposing roles for Hsc82p and Hsp82p in response to acetic acid treatment. Expression of *HSC82* or *HSP82* under a MET promoter in the respective deleted strains showed functional complementation and a reversion of the phenotype (Figure 35B and 35C). Due to the promoter's strength not only the phenotypes of the deleted cells were reverted but also Hsc82p was able to confer additional protection and Hsp82p to increase susceptibility to acetic acid (Figure 35B, 35C). These results strongly support antagonist roles for the HSP90 isoforms during acetic acid treatment. Hsc82p is suggested to be involved in a pro-survival pathway activated as a stress response while Hsp82 seems to be enrolled in a pro-death function upon acetic acid treatment. To further elucidate the HSP90 isoforms functions, wild-type, *hsc82Δ* and *hsp82Δ* cells were challenged with acetic acid in the presence of a HSP90 inhibitor, 17-allylaminogeldanamycin (17AGG). The inhibition of HSP90 in *HSP82* deleted cells had no effect on cell

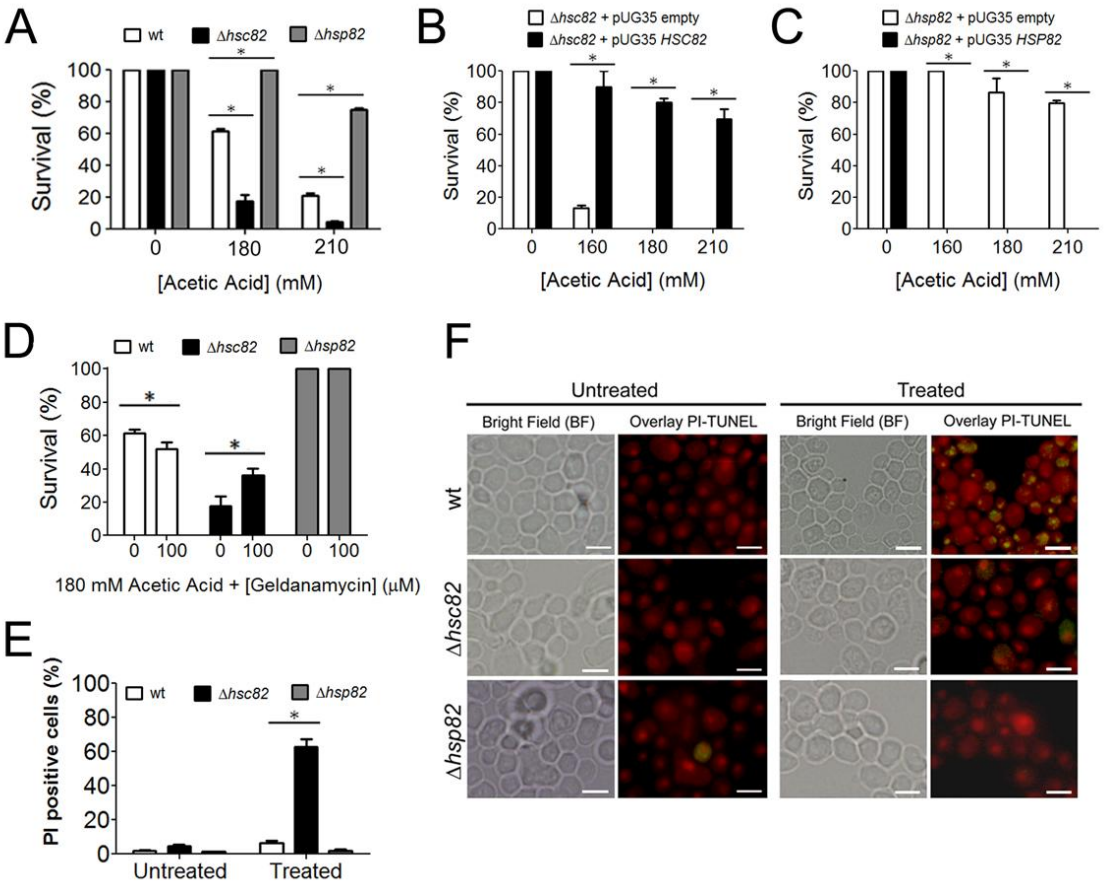

Figure 35 - Modulation of HSP90 isoforms expression suggests opposite roles for these chaperones during acetic acid treatment. (A) Comparison of the survival rates of wild type, Δ*hsc82* and Δ*hsp82 S. cerevisiae* cells after acetic acid treatment. Analysis of the survival rates of (B) Δ*hsc82* and (C) Δ*hsp82 S. cerevisiae* cells harboring a pUG35 plasmid expressing *HSC82* or *HSP82*, after treatment with acetic acid. (D) Comparison of the survival rates of wild type, Δ*hsc82* and Δ*hsp82 S. cerevisiae* cells treated with 180 mM of acetic acid after pharmacological inhibition of HSP90 activity, using 17-allylaminogeldanamycin (17AGG). (E) Propidium Iodide (PI) staining of wild type, Δ*hsc82* and Δ*hsp82 S. cerevisiae* cells after acetic acid treatment (180 mM) measured by flow cytometry. (F) Epifluorescence and bright field micrographs of untreated and acetic acid-treated (180 mM) wild-type, Δ*hsc82* and Δ*hsp82* cells displaying TUNEL reaction to visualize double-strand DNA breaks. Cells were co-stained with propidium iodide in order to facilitate nuclei visualization. Bar, 5 μm.

survival but in wild-type cells it resulted in increased acetic acid induced cell death and in *HSC82* deleted cells led to a moderated protection (Figure 35D). These data reinforce the opposite roles performed by the HSP90 isoforms in response to

acetic acid and attributes a pro-survival role for Hsc82 and a pro-death role for Hsp82.

The evaluation of the type of programmed cell death (PCD) occurring in each of the above described strains showed that despite the higher susceptibility to acetic acid treatment demonstrated by the *HSC82* deleted cells, almost no TUNEL-positive cells were observed by microscopy analysis (Figure 35F), contrarily to the well described phenotype of TUNEL-positive staining in the wild-type cells [191]. Moreover, propidium iodine (PI) staining of *HSC82* deleted cells revealed a high percentage of PI positive cells (Figure 35E), which did not occur in the *HSP82*-disrupted cells (Figure 35E), meaning that the membrane integrity of *HSC82* mutated cells was affected, therefore suggesting the occurrence of a necrotic cell death. These data also suggests that HSP90 isoforms are key molecules in governing the balance between apoptotic and necrotic cell death when cells are challenged with acetic acid. In yeast, HSP90 chaperones have been implicated in the modulation of necrotic cell death [221, 223], pointing Hsp82p as the HSP90 isoform involved in yeast necrotic cell death.

4.4.5 HSP90 regulation of Gcn2p kinase activity during acetic acid-treatment

Among the described functions of HSP90, these chaperones have a crucial role in the maturation and regulation of Gcn2p kinase activity [360]. HSP90 interaction with Gcn2p is abolished in conditions leading of accumulation of uncharged tRNAs such as amino acid starvation, derepressing the mature Gcn2p mediated phosphorylation of the subunit α of the translation initiation factor 2 (eIF2α) and consequently leading to the inhibition of cap-dependent translation [360]. However, the treatment of cells with 17AGG inhibits HSP90 activity and its release from Gcn2p, blocking the function of Gcn2p in the phosphorylation of eIF2α and translation regulation [360]. Since translation impairment has been observed upon acetic acid treatment, mediated by the Gcn2p kinase regulation of eIF2α phosphorylation (Figure 10, 11), we hypothesized if the role of HSP90 chaperones in response to acetic acid was related with the regulation of the Gcn2p kinase activity. To evaluate this hypothesis, immunoblot kinetic analysis of eIF2α

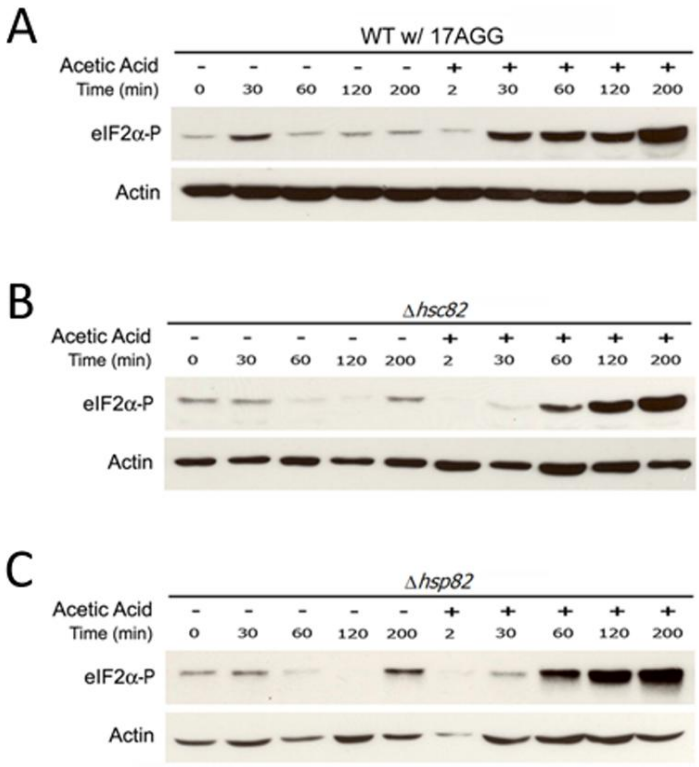

Figure 36 – HSP90 regulate Gcn2p activity at early time points of the acetic acid treatment. Immunoblot kinetic analysis of eIF2α phosphorylation in (A) wild-type *S. cerevisiae* cells after treatment with 195 mM acetic acid upon pharmacological inhibition of HSP90 activity using 17AGG, and in (B) Δ*hsc82* or (C) Δ*hsp82* cells treated with 195 mM acetic acid.

phosphorylation levels in *HSC82* and *HSP82* deleted cells and wild-type cells treated with 17AGG, was performed. The results obtained showed a delay in the phosphorylation of eIF2α in all the conditions upon acetic acid treatment (Figure 36) when compared to wild-type cells (Figure 10A), suggesting a role of HSP90 isoforms in the regulation of Gcn2p kinase activity in the first time point of acetic acid treatment, crucial for the early inhibition of cap-dependent translation initiation. However, at later time points this regulation does not occur, which could be explained by the recruitment of HSP90 chaperone for modulation of the acetic acid-induced apoptosis, and interaction with other client proteins.

4.4.6 HSP90 chaperones isoforms differential expression in mammalian cell lines

Mammalian cells contain three types of HSP90 chaperones: cytosolic HSP90, mitochondrial HSP90 (Trap-1), and endoplasmic reticulum HSP90 (Grp94) [367]. Prominent members of mammalian cytosolic HSP90 family are Hsp90alpha (HSP90AA-1, HSP90AA-2, and HSP90AB1) and Hsp90beta (HSP90B1) isoforms [141]. Hsp90beta is expressed constitutively to a higher level than Hsp90alpha, which is generally stress-inducible [141]. HSP90 chaperones are the only HSPs targeted in cancer therapy, namely in Acute Myeloid Leukemia (AML) therapy [186, 188], using the inhibitor of HSP90 activity, 17AGG.

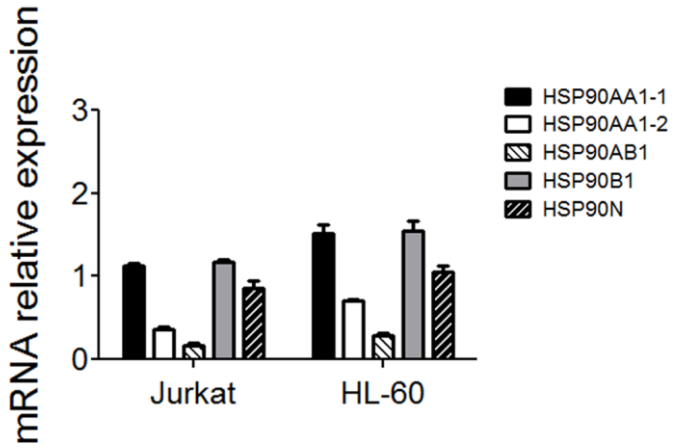

Figure 37 – HSP90 isoforms expression pattern in leukemic cell lines. RT-PCR analysis of mammalian HSP90 isoforms (HSP90AA1-1, HSP90AA1-2, HSP90AB1, HSP90B1 and HSP90N) mRNA levels in Jurkat and HL-60 cell lines.

However, the outcome is below expectations, probably due to the indiscriminated inhibition of HSP90 isoforms, instead of targeting the isoform(s) specifically implicated in AML. Our results showed that yeast HSP90 isoforms, Hsc82p and Hsp82p, are IRES-mediated translated, upon global translation impairment during PCD. The yeast data also showed the divergent roles played by each HSP90 isoform during PCD. Since HSP90 are conserved proteins from yeast to mammalian, with analogous described behavior and functions [141, 143, 188], it is of utmost importance to understand the contribution of each mammalian HSP90 isoform for the PCD process. Thus, the levels of each HSP90 isoform in human

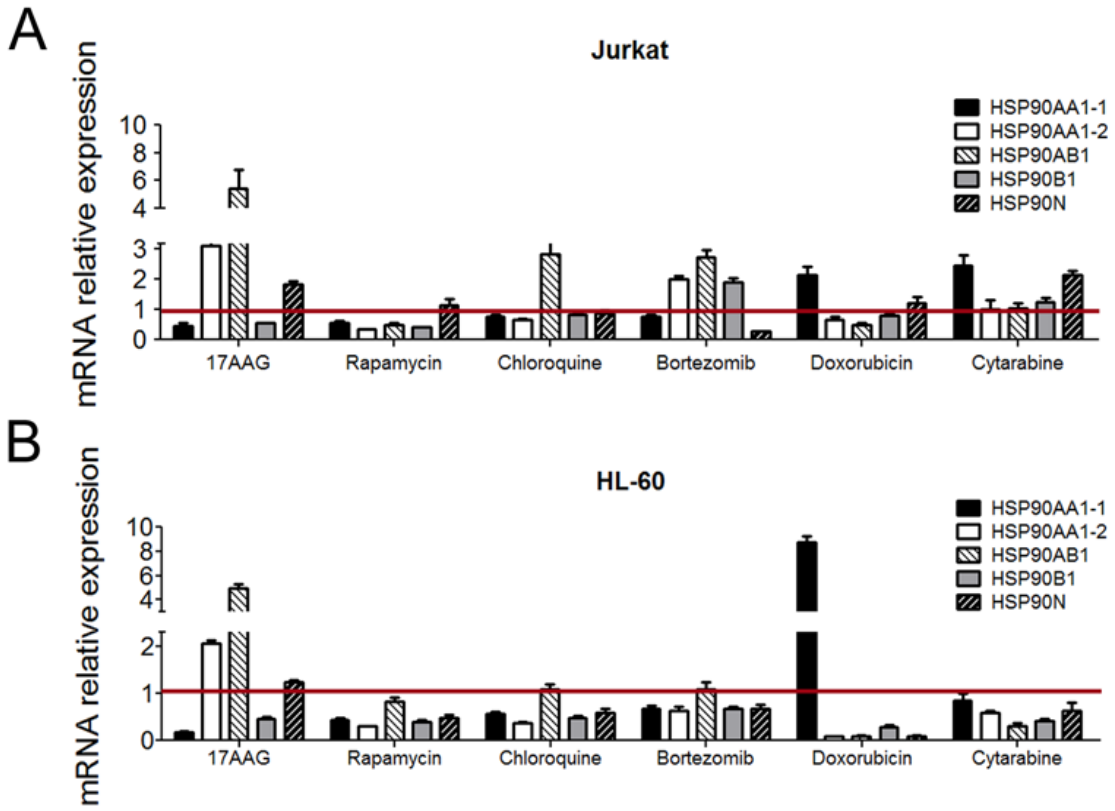

Figure 38 – HSP90 isoforms expression profile in leukemic cell lines. RT-PCR analysis of mammalian HSP90 isoforms (HSP90AA1-1, HSP90AA1-2, HSP90AB1, HSP90B1 and HSP90N) mRNA levels, relative to untreated cells, in (A) Jurkat and (B) HL-60 cell lines treated with 17AAG, rapamycin, chloroquine, doxorubicin or cytarabine.

leukemic cell lines, the AML HL-60 cell line and the acute T-lymphoblastic leukemia Jurkat cell line, were assessed. Results showed a similar pattern of expression of each HSP90 isoform both in HL-60 and Jurkat cell lines (Figure 37). However, leukemic cell lines treatment with drugs involved in the modulation of distinct cellular processes revealed the upregulation of distinct HSP90 isoforms (Figure 38A, 38B). The 17AGG inhibits HSP90 activity [174, 178, 186, 368], rapamycin inhibits TOR pathway and therefore activates the autophagic process [267, 272, 369-373], chloroquine inhibits the autophagic process [276, 277, 374], bortezomib inhibits the proteosome [375], and doxorubicin and cytarabine are two drugs widely used in AML therapy [376-379]. The data analysis revealed differential expression of the HSP90 isoforms correlated with the drug tested (Figure 38). The inhibition of HSP90 activity led to the accumulation of HSP90AA1-2 and HSP90AB1 mRNAs in the cell and the decrease in the levels of

HSP90AA1-1 and HSP90B1 mRNAs both in Jurkat and HL-60 cell line (Figure 38). In physiological conditions HSP90AA1-2 and HSP90AB1 mRNAs are more expressed that the other isoforms in these cell lines (Figure 37) and the inhibition of their activity might lead to the accumulation of correspondent mRNAs in the cell which will not be recruited for translation (Figure 38A, 38B). Activation of autophagy has been correlated with the decrease of the HSP90 activity [353, 355], which corroborated our results showing a decrease in the levels of all the HSP90 isoforms when cells were treated with rapamycin (Figure 38). The inhibition the autophagy using chloroquine did not induce a significant increase of HSP90 isoforms levels, with the exception of HSP90AB1 isoform which presented higher levels in Jurkat cell line (Figure 38A). Moreover, inhibition of proteosome by bortezomib induced an increase in the levels of HSP90AA1-2, HSP90AB1 and HSP90B1 in Jurkat cells (Figure 38A). However, the induction of apoptosis mediated by doxorubicin led to an increase in the levels of HSP90AA1-1 isoform and downregulation of all the others, particularly in HL-60 cells (Figure 38B). Cytarabine treated cells displayed higher levels of HSP90A1-1 and HSP90N isoforms in Jurkat cells and decrease in the expression of all the isoforms in HL-60 cells (Figure 38A, 38B).

These results combined suggest that each HSP90 isoform plays a distinct role in the cell, and depending on the stimulus distinct isoforms are activated. Using drugs known to affect the inter-regulatory processes of autophagy and ubiquitin-proteasome system, the HSP90 isoform HSP90AA1-2 and specially the isoform HSP90AB1 appear to be recruited and activated as modulators of these processes. However, drugs involved in the modulation of other pathways such as doxorubicin induce the translation of HSP90AA1-1 isoform. Doxorubicin and 17AGG, two drugs used in cancer therapy triggering two different apoptotic processes [160, 170, 173, 186, 379-384], induce the expression of different isoforms of HSP90, strongly suggesting the targeting of different client proteins by each HSP90 isoform involved in distinct molecular pathways. Therefore, the unveil of the specific proteins interacting with each HSP90 isoform will allow a better understanding of the mechanism regulating HSP90 isoforms functions in the cell for a more efficient cancer therapy with less secondary effects.

4.5 DISCUSSION

Over the past few years, the involvement of the translation process in the regulation of apoptosis has emerged as a crucial mechanism both in mammalian and yeast cells [59, 95, 215, 220]. Since translation is the final stage in the course of genetic information, regulation at this level leads to a direct response to changes in physiological conditions. During yeast *S. cerevisiae* acetic acid-induced apoptosis, a general amino acid starvation occurs [215] and a translation reduction might allow cells to conserve resources for a quick rearrangement of the gene expression in response to the stimulus. Microarrays kinetic analysis of polysomal mRNAs translated during acetic acid treatment, showed a decrease in the mRNA levels throughout the experiment. However, it revealed a list of up-regulated mRNAs at 15 and 30 min of acetic acid treatment, putatively involved in the cellular response to the acid stress or in the activation of the apoptotic process, since this analysis was performed at time points in which only a small percentage of the cells are undergoing apoptosis. HSP90 isoforms, *HSC82* and *HSP82,* were found upregulated in the polysomal mRNAs, although *HSP82* presented a higher fold change that *HSC82* after 30 min of acetic acid treatment. Furthermore, insertion of HSP90 isoforms 5'UTR and eIF4G at the 5'UTR of a monocistronic LacZ reporter gene harboring a hairpin showed us that translation of these chaperones as well as of eIF4G is mediated by the presence of IRES in the 5'UTR of the mRNAs allowing the translation of these isoforms by a cap-independent mechanism upon the apoptotic stimulus. These results corroborate all the previous results, pointing for the activation of an alternative IRES-mediated translation upon inhibition of cap-dependent translation during acetic acid treatment, controlling the translation of HSP90 and eIF4G. Nevertheless, the Hsc82p and the Hsp82p isoforms appear to play antagonist roles during the apoptotic process. Hsc82p play an anti-apoptotic and Hsp82p a pro-apoptotic function upon acetic acid treatment. Moreover, a balance between the two isoforms levels, during acetic acid treatment is crucial for the induction of apoptosis. The absence of Hsc82 leads to a necrotic cell death upon acetic acid treatment, probably due to the absence of an anti-apoptotic factor to balance the effect of the pro-apoptotic factor Hsp82. A role for HSP90 chaperones in the modulation of yeast necrotic cell death has been

addressed [223]. Moreover, interaction between the pro-apoptotic isoform Hsp82p and the yeast homologue of mammalian caspases, metacaspase, has been reported [209]. Therefore, a study of the role of Hsp82p in the folding of metacaspase upon its activation during the apoptotic process should be performed. Moreover, the dual role of HSP90 chaperones may be related with the fact that the different isoforms are responsible for the folding/refolding of different proteins playing distinct roles in different physiological conditions. HSP90 chaperones are target molecules for cancer therapy [141, 159, 174, 181, 185, 186, 188, 385]. The fact that in yeast, the two known isoforms of HSP90 chaperones, Hsc82p and Hsp82p, play distinct roles in the modulation of apoptotic cell death, and due to the high conservation of HSP90 chaperones from yeast to mammalians [141, 143], it is of utmost importance to understand the individual relevance of mammalian HSP90 chaperones for the PCD process in an integrated view using mammalian cells, namely AML cell lines. In fact, the levels of HSP90 isoforms, HSP90AA1-1, HSP90AA1-2, HSP90AB1, HSP90B1 and HSP90N, in cells treated with different drugs which target distinct cellular processes previously associated with a modulation of the apoptotic process [170, 177, 277, 374, 375, 384, 386-388], suggest that each HSP90 isoform has specific targets being involved in different processes which might be related to cell death or survival. These results suggest once more a conservation in the pathways/mechanism regulating PCD from yeast to mammalian cells, highlighting yeast as a good model for the study of apoptosis. Thus, future investigations using mammalian cells for the elucidation of the translation mechanisms regulating HSP90 expression, such as IRES, and the contribution of each HSP90 isoform to the PCD process is crucial for the screen of new drugs that directly act against the HSP90 isoform(s) involved in the disease for a more targeted less aggressive treatment.

Altogether, our findings reveal a new apoptotic regulatory mechanism mediated by the balance between the levels of HSP90 isoforms, Hsc82p and Hsp82p, in the presence of an apoptotic stimulus. This balance appears to be tightly regulated by the activation of an alternative mechanism of *HSC82* and *HSP82* isoforms mRNA translation mediated by the IRES sequences present in their 5'UTR. The simultaneous IRES-mediated translation of both isoforms, with

antagonistic roles in the cell during acetic acid treatment further supports a conservation of the translation regulatory mechanisms from yeast to mammalian cells placing yeast as a powerful tool in the study of the mechanism underlying the regulation of cap-independent translation during apoptosis.

CHAPTER 5

Concluding remarks and future prospectives

5.1 FRAMEWORK OF THE RESULTS

During evolution, organisms have to adapt to the surrounding environment in order to perpetuate the species, a mechanism called natural selection that Charles Darwin also liked to call “Survival of the fittest” [389]. Despite the divergent adaptation strategies undertaken by the different organism throughout evolution, they share the same origin, the same molecular basis. Therefore, the main basic and housekeeping molecular pathways regulating cells fate are most likely conserved.

The phenotypical alterations induced by the activation of different types of programmed cell death (PCD), as apoptosis and necrosis, both in yeast and mammalian cells are widely recognized [27, 28, 30]. However, the knowledge of the molecular pathways behind these phenotypes is a continuous challenge in constant update. By itself this is an intricate task, and the fact that different PCD stimuli lead to the activation of distinct PCD pathways makes it even more complex.

Over the last years, the translation process has been described as a crucial piece in mammalian cells PCD puzzle [95, 348]. Alterations in the translation machinery, such as the fragmentation of translation initiation factors eIF3, eIF4B, eIF4G mediated by caspases and post-translational modifications of eIF2α and eIF4E leading to the inhibition of the cap-dependent translation during the PCD process [59] prompt an alternative translation mechanism. This alternative translation is regulated by the presence of internal ribosome entry site (IRES) elements, usually at the 5’ untranslated region (5’UTR) of the mRNAs, which directly recruit ribosomes independent of the mRNA cap-structure [235, 390] but may also require the participation of canonical translation initiation factors such as the eIF4G, eIG4A, eIF3 and eIF2α [5, 227, 232, 235, 391-396]. IRES-mediated translation proved to be critical for cellular homeostasis and regulation of the cells fate upon triggering of the PCD process [4]. These sequences have been described not only in mRNAs related with the activation of the cell death cascade such as p53 [119], APAF-1 [109], c-myc [112], DAP5 [118] but also in mRNAs involved in the cell survival such as XIAP [132], HIAP2 [98], Bcl-2 [122] and HSP70 [125].

In yeast, the study of IRES-mediated translation is still an emergent field and a correlation between IRES and PCD has not yet been made. Nonetheless, IRES sequences have been identified in several mRNAs related to response to stress through transcriptional regulation, such as *FLO8* a transcription factor [227], *YAP1* [234], *HAP4* [228] and *MSN1* [227] transcription factors and activator, respectively, involved in the response to oxidative stress, *URE2 a* transcriptional repressor of genes involved in nitrogen catabolism [230], and eIF4G, a translation initiation factor crucial for yeast IRES-mediated translation [227].

5.2 TRANSLATION MODULATING OF YEAST PCD

A conservation in translation machinery alterations during apoptosis from yeast to mammalian cells was established by the observation of an impairment in translation initiation at early time points of acetic acid treatment through a drastic decrease in translation initiation factor eIF4A levels and the increased phosphorylation of eIF2α mediated by Gcn2p kinase, a key player in this apoptotic process. In mammalian cells, the phosphorylation of eIF2α is a common feature of different apoptotic processes [67, 72, 108, 242, 397] as well as in the response to stress conditions allowing cells to initiate a remodeling of the gene expression for a effective stress response [66, 108, 398]. The eIF2α phosphorylation or even a specific cleavage can be also mediated by caspases in the course of the apoptotic cascade as a mechanism of global translation inhibition [59, 64, 72, 399], allowing the activation of the IRES-mediated translation process [131, 390]. In yeast, the phosphorylation of eIF2α proved to be implicated in the apoptotic process since the deletion of *GCN2*, the only kinase described to be responsible for the phosphorylation of eIF2α in yeast [253, 256, 260, 261], leads to an increased resistance to acetic acid treatment together with a drastic decrease in the phosphorylation levels of eIF2α. Similar to what has been described in mammalian cells, during acetic acid treatment eIF2α phosphorylation is part of a regulatory process which inhibits global translation giving space for the activation of a selective IRES-mediated translation. In mammalian cells, IRES-mediated translation also requires the participation of canonical translation initiation factors

which vary with requirement of the IRES-containing mRNAs [4, 5]. Therefore, the analysis of our data suggests that eIF4A is not required for an IRES-mediated translation during acetic acid treatment, since the levels of this translation initiation factor decrease after 15 min of acetic acid treatment. On the other hand, the levels of eIF4G are maintained until later time points of the apoptotic process. In fact, in higher eukaryotes, IRES-mediated translation with the participation of eIF4G, with or without the interaction of eIF4A has been described [5, 400]. These evidences together with the fact that, in yeast, eIF4G is an IRES-containing factor involved in the efficient IRES-mediated translation in response to stress [227], further consolidates our hypothesis that an eIF4G-dependent IRES-mediated translation of mRNAs required for the apoptotic process, such as *AIF1*, occurs during acetic acid treatment.

Similar to mammalian cells apoptotic process, the alterations observed in translation initiation factors eIF4A and eIF2α upon acetic acid challenge appear to be mediated by metacaspase, the yeast homologue of mammalian caspases [40]. However, if this effect is mediated by the direct interaction of metacaspase with the translation factors, inducing their cleavage, or through indirect regulation of their levels is still not known and further studies should be performed. Nevertheless, metacaspase digestome analysis revealed a metacaspase substrate, the glycolytic enzyme glyceraldehyde-3-phosphate dehydrogenase (GAPDH). The extensive fragmentation of this enzyme during yeast apoptosis has been previously reported [211, 219, 401], but an association of this event to yeast metacaspase had never been made [219]. In mammalian cells, this enzyme is a known inhibitor of virus and mammalian mRNAs IRES-mediated translation [119, 134-138]. Hence, GAPDH is responsible for the inhibition/repression of cap-independent IRES-mediated translation in higher eukaryotes as a protective mechanism against opportunistic viral infections and apoptosis. Its specific cleavage by caspase-1 in mammalian cells [139] and metacaspase in yeast [219] in apoptotic conditions strongly suggests that GAPDH fragmentation might be crucial for the progression of IRES-mediated translation of apoptotic regulators mRNAs, emerging as a putative repressor of this translation mechanism both in yeast and mammalian cells. In order to clarify this possible regulation further studies are required.

Although we observed a loss-of-function by some of the translation initiation factors, such as eIF2α and eIF4A, other translation factors appear to have a gain-of-function upon the apoptotic stimulus, being recruited for the modulation of other processes, which might be unrelated with translation. That is the case of eEF1A and eEF2, which are fragmented and translocated to mitochondria during acetic acid treatment. eEF1A N-terminal fragments are even imported to the mitochondrial matrix were they appear to perform a pro-apoptotic function. Mitochondria are organelles known to contain a separate protein synthesis machinery [402-404]. In fact, most of the mitochondrial transcription/translation machinery and proteins are synthesized in cytosol and imported to mitochondria [304, 327, 402-412] Therefore, the specific translocation of eEF1A and eEF2 translation elongation factors fragments to mitochondria during acetic acid treatment might be a part of mitochondrial apoptotic cascade leading to the described severe mitochondrial alterations, such as the production of reactive oxygen species (ROS), depolarization of mitochondria outer membrane, translocation of Aif1p from mitochondria to the nucleus and release of cytochrome *c* to cytosol, culminating in mitochondria fission and fragmentation/degradation [41, 199, 200, 326, 328]. The recruitment of these factors might also be related with an alternative mitochondrial translation mechanism of important apoptotic regulators in hypothetical conditions of mitochondrial canonical translation factors degradation. Since eF1A N-terminal fragments codify for the GTP-binding domain involved in the delivery of the aminoacyl-tRNAs to ribosomes and eEF2 is involved in ribosomal translocation during protein synthesis their participation in the aminoacyl-tRNA delivery to mitochondria and translation elongation during apoptosis might be of great contribution for this process and should be further investigated.

In order to identify the mRNAs capable of being translated by the IRES-mediated translation, a screening of putative IRES-containing mRNAs translated during acetic acid treatment was performed. This study allowed us to confirm the presence of IRES in the 5'UTR of HSP90 isoforms, *HSC82* and *HSP82*, as well as in the eIF4G exposing an alternative IRES-mediated mechanism controlling HSP90 chaperones translation during acetic acid treatment. Similar to what occurs during

yeast nutrient-starvation [227], eIF4G IRES-mediated translation during acetic acid-induced amino acid starvation strongly suggests the participation of eIF4G in the IRES-mediated translation initiation, similar to what has been described regarding the IRES-mediated translation of several mammalian mRNA [5, 90, 95, 393, 394, 396, 413, 414].

Despite that, HSP90 isoforms individual translation appears to activate distinct cellular pathways. Hsc82p acts as a pro-survival molecule and Hsp82p as a pro-death molecule despite their high sequence identity (96%) and shared contribution for the regulation of Gcn2p activity during the earlier time points of the acetic acid treatment. Since these chaperones are involved in the folding/refolding of several client proteins involved in the regulation of several different processes [144, 162, 225, 226, 356-358, 360, 415-431], their antagonist role during acetic acid treatment might be related with their regulation of distinct processes, activating opposite responses to acetic acid treatment. In fact, the interaction of Hsp82p with the yeast metacaspase has been reported [209], suggesting the participation of Hsp82p in the acetic acid-induced apoptosis through interaction/folding of the active metacaspase, regulating its function in the cell. Since HSP90 are also involved in the protein delivery to mitochondria [149], a contribution of these chaperones for the translocation of eEF1A or eEF2 to mitochondria upon the apoptotic stimulus might occur. This is an aspect that deserves further attention.

In mammalian cells, a deregulation of HSP90 levels has been associated to disease [140, 162, 177, 186, 432-437], such as in acute myeloid leukemia (AML) [146, 432]. Pharmacological modulation of distinct cellular pathways using different drugs, namely 17-allylaminogeldanamycin (17AGG), a specific-inhibitor of HSP90 activity, rapamycin, the inhibitor TOR and an inducer of autophagy, chloroquine, an inhibitor of autophagy, bortezomib, an inhibitor of the proteosome and doxorubicin and cytarabine, the common AML chemotherapeutic drugs, revealed the activation of distinct isoforms of HSP90. These results strongly suggest that each HSP90 isoform interacts and is responsible for the folding of distinct proteins involved in different cellular pathways and processes [438]. In fact, similar to what occurs in yeast, in mammalian cells HSP90 chaperones are

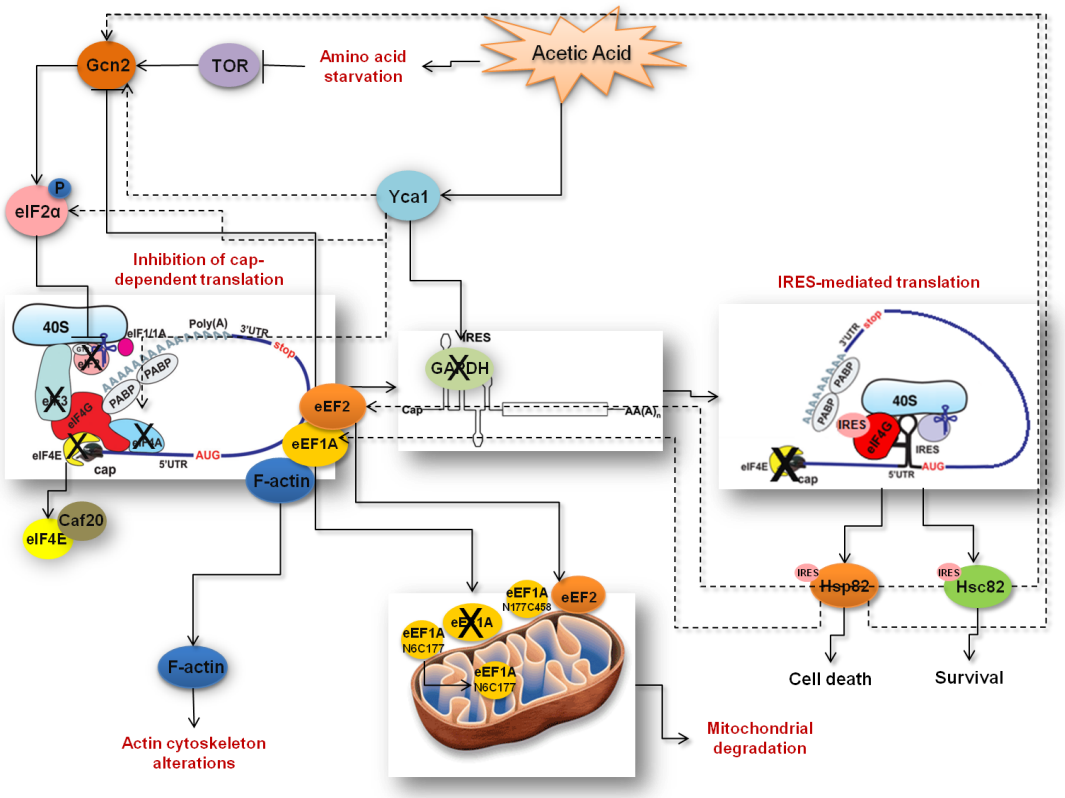

Figure 39 - Proposed illustrative scheme of the cell death pathway triggered by acetic acid, based on the main findings reported in this thesis. Dashed lines represent hypothesis that, although supported by our experiments, require further investigation.

involved in the regulation of distinct processes and client proteins. HSP90 regulate the function of proteins involved in the cell survival such as Survivin [161], RIP [173], BcR-Abl [153, 186, 439, 440], Akt [153, 156, 433, 441], Zap-7 [164], rp53 [350], p23[442], cdc37 [163] and Raf-1 [443], among others, or in the cell death such as Apaf-1 [167] and FKBP38 [171]. A deregulation of HSP90 isoforms levels in the cell may affect their interaction with client proteins leading to a rupture of the cellular homeostasis. Therefore, a thorough study of the HSP90 isoforms alternative translation mechanisms, specific client proteins and the involvement of these proteins in the disease are of utmost importance for de development of a more efficient treatment for AML and other diseases related to HSP90 deregulation.

Summing up, during acetic acid treatment an intracellular amino acid starvation occurs, blocking of TOR pathway which induces a derepression of the Gcn2p kinase. The Gcn2p active kinase phosphorylates eIF2α inhibiting the formation of

the translation initiation ternary complex (Figure 39). Activation of metacaspase directly or indirectly reduces the levels to eIF4A and regulates the phosphorylation of eIF2α, probably through interaction with Gcn2p (Figure 39). These alterations associated with the translation of Caf20p, an eIF4E binding protein, inhibit the cap-dependent translation initiation (Figure 39). The specific cleavage of GAPDH by metacaspase might favor the translation of the IRES-containing mRNAs, mediated with the participation of the canonical translation factor eIF4G, also harboring IRES (Figure 39). This mechanism will enable the translation of HSP90 in conditions of cap-dependent translation initiation impairment and their participation in the modulation of the acetic acid-induced apoptosis, Hsc82p playing a pro-survival and Hsp82p a pro-death role (Figure 39). Furthermore, at latter time points, the re-localization of eEF2 and eEF1A to mitocondria occurs, possibly regulated by HSP90 chaperones, which has also been associated with mitochondrial proteins delivery [147, 149]. eEF1A is fragmented and two of these fragments corresponding to eEF1A N-terminal sequences are imported to the mitochondria, where appear to be involved in the apoptotic process which will induced the mitochondria fission/fusion (Figure 39). The translocation of eEF1A to mitochondria reduces its binding to actin a consequently to actin cytoskeleton organization alterations. The combination of all these events culminates in the yeast cell death (Figure 39).

5.3 IMPLICATIONS FOR FUTURE RESEARCH

Altogether, the results presented in this thesis yield new insights into the translation mechanisms regulating yeast PCD, opening new perspectives for future investigations.

Microarray analysis generated a large amount of data regarding the mRNAs translated during acetic acid treatment, revealing several possible regulators of the cellular response to acetic acid treatment, namely mRNAs involved in the response to the acid stress and mRNAs involved in the activation of the acetic acid-induced apoptotic process. These mRNAs translation might be regulated by IRES. Since we have only focused in the function of the two HSP90 isoforms, Hsc82p and

Hsp82p, these data constitute a powerful database (submitted to ArrayExpress (http://www.ebi.ac.uk/arrayexpress/) for future studies.

It would be also important to clarify the role to metacaspase in the translation machinery alterations observed during acetic acid treatment. The study of the specific interactions of metacaspase with translation factors and the Gcn2p kinase is of utmost importance for the elucidation of the regulatory mechanisms controlling the remodeling of the translation process from cap-dependent to cap-independent translation. With that purpose, specific digestome analysis of translation factors with active metacaspase, followed by immunoblot analysis should be performed in order to disclose if eIF4A and eIF2α among other translation factors are in fact substrates of metacaspase during acetic acid treatment. Studies of cap-dependent and IRES-mediated translation efficiency in the absence of metacaspase, using metacaspase deleted strain, would also contribute for the disclosure of this protease role in the modulation of translation.

HPS90 chaperones play a preponderant role in cellular homeostasis. Therefore, the knowledge on the alternative translation mechanisms regulating HSP90 isoforms expression and the identification of their specific client proteins, as well as the effect of these interactions in the cell, is of great importance both in yeast and mammalian cells. The investigation of an IRES-mediated regulation of HSP90 isoforms translation in mammalian cells should be addressed. Furthermore, a yeast two-hybrid assay of HSP90 isoforms interactors both in yeast and in mammalian cells could be of great value in the understanding of the molecular pathways affected by each isoforms. In mammalian cells this information would allow a more targeted and effective cancer therapy.

The data obtained from these hypothetical experiments might be of great contribution for the continuous expansion on the knowledge of regulatory pathways controlling the apoptotic process.

REFERENCES

1. Chang, H.Y. and X. Yang, *Proteases for cell suicide: functions and regulation of caspases.* Microbiol Mol Biol Rev, 2000. **64**(4): p. 821-46.
2. Lanneau, D., et al., *Apoptosis versus cell differentiation: role of heat shock proteins HSP90, HSP70 and HSP27.* Prion, 2007. **1**(1): p. 53-60.
3. Carmona-Gutierrez, D., et al., *Apoptosis in yeast: triggers, pathways, subroutines.* Cell Death Differ, 2010. **17**(5): p. 763-73.
4. Graber, T.E. and M. Holcik, *Cap-independent regulation of gene expression in apoptosis.* Mol Biosyst, 2007. **3**(12): p. 825-34.
5. Komar, A.A. and M. Hatzoglou, *Cellular IRES-mediated translation: the war of ITAFs in pathophysiological states.* Cell Cycle, 2011. **10**(2): p. 229-40.
6. Hetts, S.W., *To die or not to die: an overview of apoptosis and its role in disease.* JAMA, 1998. **279**(4): p. 300-7.
7. Krammer, P.H., *CD95's deadly mission in the immune system.* Nature, 2000. **407**(6805): p. 789-95.
8. Jacobson, M.D., *Programmed cell death: a missing link is found.* Trends Cell Biol, 1997. **7**(12): p. 467-9.
9. Strasser, A., L. O'Connor, and V.M. Dixit, *Apoptosis signaling.* Annu Rev Biochem, 2000. **69**: p. 217-45.
10. Fuchs, Y. and H. Steller, *Programmed cell death in animal development and disease.* Cell, 2011. **147**(4): p. 742-58.
11. Bredesen, D.E., *Programmed cell death mechanisms in neurological disease.* Curr Mol Med, 2008. **8**(3): p. 173-86.
12. Elmore, S., *Apoptosis: a review of programmed cell death.* Toxicol Pathol, 2007. **35**(4): p. 495-516.
13. Lockshin, R.A. and Z. Zakeri, *Programmed cell death and apoptosis: origins of the theory.* Nat Rev Mol Cell Biol, 2001. **2**(7): p. 545-50.
14. Kerr, J.F., A.H. Wyllie, and A.R. Currie, *Apoptosis: a basic biological phenomenon with wide-ranging implications in tissue kinetics.* Br J Cancer, 1972. **26**(4): p. 239-57.
15. Wyllie, A.H., J.F. Kerr, and A.R. Currie, *Cell death: the significance of apoptosis.* Int Rev Cytol, 1980. **68**: p. 251-306.

16. Amberg, D., et al., *Cellular ageing and the actin cytoskeleton.* Subcell Biochem, 2012. **57**: p. 331-52.
17. Wlodkowic, D., et al., *Apoptosis and beyond: cytometry in studies of programmed cell death.* Methods Cell Biol, 2011. **103**: p. 55-98.
18. Proskuryakov, S.Y., V.L. Gabai, and A.G. Konoplyannikov, *Necrosis is an active and controlled form of programmed cell death.* Biochemistry (Mosc), 2002. **67**(4): p. 387-408.
19. Van Cruchten, S. and W. Van Den Broeck, *Morphological and biochemical aspects of apoptosis, oncosis and necrosis.* Anat Histol Embryol, 2002. **31**(4): p. 214-23.
20. Gumienny, T.L., et al., *Genetic control of programmed cell death in the Caenorhabditis elegans hermaphrodite germline.* Development, 1999. **126**(5): p. 1011-22.
21. Hengartner, M.O., *Programmed cell death in the nematode C. elegans.* Recent Prog Horm Res, 1999. **54**: p. 213-22; discussion 222-4.
22. Hengartner, M.O. and H.R. Horvitz, *The ins and outs of programmed cell death during C. elegans development.* Philos Trans R Soc Lond B Biol Sci, 1994. **345**(1313): p. 243-6.
23. Proskuryakov, S.Y., A.G. Konoplyannikov, and V.L. Gabai, *Necrosis: a specific form of programmed cell death?* Exp Cell Res, 2003. **283**(1): p. 1-16.
24. Kim, Y.J., et al., *Radicicol, an inhibitor of Hsp90, enhances TRAIL-induced apoptosis in human epithelial ovarian carcinoma cells by promoting activation of apoptosis-related proteins.* Mol Cell Biochem, 2012. **359**(1-2): p. 33-43.
25. Galluzzi, L., et al., *Programmed necrosis from molecules to health and disease.* Int Rev Cell Mol Biol, 2011. **289**: p. 1-35.
26. Loos, B. and A.M. Engelbrecht, *Cell death: a dynamic response concept.* Autophagy, 2009. **5**(5): p. 590-603.
27. Kanduc, D., et al., *Cell death: apoptosis versus necrosis (review).* Int J Oncol, 2002. **21**(1): p. 165-70.

28. Denecker, G., et al., *Apoptotic and necrotic cell death induced by death domain receptors.* Cell Mol Life Sci, 2001. **58**(3): p. 356-70.
29. Teng, X., et al., *Gene-dependent cell death in yeast.* Cell Death Dis, 2011. **2**: p. e188.
30. McHugh, P. and M. Turina, *Apoptosis and necrosis: a review for surgeons.* Surg Infect (Larchmt), 2006. **7**(1): p. 53-68.
31. Denecker, G., et al., *Death receptor-induced apoptotic and necrotic cell death: differential role of caspases and mitochondria.* Cell Death Differ, 2001. **8**(8): p. 829-40.
32. Vanden Berghe, T., et al., *Differential signaling to apoptotic and necrotic cell death by Fas-associated death domain protein FADD.* J Biol Chem, 2004. **279**(9): p. 7925-33.
33. Degterev, A., et al., *Identification of RIP1 kinase as a specific cellular target of necrostatins.* Nat Chem Biol, 2008. **4**(5): p. 313-21.
34. Holler, N., et al., *Fas triggers an alternative, caspase-8-independent cell death pathway using the kinase RIP as effector molecule.* Nat Immunol, 2000. **1**(6): p. 489-95.
35. Majno, G. and I. Joris, *Apoptosis, oncosis, and necrosis. An overview of cell death.* Am J Pathol, 1995. **146**(1): p. 3-15.
36. Jacobson, M.D., M. Weil, and M.C. Raff, *Programmed cell death in animal development.* Cell, 1997. **88**(3): p. 347-54.
37. Cryns, V. and J. Yuan, *Proteases to die for.* Genes Dev, 1998. **12**(11): p. 1551-70.
38. Abdelwahid, E., et al., *Mitochondrial involvement in cell death of non-mammalian eukaryotes.* Biochim Biophys Acta, 2011. **1813**(4): p. 597-607.
39. Cheng, W.C., K.M. Leach, and J.M. Hardwick, *Mitochondrial death pathways in yeast and mammalian cells.* Biochim Biophys Acta, 2008. **1783**(7): p. 1272-9.
40. Madeo, F., et al., *A caspase-related protease regulates apoptosis in yeast.* Mol Cell, 2002. **9**(4): p. 911-7.

41. Wissing, S., et al., *An AIF orthologue regulates apoptosis in yeast.* J Cell Biol, 2004. **166**(7): p. 969-74.
42. Adams, K.W. and G.M. Cooper, *Rapid turnover of mcl-1 couples translation to cell survival and apoptosis.* J Biol Chem, 2007. **282**(9): p. 6192-200.
43. Dotto, G.P. and J. Silke, *More than cell death: caspases and caspase inhibitors on the move.* Dev Cell, 2004. **7**(1): p. 2-3.
44. Earnshaw, W.C., L.M. Martins, and S.H. Kaufmann, *Mammalian caspases: structure, activation, substrates, and functions during apoptosis.* Annu Rev Biochem, 1999. **68**: p. 383-424.
45. Johnson, C.E. and S. Kornbluth, *Caspase cleavage is not for everyone.* Cell, 2008. **134**(5): p. 720-1.
46. Crawford, E.D. and J.A. Wells, *Caspase substrates and cellular remodeling.* Annu Rev Biochem, 2011. **80**: p. 1055-87.
47. Luthi, A.U. and S.J. Martin, *The CASBAH: a searchable database of caspase substrates.* Cell Death Differ, 2007. **14**(4): p. 641-50.
48. Timmer, J.C. and G.S. Salvesen, *Caspase substrates.* Cell Death Differ, 2007. **14**(1): p. 66-72.
49. Carmona-Gutierrez, D., et al., *Metacaspases are caspases. Doubt no more.* Cell Death Differ, 2010. **17**(3): p. 377-8.
50. Greenwood, M.T. and P. Ludovico, *Expressing and functional analysis of mammalian apoptotic regulators in yeast.* Cell Death Differ, 2010. **17**(5): p. 737-45.
51. Ulukaya, E., C. Acilan, and Y. Yilmaz, *Apoptosis: why and how does it occur in biology?* Cell Biochem Funct, 2011. **29**(6): p. 468-80.
52. Gupta, S., *Molecular signaling in death receptor and mitochondrial pathways of apoptosis (Review).* Int J Oncol, 2003. **22**(1): p. 15-20.
53. Reed, J.C., *Double identity for proteins of the Bcl-2 family.* Nature, 1997. **387**(6635): p. 773-6.
54. Kroemer, G. and J.C. Reed, *Mitochondrial control of cell death.* Nat Med, 2000. **6**(5): p. 513-9.

55. Khosravi-Far, R. and M.D. Esposti, *Death receptor signals to mitochondria.* Cancer Biol Ther, 2004. **3**(11): p. 1051-7.
56. Yin, X.M., *Signal transduction mediated by Bid, a pro-death Bcl-2 family proteins, connects the death receptor and mitochondria apoptosis pathways.* Cell Res, 2000. **10**(3): p. 161-7.
57. Wang, X., *The expanding role of mitochondria in apoptosis.* Genes Dev, 2001. **15**(22): p. 2922-33.
58. Fearnhead, H.O., et al., *Oncogene-dependent apoptosis is mediated by caspase-9.* Proc Natl Acad Sci U S A, 1998. **95**(23): p. 13664-9.
59. Clemens, M.J., et al., *Translation initiation factor modifications and the regulation of protein synthesis in apoptotic cells.* Cell Death Differ, 2000. **7**(7): p. 603-15.
60. Holcik, M. and T.V. Pestova, *Translation mechanism and regulation: old players, new concepts. Meeting on translational control and non-coding RNA.* EMBO Rep, 2007. **8**(7): p. 639-43.
61. Schmeing, T.M. and V. Ramakrishnan, *What recent ribosome structures have revealed about the mechanism of translation.* Nature, 2009. **461**(7268): p. 1234-42.
62. Sonenberg, N. and A.G. Hinnebusch, *Regulation of translation initiation in eukaryotes: mechanisms and biological targets.* Cell, 2009. **136**(4): p. 731-45.
63. Jackson, R.J., C.U. Hellen, and T.V. Pestova, *The mechanism of eukaryotic translation initiation and principles of its regulation.* Nat Rev Mol Cell Biol, 2010. **11**(2): p. 113-27.
64. Marissen, W.E., et al., *Identification of caspase 3-mediated cleavage and functional alteration of eukaryotic initiation factor 2alpha in apoptosis.* J Biol Chem, 2000. **275**(13): p. 9314-23.
65. Bushell, M., et al., *Changes in integrity and association of eukaryotic protein synthesis initiation factors during apoptosis.* Eur J Biochem, 2000. **267**(4): p. 1083-91.

66. Muaddi, H., et al., *Phosphorylation of eIF2alpha at serine 51 is an important determinant of cell survival and adaptation to glucose deficiency.* Mol Biol Cell, 2010. **21**(18): p. 3220-31.
67. Bevilacqua, E., et al., *eIF2alpha phosphorylation tips the balance to apoptosis during osmotic stress.* J Biol Chem, 2010. **285**(22): p. 17098-111.
68. Pushpanjali, P. and K.V. Ramaiah, *PKC activation contributes to caspase-mediated eIF2alpha phosphorylation and cell death.* Biochim Biophys Acta, 2010. **1800**(5): p. 518-25.
69. Cnop, M., et al., *Selective inhibition of eukaryotic translation initiation factor 2 alpha dephosphorylation potentiates fatty acid-induced endoplasmic reticulum stress and causes pancreatic beta-cell dysfunction and apoptosis.* J Biol Chem, 2007. **282**(6): p. 3989-97.
70. Scheuner, D., et al., *Double-stranded RNA-dependent protein kinase phosphorylation of the alpha-subunit of eukaryotic translation initiation factor 2 mediates apoptosis.* J Biol Chem, 2006. **281**(30): p. 21458-68.
71. Wek, R.C., H.Y. Jiang, and T.G. Anthony, *Coping with stress: eIF2 kinases and translational control.* Biochem Soc Trans, 2006. **34**(Pt 1): p. 7-11.
72. Saelens, X., M. Kalai, and P. Vandenabeele, *Translation inhibition in apoptosis: caspase-dependent PKR activation and eIF2-alpha phosphorylation.* J Biol Chem, 2001. **276**(45): p. 41620-8.
73. Morley, S.J., et al., *Differential requirements for caspase-8 activity in the mechanism of phosphorylation of eIF2alpha, cleavage of eIF4GI and signaling events associated with the inhibition of protein synthesis in apoptotic Jurkat T cells.* FEBS Lett, 2000. **477**(3): p. 229-36.
74. Lin, Y.M., et al., *eIF3k regulates apoptosis in epithelial cells by releasing caspase 3 from keratin-containing inclusions.* J Cell Sci, 2008. **121**(Pt 14): p. 2382-93.
75. Liang, H., et al., *Knockdown of eukaryotic translation initiation factors 3B (EIF3B) inhibits proliferation and promotes apoptosis in glioblastoma cells.* Neurol Sci, 2012.

76. Kim, J.T., et al., *Apoptosis-inducing factor (AIF) inhibits protein synthesis by interacting with the eukaryotic translation initiation factor 3 subunit p44 (eIF3g).* FEBS Lett, 2006. **580**(27): p. 6375-83.
77. Shi, J., et al., *Decreased expression of eukaryotic initiation factor 3f deregulates translation and apoptosis in tumor cells.* Oncogene, 2006. **25**(35): p. 4923-36.
78. Li, S., et al., *Translation initiation factor 4E blocks endoplasmic reticulum-mediated apoptosis.* J Biol Chem, 2004. **279**(20): p. 21312-7.
79. Li, S., et al., *Translation factor eIF4E rescues cells from Myc-dependent apoptosis by inhibiting cytochrome c release.* J Biol Chem, 2003. **278**(5): p. 3015-22.
80. Tan, A., et al., *Inhibition of Myc-dependent apoptosis by eukaryotic translation initiation factor 4E requires cyclin D1.* Oncogene, 2000. **19**(11): p. 1437-47.
81. Tee, A.R. and C.G. Proud, *Caspase cleavage of initiation factor 4E-binding protein 1 yields a dominant inhibitor of cap-dependent translation and reveals a novel regulatory motif.* Mol Cell Biol, 2002. **22**(6): p. 1674-83.
82. Marissen, W.E., et al., *Cleavage of eukaryotic translation initiation factor 4GII correlates with translation inhibition during apoptosis.* Cell Death Differ, 2000. **7**(12): p. 1234-43.
83. Bushell, M., et al., *Cleavage of polypeptide chain initiation factor eIF4GI during apoptosis in lymphoma cells: characterisation of an internal fragment generated by caspase-3-mediated cleavage.* Cell Death Differ, 2000. **7**(7): p. 628-36.
84. Roberts, L.O., et al., *Caspases are not involved in the cleavage of translation initiation factor eIF4GI during picornavirus infection.* J Gen Virol, 2000. **81**(Pt 7): p. 1703-7.
85. Morley, S.J., L. McKendrick, and M. Bushell, *Cleavage of translation initiation factor 4G (eIF4G) during anti-Fas IgM-induced apoptosis does not require signalling through the p38 mitogen-activated protein (MAP) kinase.* FEBS Lett, 1998. **438**(1-2): p. 41-8.

86. Clemens, M.J., M. Bushell, and S.J. Morley, *Degradation of eukaryotic polypeptide chain initiation factor (eIF) 4G in response to induction of apoptosis in human lymphoma cell lines.* Oncogene, 1998. **17**(22): p. 2921-31.

87. Marissen, W.E. and R.E. Lloyd, *Eukaryotic translation initiation factor 4G is targeted for proteolytic cleavage by caspase 3 during inhibition of translation in apoptotic cells.* Mol Cell Biol, 1998. **18**(12): p. 7565-74.

88. Levy-Strumpf, N., et al., *DAP-5, a novel homolog of eukaryotic translation initiation factor 4G isolated as a putative modulator of gamma interferon-induced programmed cell death.* Mol Cell Biol, 1997. **17**(3): p. 1615-25.

89. Liberman, N., et al., *The crystal structure of the C-terminal DAP5/p97 domain sheds light on the molecular basis for its processing by caspase cleavage.* J Mol Biol, 2008. **383**(3): p. 539-48.

90. Nevins, T.A., et al., *Distinct regulation of internal ribosome entry site-mediated translation following cellular stress is mediated by apoptotic fragments of eIF4G translation initiation factor family members eIF4GI and p97/DAP5/NAT1.* J Biol Chem, 2003. **278**(6): p. 3572-9.

91. Henis-Korenblit, S., et al., *The caspase-cleaved DAP5 protein supports internal ribosome entry site-mediated translation of death proteins.* Proc Natl Acad Sci U S A, 2002. **99**(8): p. 5400-5.

92. Henis-Korenblit, S., et al., *A novel form of DAP5 protein accumulates in apoptotic cells as a result of caspase cleavage and internal ribosome entry site-mediated translation.* Mol Cell Biol, 2000. **20**(2): p. 496-506.

93. Mueller, P.P. and A.G. Hinnebusch, *Multiple upstream AUG codons mediate translational control of GCN4.* Cell, 1986. **45**(2): p. 201-7.

94. Hinnebusch, A.G., *The general control of amino acid biosynthetic genes in the yeast Saccharomyces cerevisiae.* CRC Crit Rev Biochem, 1986. **21**(3): p. 277-317.

95. Holcik, M. and N. Sonenberg, *Translational control in stress and apoptosis.* Nat Rev Mol Cell Biol, 2005. **6**(4): p. 318-27.

96. Spriggs, K.A., et al., *Internal ribosome entry segment-mediated translation during apoptosis: the role of IRES-trans-acting factors.* Cell Death Differ, 2005. **12**(6): p. 585-91.
97. Van Eden, M.E., et al., *Translation of cellular inhibitor of apoptosis protein 1 (c-IAP1) mRNA is IRES mediated and regulated during cell stress.* RNA, 2004. **10**(3): p. 469-81.
98. Warnakulasuriyarachchi, D., et al., *Translational induction of the inhibitor of apoptosis protein HIAP2 during endoplasmic reticulum stress attenuates cell death and is mediated via an inducible internal ribosome entry site element.* J Biol Chem, 2004. **279**(17): p. 17148-57.
99. Lewis, S.M. and M. Holcik, *IRES in distress: translational regulation of the inhibitor of apoptosis proteins XIAP and HIAP2 during cell stress.* Cell Death Differ, 2005. **12**(6): p. 547-53.
100. Holcik, M., et al., *Translational upregulation of X-linked inhibitor of apoptosis (XIAP) increases resistance to radiation induced cell death.* Oncogene, 2000. **19**(36): p. 4174-7.
101. Holcik, M. and R.G. Korneluk, *Functional characterization of the X-linked inhibitor of apoptosis (XIAP) internal ribosome entry site element: role of La autoantigen in XIAP translation.* Mol Cell Biol, 2000. **20**(13): p. 4648-57.
102. Holcik, M., *Translational upregulation of the X-linked inhibitor of apoptosis.* Ann N Y Acad Sci, 2003. **1010**: p. 249-58.
103. Holcik, M., B.W. Gordon, and R.G. Korneluk, *The internal ribosome entry site-mediated translation of antiapoptotic protein XIAP is modulated by the heterogeneous nuclear ribonucleoproteins C1 and C2.* Mol Cell Biol, 2003. **23**(1): p. 280-8.
104. Holcik, M., et al., *Spurious splicing within the XIAP 5' UTR occurs in the Rluc/Fluc but not the betagal/CAT bicistronic reporter system.* RNA, 2005. **11**(11): p. 1605-9.
105. Yoon, A., et al., *Impaired control of IRES-mediated translation in X-linked dyskeratosis congenita.* Science, 2006. **312**(5775): p. 902-6.

106. Lewis, S.M., et al., *Subcellular re-localization of a trans-acting factor regulates XIAP IRES-dependent translation.* Mol Biol Cell, 2007. **18**(4): p. 1302-11.
107. Riley, A., L.E. Jordan, and M. Holcik, *Distinct 5' UTRs regulate XIAP expression under normal growth conditions and during cellular stress.* Nucleic Acids Res, 2010. **38**(14): p. 4665-74.
108. Thakor, N. and M. Holcik, *IRES-mediated translation of cellular messenger RNA operates in eIF2{alpha}- independent manner during stress.* Nucleic Acids Res, 2011.
109. Coldwell, M.J., et al., *Initiation of Apaf-1 translation by internal ribosome entry.* Oncogene, 2000. **19**(7): p. 899-905.
110. Mitchell, S.A., et al., *Protein factor requirements of the Apaf-1 internal ribosome entry segment: roles of polypyrimidine tract binding protein and upstream of N-ras.* Mol Cell Biol, 2001. **21**(10): p. 3364-74.
111. Ungureanu, N.H., et al., *Internal ribosome entry site-mediated translation of Apaf-1, but not XIAP, is regulated during UV-induced cell death.* J Biol Chem, 2006. **281**(22): p. 15155-63.
112. Stoneley, M., et al., *Analysis of the c-myc IRES; a potential role for cell-type specific trans-acting factors and the nuclear compartment.* Nucleic Acids Res, 2000. **28**(3): p. 687-94.
113. Chappell, S.A., et al., *A mutation in the c-myc-IRES leads to enhanced internal ribosome entry in multiple myeloma: a novel mechanism of oncogene de-regulation.* Oncogene, 2000. **19**(38): p. 4437-40.
114. Le Quesne, J.P., et al., *Derivation of a structural model for the c-myc IRES.* J Mol Biol, 2001. **310**(1): p. 111-26.
115. Subkhankulova, T., S.A. Mitchell, and A.E. Willis, *Internal ribosome entry segment-mediated initiation of c-Myc protein synthesis following genotoxic stress.* Biochem J, 2001. **359**(Pt 1): p. 183-92.
116. Shi, Y., et al., *Cyclin D1 and c-myc internal ribosome entry site (IRES)-dependent translation is regulated by AKT activity and enhanced by rapamycin through a p38 MAPK- and ERK-dependent pathway.* J Biol Chem, 2005. **280**(12): p. 10964-73.

117. Thoma, C., et al., *Translation initiation by the c-myc mRNA internal ribosome entry sequence and the poly(A) tail.* RNA, 2008. **14**(8): p. 1579-89.
118. Marash, L. and A. Kimchi, *DAP5 and IRES-mediated translation during programmed cell death.* Cell Death Differ, 2005. **12**(6): p. 554-62.
119. Grover, R., P.S. Ray, and S. Das, *Polypyrimidine tract binding protein regulates IRES-mediated translation of p53 isoforms.* Cell Cycle, 2008. **7**(14): p. 2189-98.
120. Grover, R., et al., *p53 and little brother p53/47: linking IRES activities with protein functions.* Oncogene, 2009. **28**(30): p. 2766-72.
121. Grover, R., et al., *Effect of mutations on the p53 IRES RNA structure: implications for de-regulation of the synthesis of p53 isoforms.* RNA Biol, 2011. **8**(1): p. 132-42.
122. Sherrill, K.W., et al., *BCL-2 translation is mediated via internal ribosome entry during cell stress.* J Biol Chem, 2004. **279**(28): p. 29066-74.
123. Marash, L., et al., *DAP5 promotes cap-independent translation of Bcl-2 and CDK1 to facilitate cell survival during mitosis.* Mol Cell, 2008. **30**(4): p. 447-59.
124. Willimott, S. and S.D. Wagner, *Post-transcriptional and post-translational regulation of Bcl2.* Biochem Soc Trans, 2010. **38**(6): p. 1571-5.
125. Rubtsova, M.P., et al., *Distinctive properties of the 5'-untranslated region of human hsp70 mRNA.* J Biol Chem, 2003. **278**(25): p. 22350-6.
126. Che, J., et al., *HSP70-inducible hNIS-IRES-eGFP reporter imaging: response to heat shock.* Mol Imaging, 2007. **6**(6): p. 404-16.
127. Vivinus, S., et al., *An element within the 5' untranslated region of human Hsp70 mRNA which acts as a general enhancer of mRNA translation.* Eur J Biochem, 2001. **268**(7): p. 1908-17.
128. Wang, X., et al., *Alternative translation of OCT4 by an internal ribosome entry site and its novel function in stress response.* Stem Cells, 2009. **27**(6): p. 1265-75.

129. Yeh, S.H., et al., *Translational and transcriptional control of Sp1 against ischaemia through a hydrogen peroxide-activated internal ribosomal entry site pathway.* Nucleic Acids Res, 2011. **39**(13): p. 5412-23.
130. Durie, D., et al., *RNA-binding protein HuR mediates cytoprotection through stimulation of XIAP translation.* Oncogene, 2011. **30**(12): p. 1460-9.
131. Thakor, N. and M. Holcik, *IRES-mediated translation of cellular messenger RNA operates in eIF2alpha- independent manner during stress.* Nucleic Acids Res, 2012. **40**(2): p. 541-52.
132. Holcik, M., et al., *A new internal-ribosome-entry-site motif potentiates XIAP-mediated cytoprotection.* Nat Cell Biol, 1999. **1**(3): p. 190-2.
133. Holcik, M. and R.G. Korneluk, *XIAP, the guardian angel.* Nat Rev Mol Cell Biol, 2001. **2**(7): p. 550-6.
134. Rosenstierne, M.W., et al., *Conserved CPEs in the p53 3' untranslated region influence mRNA stability and protein synthesis.* Anticancer Res, 2008. **28**(5A): p. 2553-9.
135. Yi, M., D.E. Schultz, and S.M. Lemon, *Functional significance of the interaction of hepatitis A virus RNA with glyceraldehyde 3-phosphate dehydrogenase (GAPDH): opposing effects of GAPDH and polypyrimidine tract binding protein on internal ribosome entry site function.* J Virol, 2000. **74**(14): p. 6459-68.
136. Huang, T.S. and P.D. Nagy, *Direct inhibition of tombusvirus plus-strand RNA synthesis by a dominant negative mutant of a host metabolic enzyme, glyceraldehyde-3-phosphate dehydrogenase, in yeast and plants.* J Virol, 2011. **85**(17): p. 9090-102.
137. Prasanth, K.R., et al., *Glyceraldehyde 3-phosphate dehydrogenase negatively regulates the replication of Bamboo mosaic virus and its associated satellite RNA.* J Virol, 2011. **85**(17): p. 8829-40.
138. Dollenmaier, G. and M. Weitz, *Interaction of glyceraldehyde-3-phosphate dehydrogenase with secondary and tertiary RNA structural elements of the hepatitis A virus 3' translated and non-translated regions.* J Gen Virol, 2003. **84**(Pt 2): p. 403-14.

139. Shao, W., et al., *The caspase-1 digestome identifies the glycolysis pathway as a target during infection and septic shock.* J Biol Chem, 2007. **282**(50): p. 36321-9.
140. Mosser, D.D. and R.I. Morimoto, *Molecular chaperones and the stress of oncogenesis.* Oncogene, 2004. **23**(16): p. 2907-18.
141. Sreedhar, A.S., et al., *Hsp90 isoforms: functions, expression and clinical importance.* FEBS Lett, 2004. **562**(1-3): p. 11-5.
142. Sreedhar, A.S. and P. Csermely, *Heat shock proteins in the regulation of apoptosis: new strategies in tumor therapy: a comprehensive review.* Pharmacol Ther, 2004. **101**(3): p. 227-57.
143. Lanneau, D., et al., *Heat shock proteins: essential proteins for apoptosis regulation.* J Cell Mol Med, 2008. **12**(3): p. 743-61.
144. Craig, E.A., B.D. Gambill, and R.J. Nelson, *Heat shock proteins: molecular chaperones of protein biogenesis.* Microbiol Rev, 1993. **57**(2): p. 402-14.
145. Floer, M., G.O. Bryant, and M. Ptashne, *HSP90/70 chaperones are required for rapid nucleosome removal upon induction of the GAL genes of yeast.* Proc Natl Acad Sci U S A, 2008. **105**(8): p. 2975-80.
146. Fredly, H., et al., *Immunogenic apoptosis in human acute myeloid leukemia (AML): primary human AML cells expose calreticulin and release heat shock protein (HSP) 70 and HSP90 during apoptosis.* Oncol Rep, 2011. **25**(6): p. 1549-56.
147. Li, J., et al., *Molecular chaperone Hsp70/Hsp90 prepares the mitochondrial outer membrane translocon receptor Tom71 for preprotein loading.* J Biol Chem, 2009. **284**(35): p. 23852-9.
148. Tan, S.S., et al., *GRP78 up-regulation is associated with androgen receptor status, Hsp70-Hsp90 client proteins and castrate-resistant prostate cancer.* J Pathol, 2010.
149. Young, J.C., N.J. Hoogenraad, and F.U. Hartl, *Molecular chaperones Hsp90 and Hsp70 deliver preproteins to the mitochondrial import receptor Tom70.* Cell, 2003. **112**(1): p. 41-50.

150. Csermely, P., et al., *The 90-kDa molecular chaperone family: structure, function, and clinical applications. A comprehensive review.* Pharmacol Ther, 1998. **79**(2): p. 129-68.
151. Hickey, E., et al., *Sequence and regulation of a gene encoding a human 89-kilodalton heat shock protein.* Mol Cell Biol, 1989. **9**(6): p. 2615-26.
152. Ozawa, K., et al., *Mapping of the gene family for human heat-shock protein 90 alpha to chromosomes 1, 4, 11, and 14.* Genomics, 1992. **12**(2): p. 214-20.
153. Beck, R., et al., *Hsp90 cleavage by an oxidative stress leads to its client proteins degradation and cancer cell death.* Biochem Pharmacol, 2009. **77**(3): p. 375-83.
154. Voss, A.K., T. Thomas, and P. Gruss, *Mice lacking HSP90beta fail to develop a placental labyrinth.* Development, 2000. **127**(1): p. 1-11.
155. Caplan, A.J., S. Jackson, and D. Smith, *Hsp90 reaches new heights. Conference on the Hsp90 chaperone machine.* EMBO Rep, 2003. **4**(2): p. 126-30.
156. Zhang, R., et al., *Hsp90-Akt phosphorylates ASK1 and inhibits ASK1-mediated apoptosis.* Oncogene, 2005. **24**(24): p. 3954-63.
157. Dias, S., et al., *VEGF(165) promotes survival of leukemic cells by Hsp90-mediated induction of Bcl-2 expression and apoptosis inhibition.* Blood, 2002. **99**(7): p. 2532-40.
158. Altieri, D.C., *Coupling apoptosis resistance to the cellular stress response: the IAP-Hsp90 connection in cancer.* Cell Cycle, 2004. **3**(3): p. 255-6.
159. Chiosis, G., *Targeting chaperones in transformed systems--a focus on Hsp90 and cancer.* Expert Opin Ther Targets, 2006. **10**(1): p. 37-50.
160. Okamoto, J., et al., *Inhibition of Hsp90 leads to cell cycle arrest and apoptosis in human malignant pleural mesothelioma.* J Thorac Oncol, 2008. **3**(10): p. 1089-95.
161. Suriawinata, A., *Survivin: apoptosis inhibitor and its regulation by Hsp90.* Lab Invest, 2004. **84**(4): p. 395.
162. Abbas-Terki, T., et al., *The Hsp90 co-chaperones Cdc37 and Sti1 interact physically and genetically.* Biol Chem, 2002. **383**(9): p. 1335-42.

163. Zhao, M., et al., *Apigenin inhibits proliferation and induces apoptosis in human multiple myeloma cells through targeting the trinity of CK2, Cdc37 and Hsp90.* Mol Cancer, 2011. **10**: p. 104.
164. Castro, J.E., et al., *ZAP-70 is a novel conditional heat shock protein 90 (Hsp90) client: inhibition of Hsp90 leads to ZAP-70 degradation, apoptosis, and impaired signaling in chronic lymphocytic leukemia.* Blood, 2005. **106**(7): p. 2506-12.
165. Karkoulis, P.K., et al., *17-Allylamino-17-demethoxygeldanamycin induces downregulation of critical Hsp90 protein clients and results in cell cycle arrest and apoptosis of human urinary bladder cancer cells.* BMC Cancer, 2010. **10**: p. 481.
166. Meng, Z., et al., *The ELAV RNA-stability factor HuR binds the 5'-untranslated region of the human IGF-IR transcript and differentially represses cap-dependent and IRES-mediated translation.* Nucleic Acids Res, 2005. **33**(9): p. 2962-79.
167. Pandey, P., et al., *Negative regulation of cytochrome c-mediated oligomerization of Apaf-1 and activation of procaspase-9 by heat shock protein 90.* EMBO J, 2000. **19**(16): p. 4310-22.
168. Zhao, C. and E. Wang, *Heat shock protein 90 suppresses tumor necrosis factor alpha induced apoptosis by preventing the cleavage of Bid in NIH3T3 fibroblasts.* Cell Signal, 2004. **16**(3): p. 313-21.
169. Shelton, S.N., et al., *KU135, a novel novobiocin-derived C-terminal inhibitor of the 90-kDa heat shock protein, exerts potent antiproliferative effects in human leukemic cells.* Mol Pharmacol, 2009. **76**(6): p. 1314-22.
170. Georgakis, G.V., Y. Li, and A. Younes, *The heat shock protein 90 inhibitor 17-AAG induces cell cycle arrest and apoptosis in mantle cell lymphoma cell lines by depleting cyclin D1, Akt, Bid and activating caspase 9.* Br J Haematol, 2006. **135**(1): p. 68-71.
171. Erdmann, F., et al., *Hsp90-mediated inhibition of FKBP38 regulates apoptosis in neuroblastoma cells.* FEBS Lett, 2007. **581**(29): p. 5709-14.

172. Vanden Berghe, T., et al., *Disruption of HSP90 function reverts tumor necrosis factor-induced necrosis to apoptosis.* J Biol Chem, 2003. **278**(8): p. 5622-9.
173. Lewis, J., et al., *Disruption of hsp90 function results in degradation of the death domain kinase, receptor-interacting protein (RIP), and blockage of tumor necrosis factor-induced nuclear factor-kappaB activation.* J Biol Chem, 2000. **275**(14): p. 10519-26.
174. Ayrault, O., et al., *Inhibition of Hsp90 via 17-DMAG induces apoptosis in a p53-dependent manner to prevent medulloblastoma.* Proc Natl Acad Sci U S A, 2009. **106**(40): p. 17037-42.
175. Hostein, I., et al., *Inhibition of signal transduction by the Hsp90 inhibitor 17-allylamino-17-demethoxygeldanamycin results in cytostasis and apoptosis.* Cancer Res, 2001. **61**(10): p. 4003-9.
176. Lopez-Maderuelo, M.D., et al., *Opposite effects of the Hsp90 inhibitor Geldanamycin: induction of apoptosis in PC12, and differentiation in N2A cells.* FEBS Lett, 2001. **490**(1-2): p. 23-7.
177. Vaseva, A.V., et al., *Blockade of Hsp90 by 17AAG antagonizes MDMX and synergizes with Nutlin to induce p53-mediated apoptosis in solid tumors.* Cell Death Dis, 2011. **2**: p. e156.
178. Yu, W., et al., *The Hsp90 inhibitor 17-allylamide-17-demethoxygeldanamycin induces apoptosis and differentiation of Kasumi-1 harboring the Asn822Lys KIT mutation and down-regulates KIT protein level.* Leuk Res, 2006. **30**(5): p. 575-82.
179. Zhang, M.H., et al., *HSP90 protects apoptotic cleavage of vimentin in geldanamycin-induced apoptosis.* Mol Cell Biochem, 2006. **281**(1-2): p. 111-21.
180. Chatterjee, M., et al., *STAT3 and MAPK signaling maintain overexpression of heat shock proteins 90alpha and beta in multiple myeloma cells, which critically contribute to tumor-cell survival.* Blood, 2007. **109**(2): p. 720-8.
181. Chiosis, G. and L. Neckers, *Tumor selectivity of Hsp90 inhibitors: the explanation remains elusive.* ACS Chem Biol, 2006. **1**(5): p. 279-84.

182. Chiosis, G. and H. Tao, *Purine-scaffold Hsp90 inhibitors.* IDrugs, 2006. **9**(11): p. 778-82.
183. Chiosis, G., *Discovery and development of purine-scaffold Hsp90 inhibitors.* Curr Top Med Chem, 2006. **6**(11): p. 1183-91.
184. Chiosis, G., E. Caldas Lopes, and D. Solit, *Heat shock protein-90 inhibitors: a chronicle from geldanamycin to today's agents.* Curr Opin Investig Drugs, 2006. **7**(6): p. 534-41.
185. Richardson, P.G., et al., *Inhibition of heat shock protein 90 (HSP90) as a therapeutic strategy for the treatment of myeloma and other cancers.* Br J Haematol, 2011. **152**(4): p. 367-79.
186. Neckers, L., *Hsp90 inhibitors as novel cancer chemotherapeutic agents.* Trends Mol Med, 2002. **8**(4 Suppl): p. S55-61.
187. Shipp, C., K. Watson, and G.L. Jones, *Associations of HSP90 client proteins in human breast cancer.* Anticancer Res, 2011. **31**(6): p. 2095-101.
188. Reikvam, H., E. Ersvaer, and O. Bruserud, *Heat shock protein 90 - a potential target in the treatment of human acute myelogenous leukemia.* Curr Cancer Drug Targets, 2009. **9**(6): p. 761-76.
189. Madeo, F., E. Frohlich, and K.U. Frohlich, *A yeast mutant showing diagnostic markers of early and late apoptosis.* J Cell Biol, 1997. **139**(3): p. 729-34.
190. Madeo, F., et al., *Oxygen stress: a regulator of apoptosis in yeast.* J Cell Biol, 1999. **145**(4): p. 757-67.
191. Ludovico, P., et al., *Saccharomyces cerevisiae commits to a programmed cell death process in response to acetic acid.* Microbiology, 2001. **147**(Pt 9): p. 2409-15.
192. Madeo, F., et al., *Apoptosis in yeast.* Curr Opin Microbiol, 2004. **7**(6): p. 655-60.
193. Knorre, D.A., E.A. Smirnova, and F.F. Severin, *Natural conditions inducing programmed cell death in the yeast Saccharomyces cerevisiae.* Biochemistry (Mosc), 2005. **70**(2): p. 264-6.

194. Severin, F.F. and A.A. Hyman, *Pheromone induces programmed cell death in S. cerevisiae.* Curr Biol, 2002. **12**(7): p. R233-5.
195. Herker, E., et al., *Chronological aging leads to apoptosis in yeast.* J Cell Biol, 2004. **164**(4): p. 501-7.
196. Frohlich, K.U. and F. Madeo, *Apoptosis in yeast: a new model for aging research.* Exp Gerontol, 2001. **37**(1): p. 27-31.
197. Walter, D., et al., *The inhibitor-of-apoptosis protein Bir1p protects against apoptosis in S. cerevisiae and is a substrate for the yeast homologue of Omi/HtrA2.* J Cell Sci, 2006. **119**(Pt 9): p. 1843-51.
198. Buttner, S., et al., *Endonuclease G regulates budding yeast life and death.* Mol Cell, 2007. **25**(2): p. 233-46.
199. Ludovico, P., et al., *Cytochrome c release and mitochondria involvement in programmed cell death induced by acetic acid in Saccharomyces cerevisiae.* Mol Biol Cell, 2002. **13**(8): p. 2598-606.
200. Fannjiang, Y., et al., *Mitochondrial fission proteins regulate programmed cell death in yeast.* Genes Dev, 2004. **18**(22): p. 2785-97.
201. Pereira, C., et al., *Mitochondrial degradation in acetic acid-induced yeast apoptosis: the role of Pep4 and the ADP/ATP carrier.* Mol Microbiol, 2010. **76**(6): p. 1398-410.
202. Gourlay, C.W., et al., *A role for the actin cytoskeleton in cell death and aging in yeast.* J Cell Biol, 2004. **164**(6): p. 803-9.
203. Gourlay, C.W. and K.R. Ayscough, *A role for actin in aging and apoptosis.* Biochem Soc Trans, 2005. **33**(Pt 6): p. 1260-4.
204. Gourlay, C.W. and K.R. Ayscough, *The actin cytoskeleton in ageing and apoptosis.* FEMS Yeast Res, 2005. **5**(12): p. 1193-8.
205. Uren, A.G., et al., *Identification of paracaspases and metacaspases: two ancient families of caspase-like proteins, one of which plays a key role in MALT lymphoma.* Mol Cell, 2000. **6**(4): p. 961-7.
206. Tsiatsiani, L., et al., *Metacaspases.* Cell Death Differ, 2011. **18**(8): p. 1279-88.

207. Low, C.P., et al., *Caspase-dependent and -independent lipotoxic cell-death pathways in fission yeast.* J Cell Sci, 2008. **121**(Pt 16): p. 2671-84.
208. Lee, R.E., et al., *A non-death role of the yeast metacaspase: Yca1p alters cell cycle dynamics.* PLoS One, 2008. **3**(8): p. e2956.
209. Lee, R.E., et al., *Metacaspase Yca1 is required for clearance of insoluble protein aggregates.* Proc Natl Acad Sci U S A, 2010. **107**(30): p. 13348-53.
210. Belenghi, B., et al., *Metacaspase activity of Arabidopsis thaliana is regulated by S-nitrosylation of a critical cysteine residue.* J Biol Chem, 2007. **282**(2): p. 1352-8.
211. Almeida, B., et al., *NO-mediated apoptosis in yeast.* J Cell Sci, 2007. **120**(Pt 18): p. 3279-88.
212. Osorio, N.S., et al., *Nitric oxide signaling is disrupted in the yeast model for Batten disease.* Mol Biol Cell, 2007. **18**(7): p. 2755-67.
213. Sundstrom, J.F., et al., *Tudor staphylococcal nuclease is an evolutionarily conserved component of the programmed cell death degradome.* Nat Cell Biol, 2009. **11**(11): p. 1347-54.
214. Mazzoni, C. and C. Falcone, *Caspase-dependent apoptosis in yeast.* Biochim Biophys Acta, 2008. **1783**(7): p. 1320-7.
215. Almeida, B., et al., *Yeast protein expression profile during acetic acid-induced apoptosis indicates causal involvement of the TOR pathway.* Proteomics, 2009. **9**(3): p. 720-32.
216. Mroczek, S. and J. Kufel, *Apoptotic signals induce specific degradation of ribosomal RNA in yeast.* Nucleic Acids Res, 2008. **36**(9): p. 2874-88.
217. Guaragnella, N., et al., *YCA1 participates in the acetic acid induced yeast programmed cell death also in a manner unrelated to its caspase-like activity.* FEBS Lett, 2006. **580**(30): p. 6880-4.
218. Mazzoni, C., et al., *Yeast caspase 1 links messenger RNA stability to apoptosis in yeast.* EMBO Rep, 2005. **6**(11): p. 1076-81.

219. Silva, A., et al., *Glyceraldehyde-3-phosphate dehydrogenase (GAPDH) is a specific substrate of yeast metacaspase.* Biochim Biophys Acta, 2011. **1813**(12): p. 2044-9.
220. Shenton, D., et al., *Global translational responses to oxidative stress impact upon multiple levels of protein synthesis.* J Biol Chem, 2006. **281**(39): p. 29011-21.
221. Eisenberg, T., et al., *Necrosis in yeast.* Apoptosis, 2010. **15**(3): p. 257-68.
222. Eisenberg, T., et al., *Induction of autophagy by spermidine promotes longevity.* Nat Cell Biol, 2009. **11**(11): p. 1305-14.
223. Dudgeon, D.D., et al., *Nonapoptotic death of Saccharomyces cerevisiae cells that is stimulated by Hsp90 and inhibited by calcineurin and Cmk2 in response to endoplasmic reticulum stresses.* Eukaryot Cell, 2008. **7**(12): p. 2037-51.
224. Caplan, A.J., *What is a co-chaperone?* Cell Stress Chaperones, 2003. **8**(2): p. 105-7.
225. Piper, P.W., et al., *Hsp90 chaperone control over transcriptional regulation by the yeast Slt2(Mpk1)p and human ERK5 mitogen-activated protein kinases (MAPKs).* Biochem Soc Trans, 2006. **34**(Pt 5): p. 783-5.
226. Truman, A.W., et al., *In the yeast heat shock response, Hsf1-directed induction of Hsp90 facilitates the activation of the Slt2 (Mpk1) mitogen-activated protein kinase required for cell integrity.* Eukaryot Cell, 2007. **6**(4): p. 744-52.
227. Gilbert, W.V., et al., *Cap-independent translation is required for starvation-induced differentiation in yeast.* Science, 2007. **317**(5842): p. 1224-7.
228. Seino, A., et al., *Translational control by internal ribosome entry site in Saccharomyces cerevisiae.* Biochim Biophys Acta, 2005. **1681**(2-3): p. 166-74.
229. Das, S., et al., *Sequences within a small yeast RNA required for inhibition of internal initiation of translation: interaction with La and other cellular proteins influences its inhibitory activity.* J Virol, 1996. **70**(3): p. 1624-32.

230. Komar, A.A., et al., *Internal initiation drives the synthesis of Ure2 protein lacking the prion domain and affects [URE3] propagation in yeast cells.* EMBO J, 2003. **22**(5): p. 1199-209.
231. Reineke, L.C. and W.C. Merrick, *Characterization of the functional role of nucleotides within the URE2 IRES element and the requirements for eIF2A-mediated repression.* RNA, 2009. **15**(12): p. 2264-77.
232. Reineke, L.C., et al., *Insights into the role of yeast eIF2A in IRES-mediated translation.* PLoS One, 2011. **6**(9): p. e24492.
233. Reineke, L.C., et al., *A small stem loop element directs internal initiation of the URE2 internal ribosome entry site in Saccharomyces cerevisiae.* J Biol Chem, 2008. **283**(27): p. 19011-25.
234. Zhou, W., G.M. Edelman, and V.P. Mauro, *Transcript leader regions of two Saccharomyces cerevisiae mRNAs contain internal ribosome entry sites that function in living cells.* Proc Natl Acad Sci U S A, 2001. **98**(4): p. 1531-6.
235. Fitzgerald, K.D. and B.L. Semler, *Bridging IRES elements in mRNAs to the eukaryotic translation apparatus.* Biochim Biophys Acta, 2009. **1789**(9-10): p. 518-28.
236. Cherkasova, V.A. and A.G. Hinnebusch, *Translational control by TOR and TAP42 through dephosphorylation of eIF2alpha kinase GCN2.* Genes Dev, 2003. **17**(7): p. 859-72.
237. Hinnebusch, A.G., et al., *Study of translational control of eukaryotic gene expression using yeast.* Ann N Y Acad Sci, 2004. **1038**: p. 60-74.
238. Hinnebusch, A.G., *Translational regulation of GCN4 and the general amino acid control of yeast.* Annu Rev Microbiol, 2005. **59**: p. 407-50.
239. Polunovsky, V.A., et al., *Translational control of programmed cell death: eukaryotic translation initiation factor 4E blocks apoptosis in growth-factor-restricted fibroblasts with physiologically expressed or deregulated Myc.* Mol Cell Biol, 1996. **16**(11): p. 6573-81.
240. Moon, S.H., et al., *Cap-independent protein translation is initially responsible for 4-(N-methylnitrosamino)-1-(3-pyridyl)-butanone (NNK)-*

induced apoptosis in normal human bronchial epithelial cells. J Vet Sci, 2004. **5**(4): p. 369-78.

241. Paschen, W., *Shutdown of translation: lethal or protective? Unfolded protein response versus apoptosis.* J Cereb Blood Flow Metab, 2003. **23**(7): p. 773-9.
242. Parker, S.H., et al., *The roles of translation initiation regulation in ultraviolet light-induced apoptosis.* Mol Cell Biochem, 2006. **293**(1-2): p. 173-81.
243. Holcik, M., N. Sonenberg, and R.G. Korneluk, *Internal ribosome initiation of translation and the control of cell death.* Trends Genet, 2000. **16**(10): p. 469-73.
244. Mazzoni, C. and C. Falcone, *mRNA stability and control of cell proliferation.* Biochem Soc Trans, 2011. **39**(5): p. 1461-5.
245. Mazzoni, C., et al., *HIR1, the co-repressor of histone gene transcription of Saccharomyces cerevisiae, acts as a multicopy suppressor of the apoptotic phenotypes of the LSM4 mRNA degradation mutant.* FEMS Yeast Res, 2005. **5**(12): p. 1229-35.
246. Mazzoni, C., et al., *A truncated form of KILsm4p and the absence of factors involved in mRNA decapping trigger apoptosis in yeast.* Mol Biol Cell, 2003. **14**(2): p. 721-9.
247. Grallert, B. and E. Boye, *The Gcn2 kinase as a cell cycle regulator.* Cell Cycle, 2007. **6**(22): p. 2768-72.
248. Menacho-Marquez, M., et al., *Gcn2p regulates a G1/S cell cycle checkpoint in response to DNA damage.* Cell Cycle, 2007. **6**(18): p. 2302-5.
249. Ecker, N., et al., *Induction of autophagic flux by amino acid deprivation is distinct from nitrogen starvation-induced macroautophagy.* Autophagy, 2010. **6**(7): p. 879-90.
250. Vida, T.A. and S.D. Emr, *A new vital stain for visualizing vacuolar membrane dynamics and endocytosis in yeast.* J Cell Biol, 1995. **128**(5): p. 779-92.

251. Ohlmeier, S., et al., *The yeast mitochondrial proteome, a study of fermentative and respiratory growth.* J Biol Chem, 2004. **279**(6): p. 3956-79.
252. Ludovico, P., F. Madeo, and M. Silva, *Yeast programmed cell death: an intricate puzzle.* IUBMB Life, 2005. **57**(3): p. 129-35.
253. Hinnebusch, A.G., *The eIF-2 alpha kinases: regulators of protein synthesis in starvation and stress.* Semin Cell Biol, 1994. **5**(6): p. 417-26.
254. Hinnebusch, A.G., *Gene-specific translational control of the yeast GCN4 gene by phosphorylation of eukaryotic initiation factor 2.* Mol Microbiol, 1993. **10**(2): p. 215-23.
255. Rolfes, R.J. and A.G. Hinnebusch, *Translation of the yeast transcriptional activator GCN4 is stimulated by purine limitation: implications for activation of the protein kinase GCN2.* Mol Cell Biol, 1993. **13**(8): p. 5099-111.
256. Dever, T.E., et al., *Phosphorylation of initiation factor 2 alpha by protein kinase GCN2 mediates gene-specific translational control of GCN4 in yeast.* Cell, 1992. **68**(3): p. 585-96.
257. Lewis, S.M., et al., *The eIF4G homolog DAP5/p97 supports the translation of select mRNAs during endoplasmic reticulum stress.* Nucleic Acids Res, 2008. **36**(1): p. 168-78.
258. Clarkson, B.K., W.V. Gilbert, and J.A. Doudna, *Functional overlap between eIF4G isoforms in Saccharomyces cerevisiae.* PLoS One, 2010. **5**(2): p. e9114.
259. Imataka, H. and N. Sonenberg, *Human eukaryotic translation initiation factor 4G (eIF4G) possesses two separate and independent binding sites for eIF4A.* Mol Cell Biol, 1997. **17**(12): p. 6940-7.
260. Hinnebusch, A.G., *Evidence for translational regulation of the activator of general amino acid control in yeast.* Proc Natl Acad Sci U S A, 1984. **81**(20): p. 6442-6.
261. Wek, R.C., et al., *Identification of positive-acting domains in GCN2 protein kinase required for translational activation of GCN4 expression.* Mol Cell Biol, 1990. **10**(6): p. 2820-31.

262. Hall, M.N., *The TOR signalling pathway and growth control in yeast.* Biochem Soc Trans, 1996. **24**(1): p. 234-9.
263. Cutler, N.S., J. Heitman, and M.E. Cardenas, *TOR kinase homologs function in a signal transduction pathway that is conserved from yeast to mammals.* Mol Cell Endocrinol, 1999. **155**(1-2): p. 135-42.
264. Dann, S.G. and G. Thomas, *The amino acid sensitive TOR pathway from yeast to mammals.* FEBS Lett, 2006. **580**(12): p. 2821-9.
265. Sampaio-Marques, B., et al., *Yeast chronological lifespan and proteotoxic stress: is autophagy good or bad?* Biochem Soc Trans, 2011. **39**(5): p. 1466-70.
266. Stephan, J.S., et al., *The Tor and cAMP-dependent protein kinase signaling pathways coordinately control autophagy in Saccharomyces cerevisiae.* Autophagy, 2010. **6**(2): p. 294-5.
267. Kamada, Y., et al., *Tor directly controls the Atg1 kinase complex to regulate autophagy.* Mol Cell Biol, 2010. **30**(4): p. 1049-58.
268. Alvers, A.L., et al., *Autophagy is required for extension of yeast chronological life span by rapamycin.* Autophagy, 2009. **5**(6): p. 847-9.
269. Chang, Y.Y., et al., *Nutrient-dependent regulation of autophagy through the target of rapamycin pathway.* Biochem Soc Trans, 2009. **37**(Pt 1): p. 232-6.
270. Diaz-Troya, S., et al., *The role of TOR in autophagy regulation from yeast to plants and mammals.* Autophagy, 2008. **4**(7): p. 851-65.
271. Kamada, Y., T. Sekito, and Y. Ohsumi, *Autophagy in yeast: a TOR-mediated response to nutrient starvation.* Curr Top Microbiol Immunol, 2004. **279**: p. 73-84.
272. Noda, T. and Y. Ohsumi, *Tor, a phosphatidylinositol kinase homologue, controls autophagy in yeast.* J Biol Chem, 1998. **273**(7): p. 3963-6.
273. Shpilka, T., et al., *Atg8: an autophagy-related ubiquitin-like protein family.* Genome Biol, 2011. **12**(7): p. 226.
274. Trout, J.J., W.T. Stauber, and B.A. Schottelius, *Increased autophagy in chloroquine-treated tonic and phasic muscles: an alternative view.* Tissue Cell, 1981. **13**(2): p. 393-401.

275. Suzuki, T., et al., *The first molecular evidence that autophagy relates rimmed vacuole formation in chloroquine myopathy.* J Biochem, 2002. **131**(5): p. 647-51.
276. Yoon, Y.H., et al., *Induction of lysosomal dilatation, arrested autophagy, and cell death by chloroquine in cultured ARPE-19 cells.* Invest Ophthalmol Vis Sci, 2010. **51**(11): p. 6030-7.
277. Wilson, E.N., et al., *A switch between cytoprotective and cytotoxic autophagy in the radiosensitization of breast tumor cells by chloroquine and vitamin D.* Horm Cancer, 2011. **2**(5): p. 272-85.
278. Shintani, T. and D.J. Klionsky, *Autophagy in health and disease: a double-edged sword.* Science, 2004. **306**(5698): p. 990-5.
279. Floto, R.A., et al., *Small molecule enhancers of rapamycin-induced TOR inhibition promote autophagy, reduce toxicity in Huntington's disease models and enhance killing of mycobacteria by macrophages.* Autophagy, 2007. **3**(6): p. 620-2.
280. Sarkar, S., et al., *Trehalose, a novel mTOR-independent autophagy enhancer, accelerates the clearance of mutant huntingtin and alpha-synuclein.* J Biol Chem, 2007. **282**(8): p. 5641-52.
281. Aguib, Y., et al., *Autophagy induction by trehalose counteracts cellular prion infection.* Autophagy, 2009. **5**(3): p. 361-9.
282. Casarejos, M.J., et al., *The accumulation of neurotoxic proteins, induced by proteasome inhibition, is reverted by trehalose, an enhancer of autophagy, in human neuroblastoma cells.* Neurochem Int, 2011. **58**(4): p. 512-20.
283. Vahsen, N., et al., *AIF deficiency compromises oxidative phosphorylation.* EMBO J, 2004. **23**(23): p. 4679-89.
284. Silva, R.D., et al., *Hyperosmotic stress induces metacaspase- and mitochondria-dependent apoptosis in Saccharomyces cerevisiae.* Mol Microbiol, 2005. **58**(3): p. 824-34.
285. Eisenberg, T., et al., *The mitochondrial pathway in yeast apoptosis.* Apoptosis, 2007. **12**(5): p. 1011-23.

286. Morley, S.J., M.J. Coldwell, and M.J. Clemens, *Initiation factor modifications in the preapoptotic phase.* Cell Death Differ, 2005. **12**(6): p. 571-84.
287. Mateyak, M.K. and T.G. Kinzy, *eEF1A: thinking outside the ribosome.* J Biol Chem, 2010. **285**(28): p. 21209-13.
288. Gavin, A.C., et al., *Proteome survey reveals modularity of the yeast cell machinery.* Nature, 2006. **440**(7084): p. 631-6.
289. Yu, X. and M. Cai, *The yeast dynamin-related GTPase Vps1p functions in the organization of the actin cytoskeleton via interaction with Sla1p.* J Cell Sci, 2004. **117**(Pt 17): p. 3839-53.
290. Almeida, B., *Elucidation of molecular pathways involved in Saccharomyces cerevisiae apoptotic cell death*, in *School of Health Sciences, ICVS*2009, University of Minho: Braga, Portugal.
291. Khacho, M., et al., *eEF1A is a novel component of the mammalian nuclear protein export machinery.* Mol Biol Cell, 2008. **19**(12): p. 5296-308.
292. Thornton, S., et al., *Not just for housekeeping: protein initiation and elongation factors in cell growth and tumorigenesis.* J Mol Med (Berl), 2003. **81**(9): p. 536-48.
293. Lamberti, A., et al., *The translation elongation factor 1A in tumorigenesis, signal transduction and apoptosis: review article.* Amino Acids, 2004. **26**(4): p. 443-8.
294. Magazinnik, T., et al., *Interplay between GCN2 and GCN4 expression, translation elongation factor 1 mutations and translational fidelity in yeast.* Nucleic Acids Res, 2005. **33**(14): p. 4584-92.
295. Munshi, R., et al., *Overexpression of translation elongation factor 1A affects the organization and function of the actin cytoskeleton in yeast.* Genetics, 2001. **157**(4): p. 1425-36.
296. Kandl, K.A., et al., *Identification of a role for actin in translational fidelity in yeast.* Mol Genet Genomics, 2002. **268**(1): p. 10-8.
297. Gross, S.R. and T.G. Kinzy, *Translation elongation factor 1A is essential for regulation of the actin cytoskeleton and cell morphology.* Nat Struct Mol Biol, 2005. **12**(9): p. 772-8.

298. Gross, S.R. and T.G. Kinzy, *Improper organization of the actin cytoskeleton affects protein synthesis at initiation.* Mol Cell Biol, 2007. **27**(5): p. 1974-89.
299. Leadsham, J.E., et al., *Apoptosis and the yeast actin cytoskeleton.* Cell Death Differ, 2010. **17**(5): p. 754-62.
300. Pittman, Y.R., et al., *Coordination of eukaryotic translation elongation factor 1A (eEF1A) function in actin organization and translation elongation by the guanine nucleotide exchange factor eEF1Balpha.* J Biol Chem, 2009. **284**(7): p. 4739-47.
301. Bouzaidi-Tiali, N., et al., *Elongation factor 1a mediates the specificity of mitochondrial tRNA import in T. brucei.* EMBO J, 2007. **26**(20): p. 4302-12.
302. Paris, Z., et al., *Mitochondrial tRNA import in Trypanosoma brucei is independent of thiolation and the Rieske protein.* RNA, 2009. **15**(7): p. 1398-406.
303. Tarassov, I.A. and R.P. Martin, *Mechanisms of tRNA import into yeast mitochondria: an overview.* Biochimie, 1996. **78**(6): p. 502-10.
304. Kamenski, P., et al., *tRNA mitochondrial import in yeast: Mapping of the import determinants in the carrier protein, the precursor of mitochondrial lysyl-tRNA synthetase.* Mitochondrion, 2010. **10**(3): p. 284-93.
305. Alfonzo, J.D. and D. Soll, *Mitochondrial tRNA import--the challenge to understand has just begun.* Biol Chem, 2009. **390**(8): p. 717-22.
306. Schirmaier, F. and P. Philippsen, *Identification of two genes coding for the translation elongation factor EF-1 alpha of S. cerevisiae.* EMBO J, 1984. **3**(13): p. 3311-5.
307. Cottrelle, P., et al., *Cloning, nucleotide sequence, and expression of one of two genes coding for yeast elongation factor 1 alpha.* J Biol Chem, 1985. **260**(5): p. 3090-6.
308. Cottrelle, P., et al., *Either one of the two yeast EF-1 alpha genes is required for cell viability.* Curr Genet, 1985. **9**(8): p. 693-7.

309. Soares, D.C., et al., *Structural models of human eEF1A1 and eEF1A2 reveal two distinct surface clusters of sequence variation and potential differences in phosphorylation.* PLoS One, 2009. **4**(7): p. e6315.
310. Tomlinson, V.A., et al., *Translation elongation factor eEF1A2 is a potential oncoprotein that is overexpressed in two-thirds of breast tumours.* BMC Cancer, 2005. **5**: p. 113.
311. Newbery, H.J., et al., *Translation elongation factor eEF1A2 is essential for post-weaning survival in mice.* J Biol Chem, 2007. **282**(39): p. 28951-9.
312. Tomlinson, V.A., et al., *Expression of eEF1A2 is associated with clear cell histology in ovarian carcinomas: overexpression of the gene is not dependent on modifications at the EEF1A2 locus.* Br J Cancer, 2007. **96**(10): p. 1613-20.
313. Abbott, C.M., et al., *eEF1A2 and neuronal degeneration.* Biochem Soc Trans, 2009. **37**(Pt 6): p. 1293-7.
314. Tristan, C., et al., *The diverse functions of GAPDH: views from different subcellular compartments.* Cell Signal, 2011. **23**(2): p. 317-23.
315. Nicholls, C., H. Li, and J.P. Liu, *GAPDH: A common enzyme with uncommon functions.* Clin Exp Pharmacol Physiol, 2011.
316. Berry, M.D. and A.A. Boulton, *Glyceraldehyde-3-phosphate dehydrogenase and apoptosis.* J Neurosci Res, 2000. **60**(2): p. 150-4.
317. Backlund, M., et al., *Posttranscriptional regulation of angiotensin II type 1 receptor expression by glyceraldehyde 3-phosphate dehydrogenase.* Nucleic Acids Res, 2009. **37**(7): p. 2346-58.
318. Chen, R.W., et al., *Involvement of glyceraldehyde-3-phosphate dehydrogenase (GAPDH) and p53 in neuronal apoptosis: evidence that GAPDH is upregulated by p53.* J Neurosci, 1999. **19**(21): p. 9654-62.
319. Vercammen, D., et al., *Are metacaspases caspases?* J Cell Biol, 2007. **179**(3): p. 375-80.
320. Watanabe, N. and E. Lam, *Two Arabidopsis metacaspases AtMCP1b and AtMCP2b are arginine/lysine-specific cysteine proteases and activate apoptosis-like cell death in yeast.* J Biol Chem, 2005. **280**(15): p. 14691-9.

321. Kruger, N.J., *The Bradford method for protein quantitation.* Methods Mol Biol, 1994. **32**: p. 9-15.
322. Ricci, J.E., et al., *Disruption of mitochondrial function during apoptosis is mediated by caspase cleavage of the p75 subunit of complex I of the electron transport chain.* Cell, 2004. **117**(6): p. 773-86.
323. Zhou, Y., et al., *The multifunctional protein glyceraldehyde-3-phosphate dehydrogenase is both regulated and controls colony-stimulating factor-1 messenger RNA stability in ovarian cancer.* Mol Cancer Res, 2008. **6**(8): p. 1375-84.
324. Teng, X. and J.M. Hardwick, *Reliable method for detection of programmed cell death in yeast.* Methods Mol Biol, 2009. **559**: p. 335-42.
325. Giannattasio, S., et al., *Cytochrome c is released from coupled mitochondria of yeast en route to acetic acid-induced programmed cell death and can work as an electron donor and a ROS scavenger.* FEBS Lett, 2008. **582**(10): p. 1519-25.
326. Pereira, C., et al., *ADP/ATP carrier is required for mitochondrial outer membrane permeabilization and cytochrome c release in yeast apoptosis.* Mol Microbiol, 2007. **66**(3): p. 571-82.
327. Breitenbach, M., et al., *The role of mitochondria in the aging processes of yeast.* Subcell Biochem, 2012. **57**: p. 55-78.
328. Pereira, C., et al., *Mitochondria-dependent apoptosis in yeast.* Biochim Biophys Acta, 2008. **1783**(7): p. 1286-302.
329. Bereiter-Hahn, J., et al., *Structural implications of mitochondrial dynamics.* Biotechnol J, 2008. **3**(6): p. 765-80.
330. Reyes, A., et al., *Actin and myosin contribute to mammalian mitochondrial DNA maintenance.* Nucleic Acids Res, 2011. **39**(12): p. 5098-108.
331. Swayne, T.C., I.R. Boldogh, and L.A. Pon, *Imaging of the cytoskeleton and mitochondria in fixed budding yeast cells.* Methods Mol Biol, 2009. **586**: p. 171-84.
332. Lackner, L.L., J.S. Horner, and J. Nunnari, *Mechanistic analysis of a dynamin effector.* Science, 2009. **325**(5942): p. 874-7.

333. Palermo, V., C. Falcone, and C. Mazzoni, *Apoptosis and aging in mitochondrial morphology mutants of S. cerevisiae.* Folia Microbiol (Praha), 2007. **52**(5): p. 479-83.
334. Kimball, S.R., *Regulation of translation initiation by amino acids in eukaryotic cells.* Prog Mol Subcell Biol, 2001. **26**: p. 155-84.
335. Visweswaraiah, J., et al., *Evidence that eukaryotic translation elongation factor 1A (eEF1A) binds the Gcn2 protein C terminus and inhibits Gcn2 activity.* J Biol Chem, 2011. **286**(42): p. 36568-79.
336. Hardwick, J.M. and W.C. Cheng, *Mitochondrial programmed cell death pathways in yeast.* Dev Cell, 2004. **7**(5): p. 630-2.
337. Kahns, S., et al., *The elongation factor 1 A-2 isoform from rabbit: cloning of the cDNA and characterization of the protein.* Nucleic Acids Res, 1998. **26**(8): p. 1884-90.
338. Kulkarni, G., et al., *Expression of protein elongation factor eEF1A2 predicts favorable outcome in breast cancer.* Breast Cancer Res Treat, 2007. **102**(1): p. 31-41.
339. Amiri, A., et al., *eEF1A2 activates Akt and stimulates Akt-dependent actin remodeling, invasion and migration.* Oncogene, 2007. **26**(21): p. 3027-40.
340. Anand, N., et al., *Protein elongation factor EEF1A2 is a putative oncogene in ovarian cancer.* Nat Genet, 2002. **31**(3): p. 301-5.
341. Zhang, J., et al., *EF1A1-actin interactions alter mRNA stability to determine differential osteopontin expression in HepG2 and Hep3B cells.* Exp Cell Res, 2009. **315**(2): p. 304-12.
342. Mukamel, Z. and A. Kimchi, *Death-associated protein 3 localizes to the mitochondria and is involved in the process of mitochondrial fragmentation during cell death.* J Biol Chem, 2004. **279**(35): p. 36732-8.
343. Thangima Zannat, M., R.B. Bhattacharjee, and J. Bag, *In the absence of cellular poly (A) binding protein, the glycolytic enzyme GAPDH translocated to the cell nucleus and activated the GAPDH mediated*

apoptotic pathway by enhancing acetylation and serine 46 phosphorylation of p53. Biochem Biophys Res Commun, 2011. **409**(2): p. 171-6.

344. Bonafe, N., et al., *Glyceraldehyde-3-phosphate dehydrogenase binds to the AU-Rich 3' untranslated region of colony-stimulating factor-1 (CSF-1) messenger RNA in human ovarian cancer cells: possible role in CSF-1 posttranscriptional regulation and tumor phenotype.* Cancer Res, 2005. **65**(9): p. 3762-71.
345. Anand, M., et al., *Translation elongation factor 1 functions in the yeast Saccharomyces cerevisiae.* Cold Spring Harb Symp Quant Biol, 2001. **66**: p. 439-48.
346. Drubin, D.G., H.D. Jones, and K.F. Wertman, *Actin structure and function: roles in mitochondrial organization and morphogenesis in budding yeast and identification of the phalloidin-binding site.* Mol Biol Cell, 1993. **4**(12): p. 1277-94.
347. Morrish, B.C. and M.G. Rumsby, *The 5' untranslated region of protein kinase Cdelta directs translation by an internal ribosome entry segment that is most active in densely growing cells and during apoptosis.* Mol Cell Biol, 2002. **22**(17): p. 6089-99.
348. Holcik, M., *Targeting translation for treatment of cancer--a novel role for IRES?* Curr Cancer Drug Targets, 2004. **4**(3): p. 299-311.
349. Picard, D., *Heat-shock protein 90, a chaperone for folding and regulation.* Cell Mol Life Sci, 2002. **59**(10): p. 1640-8.
350. Kim, T.S., et al., *Interaction of Hsp90 with ribosomal proteins protects from ubiquitination and proteasome-dependent degradation.* Mol Biol Cell, 2006. **17**(2): p. 824-33.
351. Busconi, L., J. Guan, and B.M. Denker, *Degradation of heterotrimeric Galpha(o) subunits via the proteosome pathway is induced by the hsp90-specific compound geldanamycin.* J Biol Chem, 2000. **275**(3): p. 1565-9.
352. Wang, W.B., et al., *Paraptosis accompanied by autophagy and apoptosis was induced by celastrol, a natural compound with influence on proteasome, ER stress and Hsp90.* J Cell Physiol, 2012. **227**(5): p. 2196-206.

353. Liu, K.S., et al., *SNX-2112, an Hsp90 inhibitor, induces apoptosis and autophagy via degradation of Hsp90 client proteins in human melanoma A-375 cells.* Cancer Lett, 2011.

354. Shen, S., et al., *Cyclodepsipeptide toxin promotes the degradation of Hsp90 client proteins through chaperone-mediated autophagy.* J Cell Biol, 2009. **185**(4): p. 629-39.

355. Qing, G., P. Yan, and G. Xiao, *Hsp90 inhibition results in autophagy-mediated proteasome-independent degradation of IkappaB kinase (IKK).* Cell Res, 2006. **16**(11): p. 895-901.

356. McClellan, A.J., et al., *Diverse cellular functions of the Hsp90 molecular chaperone uncovered using systems approaches.* Cell, 2007. **131**(1): p. 121-35.

357. Louvion, J.F., T. Abbas-Terki, and D. Picard, *Hsp90 is required for pheromone signaling in yeast.* Mol Biol Cell, 1998. **9**(11): p. 3071-83.

358. Franzosa, E.A., et al., *Heterozygous yeast deletion collection screens reveal essential targets of Hsp90.* PLoS One, 2011. **6**(11): p. e28211.

359. Millson, S.H., et al., *A two-hybrid screen of the yeast proteome for Hsp90 interactors uncovers a novel Hsp90 chaperone requirement in the activity of a stress-activated mitogen-activated protein kinase, Slt2p (Mpk1p).* Eukaryot Cell, 2005. **4**(5): p. 849-60.

360. Donze, O. and D. Picard, *Hsp90 binds and regulates Gcn2, the ligand-inducible kinase of the alpha subunit of eukaryotic translation initiation factor 2 [corrected].* Mol Cell Biol, 1999. **19**(12): p. 8422-32.

361. Altmann, M., et al., *A Saccharomyces cerevisiae homologue of mammalian translation initiation factor 4B contributes to RNA helicase activity.* EMBO J, 1993. **12**(10): p. 3997-4003.

362. Mueller, P.P., S. Harashima, and A.G. Hinnebusch, *A segment of GCN4 mRNA containing the upstream AUG codons confers translational control upon a heterologous yeast transcript.* Proc Natl Acad Sci U S A, 1987. **84**(9): p. 2863-7.

363. Mira, N.P., J.D. Becker, and I. Sa-Correia, *Genomic expression program involving the Haa1p-regulon in Saccharomyces cerevisiae response to acetic acid.* OMICS, 2010. **14**(5): p. 587-601.
364. Altmann, M., et al., *A novel inhibitor of cap-dependent translation initiation in yeast: p20 competes with eIF4G for binding to eIF4E.* EMBO J, 1997. **16**(5): p. 1114-21.
365. Warnakulasuriyarachchi, D., N.H. Ungureanu, and M. Holcik, *The translation of an antiapoptotic protein HIAP2 is regulated by an upstream open reading frame.* Cell Death Differ, 2003. **10**(8): p. 899-904.
366. Baird, S.D., et al., *A search for structurally similar cellular internal ribosome entry sites.* Nucleic Acids Res, 2007. **35**(14): p. 4664-77.
367. Chen, B., et al., *The HSP90 family of genes in the human genome: insights into their divergence and evolution.* Genomics, 2005. **86**(6): p. 627-37.
368. Smith, V., et al., *Comparison of 17-dimethylaminoethylamino-17-demethoxy-geldanamycin (17DMAG) and 17-allylamino-17-demethoxygeldanamycin (17AAG) in vitro: effects on Hsp90 and client proteins in melanoma models.* Cancer Chemother Pharmacol, 2005. **56**(2): p. 126-37.
369. Neufeld, T.P., *TOR-dependent control of autophagy: biting the hand that feeds.* Curr Opin Cell Biol, 2010. **22**(2): p. 157-68.
370. Nakatsu, Y., et al., *Involvement of autophagy via mammalian target of rapamycin (mTOR) inhibition in tributyltin-induced neuronal cell death.* J Toxicol Sci, 2010. **35**(2): p. 245-51.
371. Yu, J., A.A. Parkhitko, and E.P. Henske, *Mammalian target of rapamycin signaling and autophagy: roles in lymphangioleiomyomatosis therapy.* Proc Am Thorac Soc, 2010. **7**(1): p. 48-53.
372. Carames, B., et al., *Autophagy activation by rapamycin reduces severity of experimental osteoarthritis.* Ann Rheum Dis, 2011.
373. Sekiguchi, A., et al., *Rapamycin Promotes Autophagy and Reduces Neural Tissue Damage and Locomotor Impairment after Spinal Cord Injury in Mice.* J Neurotrauma, 2011.

374. Wang, Y., et al., *Chloroquine enhances the cytotoxicity of topotecan by inhibiting autophagy in lung cancer cells.* Chin J Cancer, 2011. **30**(10): p. 690-700.
375. Colado, E., et al., *The effect of the proteasome inhibitor bortezomib on acute myeloid leukemia cells and drug resistance associated with the CD34+ immature phenotype.* Haematologica, 2008. **93**(1): p. 57-66.
376. Butturini, A., et al., *GM-CSF incubation prior to treatment with cytarabine or doxorubicin enhances drug activity against AML cells in vitro: a model for leukemia chemotherapy.* Leuk Res, 1990. **14**(9): p. 743-9.
377. Pogliani, E.M., et al., *Idarubicin in combination with cytarabine and VP-16 in the treatment of post myelodysplastic syndrome acute myeloblastic leukemia (MDS-AML).* Leuk Lymphoma, 1995. **19**(5-6): p. 473-7.
378. Arnaout, M.K., et al., *Treatment of childhood acute myelogenous leukemia with an intensive regimen (AML-87) that individualizes etoposide and cytarabine dosages: short- and long-term effects.* Leukemia, 2000. **14**(10): p. 1736-42.
379. Limonta, M., et al., *Doxorubicin and m-AMSA induced DNA damage in blast cells from AML patients.* Leuk Res, 1991. **15**(1): p. 19-24.
380. Kim, H.S., T.B. Lee, and C.H. Choi, *Down-regulation of catalase gene expression in the doxorubicin-resistant AML subline AML-2/DX100.* Biochem Biophys Res Commun, 2001. **281**(1): p. 109-14.
381. Choi, C.H., et al., *Balance of NF-kappaB and p38 MAPK is a determinant of radiosensitivity of the AML-2 and its doxorubicin-resistant cell lines.* Leuk Res, 2007. **31**(9): p. 1267-76.
382. Lee, T.B., Y.S. Moon, and C.H. Choi, *Histone H4 deacetylation down-regulates catalase gene expression in doxorubicin-resistant AML subline.* Cell Biol Toxicol, 2012. **28**(1): p. 11-8.
383. Schnaider, T., et al., *The Hsp90-specific inhibitor, geldanamycin, blocks CD28-mediated activation of human T lymphocytes.* Life Sci, 1998. **63**(11): p. 949-54.

384. Taiyab, A., A.S. Sreedhar, and M. Rao Ch, *Hsp90 inhibitors, GA and 17AAG, lead to ER stress-induced apoptosis in rat histiocytoma.* Biochem Pharmacol, 2009. **78**(2): p. 142-52.
385. Chiosis, G., A. Rodina, and K. Moulick, *Emerging Hsp90 inhibitors: from discovery to clinic.* Anticancer Agents Med Chem, 2006. **6**(1): p. 1-8.
386. Zheng, Y., et al., *Chloroquine inhibits colon cancer cell growth in vitro and tumor growth in vivo via induction of apoptosis.* Cancer Invest, 2009. **27**(3): p. 286-92.
387. Kim, E.L., et al., *Chloroquine activates the p53 pathway and induces apoptosis in human glioma cells.* Neuro Oncol, 2010. **12**(4): p. 389-400.
388. Chiu, W.T., et al., *Inhibition of HSP90-dependent telomerase activity in amyloid beta-induced apoptosis of cerebral endothelial cells.* J Cell Physiol, 2011. **226**(8): p. 2041-51.
389. Darwin, C., *The origin of the species*. Barnes & noble classics. 2003, New York, NY: Fine Creative Media. p.
390. Hellen, C.U., *IRES-induced conformational changes in the ribosome and the mechanism of translation initiation by internal ribosomal entry.* Biochim Biophys Acta, 2009. **1789**(9-10): p. 558-70.
391. King, H.A., L.C. Cobbold, and A.E. Willis, *The role of IRES trans-acting factors in regulating translation initiation.* Biochem Soc Trans, 2010. **38**(6): p. 1581-6.
392. Khan, M.A., et al., *Effects of poly(A)-binding protein on the interactions of translation initiation factor eIF4F and eIF4F.4B with internal ribosome entry site (IRES) of tobacco etch virus RNA.* Biochim Biophys Acta, 2008. **1779**(10): p. 622-7.
393. Byrd, M.P., M. Zamora, and R.E. Lloyd, *Translation of eukaryotic translation initiation factor 4GI (eIF4GI) proceeds from multiple mRNAs containing a novel cap-dependent internal ribosome entry site (IRES) that is active during poliovirus infection.* J Biol Chem, 2005. **280**(19): p. 18610-22.

394. Lopez de Quinto, S., E. Lafuente, and E. Martinez-Salas, *IRES interaction with translation initiation factors: functional characterization of novel RNA contacts with eIF3, eIF4B, and eIF4GII.* RNA, 2001. **7**(9): p. 1213-26.
395. Ali, I.K., et al., *Activity of the hepatitis A virus IRES requires association between the cap-binding translation initiation factor (eIF4E) and eIF4G.* J Virol, 2001. **75**(17): p. 7854-63.
396. Hayashi, S., et al., *Increase in cap- and IRES-dependent protein synthesis by overproduction of translation initiation factor eIF4G.* Biochem Biophys Res Commun, 2000. **277**(1): p. 117-23.
397. Robert, F., et al., *Blocking UV-induced eIF2alpha phosphorylation with small molecule inhibitors of GCN2.* Chem Biol Drug Des, 2009. **74**(1): p. 57-67.
398. Cai, Q. and H.L. Brooks, *Phosphorylation of eIF2alpha via the general control kinase, GCN2, modulates the ability of renal medullary cells to survive high urea stress.* Am J Physiol Renal Physiol, 2011. **301**(6): p. F1202-7.
399. Satoh, S., et al., *Caspase-mediated cleavage of eukaryotic translation initiation factor subunit 2alpha.* Biochem J, 1999. **342 (Pt 1)**: p. 65-70.
400. Lomakin, I.B., C.U. Hellen, and T.V. Pestova, *Physical association of eukaryotic initiation factor 4G (eIF4G) with eIF4A strongly enhances binding of eIF4G to the internal ribosomal entry site of encephalomyocarditis virus and is required for internal initiation of translation.* Mol Cell Biol, 2000. **20**(16): p. 6019-29.
401. Magherini, F., et al., *Protein expression profiles in Saccharomyces cerevisiae during apoptosis induced by H2O2.* Proteomics, 2007. **7**(9): p. 1434-45.
402. Smits, P., J. Smeitink, and L. van den Heuvel, *Mitochondrial translation and beyond: processes implicated in combined oxidative phosphorylation deficiencies.* J Biomed Biotechnol, 2010. **2010**: p. 737385.
403. Chiron, S., A. Suleau, and N. Bonnefoy, *Mitochondrial translation: elongation factor tu is essential in fission yeast and depends on an*

exchange factor conserved in humans but not in budding yeast. Genetics, 2005. **169**(4): p. 1891-901.

404. McKee, E.E., *Mitochondrial gene expression in Saccharomyces cerevisiae. IV. Effects of yeast cytosol on mitochondrial protein synthesis, degradation, and respiration.* Biochim Biophys Acta, 1994. **1201**(2): p. 235-44.
405. Schneider, A., *Mitochondrial tRNA import and its consequences for mitochondrial translation.* Annu Rev Biochem, 2011. **80**: p. 1033-53.
406. Gadir, N., et al., *Localization of mRNAs coding for mitochondrial proteins in the yeast Saccharomyces cerevisiae.* RNA, 2011. **17**(8): p. 1551-65.
407. Dieckmann, C.L. and R.R. Staples, *Regulation of mitochondrial gene expression in Saccharomyces cerevisiae.* Int Rev Cytol, 1994. **152**: p. 145-81.
408. Costanzo, M.C. and T.D. Fox, *Control of mitochondrial gene expression in Saccharomyces cerevisiae.* Annu Rev Genet, 1990. **24**: p. 91-113.
409. Attardi, G. and G. Schatz, *Biogenesis of mitochondria.* Annu Rev Cell Biol, 1988. **4**: p. 289-333.
410. Tzagoloff, A. and A.M. Myers, *Genetics of mitochondrial biogenesis.* Annu Rev Biochem, 1986. **55**: p. 249-85.
411. Biswas, T.K. and G.S. Getz, *Requirement of different mitochondrial targeting sequences of the yeast mitochondrial transcription factor Mtf1p when synthesized in alternative translation systems.* Biochem J, 2004. **383**(Pt 2): p. 383-91.
412. Grivell, L.A., *Nucleo-mitochondrial interactions in mitochondrial gene expression.* Crit Rev Biochem Mol Biol, 1995. **30**(2): p. 121-64.
413. Yu, Y., et al., *The mechanism of translation initiation on Aichivirus RNA mediated by a novel type of picornavirus IRES.* EMBO J, 2011. **30**(21): p. 4423-36.
414. Hernandez, G., *Was the initiation of translation in early eukaryotes IRES-driven?* Trends Biochem Sci, 2008. **33**(2): p. 58-64.
415. Moosavi, B., J. Wongwigkarn, and M.F. Tuite, *Hsp70/Hsp90 co-chaperones are required for efficient Hsp104-mediated elimination of the*

yeast [PSI(+)] prion but not for prion propagation. Yeast, 2010. **27**(3): p. 167-79.

416. Tapia, H. and K.A. Morano, *Hsp90 nuclear accumulation in quiescence is linked to chaperone function and spore development in yeast.* Mol Biol Cell, 2010. **21**(1): p. 63-72.
417. Ahner, A., F.M. Whyte, and J.L. Brodsky, *Distinct but overlapping functions of Hsp70, Hsp90, and an Hsp70 nucleotide exchange factor during protein biogenesis in yeast.* Arch Biochem Biophys, 2005. **435**(1): p. 32-41.
418. Mishra, M., et al., *Hsp90 protein in fission yeast Swo1p and UCS protein Rng3p facilitate myosin II assembly and function.* Eukaryot Cell, 2005. **4**(3): p. 567-76.
419. Goeckeler, J.L., et al., *Overexpression of yeast Hsp110 homolog Sse1p suppresses ydj1-151 thermosensitivity and restores Hsp90-dependent activity.* Mol Biol Cell, 2002. **13**(8): p. 2760-70.
420. Stemmann, O., et al., *Hsp90 enables Ctf13p/Skp1p to nucleate the budding yeast kinetochore.* Proc Natl Acad Sci U S A, 2002. **99**(13): p. 8585-90.
421. Lee, H.C., T. Hon, and L. Zhang, *The molecular chaperone Hsp90 mediates heme activation of the yeast transcriptional activator Hap1.* J Biol Chem, 2002. **277**(9): p. 7430-7.
422. Ki, S.W., et al., *Radicicol binding to Swo1/Hsp90 and inhibition of growth of specific temperature-sensitive cell cycle mutants of fission yeast.* Biosci Biotechnol Biochem, 2001. **65**(11): p. 2528-34.
423. Abbas-Terki, T., et al., *Hsp104 interacts with Hsp90 cochaperones in respiring yeast.* Mol Cell Biol, 2001. **21**(22): p. 7569-75.
424. Grandin, N. and M. Charbonneau, *Hsp90 levels affect telomere length in yeast.* Mol Genet Genomics, 2001. **265**(1): p. 126-34.
425. Goes, F.S. and J. Martin, *Hsp90 chaperone complexes are required for the activity and stability of yeast protein kinases Mik1, Wee1 and Swe1.* Eur J Biochem, 2001. **268**(8): p. 2281-9.

426. Abbas-Terki, T., O. Donze, and D. Picard, *The molecular chaperone Cdc37 is required for Ste11 function and pheromone-induced cell cycle arrest.* FEBS Lett, 2000. **467**(1): p. 111-6.
427. Liu, X.D., K.A. Morano, and D.J. Thiele, *The yeast Hsp110 family member, Sse1, is an Hsp90 cochaperone.* J Biol Chem, 1999. **274**(38): p. 26654-60.
428. Munoz, M.J. and J. Jimenez, *Genetic interactions between Hsp90 and the Cdc2 mitotic machinery in the fission yeast Schizosaccharomyces pombe.* Mol Gen Genet, 1999. **261**(2): p. 242-50.
429. Fang, Y., et al., *SBA1 encodes a yeast hsp90 cochaperone that is homologous to vertebrate p23 proteins.* Mol Cell Biol, 1998. **18**(7): p. 3727-34.
430. Zarzov, P., H. Boucherie, and C. Mann, *A yeast heat shock transcription factor (Hsf1) mutant is defective in both Hsc82/Hsp82 synthesis and spindle pole body duplication.* J Cell Sci, 1997. **110 (Pt 16)**: p. 1879-91.
431. Zhao, R. and W.A. Houry, *Molecular interaction network of the Hsp90 chaperone system.* Adv Exp Med Biol, 2007. **594**: p. 27-36.
432. Minami, Y., et al., *Selective apoptosis of tandemly duplicated FLT3-transformed leukemia cells by Hsp90 inhibitors.* Leukemia, 2002. **16**(8): p. 1535-40.
433. Redlak, M.J. and T.A. Miller, *Targeting PI3K/Akt/HSP90 signaling sensitizes gastric cancer cells to deoxycholate-induced apoptosis.* Dig Dis Sci, 2011. **56**(2): p. 323-9.
434. Tan, S.S., et al., *GRP78 up-regulation is associated with androgen receptor status, Hsp70-Hsp90 client proteins and castrate-resistant prostate cancer.* J Pathol, 2011. **223**(1): p. 81-7.
435. Williams, C.R., et al., *Intratumor injection of the Hsp90 inhibitor 17AAG decreases tumor growth and induces apoptosis in a prostate cancer xenograft model.* J Urol, 2007. **178**(4 Pt 1): p. 1528-32.
436. Kim, H.L., et al., *HIF-1alpha and STAT3 client proteins interacting with the cancer chaperone Hsp90: therapeutic considerations.* Cancer Biol Ther, 2008. **7**(1): p. 10-4.

437. Messaoudi, S., et al., *Recent advances in Hsp90 inhibitors as antitumor agents.* Anticancer Agents Med Chem, 2008. **8**(7): p. 761-82.
438. Millson, S.H., et al., *Expressed as the sole Hsp90 of yeast, the alpha and beta isoforms of human Hsp90 differ with regard to their capacities for activation of certain client proteins, whereas only Hsp90beta generates sensitivity to the Hsp90 inhibitor radicicol.* FEBS J, 2007. **274**(17): p. 4453-63.
439. Lu, Z., et al., *Celastrol, a novel HSP90 inhibitor, depletes Bcr-Abl and induces apoptosis in imatinib-resistant chronic myelogenous leukemia cells harboring T315I mutation.* Cancer Lett, 2010. **290**(2): p. 182-91.
440. Tong, W.G., et al., *The synthetic heat shock protein 90 (Hsp90) inhibitor EC141 induces degradation of Bcr-Abl p190 protein and apoptosis of Ph-positive acute lymphoblastic leukemia cells.* Invest New Drugs, 2011. **29**(6): p. 1206-12.
441. Bai, L., et al., *Blocking NF-kappaB and Akt by Hsp90 inhibition sensitizes Smac mimetic compound 3-induced extrinsic apoptosis pathway and results in synergistic cancer cell death.* Apoptosis, 2011. **16**(1): p. 45-54.
442. McLaughlin, S.H., et al., *The co-chaperone p23 arrests the Hsp90 ATPase cycle to trap client proteins.* J Mol Biol, 2006. **356**(3): p. 746-58.
443. Zhao, Y.S., et al., *beta-Elemene inhibits Hsp90/Raf-1 molecular complex inducing apoptosis of glioblastoma cells.* J Neurooncol, 2011.

ATTACHMENTS

Attachment I

Biochimica et Biophysica Acta 1813 (2011) 2044–2049

Contents lists available at SciVerse ScienceDirect

Biochimica et Biophysica Acta

journal homepage: www.elsevier.com/locate/bbamcr

Glyceraldehyde-3-phosphate dehydrogenase (GAPDH) is a specific substrate of yeast metacaspase

A. Silva [a,b], B. Almeida [a,b,1], B. Sampaio-Marques [a,b], M.I.R. Reis [c,d], S. Ohlmeier [e], F. Rodrigues [a,b], A. do Vale [c], P. Ludovico [a,b,*]

[a] Life and Health Sciences Research Institute (ICVS), School of Health Sciences, University of Minho, Braga, Portugal
[b] ICVS/3B's - PT Government Associate Laboratory, Braga/Guimarães, Portugal
[c] Fish Immunology and Vaccinology Group, IBMC - Instituto de Biologia Molecular e Celular, Universidade do Porto, Porto, Portugal
[d] Instituto de Ciências Biomédicas Abel Salazar (ICBAS), Universidade do Porto, Porto, Portugal
[e] Proteomics Core Facility, Biocenter Oulu, Department of Biochemistry, University of Oulu, Oulu, Finland

ARTICLE INFO

Article history:
Received 21 June 2011
Received in revised form 21 September 2011
Accepted 23 September 2011
Available online 1 October 2011

Keywords:
H_2O_2-induced yeast apoptosis
Yeast metacaspase
Glyceraldehyde-3-phosphate dehydrogenase
Nitric oxide

ABSTRACT

Yeast metacaspase (Yca1p) is required for the execution of apoptosis upon a wide range of stimuli. However, the specific degradome of this yeast protease has not been unraveled so far. By combining different methodologies described as requisites for a protein to be considered a protease substrate, such as digestome analysis, cleavage of recombinant GAPDH by metacaspase and evaluation of protein levels in vivo, we show that upon H_2O_2-induced apoptosis, the metabolic enzyme glyceraldehyde-3-phosphate dehydrogenase (GAPDH) is a specific target of metacaspase. Nitric oxide (NO) signaling, which mediates H_2O_2-induced apoptosis, is required for metacaspase specific GAPDH cleavage. In conclusion, in this work we identified GAPDH as the first direct yeast metacaspase substrate described so far. Although mammalian caspases and yeast metacaspase apparently have distinct target cleavage sites, GAPDH arises as a common substrate for these proteases.

1. Introduction

Over a decade ago, a family of proteases presenting structural similarities to caspases was identified in protists, fungi and plants [1]. These proteases were named metacaspases and classified, according to the presence or absence of a N-terminal prodomain containing a proline-rich repeat motif, as type I or type II, respectively. In spite of the structural similarity with the remotely related caspases, a large body of accumulating evidence shows that all metacaspases are highly specific for P1-Arg and P1-Lys substrates (reviewed in [2]).

Yeast cells have a single gene, *YCA1*, encoding a type I metacaspase that was first implicated in the execution of oxidative stress induced cell death [3] but that is estimated to participate in approximately 40% of the described yeast apoptotic scenarios [4]. Nevertheless, non-death functions have also been assigned to yeast metacaspase such as cell cycle regulation [5] and protein catabolism [6]. Although the mechanisms regulating this multifunctional protein, metacaspase, still remain elusive, it is known that metacaspase activity is regulated through S-nitrosation and thus dependent on the endogenous levels of nitric oxide (NO) [7]. S-nitrosation of one metacaspase Cys residue keeps it inactive. However, a second catalytic Cys residue, highly conserved in all known metacaspases but absent in all members of caspases, can rescue metacaspase activity in the presence of high NO levels [7]. Accordingly, in yeast H_2O_2-induced apoptotic conditions [3,8], a cell death process dependent on metacaspase activity and NO generation, metacaspase activity and cell death are abolished in the presence of L-NAME, an inhibitor of NO synthesis [9,10].

One of the major mechanistic challenges for understanding the role of metacaspases in cell survival and death is still the identification of their natural substrates. At the present the only protein found to be cleaved by metacaspases in vivo is the evolutionarily conserved TSN (Tudor staphylococcal nuclease) [11] found in all eukaryotes except in budding yeast [11]. Thus, although in yeast, metacaspase is essential for apoptosis execution upon a wide range of either physiological or external stimuli [3,12], the substrates targeted by this protease are still unknown.

In this context, the identification of yeast metacaspase specific degradome is crucial for unraveling the signaling pathways regulated by yeast metacaspase and to clarify its function in cell death. Using a digestome analysis, together with in vitro and in vivo protein processing assays, we found evidence indicating that the yeast metabolic enzyme glyceraldehyde-3-phosphate dehydrogenase (GAPDH) is a specific substrate of yeast metacaspase.

Abbreviations: Yca1p, metacaspase; GAPDH, glyceraldehyde-3-phosphate dehydrogenase; NO, nitric oxide; L-NAME, Nω-nitro-L-arginine methyl ester

* Corresponding author at: Life and Health Sciences Research Institute (ICVS), School of Health Sciences, University of Minho, Campus de Gualtar, 4710-057 Braga, Portugal. Tel.: +351 253604812; fax: +351 253604809.
E-mail address: pludovico@ecsaude.uminho.pt (P. Ludovico).
[1] Present address: IBMC-Instituto de Biologia Molecular e Celular, Universidade do Porto, Porto, Portugal.

0167-4889/$ – see front matter © 2011 Elsevier B.V. All rights reserved.
doi:10.1016/j.bbamcr.2011.09.010

2. Materials and methods

2.1. Yeast strains and plasmids

Saccharomyces cerevisiae BY4742 (*MATα his3*Δ1 *leu2*Δ0 *lys2*Δ0 *ura3*Δ0) strain and its isogenic derivative Δ*yca1* (EUROSCARF, Frankfurt, Germany) were used. For construction of the metacaspase-overexpressing strain, *YCA1* was amplified by PCR (primers 5′-ccgggaattcgatgtatccaggtagtggacgt-3′ and 5′-ccggggatccctacataat aaattgcagatttacgtc-3′), using genomic DNA, isolated from BY4742 strain and cloned into the EcoRI and BamHI sites of pGREG546 (EUROSCARF, Frankfurt, Germany), which displays GST at N-terminal and a galactose-inducible promoter, generating pGREG546*YCA1*. Strain Δ*yca1* was transformed with pGREG546*YCA1*, generating strain *YCA1*^{overexp}.

2.2. Metacaspase overexpression and activation

YCA1^{overexp} cells were grown until exponential growth phase ($OD_{640nm} = 0.5$) on synthetic complete (SC) medium containing glucose (2%, w/v), yeast nitrogen base (0.17%, w/v, Difco), 300 mg/l of L-leucine, 50 mg/l of L-histidine and 50 mg/l of L-lysine. Cells were washed, ressuspended in SC medium containing galactose (2%, w/v) and incubated at 26 °C with stirring (150 r.p.m.) to induce metacaspase overexpression. After 16 h, 10^7 cells/ml were harvested and resuspended in fresh SC medium with galactose (2%, w/v), and metacaspase was activated by the addition of 2 mM of H_2O_2 [3] and incubation for 200 min at 26 °C with stirring (150 r.p.m.).

2.3. Inhibition of NO production

Inhibition of NO production was achieved by pre-incubation of yeast cells for 1 h with the non-metabolized L-arginine analog, Nω-nitro-L-arginine methyl ester (L-NAME; Sigma-Aldrich), as described [8,9].

2.4. Protein extracts

Total protein extracts were prepared from untreated and H_2O_2-treated yeast cells as described [9]. Protein concentration was determined by Bradford method [13].

2.5. Digestome analysis

Digestome analysis was performed according to the methodology previously described in [14], with adaptations. Four hundred micrograms of total protein extracts obtained from untreated wild-type yeast cells were resolved by SDS-PAGE 12% (first dimension). After migration, the lanes were excised and treated as described in [14], soaked in digestion buffer [50 mM Tris-HCl, 150 mM NaCl and 10 mM DTT] with 5 mg of either active metacaspase-enriched extracts (obtained from H_2O_2-treated *YCA1*^{overexp} cells) or inactive metacaspase-enriched extracts (obtained from H_2O_2-treated Δ*yca1* or untreated *YCA1*^{overexp} cells), incubated overnight at 37 °C, washed with ultrapure water and incubated in loading buffer [50 mM Tris (pH 6.8), 2% SDS, 0.1% bromophenol blue, 10% glycerol, 2.5% β-mercaptoethanol] for 10 min at 95 °C. After cooling, lanes were subjected to a second dimension SDS-PAGE. Proteins in the gels were immunoblotted as described below or stained using Colloidal Blue Staining Kit (Invitrogen) and the spots located below the diagonal, corresponding to cleaved proteins, were excised from the gels and identified by MALDI-TOF mass spectrometry as described in [13].

2.6. Assessment of intracellular reactive oxygen species (ROS)

Free intracellular ROS were detected with dihydrorhodamine 123 (DHR123) (Molecular Probes, Eugene, OR, USA). DHR123 was added from a 1 mg/ml stock solution in ethanol, to 5×10^6 cells/ml suspended in PBS, reaching a final concentration of 15 μg/ml. Cells were incubated for 90 min at 30 °C in the dark, washed in PBS and analyzed by flow cytometry. Flow cytometric assays were performed on a BD LSR II™ (Becton Dickinson, NJ, USA) using BD FACSDiva Software 6.0 (Becton Dickinson, NJ, USA). Twenty thousand cells per sample were analyzed using the FlowJo software (Tree Star, Ashland, OR, USA).

2.7. TUNEL assay

DNA strand breaks were assessed by a TUNEL assay with the In situ Cell Death Detection Kit, POD (Roche Applied Science, Indianapolis, IN). Yeast cells were initially fixed with 3.7% formaldehyde followed by digestion of the cell walls with lyticase. After preparation of cytospins, the slides were rinsed with PBS, incubated in permeabilization solution (0.1%, v/v, Triton X-100 and 0.1%, w/v, sodium citrate) for 3 min on ice, rinsed twice with PBS, and incubated with 10 μL of TUNEL reaction mixture (terminal deoxynucleotidyl transferase and FITC-dUTP) for 60 min at 37 °C . Finally, the slides were rinsed three times with PBS and a coverslip was mounted with a drop of anti-fading agent Vectashield (Molecular Probes, Eugene, OR) and with 2 μL of 50 μg/mL propidium iodide (PI, Molecular Probes) solution in Tris buffer (10 mM, pH 7.0) with $MgCl_2$ (5 mM) and RNase (0.5 μg/mL). Cells were visualized with an Olympus PlanApo 60X/oil objective, with a numerical aperture of 1.42. For quantification of the number TUNEL-positive cells, at least 400 cells from three independent assays were counted. Data express the percentage of TUNEL-positive cells compared to the total number of counted cells.

2.8. Recombinant protein expression and cleavage assay

For production of recombinant GAPDH, yeast GAPDH (*TDH3*) was amplified by PCR (primers 5′-ggggacaagtttgtacaaaaaagcaggctccatggttagagttgctatt-3′ and 5′-ggggaccactttgtacaagaaagctgggtcttaagccttggcaacgtg-3′) from wild-type genomic DNA. PCR product was then inserted into pDEST17 vector (Invitrogen) using the gateway® technology (Invitrogen), generating the plasmid pDEST17GAPDH. *E. coli* strain BL21 pLys was transformed with vectors pDEST17GAPDH or pET23a*YCA1* (kindly provided by Dr. E. Lam).

Recombinant GAPDH and metacaspase expression was induced with 1 or 0.4 mM isopropyl-1-thio-β-D-galactopyranoside (IPTG), respectively, at 37 °C (GAPDH) or 28 °C (metacaspase). GAPDH was obtained as inclusion bodies that were solubilised in 50 mM Tris–HCl, 0.2 M NaCl, 2 mM EDTA, pH 8.0. Refolding conditions were screened using the iFOLD Protein Refolding System 2 (Novagen). The protein was refolded by dilution in 50 volumes of refolding buffer [50 mM TAPS, pH 8.5, 1.5 M Sorbitol, 24 mM NaCl, 1 mM KCl, 1 mM TCEP] overnight at 22 °C with mild agitation. Bacterial cells expressing *YCA1* were broken by sonication as described in [15], and the resulting supernatants used as described hereafter.

Metacaspase cleavage of GAPDH was assayed by incubating 500 μl of recombinant GAPDH in refolding buffer with 20 μl of bacterial extracts obtained upon expression of metacaspase and 520 μl of 2× buffer A [0.2% (w/v) CHAPS, 0.2 M HEPES, 20% (w/v) Sucrose, 20 mM TCEP, pH 7.5]. As a negative control, GAPDH was incubated with bacterial extracts obtained from *E. coli* cells expressing the empty vector, pET23a, and as a positive control, 500 μl of recombinant GAPDH in refolding buffer was mixed with 100 μl of sea bass recombinant active caspase-1 in refolding buffer and with 600 μl of 2× buffer A. Samples were incubated overnight at 22 °C, precipitated with trichloroacetic acid, resolved by SDS-PAGE and immunoblotted.

2.9. Immunoblotting

Proteins in the gels were transferred to nitrocellulose membranes. Total protein extracts were probed with monoclonal mouse anti-

GAPDH (MAB474, Chemicon) as described [9] or with the monoclonal goat anti-actin (kindly provided by Dr. C.W. Gourlay) at a dilution of 1:5000. IgGs on the blots were detected with horseradish peroxidase-conjugated anti-mouse, anti-rabbit or anti-goat IgG secondary antibodies (Cell Signaling Technology) using an enhanced chemiluminescence kit (Pierce). The expression of active metacaspase in *E. coli* harboring the pET23a*YCA1* plasmid was confirmed using polyclonal rabbit anti-Yca1p antibody (kindly supplied by Dr. F. Madeo).

2.10. Statistical analysis

The arithmetic means for the free intracellular ROS and TUNEL staining quantification and comparison of cell survival rates are presented with standard deviation with a 95% confidence value. Statistical analysis was carried out using independent samples *t*-test analysis. A p-value lower than 0.05 was assumed to denote a significant difference.

3. Results

3.1. Digestome analysis reveals GAPDH as a cleavage target of metacaspase

To identify specific targets of yeast metacaspase we performed a digestome analysis, as previously described [14]. Although digestome analysis, an in vitro assay, does not mimic cellular physiological conditions, it represents a starting point for searching putative specific substrates of proteases. In a first dimension SDS-PAGE, total protein extracts from untreated wild-type yeast cells were resolved. Upon protein separation, gel lanes were excised and incubated with active metacaspase-enriched extracts obtained from *YCA1*^{overexp} cells undergoing apoptosis induced by H_2O_2 treatment (a condition known to induce metacaspase activation [3]). After incubation, gel lanes were mounted on a second SDS-PAGE gel and proteins resolved a second time by molecular weight. Digestome analysis of total protein extracts revealed numerous spots below the diagonal, corresponding to protein fragments that originated from cleavage during the incubation of the gel lane with active metacaspase-enriched extracts (Fig. 1A). Three spots (Fig. 1A, spot 1, 2 and 3) were analyzed by mass spectrometry and indicate the presence of peptide fragments of the isoforms 2 or 3 (Tdh2p/Tdh3p), but not of the isoform 1 (Tdh1p), of the glycolytic enzyme glyceraldehyde-3-phosphate dehydrogenase (GAPDH) (Fig. 1B). Immunoblotting of the digestome analysis gel with an anti-GAPDH antibody showed three GAPDH fragments immediately below the diagonal (Fig. 1C1, spots 4, 5 and 6). Some of these labeled fragments are most likely the complementary GAPDH protein fragments of the peptides identified by mass spectrometry (Fig. 1A and B).

The question whether GAPDH cleavage observed was due to metacaspase or to other activated proteases was addressed. For such purpose, gel lanes were also incubated either with extracts from untreated *YCA1*^{overexp} cells or H_2O_2-treated Δ*yca1* cells, two paradigmatic conditions of absence of metacaspase activity. Digestome analysis showed that the absence of metacaspase activity (Fig. 1C2 and C3) resulted in the appearance of a GAPDH fragment (spot 6) below the full-length GAPDH protein that is also present in the digestome obtained with H_2O_2-treated *YCA1*^{overexp} cells, indicating that this is a biological phenomenon independent of metacaspase activity. However, two other spots (spots 4 and 5) were detected in the digestome analysis under active metacaspase conditions (Fig. 1C) and were not generated when active metacaspase was absent. These data suggest that GAPDH is cleaved by metacaspase and that specific cleavage products only occur when metacaspase is active.

The observed in vitro cleavage of GAPDH by active metacaspase-enriched extracts suggests a relevant role of metacaspase proteolytic activity in targeting a crucial metabolic enzyme during yeast apoptosis. In mammals, the targeting of metabolic enzymes by caspases is not a newly described phenomenon as evidenced in the caspase substrate database (CASBAH database) [16].

3.2. Recombinant GAPDH is cleaved in vitro by recombinant metacaspase

To further support the specific cleavage of GAPDH by active metacaspase, recombinant metacaspase-enriched bacterial extracts were added to recombinant GAPDH (isoform 3 - Tdh3p, the main target of fragmentation during H_2O_2-induced apoptosis [9]). As shown in Fig. 2, the addition of a metacaspase-enriched bacterial extract to recombinant GAPDH was sufficient to induce its fragmentation, with the appearance of fragments with molecular weights similar to the ones detected in the immunoblot of the digestome gel (Fig. 1C1). When protein extracts from *E. coli* cells expressing the empty vector were added to GAPDH, no fragmentation was observed (Fig. 2). GAPDH has also been reported to be specifically cleaved by caspase-1 in higher eukaryotic cells [17]. Since GAPDH sequence is highly conserved among species, as a positive control, we added recombinant fish caspase-1 to recombinant yeast GAPDH. As expected, fish caspase-1 was able to cleave yeast GAPDH (Fig. 2), although the four resulting GAPDH fragments were distinct from the ones produced by incubation with recombinant yeast metacaspase, showing that these proteases have distinct cleavage target sites. Our results indicate that yeast metacaspase recognizes target sequences distinct from the ones recognized by caspases of higher eukaryotes corroborating previous results that attributed to metacaspase an arginine/lysine-specific endopeptidase activity in contrast to the cysteine-aspartic proteases of caspases [15].

Altogether, these results show that although metacaspases have a proteolytic activity distinct from caspases, their targeted molecular pathways upon an apoptotic stimulus display similarities and during apoptotic cell death both of them degrade metabolic enzymes. Next, we went on to evaluate if cleavage of GAPDH by metacaspase also occurs during in vivo induction of yeast apoptosis by H_2O_2 [3].

3.3. In vivo metacaspase cleavage of GAPDH during H_2O_2-induced apoptosis is dependent on NO levels

Several proteins shown to be specifically cleaved by in vitro methodologies, such as the digestome analysis, proved later not to be substrates of the caspases under in vivo apoptotic conditions. Thus, metacaspase specific GAPDH fragmentation was evaluated by immunoblot analysis of the GAPDH levels, in total protein extracts from wild-type and Δ*yca1* cells challenged with H_2O_2. As expected, H_2O_2 (concentrations ranging from 0.5 mM to 2 mM) induced apoptotic cell death of wild-type cells as revealed by the increasing percentage of cells displaying TUNEL positive phenotype and high levels of reactive oxygen species (ROS) (Fig. 3). In contrast, Δ*yca1* cells were more resistant to H_2O_2 and thus have increased survival, TUNEL negative phenotype and lower percentage of cells with high ROS levels (Fig. 3). Moreover, apoptotic cell death of wild-type cells was accompanied by a clear reduction of the GAPDH levels that was not observed in Δ*yca1* cells (Fig. 3E), suggesting the requirement of metacaspase for the occurrence of fragmentation of this protein in vivo. Simultaneously, it was possible to detect a GAPDH fragment with lower molecular weight (15 kDa) (Fig. 3E) compatible with one of the fragments observed by digestome analysis (Fig. 1C1). The absence of other fragments in the immunoblot analysis, as observed by in vitro digestome assay, suggests that the peptides liberated from the precursor protein, can be further processed, resulting in fragments that are released or degraded.

These results suggest that GAPDH is a specific target of metacaspase during H_2O_2-induced apoptosis, reinforcing the link between metabolism and cell death.

Our previous data have demonstrated that upon H_2O_2-induced apoptosis, yeast cells are able to synthesize nitric oxide (NO) leading to

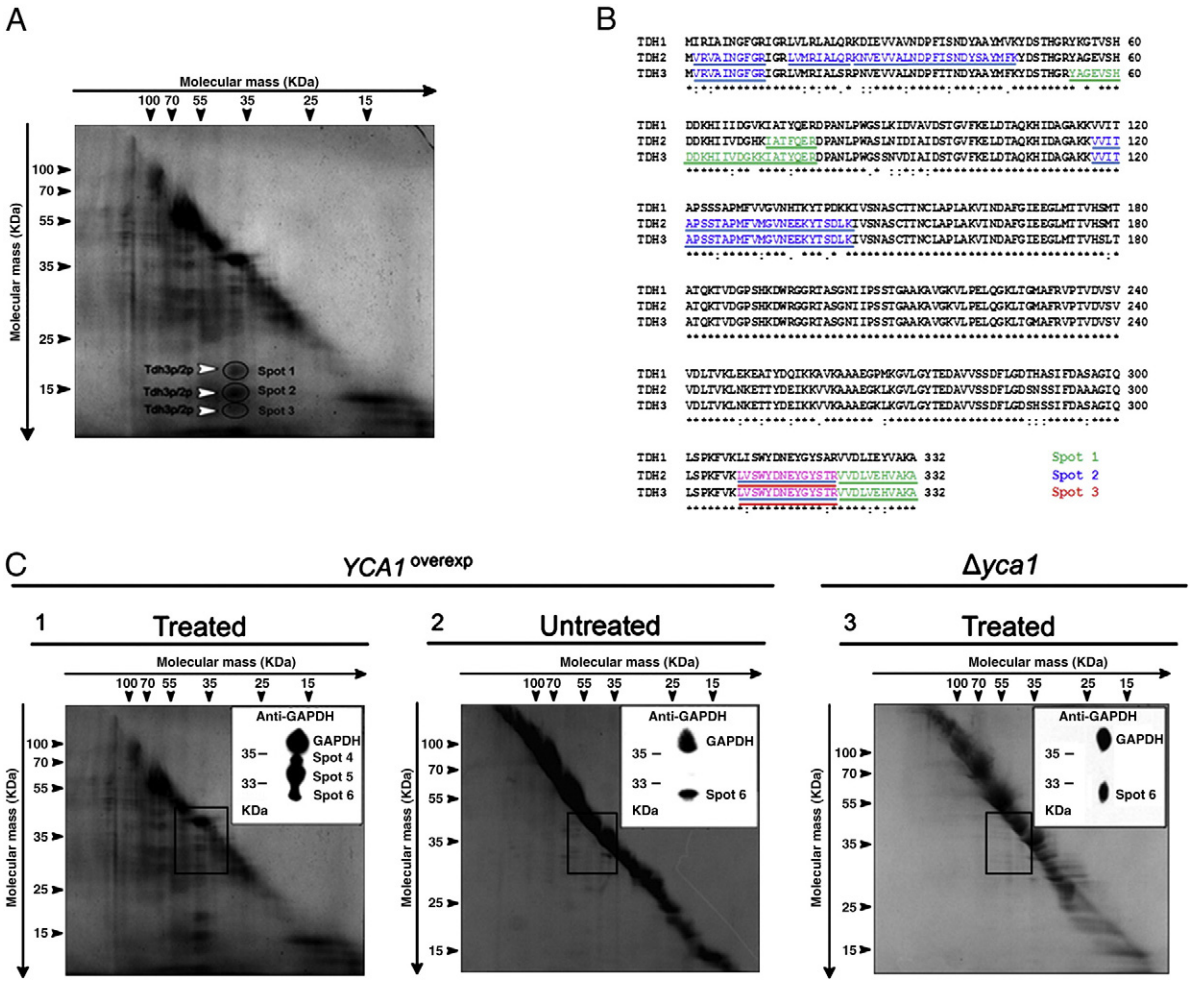

Fig. 1. GAPDH is a target of cleavage by metacaspase-enriched protein extracts. (A) Total protein extracts from untreated wild-type cells subjected to SDS-PAGE, incubated with active metacaspase-enriched extracts (from H_2O_2-treated *YCA1*^{overexp} cells) and then subjected to a second SDS-PAGE. The gel was Coomassie blue-stained. Spots below diagonal (1, 2 and 3), corresponding to cleaved proteins, were excised and analyzed by MALDI-TOF mass spectrometry. (B) Sequence of GAPDH isoforms Tdh1p (NP_012483.1), Tdh2p (NP_012542) and Tdh3p (NP_011708) retrieved from NCBI. Mass spectrometry analyses of the three spots identified peptides matches to Tdh2p and Tdh3p but not Tdh1p. Sequence parts covered by the detected peptides are indicated with different colors. Pink colored peptide was identified both in spot 2 and 3. (C) Coomassie-stained diagonal gels of protein extracts from wild-type untreated cells incubated with protein extracts from (1) H_2O_2-treated *YCA1*^{overexp} cells; (2) untreated *YCA1*^{overexp} cells and (3) H_2O_2-treated Δ*yca1* cells, and respective immunoblot analysis with a monoclonal anti-GAPDH antibody reveal spots 4, 5 and 6. Data are representative of at least three independent experiments.

the S-nitrosation of GAPDH [9]. Therefore, we wondered if the metacaspase specific GAPDH cleavage and NO signaling are correlated. To elucidate if GAPDH metacaspase-dependent fragmentation requires its previous S-nitrosation, NO synthesis was inhibited, through the pre-incubation of cells with the L-arginine analog N_ω-nitro-L-arginine methyl ester (L-NAME) [9,10], and the in vivo GAPDH levels assessed by immunoblot. NO synthesis inhibition resulted in the maintenance of GAPDH levels, in contrast with the H_2O_2-treated wild-type cells without L-NAME pre-incubation (Fig. 3F). These results revealed a causal relation between metacaspase activity and NO levels, as previously reported [7,10] indicating that the in vivo occurrence of metacaspase specific GAPDH cleavage upon H_2O_2-induced apoptosis requires NO signaling.

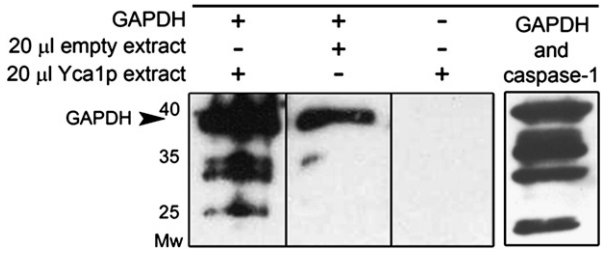

Fig. 2. In vitro cleavage of recombinant GAPDH by metacaspase-enriched bacterial extracts and purified caspase-1. Immunoblot of recombinant GAPDH incubated with 20 µl of protein extracts from bacteria harboring pET23a empty vector, 20 µl of protein extracts from bacteria expressing metacaspase or recombinant purified caspase-1. Twenty microliters of protein extracts from bacterial cells expressing metacaspase were loaded as control. Data are representative of at least three independent experiments.

4. Discussion

Metacaspase seems to be an executor of the apoptotic events observed in *S. cerevisiae* (reviewed in [4,12]). Although significant efforts have gone into the clarification of the role of metacaspase in yeast cell death processes, its role is still enigmatic. The routes to unravel yeast metacaspase functions undoubtedly have to pass through understanding how metacaspase recognizes its substrates, the identification of its specific substrates and how substrate cleavage is involved in the apoptotic phenotype. Although it was described that in vivo metacaspases cleave the evolutionarily conserved TSN (Tudor staphylococcal nuclease) [11], TSN is absent in budding yeast [11] and thus the substrates targeted by yeast metacaspase are still unknown.

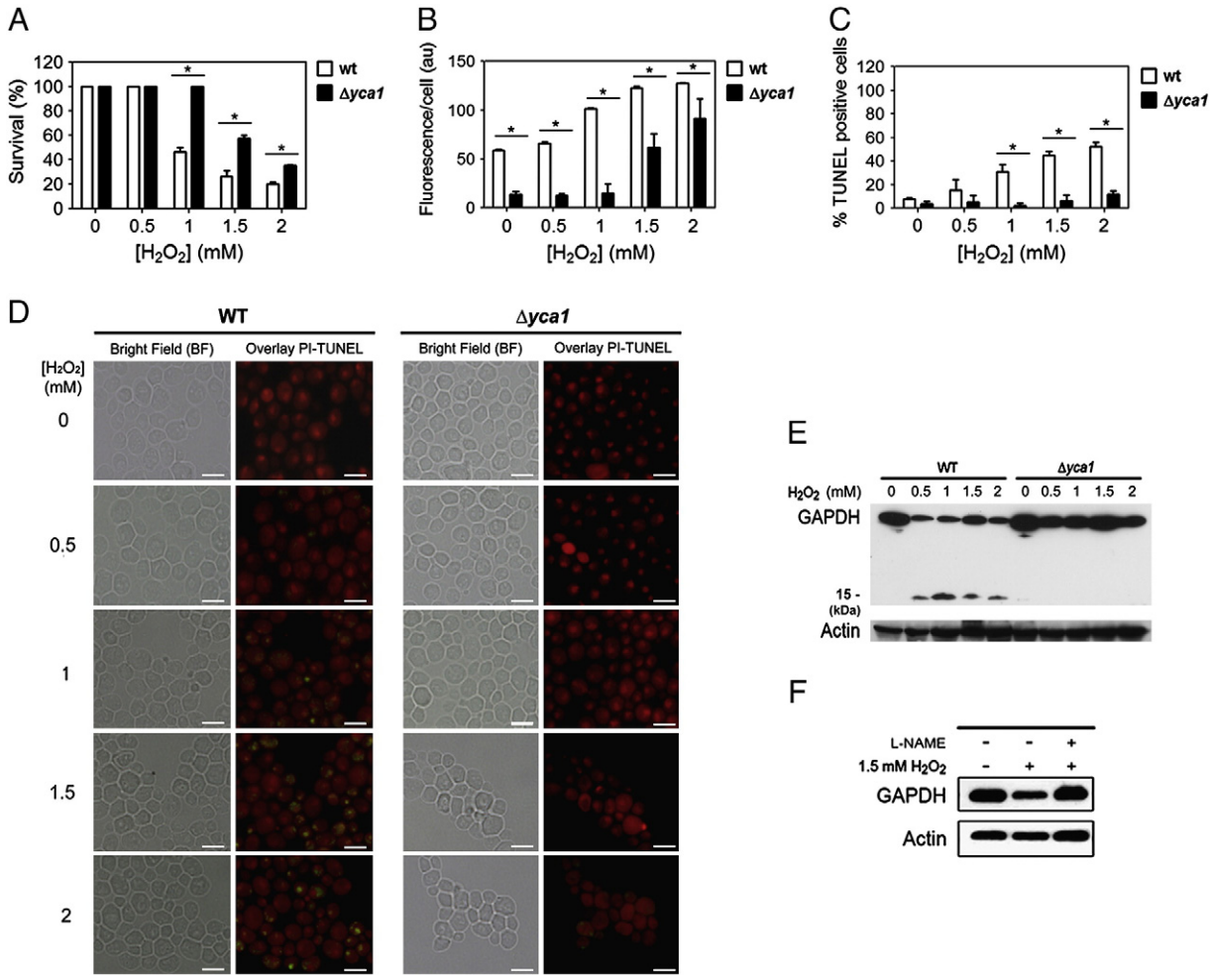

Fig. 3. GAPDH specific cleavage by metacaspase during H_2O_2-induced apoptosis is dependent on NO levels. (A) Comparison of the survival rate of wild-type and Δ*yca1* cells upon H_2O_2 treatment. (B) Percentage of wild-type and Δ*yca1* cells exhibiting high levels of intracellular ROS detected by FACS measurements of the dihydrorhodamine 123 fluorescence. (C) Percentage of wild-type and Δ*yca1* cells displaying TUNEL positive phenotype. (D) Epifluorescence and bright field micrographs of untreated and H_2O_2-treated wild-type and Δ*yca1* cells displaying TUNEL reaction to visualize double-strand DNA breaks. Cells were co-stained with propidium iodide in order to facilitate nuclei visualization. Bar, 5 μm. (E) Immunoblot analysis of GAPDH and actin protein levels in 40 μg of total protein extracts of H_2O_2-treated and untreated wild-type and Δ*yca1* cells. (F) Immunoblot analysis of GAPDH levels in 40 μg of total protein extracts of untreated and H_2O_2-treated wild-type yeast cells after pre-incubation with the L-arginine analog, L-NAME. Statistical significance (*$P<0.05$) was determined by Student's *t*-test.

The use of different methodologies described as requisites for a protein to be considered a caspase substrate [18] allows us to assign GAPDH as a metacaspase specific substrate. GAPDH cleavage was observed in vitro by digestome analysis complemented with mass spectrometry and immunoblot and validated by its specific cleavage after incubation of recombinant GAPDH with recombinant metacaspase. Moreover, the occurrence of GAPDH metacaspase-dependent cleavage was further confirmed by an in vivo assay in cells undergoing apoptosis with GAPDH displaying reduced levels. Moreover, the physiological relevance of GAPDH fragmentation is also supported by previous results showing that GAPDH is a target of extensive fragmentation upon H_2O_2-induced apoptosis [9,19]. It is important to acknowledge that, proteolytic cleavage of GAPDH, as that of any protein, can result in a gain- or loss-of-function for the protein. It is well known that H_2O_2 treatment (1.5 mM) of *S. cerevisiae* cells results in the decrease of GAPDH activity associated with a drop of the ATP levels [20]. The reduced ATP levels affect cellular homeostasis and can decrease the efficiency of energy-dependent processes and ATP-mediated cell signal transduction such as actin dynamics [21] increasing the sensitivity to apoptotic insult. Nevertheless, the hypothesis that GAPDH cleavage results in a gain-of-function is also acceptable in the light of our previous results [9] showing an increased survival of *TDH2*- and *TDH3*-disrupted cells exposed to H_2O_2-induced apoptosis. The GAPDH pleiotropic functions, linked to the various intracellular localizations of the enzyme, as well as the observation that GAPDH overexpressing cells behave as wild-type cells when challenged with H_2O_2 (data not shown) further complicates the elucidation of this aspect. Nonetheless, the accumulating evidence indicates that yeast GAPDH cleavage by metacaspase could contribute to H_2O_2-induced apoptosis independently of whether or not this proteolysis results in a gain- or loss-of-function. We and others have shown that GAPDH is S-nitrosated by the NO generated upon H_2O_2-induced apoptosis [9], and that inhibition of NO synthesis in yeast cell leads to a dramatic reduction of metacaspase activity [10]. Herein we show that NO production is needed for the metacaspase specific cleavage of GAPDH upon H_2O_2-induced apoptosis, similar to what occurs in higher eukaryotic cells, in which NO has already been ascertained as a signaling molecule with the capacity to promote caspase activation [22]. The observed NO-dependent metacaspase specific cleavage of GAPDH might also be explained by the capacity of NO in activating metacaspase as previously reported [7]. Further studies might help in elucidating the relation between NO signaling and metacaspase specific GAPDH cleavage. Nonetheless, all these results call attention to the relevance of metabolic enzyme cleavage during H_2O_2-induced apoptosis. Metabolic enzymes have complex roles, having proved their multi-functional relation with different cellular processes, including cell death [23,24]. In fact, GAPDH has been extensively implicated in

several mammalian apoptotic processes [25]. Additionally, alterations in metabolic pathways are often related to neurodegenerative diseases, cell damaging processes and cancers [23,25]. Our findings herein described demonstrate for the first time a yeast metacaspase specific substrate, GAPDH. The data obtained open new perspectives for the precise identification of the molecular cascade regulated by metacaspase activation and its relevance to yeast apoptotic cell death.

Funding

This work was supported by a grant from FCT - Fundação para a Ciência e Tecnologia [PTDC/BIA-MIC/114116/2009]. A.S., B.S.M. and M.I.R.R. have fellowships from FCT [SFRH/BD/33125/2007, SRFH/BD/41674/2007 and SFRH/BD/37717/2007, respectively] and AdV was supported by Programa Ciência — financed by POPH - QREN - Tipologia 4.2 - Promoção do Emprego Científico, co-funded by Fundo Social Europeu and National funding from MCTES.

References

[1] A.G. Uren, K. O'Rourke, L.A. Aravind, M.T. Pisabarro, S. Seshagiri, E.V. Koonin, V.M. Dixit, Identification of paracaspases and metacaspases: two ancient families of caspase-like proteins, one of which plays a key role in MALT lymphoma, Mol. Cell 6 (2000) 961–967.
[2] L. Tsiatsiani, F. Van Breusegem, P. Gallois, A. Zavialov, E. Lam, P.V. Bozhkov, Metacaspases, Cell Death Differ. 8 (2011) 1279–1288.
[3] F. Madeo, E. Herker, C. Maldener, S. Wissing, S. Lachelt, M. Herlan, M. Fehr, K. Lauber, S.J. Sigrist, S. Wesselborg, K.U. Frohlich, A caspase-related protease regulates apoptosis in yeast, Mol. Cell 9 (2002) 911–917.
[4] F. Madeo, D. Carmona-Gutierrez, J. Ring, S. Büttner, T. Eisenberg, G. Kroemer, Caspase-dependent and caspase-independent cell death pathways in yeast, Biochem. Biophys. Res. Commun. 2 (2009) 227–231.
[5] R.E. Lee, L.G. Puente, M. Kaern, L.A. Megeney, A non-death role of the yeast metacaspase: Yca1p alters cell cycle dynamics, PLoS One 8 (2008) e2956.
[6] R.E. Lee, S. Brunette, L.G. Puente, L.A. Megeney, Metacaspase Yca1 is required for clearance of insoluble protein aggregates, Proc. Natl. Acad. Sci. U. S. A. 30 (2010) 13348–13353.
[7] B. Belenghi, M.C. Romero-Puertas, D. Vercammen, A. Brackenier, D. Inze, M. Delledonne, F. Van Breusegem, Metacaspase activity of *Arabidopis thaliana* is regulated by S-nitrosylation of a critical cysteine residue, J. Biol. Chem. 282 (2007) 1352–1358.
[8] F. Madeo, E. Fröhlich, M. Ligr, M. Grey, S.J. Sigrist, D.H. Wolf, K.U. Fröhlich, Oxygen stress: a regulator of apoptosis in yeast, J. Cell Biol. 145 (1999) 757–767.
[9] B. Almeida, S. Buttner, S. Ohlmeier, A. Silva, A. Mesquita, B. Sampaio-Marques, N.S. Osorio, A. Kollau, B. Mayer, C. Leao, J. Laranjinha, F. Rodrigues, F. Madeo, P. Ludovico, NO-mediated apoptosis in yeast, J. Cell Sci. 120 (2007) 3279–3288.
[10] N.S. Osorio, A. Carvalho, A.J. Almeida, S. Padilla-Lopez, C. Leao, J. Laranjinha, P. Ludovico, D.A. Pearce, F. Rodrigues, Nitric oxide signaling is disrupted in the yeast model for Batten disease, Mol. Biol. Cell 18 (2007) 2755–2767.
[11] J.F. Sundström, A. Vaculova, A.P. Smertenko, E.I. Savenkov, A. Golovko, E. Minina, B.S. Tiwari, S. Rodriguez-Nieto, A.A. Jr Zamyatnin, T. Välineva, J. Saarikettu, M.J. Frilander, M.F. Suarez, A. Zavialov, U. Ståhl, P.J. Hussey, O. Silvennoinen, E. Sundberg, B. Zhivotovsky, P.V. Bozhkov, Tudor staphylococcal nuclease is an evolutionarily conserved component of the programmed cell death degradome, Nat. Cell Biol. 11 (2009) 1347–1354.
[12] C. Mazzoni, C. Falcone, Caspase-dependent apoptosis in yeast, Biochim. Biophys. Acta 1783 (2008) 1320–1327.
[13] N.J. Kruger, The Bradford method for protein quantitation, Methods Mol. Biol. 32 (1994) 9–15.
[14] J.E. Ricci, C. Munoz-Pinedo, P. Fitzgerald, B. Bailly-Maitre, G.A. Perkins, N. Yadava, I.E. Scheffler, M.H. Ellisman, D.R. Green, Disruption of mitochondrial function during apoptosis is mediated by caspase cleavage of the p75 subunit of complex I of the electron transport chain, Cell 117 (2004) 773–786.
[15] N. Watanabe, E. Lam, Two *Arabidopsis* metacaspases AtMCP1b and AtMCP2b are arginine/lysine-specific cysteine proteases and activate apoptosis-like cell death in yeast, J. Biol. Chem. 280 (2005) 14691–14699.
[16] A.U. Lüthi, S.J. Martin, The CASBAH: a searchable database of caspase substrates, Cell Death Differ. 14 (2007) 641–650.
[17] W. Shao, G. Yeretssian, K. Doiron, S.N. Hussain, M. Saleh, The caspase-1 digestome identifies the glycolysis pathway as a target during infection and septic shock, J. Biol. Chem. 282 (2007) 36321–36329.
[18] J.C. Timmer, G.S. Salvesen, Caspase substrates, Cell Death Differ. 14 (2007) 66–72.
[19] F. Magherini, C. Tani, T. Gamberi, A. Caselli, L. Bianchi, L. Bini, A. Modesti, Protein expression profiles in *Saccharomyces cerevisiae* during apoptosis induced by H_2O_2, Proteomics 7 (2007) 1434–1445.
[20] H. Osório, P. Moradas-Ferreira, M.A. Günther Sillero, A. Sillero In, *Saccharomyces cerevisiae*, the effect of H2O2 on ATP, but not on glyceraldehyde-3-phosphate dehydrogenase, depends on the glucose concentration, Arch. Microbiol. 181 (2004) 231–236.
[21] C.W. Gourlay, K.R. Ayscough, The actin cytoskeleton: a key regulator of apoptosis and ageing? Nat. Rev. Mol. Cell Biol. 6 (2005) 583–589.
[22] C.E. Johnson, S. Kornbluth, Caspase cleavage is not for everyone, Cell 134 (2008) 720–721.
[23] D.R. Plas, C.B. Thompson, Cell metabolism in the regulation of programmed cell death, Trends Endocrinol. Metab. 13 (2002) 75–78.
[24] J.W. Kim, C.V. Dang, Multifaceted roles of glycolitic enzymes, Trends Biochem. Sci. 30 (2005) 142–150.
[25] M.D. Berry, A.A. Boulton, Glyceraldehyde-3-phosphate dehydrogenase and apoptosis, J. Neurosci. Res. 60 (2000) 150–154.

Attachment II

Table 1 - Microarrays analysis results of polysomal fractions of untreated and 15 min acetic acid treated cells. 412 genes were found up-regulated (more than two fold) upon acetic acid treatment.

Probe ID	Gene symbol	Fold change	p-value
YCL027C-A	#N/A	2.434	1,25E-05
YMR178W	0	3.422	1,58E-03
YNL149C	0	3.233	4,12E-04
YMR074C	0	4.601	6,56E-03
YBR231C	0	2.564	1,64E-03
YCR051W	0	2.235	7,55E-03
YGR173W	0	2.826	9.31E-6
YGR277C	0	2.37	7.62E-7
YFL046W	0	2.257	1,99E-03
YPR118W	0	2.738	5,41E-03
YCR090C	0	2.084	3,92E-03
YHR020W	0	3.376	4,93E-04
YDR533C	0	2.976	1,10E-03
YOR164C	0	3.51	8,15E-04
YMR067C	0	1.619	7.9E-6
YJR085C	0	2.671	4,15E-03
YNL081C	0	2.679	2.96E-8
YBR052C	0	5.027	2,58E-05
YNL208W	0	2.902	2,40E-03
YDR287W	0	1.661	6,33E-04
YDL158C	0	6.249	4,09E-03
YGR021W	0	2.169	2,65E-03
YGR017W	0	2.13	2,83E-03
YHR121W	0	3.589	1,55E-04
YER067W	0	4.324	2,36E-03
YDR286C	0	4.045	2,80E-03
YGL245W	0	3.033	1,32E-03
YER030W	0	3.435	3,62E-03
YER093C-A	0	2.085	8,70E-03
YOR091W	0	1.676	8,03E-03
YER138W-A	0	2.876	3,90E-03
YOL026C	0	2.159	8,46E-03
YPR188C	0	3.869	9,90E-03
YPL098C	0	3.668	3,18E-03
YGL068W	0	3.297	2,84E-03
YKL018C-A	0	2.366	3,53E-05
YPL183W-A	0	2.352	1.38E-6
YLR408C	0	1.864	3,84E-03
YDR071C	0	2.738	3,65E-03
YPL267W	0	2.049	6,40E-03
YNL134C	0	3.529	1,05E-03
YOR112W	0	2.333	2,01E-05
YNL201C	0	1.948	3,09E-03
YLR022C	0	3.4	6,03E-03
YKR065C	0	2.333	3.76E-6
YIR036C	0	2.501	4,61E-04
YMR226C	0	3.537	1,23E-04
YPL225W	0	5.758	1,11E-04
YNR046W	0	1.997	9.79E-6
YNL168C	0	4.206	1,42E-04
YJL217W	0	3.762	1,46E-04
YIR035C	0	3.216	1,07E-03
YMR009W	0	1.975	6,39E-03
YDR063W	0	3.346	1,82E-04
YBR137W	0	2.834	7,45E-04
YER163C	0	2.029	4,34E-04
YDR514C	0	2.185	6,67E-03
YGR111W	0	2.046	6,89E-04
YJL062W-A	0	4.087	6,51E-06
YGL232W	0	5.921	7,52E-04
YJR024C	0	2.433	3,41E-04
YKL206C	0	1.818	5,36E-03
YOR285W	0	8.172	1,14E-05

YGL231C	0	3.882	1,76E-03
YHR034C	0	2.04	8,78E-03
YGR001C	0	3.286	5,94E-05
YNR040W	0	2.335	1,61E-04
YHR029C	0	4.209	4,20E-06
YNR036C	0	7.03	5,93E-05
YFR043C	0	3.038	3,42E-03
YER010C	0	1.768	1,70E-04
YOR203W	0	6.442	1.98E-6
YIL041W	0	2.889	2,27E-03
YJL181W	0	1.464	9.96E-6
YDR196C	0	2.919	6,97E-04
YPR063C	0	2.325	9,01E-05
YGR137W	0	3.523	4,75E-03
YGL047W	0	3.509	5,25E-06
YMR184W	0	3.766	3,12E-05
YCL033C	0	8.464	1,92E-06
YLL022C	0	1.739	9,28E-03
YOR169C	0	5.731	9,45E-03
YOL111C	0	2.781	2,51E-06
YMR315W	0	4.836	5,59E-05
YDR433W	0	3.77	9,92E-03
YDR154C	0	3.021	6,36E-03
YDL099W	0	3.714	5,89E-03
YNL045W	0	2.521	4,52E-03
YLR027C	AAT2	2.636	1,27E-03
YGR037C	ACB1	2.728	4,03E-03
YKL192C	ACP1	3.18	5,30E-05
YOR128C	ADE2	1.877	2.11E-6
YDR408C	ADE8	1.81	8,64E-03
YDR226W	ADK1	3.878	2,62E-04
YDR214W	AHA1	2.064	5,44E-03
YJR047C	ANB1	5.128	8,29E-04
YPR128C	ANT1	2.26	7,26E-05
YLR102C	APC9	2.273	9,67E-03
YML022W	APT1	2.876	3,78E-03
YBR149W	ARA1	2.426	1,49E-03
YGL105W	ARC1	2.939	5,49E-03
YIL062C	ARC15	3.016	9,90E-04
YKL013C	ARC19	2.217	2,38E-03
YHR013C	ARD1	4.797	1,96E-04
YDL100C	ARR4	2.466	3,97E-03
YGL017W	ATE1	1.868	3.14E-7
YNL315C	ATP11	2.295	2.14E-6
YDR298C	ATP5	1.793	1,60E-04
YKL016C	ATP7	2.657	1,57E-04
YFL010W-A	AUA1	3.524	1,31E-03
YER155C	BEM2	1.437	5,06E-03
YIL004C	BET1	1.926	4,76E-03
YPR176C	BET2	2.356	1,33E-04
YJL031C	BET4	4.849	9,39E-04
YFR047C	BNA6	4.461	1,72E-04
YLR078C	BOS1	2.565	2,55E-03
YHR114W	BZZ1	2.446	7,20E-04
YOR276W	CAF20	6.022	3,49E-06
YNL288W	CAF40	2.324	9,24E-05
YER048C	CAJ1	2.757	5,77E-05
YOR125C	CAT5	2.415	1,97E-04
YPL178W	CBC2	2.951	4,30E-04
YPL215W	CBP3	2.264	4.44E-6
YIL142W	CCT2	1.739	6.42E-6
YDL143W	CCT4	3.126	1,75E-04
YCR002C	CDC10	2.249	1,11E-03
YDL165W	CDC36	1.742	1,73E-03
YDR168W	CDC37	2.214	8,91E-04
YDL126C	CDC48	2.643	1,80E-03
YLR418C	CDC73	2.671	5,06E-05
YJR057W	CDC8	2.132	4,20E-03
YBR109C	CMD1	2.157	6,21E-05
YLL009C	COX17	5.469	1,27E-05
YIL111W	COX5B	3.615	1.03E-6
YML078W	CPR3	4.73	1,11E-04
YLR216C	CPR6	2.827	3,81E-03
YNL027W	CRZ1	2.014	4,21E-04

YHR191C	CTF8	2.503	2,84E-04
YOR042W	CUE5	3.479	9,22E-05
YGL166W	CUP2	1.685	6.81E-6
YDR163W	CWC15	3.032	1,69E-03
YKL096W	CWP1	5.528	3,12E-04
YAL039C	CYC3	2.265	6,19E-03
YAL012W	CYS3	3.644	1,54E-04
YGR155W	CYS4	2.777	1,81E-03
YML113W	DAT1	1.425	5,27E-03
YOR046C	DBP5	3.551	2,58E-05
YOL149W	DCP1	3.133	6.21E-6
YOR163W	DDP1	3.187	8,42E-04
YKL054C	DEF1	2.426	2,03E-03
YIR004W	DJP1	1.734	1.28E-6
YDR121W	DPB4	2.376	1,39E-03
YMR276W	DSK2	4.415	2.22E-6
YDR424C	DYN2	2.817	2,04E-04
YLR390W	ECM19	4.296	1,21E-03
YHL030W	ECM29	3.324	4,05E-04
YBL047C	EDE1	2.482	5,94E-03
YHR193C	EGD2	3.567	9,13E-03
YNL084C	END3	3.195	3,10E-04
YJR125C	ENT3	5.058	1,33E-05
YDR153C	ENT5	2.176	1,67E-03
YPL028W	ERG10	3.242	3,37E-03
YML126C	ERG13	3.009	7,82E-03
YJL167W	ERG20	3.215	7,46E-05
YGL001C	ERG26	3.343	9,03E-05
YLR100W	ERG27	2.974	1,25E-04
YHR190W	ERG9	2.347	4,07E-03
YDL166C	FAP7	3.001	5,90E-03
YPL231W	FAS2	1.648	2,32E-03
YPR062W	FCY1	2.466	7,16E-03
YIL065C	FIS1	2.633	2,87E-03
YIL098C	FMC1	2.095	3,99E-04
YNL135C	FPR1	3.371	4,88E-05
YML074C	FPR3	2.746	6,42E-04

YFL022C	FRS2	2.1	7,54E-03
YHR049W	FSH1	4.94	1,52E-04
YMR222C	FSH2	3.703	1,33E-03
YAL035W	FUN12	2.554	2,14E-04
YER027C	GAL83	2.013	5,72E-03
YCL011C	GBP2	1.689	6,76E-03
YGR083C	GCD2	2.863	6.52E-8
YFR009W	GCN20	2.502	3,48E-03
YAL044C	GCV3	2.937	3,96E-04
YLR094C	GIS3	2.004	2,38E-03
YOR168W	GLN4	6.049	3,46E-04
YML004C	GLO1	3.932	1,81E-03
YDR272W	GLO2	5.923	1,07E-04
YHL031C	GOS1	2.473	5,79E-03
YLR293C	GSP1	2.273	7,36E-03
YGL181W	GTS1	2.211	5,20E-04
YIR038C	GTT1	3.554	5,01E-04
YNL281W	HCH1	2.306	1.28E-6
YLR192C	HCR1	1.859	1,06E-03
YOR176W	HEM15	5.048	3,09E-08
YBR248C	HIS7	2.32	8,05E-03
YDL125C	HNT1	5.896	4,54E-04
YDR305C	HNT2	2.761	2.52E-6
YJR139C	HOM6	2.998	1,46E-03
YEL066W	HPA3	2.762	3,01E-04
YMR186W	HSC82	2.721	5,86E-03
YHL002W	HSE1	3.497	5,51E-03
YOR020C	HSP10	3.255	4,77E-03
YLR259C	HSP60	2.511	3,01E-03
YIR037W	HYR1	5.356	8.62E-8
YJR016C	ILV3	2.484	3,29E-03
YCR046C	IMG1	2.95	5,51E-03
YBR011C	IPP1	2.55	2.77E-7
YNL265C	IST1	3.325	2,55E-03
YBR245C	ISW1	1.597	1,86E-03
YPR133C	IWS1	2.951	5,75E-04
YGL173C	KEM1	2.363	5,06E-04

YDR148C	KGD2	1.678	2,54E-03
YKL183W	LOT5	3.299	1,89E-03
YBL026W	LSM2	3.704	2,66E-03
YER112W	LSM4	1.831	2,44E-03
YPL004C	LSP1	3.811	4,17E-03
YMR038C	LYS7	3.017	3,75E-04
YGL086W	MAD1	3.233	2,86E-03
YIL070C	MAM33	6.55	2,58E-04
YBL091C	MAP2	2.878	4,33E-03
YOR197W	MCA1	3.586	2,24E-04
YDL078C	MDH3	6.345	5,33E-04
YLR303W	MET17	2.443	3,06E-03
YOR241W	MET7	1.639	5,78E-03
YOR232W	MGE1	3.441	6,51E-03
YKR095W	MLP1	1.454	3,00E-03
YIL051C	MMF1	3.26	7,05E-05
YJR074W	MOG1	2.8	1,43E-04
YDR347W	MRP1	3.939	2,87E-03
YKL003C	MRP17	1.774	1,73E-03
YBL038W	MRPL16	2.409	1,83E-03
YKR085C	MRPL20	4.251	2,04E-03
YOR150W	MRPL23	2.277	3,53E-03
YBR282W	MRPL27	2.591	9,64E-04
YDR462W	MRPL28	2.275	6,69E-03
YKL138C	MRPL31	1.971	6,68E-03
YJL096W	MRPL49	5.127	4,39E-04
YPR100W	MRPL51	2.169	6,48E-04
YJL063C	MRPL8	3.006	1,13E-04
YGR220C	MRPL9	2.309	5,45E-03
YBR251W	MRPS5	1.92	4,74E-04
YMR158W	MRPS8	3.957	1,07E-03
YOR354C	MSC6	1.391	8,35E-03
YGL122C	NAB2	2.121	1,78E-03
YGR232W	NAS6	3.63	1,38E-04
YDL040C	NAT1	2.23	1,60E-03
YPR052C	NHP6A	2.297	3,51E-03
YBR089C-A	NHP6B	2.994	7.69E-8
YGL221C	NIF3	2.169	8,73E-03
YPL211W	NIP7	2.348	3,68E-03
YLR351C	NIT3	3.165	2,26E-04
YOL041C	NOP12	2.204	2,14E-03
YNL175C	NOP13	4.616	2.44E-6
YPR072W	NOT5	4.422	3,14E-04
YMR091C	NPL6	1.761	2,63E-03
YER126C	NSA2	2.309	5.19E-6
YER009W	NTF2	3.864	2,01E-03
YER006W	NUG1	3.111	2.72E-6
YIL115C	NUP159	2.266	1,98E-03
YBR129C	OPY1	1.948	3,88E-03
YHR063C	PAN5	2.194	5,26E-05
YDR228C	PCF11	1.602	3,89E-03
YNL231C	PDR16	1.794	1.74E-6
YER153C	PET122	3.809	1,71E-03
YOR158W	PET123	1.546	3,02E-03
YOL044W	PEX15	4.079	1,59E-04
YPL112C	PEX25	2.616	4,14E-03
YOR122C	PFY1	2.83	4,22E-04
YGL025C	PGD1	2.401	8,95E-03
YPL031C	PHO85	3.07	4,32E-03
YNL055C	POR1	3.258	8,57E-04
YDL134C	PPH21	1.996	2,40E-03
YDL188C	PPH22	2.871	6,01E-03
YMR314W	PRE5	2.453	2,26E-04
YOR323C	PRO2	3.161	4,17E-04
YBL068W	PRS4	3.243	7,72E-05
YJL166W	QCR8	1.466	6,71E-03
YDL103C	QRI1	3.576	2,00E-03
YMR022W	QRI8	2.397	3,89E-04
YER095W	RAD51	1.688	3,06E-03
YNL216W	RAP1	1.884	4.46E-6
YCR036W	RBK1	2.185	2,69E-04
YLR248W	RCK2	3.24	2,12E-04
YJL204C	RCY1	1.679	2,97E-03
YNL312W	RFA2	2.224	2,53E-03

YJL173C	RFA3	1.824	8,74E-03
YDR487C	RIB3	2.803	2,97E-04
YER083C	RMD7	3.565	3,26E-04
YCL028W	RNQ1	4.784	1,63E-05
YDR156W	RPA14	2.239	1,90E-04
YOL005C	RPB11	3.302	7,65E-04
YJL140W	RPB4	4.935	3,93E-03
YDR404C	RPB7	1.394	8,89E-03
YJL121C	RPE1	4.233	1.03E-6
YMR121C	RPL15B	3.335	4.34E-6
YNL069C	RPL16B	4.102	5,61E-03
YPL079W	RPL21B	4.027	1,50E-03
YBL087C	RPL23A	2.059	2,01E-03
YDR471W	RPL27B	3.546	2,94E-04
YBR031W	RPL4A	4.197	5,85E-03
YDR012W	RPL4B	3.28	2,90E-03
YLL045C	RPL8B	2.614	6,70E-03
YDL097C	RPN6	3.027	4,64E-03
YPR187W	RPO26	5.196	4,23E-03
YDR064W	RPS13	3.576	1,84E-03
YCR031C	RPS14A	2.179	2.6E-6
YJL191W	RPS14B	2.456	1,99E-03
YOL121C	RPS19A	3.619	9,20E-03
YJL190C	RPS22A	5.264	6,38E-03
YLR367W	RPS22B	2.913	1,35E-03
YKL156W	RPS27A	2.049	9,22E-03
YLR167W	RPS31	5.439	6,48E-03
YPL090C	RPS6A	3.674	7,29E-03
YKL145W	RPT1	2.805	4,85E-04
YMR131C	RRB1	2.279	9,35E-03
YDL111C	RRP42	1.592	5,89E-03
YER050C	RSM18	3.008	1,48E-03
YJR113C	RSM7	3.909	3,85E-03
YGL244W	RTF1	1.839	2,59E-03
YOR216C	RUD3	3.518	2,02E-03
YPL235W	RVB2	2.213	6,73E-03
YCR009C	RVS161	2.804	2,84E-05
YDR388W	RVS167	2.668	3,95E-04
YLR180W	SAM1	2.834	9,18E-04
YMR263W	SAP30	3.162	2,72E-04
YPL218W	SAR1	4.355	1,40E-03
YHL034C	SBP1	3.199	9,23E-03
YGL011C	SCL1	2.202	1,05E-03
YJL080C	SCP160	3.62	1,87E-03
YER120W	SCS2	4.536	5,15E-04
YPL085W	SEC16	1.794	2,49E-04
YBL050W	SEC17	2.83	2,29E-04
YLR268W	SEC22	3.154	2,99E-03
YDR170C	SEC7	2.773	7.48E-7
YLR292C	SEC72	2.732	7,77E-04
YGR009C	SEC9	2.846	2,44E-03
YIL074C	SER33	1.809	7,77E-03
YDL168W	SFA1	1.956	5,51E-04
YJL145W	SFH5	3.227	2,67E-04
YJR134C	SGM1	1.912	3,53E-03
YKL130C	SHE2	2.044	8,07E-03
YBR258C	SHG1	3.595	7,61E-05
YBL058W	SHP1	3.181	4,82E-03
YNL236W	SIN4	2.888	4,57E-03
YGL208W	SIP2	2.165	7,16E-03
YDR328C	SKP1	2.64	3,24E-03
YML058W	SML1	1.965	9,67E-03
YFL017W-A	SMX2	4.721	5,12E-04
YPR182W	SMX3	5.104	3,49E-03
YKL079W	SMY1	3.442	6,56E-04
YAL030W	SNC1	4.013	1,46E-03
YGL115W	SNF4	4.644	1.56E-6
YJR104C	SOD1	5.51	8,67E-05
YHR163W	SOL3	2.077	4,89E-04
YGL093W	SPC105	2.844	5,74E-04
YER018C	SPC25	2.297	6,38E-03
YPR069C	SPE3	3.145	3.49E-6
YGL207W	SPT16	1.746	9.49E-6
YDR292C	SRP101	2.05	8,60E-03

YOR027W	STI1	4.129	5,54E-04
YLR150W	STM1	3.327	4,83E-03
YPL237W	SUI3	4.088	1,74E-03
YDR172W	SUP35	3.036	9,06E-05
YDR167W	TAF10	2.04	1,02E-03
YJL052W	TDH1	1.642	4,01E-03
YHR025W	THR1	1.739	9,45E-03
YMR146C	TIF34	2.579	2,61E-03
YGL049C	TIF4632	1.825	1,53E-04
YJL143W	TIM17	2.285	1,04E-03
YJR135W-A	TIM8	3.72	2,67E-04
YEL020W-A	TIM9	4.506	3,58E-06
YER011W	TIR1	2.279	4,51E-04
YIL011W	TIR3	1.915	3,96E-03
YNL070W	TOM7	3.081	2,72E-03
YAL016W	TPD3	2.92	2,96E-03
YDR353W	TRR1	1.966	1,18E-03
YOR115C	TRS33	3.016	7,10E-03
YGR209C	TRX2	4.381	5,92E-04
YCR083W	TRX3	2.845	3,46E-04
YML028W	TSA1	3.582	1,42E-05
YBR058C-A	TSC3	3.442	2,36E-03
YDR513W	TTR1	3.059	8,01E-03
YER100W	UBC6	2.465	1,69E-04
YLL039C	UBI4	3.689	6,60E-03
YFR010W	UBP6	2.65	5,26E-03
YKL024C	URA6	2.55	5,45E-04
YDR400W	URH1	2.39	2,09E-03
YDL058W	USO1	2.52	5,15E-04
YGR128C	UTP8	1.858	4,91E-03
YEL038W	UTR4	1.794	4,15E-03
YHR039C-A	VMA10	7.892	3,15E-03
YPR036W	VMA13	2.925	2,40E-03
YOR132W	VPS17	2.364	8.94E-6
YKL041W	VPS24	1.319	6,31E-03
YFL010C	WWM1	3.368	9,91E-06
YPL252C	YAH1	2.687	5,79E-04
YHR135C	YCK1	1.986	7,08E-03
YDL120W	YFH1	1.969	2,08E-04
YDL198C	YHM1	5.2	8,22E-05
YNL263C	YIF1	2.105	9,55E-04
YNL044W	YIP3	2.339	5,80E-03
YLR200W	YKE2	1.633	2,08E-03
YML025C	YML6	1.743	7,93E-03
YKL067W	YNK1	2.594	3,91E-04
YPR028W	YOP1	2.444	5,75E-04
YML027W	YOX1	1.926	6,88E-03
YDL235C	YPD1	2.353	8,33E-03
YDR368W	YPR1	1.847	2,13E-03
YFL038C	YPT1	2.348	1,65E-03
YML001W	YPT7	4.534	2,95E-05
YIL063C	YRB2	2.304	9,77E-03

Table 2 - Microarrays analysis results of polysomal fractions of untreated and 15 min acetic acid treated cells. 457 genes were found down-regulated upon acetic acid treatment.

Probe ID	Gene symbol	Fold change	p-value
YGL217C	0	0,301	3,45E-04
YAL064W-B	0	0,304	5,74E-02
YOR343C	0	0,149	3,57E-02
YLR361C	0	0,364	3,28E-02
YLR077W	0	0,567	4,07E-02
YLL055W	0	0,543	8,34E-02
YOR378W	0	0,17	4,65E-02
YOR019W	0	0,379	5,85E-02
YBL029W	0	0,185	6,06E-02
YBR095C	0	0,572	3,51E-02
YIL177C	0	0,269	3,20E-02
YBR094W	0	0,387	2,93E-02
YNL083W	0	0,545	8,44E-02
YJR115W	0	0,293	6,92E-04
YJL065C	0	0,625	7,27E-05
YBR162C	0	0,212	5,47E-04
YER076C	0	0,232	7,72E-03
YIR014W	0	0,06	8,00E-03
YLR463C	0	0,27	4,56E-05
YLR462W	0	0,45	4,63E-06
YPR157W	0	0,121	1,36E-02
YHL035C	0	0,104	6,13E-02
YLL053C	0	0,206	1,73E-02
YGL146C	0	0,469	8,11E-03
YDL096C	0	0,168	2,22E-03
YKR106W	0	0,253	6,28E-02
YCR006C	0	0,242	3,99E-02
YIL082W-A	0	0,313	3,40E-06
YLL012W	0	0,265	1,80E-02
YMR278W	0	0,567	3,78E-02
YPL278C	0	0,152	4,99E-02
YMR134W	0	0,376	6,11E-03
YHR199C	0	0,495	4,01E-02
YBR012C	0	0,309	9,99E-02
YLR073C	0	0,535	1,78E-02
YPL277C	0	0,235	2,30E-03
YOL029C	0	0,488	5,30E-03
YPL201C	0	0,284	1,32E-02
YML003W	0	0,239	5,22E-02
YKR040C	0	0,375	1,35E-02
YGR125W	0	0,55	1,74E-05
YGL139W	0	0,257	1,26E-02
YLR312C	0	0,221	9,29E-02
YDR459C	0	0,251	4,81E-02
YIL172C	0	0,351	7,48E-02
YDL156W	0	0,489	8,28E-03
YBR113W	0	0,421	4,85E-02
YLR414C	0	0,275	1,06E-02
YHL026C	0	0,383	6,21E-04
YLR241W	0	0,328	5,71E-02
YDR352W	0	0,375	1,67E-05
YHR219W	0	0,26	1,07E-02
YDL010W	0	0,367	1,04E-02
YNL176C	0	0,379	1,39E-03
YHR218W	0	0,477	1,63E-02
YPR150W	0	0,307	7,60E-02
YFR020W	0	0,475	2,32E-02
YLR063W	0	0,49	6,95E-03
YOR364W	0	0,2	1,46E-03
YGR012W	0	0,471	9,03E-03
YEL077C	0	0,2	4,90E-03
YFR055W	0	0,482	5,38E-02
YMR086C-A	0	0,244	1,02E-03
YMR266W	0	0,271	4,38E-02
YHR112C	0	0,534	6,32E-02
YGR259C	0	0,133	6,15E-03

YER097W	0	0,314	8,30E-03
YHL017W	0	0,293	2,83E-04
YLR125W	0	0,204	1,51E-02
YLR057W	0	0,255	2,18E-02
YBR139W	0	0,301	4,98E-02
YJL193W	0	0,31	3,36E-02
YEL075C	0	0,463	7,09E-02
YIL092W	0	0,598	6,04E-02
YBR178W	0	0,17	4,59E-03
YLR376C	0	0,455	2,19E-03
YDL038C	0	0,163	1,46E-02
YOR314W-A	0	0,075	7,68E-02
YER053C-A	0	0,481	2,11E-02
YOR105W	0	0,41	3,05E-02
YOR396W	0	0,269	1,02E-02
YFL066C	0	0,423	1,95E-05
YMR088C	0	0,546	4,44E-02
YOR356W	0	0,455	2,36E-02
YMR155W	0	0,646	9,24E-02
YCR026C	0	0,443	3,15E-02
YDR338C	0	0,277	6,86E-02
YIL090W	0	0,312	9,71E-02
YMR007W	0	0,322	8,79E-04
YML133C	0	0,266	2,25E-02
YPR204W	0	0,292	1,31E-02
YEL068C	0	0,266	6,28E-07
YIL006W	0	0,326	7,80E-03
YJR129C	0	0,323	3,80E-06
YLL032C	0	0,639	7,69E-02
YOL092W	0	0,465	8,63E-02
YMR085W	0	0,224	5,25E-05
YEL067C	0	0,363	5,22E-02
YLL067C	0	0,231	3,03E-06
YBL113C	0	0,207	3,29E-03
YLR224W	0	0,401	2,99E-03
YIL152W	0	0,274	6,12E-04
YMR221C	0	0,469	2,80E-02

YOR389W	0	0,196	8,88E-02
YCR099C	0	0,197	8,81E-02
YPR202W	0	0,341	6,63E-03
YBL108W	0	0,091	5,52E-04
YNL095C	0	0,284	7,42E-04
YLL066C	0	0,268	1,55E-05
YLL030C	0	0,155	5,21E-02
YHL008C	0	0,282	3,64E-02
YHR033W	0	0,4	3,88E-02
YDL033C	0	0,276	8,06E-03
YOR205C	0	0,267	8,31E-07
YML018C	0	0,272	1,46E-02
YBL111C	0	0,477	1,98E-02
YIL082W	0	0,283	1,40E-02
YHL050C	0	0,323	4,06E-03
YER189W	0	0,531	8,14E-02
YMR317W	0	0,162	8,36E-03
YMR293C	0	0,469	1,97E-02
YHR202W	0	0,229	8,53E-02
YKL174C	0	0,587	2,79E-02
YLL059C	0	0,284	7,22E-02
YNL087W	0	0,245	1,59E-04
YLR112W	0	0,149	5,59E-03
YDR048C	0	0,326	3,01E-02
YDL237W	0	0,48	1,82E-02
YJR015W	0	0,372	2,26E-02
YGL114W	0	0,406	2,52E-03
YPL207W	0	0,24	3,45E-04
YNR068C	0	0,187	3,09E-05
YJR013W	0	0,203	2,52E-02
YNL217W	0	0,541	1,30E-02
YBR124W	0	0,384	6,55E-06
YKL134C	40817	0,351	2,68E-06
YJR155W	AAD10	0,224	1,96E-02
YFL057C	AAD16	0,316	2,97E-02
YBL015W	ACH1	0,543	1,88E-02
YGL256W	ADH4	0,314	5,50E-02

YEL052W	AFG1	0,35	1,14E-02
YER017C	AFG3	0,212	1,53E-06
YCL025C	AGP1	0,194	3,68E-03
Q0050	AI1	0,507	9,30E-02
YBR110W	ALG1	0,589	3,51E-02
YNL048W	ALG11	0,445	9,52E-02
YBR243C	ALG7	0,375	6,60E-04
YNL219C	ALG9	0,387	2,71E-02
YFL050C	ALR2	0,483	5,32E-02
YBR158W	AMN1	0,569	5,80E-02
YGL156W	AMS1	0,285	6,17E-03
YBR286W	APE3	0,403	4,47E-02
YPL195W	APL5	0,512	7,08E-03
YPR192W	AQY1	0,305	8,68E-04
YHL040C	ARN1	0,282	5,96E-02
YHL047C	ARN2	0,229	4,61E-02
YPR034W	ARP7	0,633	6,66E-02
YLR155C	ASP3-1	0,267	6,64E-03
YLR157C	ASP3-2	0,259	1,77E-02
YLR158C	ASP3-3	0,265	1,38E-02
YLR160C	ASP3-4	0,255	1,31E-02
YCR068W	ATG15	0,213	2,89E-03
YPR026W	ATH1	0,291	9,11E-02
YKL004W	AUR1	0,393	2,57E-02
YLR465C	BSC3	0,574	5,69E-02
YOL137W	BSC6	0,388	5,57E-02
YFL025C	BST1	0,286	6,00E-02
YLR353W	BUD8	0,43	2,99E-02
YEL063C	CAN1	0,255	5,42E-03
YML042W	CAT2	0,269	2,46E-02
YHL038C	CBP2	0,235	5,22E-04
YDR270W	CCC2	0,329	5,17E-02
YGR217W	CCH1	0,253	8,39E-02
YBR131W	CCZ1	0,447	9,89E-03
YLR307W	CDA1	0,231	4,51E-02
YDR182W	CDC1	0,421	2,28E-02
YGL116W	CDC20	0,378	6,20E-02
YDR364C	CDC40	0,28	5,29E-02
YBR202W	CDC47	0,436	8,87E-02
YDL164C	CDC9	0,437	3,01E-02
YLR245C	CDD1	0,482	3,79E-02
YBR029C	CDS1	0,298	7,44E-04
YER061C	CEM1	0,37	7,79E-02
YBR038W	CHS2	0,525	8,48E-02
YCR005C	CIT2	0,186	7,69E-05
YKL219W	COS9	0,41	8,63E-03
YOR316C	COT1	0,49	6,53E-02
Q0045	COX1	0,198	9,74E-02
YER141W	COX15	0,371	2,52E-02
YLL018C-A	COX19	0,572	2,68E-05
Q0275	COX3	0,128	5,48E-02
YJL172W	CPS1	0,209	2,10E-02
YNL130C	CPT1	0,509	1,33E-02
YOR031W	CRS5	0,229	2,61E-02
YBR161W	CSH1	0,298	3,30E-02
YPR124W	CTR1	0,334	9,56E-04
YDL209C	CWC2	0,528	1,81E-02
YGL027C	CWH41	0,359	1,55E-02
YCR017C	CWH43	0,2	4,82E-02
YML054C	CYB2	0,299	2,88E-02
YJR152W	DAL5	0,188	2,15E-03
YLR037C	DAN2	0,327	9,11E-02
YKL046C	DCW1	0,236	3,04E-04
YBR163W	DEM1	0,642	5,67E-05
YDL024C	DIA3	0,233	2,84E-02
YPL265W	DIP5	0,167	1,39E-02
YER166W	DNF1	0,41	2,67E-03
YDR093W	DNF2	0,349	2,55E-02
YAL026C	DRS2	0,256	1,21E-03
YHR132C	ECM14	0,35	3,95E-03
YLR436C	ECM30	0,47	2,32E-02
YBR078W	ECM33	0,331	7,08E-04
YLR443W	ECM7	0,358	1,65E-02
YKR004C	ECM9	0,387	8,57E-03

YLR083C	EMP70	0,317	4,07E-05
YDR040C	ENA1	0,264	3,85E-02
YLL038C	ENT4	0,521	1,06E-02
YIL005W	EPS1	0,356	1,82E-03
YHR007C	ERG11	0,3	8,72E-04
YGR060W	ERG25	0,358	1,01E-02
YML067C	ERV41	0,496	4,60E-02
YMR219W	ESC1	0,599	3,88E-02
YDR261C	EXG2	0,504	5,81E-02
YBR041W	FAT1	0,352	5,13E-03
YLR377C	FBP1	0,219	6,26E-03
YMR058W	FET3	0,287	8,26E-02
YMR319C	FET4	0,33	4,10E-02
YFL041W	FET5	0,264	1,24E-02
YBR040W	FIG1	0,186	3,19E-02
YLR342W	FKS1	0,278	1,92E-03
YHR211W	FLO5	0,309	7,44E-02
YER109C	FLO8	0,586	4,87E-02
YHR176W	FMO	0,495	9,43E-06
YLR214W	FRE1	0,179	1,64E-02
YKL220C	FRE2	0,245	9,52E-02
YOR381W	FRE3	0,214	2,59E-02
YJL221C	FSP2	0,373	9,67E-02
YBL042C	FUI1	0,165	5,44E-04
YBR021W	FUR4	0,331	2,46E-02
YBR179C	FZO1	0,55	9,52E-02
YLR088W	GAA1	0,391	5,25E-03
YML051W	GAL80	0,311	4,71E-05
YMR307W	GAS1	0,303	3,99E-02
YMR215W	GAS3	0,516	6,40E-02
YOL030W	GAS5	0,439	1,11E-02
YAL062W	GDH3	0,438	1,83E-02
YJR040W	GEF1	0,422	4,45E-02
YCL039W	GID7	0,385	7,94E-02
YKR030W	GMH1	0,48	3,92E-02
YDR508C	GNP1	0,309	1,31E-03
YER020W	GPA2	0,328	3,66E-03
YOR371C	GPB1	0,222	9,65E-03
YAL056W	GPB2	0,188	3,54E-02
YLL031C	GPI13	0,283	2,38E-02
YHR188C	GPI16	0,272	3,04E-06
YKR067W	GPT2	0,457	1,44E-02
YGR032W	GSC2	0,261	6,28E-04
YGL084C	GUP1	0,219	6,62E-03
YHL032C	GUT1	0,348	7,41E-02
YIL155C	GUT2	0,136	5,29E-03
YJL091C	GWT1	0,246	2,85E-02
YFL031W	HAC1	0,509	6,22E-03
YNL014W	HEF3	0,351	1,84E-02
YER014W	HEM14	0,487	8,52E-02
YMR207C	HFA1	0,332	1,56E-02
YDR528W	HLR1	0,618	5,13E-02
YML075C	HMG1	0,562	8,39E-02
YLR205C	HMX1	0,458	2,53E-02
YMR032W	HOF1	0,489	1,01E-02
YCR021C	HSP30	0,211	6,84E-02
YJL077C	ICS3	0,372	2,65E-02
YER086W	ILV1	0,425	2,42E-02
YMR081C	ISF1	0,28	5,20E-05
YBR086C	IST2	0,607	3,26E-05
YOL103W	ITR2	0,568	8,62E-02
YJL034W	KAR2	0,341	1,13E-03
YGL203C	KEX1	0,453	4,83E-03
YNL238W	KEX2	0,508	5,73E-03
YJL094C	KHA1	0,307	8,82E-05
YOR336W	KRE5	0,347	1,70E-02
YPR159W	KRE6	0,331	6,05E-03
YKL110C	KTI12	0,442	4,62E-02
YNL029C	KTR5	0,584	8,83E-02
YPL053C	KTR6	0,307	3,36E-05
YHL003C	LAG1	0,234	1,28E-02
YJL062W	LAS21	0,17	2,90E-03
YDR062W	LCB2	0,356	4,58E-03
YOR108W	LEU9	0,297	4,70E-02

YNR008W	LRO1	0,303	1,69E-04
YNL268W	LYP1	0,226	5,53E-03
YGR289C	MAL11	0,165	3,51E-02
YER106W	MAM1	0,221	1,85E-03
YOL060C	MAM3	0,394	5,26E-02
YKL165C	MCD4	0,253	1,84E-03
YDL054C	MCH1	0,363	9,10E-02
YLR188W	MDL1	0,338	3,44E-03
YML104C	MDM1	0,393	1,11E-05
YOR147W	MDM32	0,43	5,02E-05
YJL112W	MDV1	0,582	2,84E-02
YLR069C	MEF1	0,258	1,25E-03
YNL142W	MEP2	0,129	1,40E-02
YPR138C	MEP3	0,324	3,02E-03
YNL277W	MET2	0,422	4,08E-02
YIL046W	MET30	0,447	6,04E-02
YOR211C	MGM1	0,379	3,12E-02
YNL291C	MID1	0,469	6,60E-03
YBR084W	MIS1	0,331	7,34E-02
YDR144C	MKC7	0,365	1,63E-02
YPL140C	MKK2	0,597	5,57E-05
YPL164C	MLH3	0,34	2,96E-02
YHR204W	MNL1	0,426	4,43E-02
YER001W	MNN1	0,322	3,79E-03
YBR015C	MNN2	0,49	7,46E-02
YKL201C	MNN4	0,344	6,43E-02
YPL050C	MNN9	0,26	7,36E-03
YGL257C	MNT2	0,406	7,91E-02
YIL014W	MNT3	0,488	7,53E-03
YIR021W	MRS1	0,623	6,26E-02
YOR370C	MRS6	0,577	3,93E-02
YGR014W	MSB2	0,533	3,19E-02
YLR219W	MSC3	0,512	3,40E-02
YHR120W	MSH1	0,351	8,78E-05
YKL194C	MST1	0,31	7,57E-03
YGR055W	MUP1	0,338	7,35E-02
YHL036W	MUP3	0,18	7,81E-04
YOR326W	MYO2	0,542	8,28E-02
YMR080C	NAM7	0,644	8,92E-02
YPR155C	NCA2	0,48	4,16E-03
YJL116C	NCA3	0,138	1,09E-02
YPR149W	NCE102	0,445	5,73E-02
YHR042W	NCP1	0,46	3,15E-03
YMR145C	NDE1	0,298	1,74E-06
YOL104C	NDJ1	0,114	5,83E-02
Q0130	OLI1	0,515	2,48E-02
YOR085W	OST3	0,433	1,46E-03
YER154W	OXA1	0,336	4,15E-04
YEL049W	PAU2	0,409	7,02E-02
YBR233W	PBP2	0,422	3,10E-02
YPR002W	PDH1	0,349	7,67E-02
YOR328W	PDR10	0,447	7,17E-02
YOR153W	PDR5	0,332	3,59E-05
YBL017C	PEP1	0,355	2,46E-02
YPL154C	PEP4	0,412	5,73E-02
YCL004W	PGS1	0,24	1,67E-03
YKL043W	PHD1	0,213	7,39E-07
YAR071W	PHO11	0,27	8,77E-03
YHR215W	PHO12	0,357	4,81E-02
YBR092C	PHO3	0,272	2,00E-02
YBR093C	PHO5	0,118	3,89E-03
YDR481C	PHO8	0,39	2,29E-05
YML123C	PHO84	0,138	1,26E-03
YJL198W	PHO90	0,477	3,05E-02
YNR013C	PHO91	0,371	4,15E-02
YML061C	PIF1	0,456	8,32E-02
YOL011W	PLB3	0,169	2,40E-04
YGL008C	PMA1	0,389	3,26E-02
YCR024C-A	PMP1	0,43	3,38E-02
YGL167C	PMR1	0,462	5,14E-05
YDL095W	PMT1	0,257	2,24E-07
YAL023C	PMT2	0,331	1,40E-02
YOR321W	PMT3	0,272	5,62E-02
YJR143C	PMT4	0,368	2,97E-02

YDL093W	PMT5	0,465	5,34E-02
YGR199W	PMT6	0,234	3,60E-03
YBR088C	POL30	0,562	3,30E-02
YMR129W	POM152	0,334	1,51E-03
YNL282W	POP3	0,463	1,41E-02
YIL037C	PRM2	0,255	2,19E-02
YPL156C	PRM4	0,275	5,84E-05
YDL039C	PRM7	0,271	5,51E-02
YBR237W	PRP5	0,518	7,84E-02
YKR013W	PRY2	0,47	6,88E-03
YGR170W	PSD2	0,435	1,16E-02
YMR137C	PSO2	0,601	7,57E-02
YKL039W	PTM1	0,242	2,97E-05
YGL063W	PUS2	0,165	3,56E-02
YLR142W	PUT1	0,122	2,47E-03
YGR258C	RAD2	0,449	1,48E-02
YDL059C	RAD59	0,455	4,14E-02
YOR380W	RDR1	0,403	3,87E-03
YBL020W	RFT1	0,264	6,42E-03
YMR182C	RGM1	0,325	1,29E-02
YOR107W	RGS2	0,34	3,79E-05
YBL082C	RHK1	0,361	2,07E-03
YLL046C	RNP1	0,28	2,16E-02
YBR229C	ROT2	0,366	4,35E-03
YIL075C	RPN2	0,417	2,78E-02
YIR015W	RPR2	0,436	1,58E-03
YMR030W	RSF1	0,279	8,50E-03
YJR004C	SAG1	0,182	2,28E-03
YER147C	SCC4	0,44	9,72E-02
YMR214W	SCJ1	0,522	3,93E-02
YGL126W	SCS3	0,591	4,01E-02
YLR378C	SEC61	0,348	1,39E-03
YOR254C	SEC63	0,52	3,38E-02
YLR430W	SEN1	0,592	3,07E-02
YJR095W	SFC1	0,162	3,70E-03
YIL099W	SGA1	0,069	7,32E-03
YPR198W	SGE1	0,378	4,03E-03
YCL010C	SGF29	0,424	5,03E-03
YGR112W	SHY1	0,368	3,88E-02
YEL065W	SIT1	0,187	3,46E-02
YBL061C	SKT5	0,452	3,18E-02
YOR307C	SLY41	0,462	5,14E-02
YOR149C	SMP3	0,395	1,30E-02
YFL060C	SNO3	0,39	2,38E-02
YDR011W	SNQ2	0,334	1,07E-02
YEL031W	SPF1	0,512	1,80E-02
YCR018C	SRD1	0,478	8,11E-02
YPL092W	SSU1	0,435	5,08E-02
YHR084W	STE12	0,407	8,98E-02
YOR219C	STE13	0,395	1,23E-02
YDR103W	STE5	0,592	7,54E-02
YKL209C	STE6	0,379	6,59E-04
YGL022W	STT3	0,354	2,05E-03
YGL169W	SUA5	0,587	2,83E-02
YLR092W	SUL2	0,284	5,31E-02
YPL057C	SUR1	0,442	7,15E-03
YLR372W	SUR4	0,359	1,64E-03
YIL047C	SYG1	0,214	5,79E-03
YBR069C	TAT1	0,438	1,24E-02
YOL020W	TAT2	0,508	1,95E-02
YKL028W	TFA1	0,58	5,63E-05
YKL140W	TGL1	0,383	7,14E-02
YPL258C	THI21	0,226	8,03E-03
YPR121W	THI22	0,224	8,24E-05
YDL080C	THI3	0,612	4,80E-02
YDR105C	TMS1	0,344	9,55E-03
YJL093C	TOK1	0,37	3,46E-03
YLR234W	TOP3	0,367	4,93E-02
YGL096W	TOS8	0,428	9,06E-02
YGR138C	TPO2	0,28	8,14E-03
YJL129C	TRK1	0,31	3,24E-02
YDR120C	TRM1	0,498	8,71E-03
YKL034W	TUL1	0,415	9,24E-02
YKR042W	UTH1	0,227	2,96E-04

YEL040W	UTR2	0,414	4,50E-02	**YGR296W**	YRF1-3	0,276	2,51E-02
YGL225W	VRG4	0,452	9,18E-02	**YLR466W**	YRF1-4	0,273	1,61E-02
YNL197C	WHI3	0,646	8,84E-05	**YLR467W**	YRF1-5	0,281	2,64E-02
YNL283C	WSC2	0,483	1,87E-02	**YNL339C**	YRF1-6	0,295	1,25E-02
YAR035W	YAT1	0,294	3,72E-07	**YPL283C**	YRF1-7	0,277	2,20E-02
YCR059C	YIH1	0,528	2,40E-02	**YMR089C**	YTA12	0,412	1,34E-02
YMR106C	YKU80	0,388	1,03E-03	**YMR243C**	ZRC1	0,552	7,59E-02
YPR024W	YME1	0,237	2,44E-02	**YGL255W**	ZRT1	0,247	1,59E-02
YDR545W	YRF1-1	0,27	1,04E-02	**YLR130C**	ZRT2	0,25	2,55E-03
YER190W	YRF1-2	0,278	4,35E-02				

Table 3 - Microarrays analysis results of polysomal fractions of untreated and 30 min acetic acid treated cells. 211 genes were found up-regulated (more than two fold) upon acetic acid treatment.

Probe ID	Gene symbol	Fold change	p-value
YJL012C-A	0	2.791	2.87E-03
YGR001C	0	3.0	7.04E-03
YNL149C	0	3.317	8.31E-03
YOR285W	0	8.996	8.04E-03
YDR248C	0	2.358	4.05E-02
YBL107W-A	0	2.287	2.66E-02
YNL045W	0	2.624	9.66E-02
YPR063C	0	2.235	3.03E-03
YCL047C	0	1.783	2.12E-02
YER138W-A	0	2.0	5.07E-5
YLR022C	0	4.056	2.79E-5
YOL087C	0	2.148	1.0E-5
YHR020W	0	2.822	1.89E-02
YMR315W	0	4.626	9.06E-02
YMR126C	0	1.767	5.08E-02
YKL084W	0	2.843	3.63E-5
YPL221W	0	1.71	3.08E-03
YHR138C	0	3.648	4.29E-02
YJL062W-A	0	4.499	1.76E-04
YNL058C	0	1.584	4.32E-02
YNL081C	0	3.08	8.62E-7
YGL232W	0	4.364	9.85E-02
YKR007W	0	2.784	1.37E-02
YLR345W	0	2.171	3.24E-02
YMR122W-A	0	3.154	7.20E-04
YMR226C	0	4.189	1.93E-02
YML072C	0	3.117	3.49E-02
YNL157W	0	2.086	2.75E-02
YIR035C	0	2.959	5.52E-02
YDL110C	0	2.846	5.75E-02
YDR034W-B	0	4.306	3.68E-02
YER053C	0	2.075	3.81E-02
YNR034W-A	0	4.499	8.53E-04
YIL108W	0	3.044	2.18E-02
YPR172W	0	3.702	6.92E-02
YKL161C	0	1.873	4.91E-03
YER067W	0	6.093	2.01E-02
YLR187W	0	1.832	5.65E-02
YKL160W	0	2.278	5.91E-02
YIL130W	0	2.043	6.35E-03
YNL201C	0	2.541	6.38E-7
YLR356W	0	1.467	8.79E-02
YOR227W	0	1.778	1.10E-02
YDR063W	0	2.787	1.95E-03
YCL033C	0	6.6	5.49E-02
YKL069W	0	1.947	5.53E-02
YKL192C	ACP1	2.834	2.38E-03
YDR226W	ADK1	3.193	1.02E-02
YBR059C	AKL1	2.697	2.52E-02
YOR374W	ALD4	2.731	3.01E-02
YJR047C	ANB1	3.461	2.26E-02
YIL062C	ARC15	4.145	7.00E-02
YKL185W	ASH1	4.779	4.18E-02
YGR097W	ASK10	1.937	2.22E-5
YKL016C	ATP7	3.07	6.02E-02
YER155C	BEM2	1.593	7.74E-02
YPR176C	BET2	1.537	4.39E-02
YJL060W	BNA3	2.334	8.40E-02
YOR276W	CAF20	6.567	3.49E-02
YNL288W	CAF40	2.018	1.18E-02
YER048C	CAJ1	2.014	8.08E-02
YDL126C	CDC48	2.805	2.76E-02
YER164W	CHD1	2.106	1.51E-6
YLL009C	COX17	4.073	4.60E-02

YML078W	CPR3	4.431	1.22E-02
YOR042W	CUE5	2.639	1.58E-03
YAL012W	CYS3	3.064	5.02E-03
YGR155W	CYS4	2.475	9.78E-03
YKL054C	DEF1	2.362	8.46E-02
YBR201W	DER1	1.837	5.48E-03
YLL001W	DNM1	1.676	5.88E-02
YNR067C	DSE4	2.2	3.02E-02
YKR076W	ECM4	3.079	6.20E-03
YNL327W	EGT2	1.984	6.72E-02
YGR175C	ERG1	2.019	8.72E-02
YML126C	ERG13	3.529	1.16E-02
YLR100W	ERG27	2.589	3.27E-02
YOR280C	FSH3	1.758	1.64E-02
YLR094C	GIS3	2.715	5.98E-02
YMR311C	GLC8	2.052	1.56E-02
YOR168W	GLN4	3.645	9.80E-03
YPR160W	GPH1	4.009	7.57E-02
YLR293C	GSP1	2.103	2.40E-02
YDL223C	HBT1	3.506	9.13E-03
YOR176W	HEM15	4.481	1.83E-02
YML075C	HMG1	1.406	9.45E-02
YDL125C	HNT1	5.18	1.43E-02
YJR139C	HOM6	2.872	6.67E-02
YMR186W	HSC82	2.815	3.68E-03
YFL014W	HSP12	2.417	1.13E-02
YLR259C	HSP60	2.624	2.30E-02
YPL240C	HSP82	3.203	2.08E-02
YJR016C	ILV3	2.426	7.55E-02
YCL009C	ILV6	2.376	8.14E-03
YGL173C	KEM1	1.715	4.73E-02
YNL132W	KRE33	1.688	2.69E-02
YIL070C	MAM33	2.56	6.88E-02
YBL091C	MAP2	3.129	9.12E-02
YGL209W	MIG2	2.872	9.12E-02
YPL082C	MOT1	3.345	9.15E-5
YPR166C	MRP2	2.01	7.13E-7
YKR085C	MRPL20	3.509	2.99E-5
YOR150W	MRPL23	2.162	4.36E-03
YBR282W	MRPL27	2.756	2.4E-5
YJL096W	MRPL49	4.329	3.95E-02
YGR220C	MRPL9	2.177	7.83E-04
YMR158W	MRPS8	2.657	3.64E-02
YOR354C	MSC6	1.475	1.61E-02
YMR109W	MYO5	2.693	7.07E-04
YNL137C	NAM9	1.991	9.98E-02
YGR232W	NAS6	4.102	4.04E-02
YDR176W	NGG1	1.234	3.23E-02
YPR052C	NHP6A	3.173	1.59E-03
YOL041C	NOP12	2.043	9.83E-04
YNL175C	NOP13	3.319	3.36E-02
YMR091C	NPL6	1.572	5.41E-5
YJR042W	NUP85	1.337	1.11E-02
YIR006C	PAN1	3.828	3.37E-02
YNL015W	PBI2	2.98	7.54E-03
YLR134W	PDC5	1.926	4.19E-02
YER153C	PET122	2.863	4.85E-02
YKL164C	PIR1	1.782	2.50E-02
YNL055C	POR1	3.055	4.94E-5
YDL188C	PPH22	4.072	1.64E-5
YBL068W	PRS4	2.918	4.27E-5
YDR055W	PST1	3.4	1.27E-02
YOR265W	RBL2	2.152	6.48E-02
YCL028W	RNQ1	4.701	2.93E-03
YDR156W	RPA14	3.761	1.66E-03
YOL005C	RPB11	3.363	1.35E-02
YDR418W	RPL12B	2.468	1.91E-02
YNL069C	RPL16B	3.118	2.98E-03
YBR191W	RPL21A	2.057	5.67E-02
YBL087C	RPL23A	1.71	8.54E-03
YDR471W	RPL27B	3.573	5.24E-03
YFL036W	RPO41	2.213	6.43E-03
YDR064W	RPS13	2.752	1.46E-02
YJL191W	RPS14B	1.911	9.91E-02

YOL040C	RPS15	2.061	4.92E-02
YOL121C	RPS19A	2.897	1.93E-02
YER074W	RPS24A	2.416	1.36E-04
YIL069C	RPS24B	2.626	7.16E-04
YGR027C	RPS25A	2.247	9.46E-02
YGL189C	RPS26A	3.573	1.64E-03
YER131W	RPS26B	2.977	8.33E-02
YKL156W	RPS27A	2.232	4.07E-02
YDL061C	RPS29B	3.668	1.75E-02
YJR145C	RPS4A	2.117	1.39E-02
YHR203C	RPS4B	1.816	6.49E-02
YPL090C	RPS6A	2.771	1.04E-02
YBR181C	RPS6B	3.536	4.04E-02
YOR096W	RPS7A	1.931	5.38E-02
YDL111C	RRP42	1.896	2.85E-02
YMR229C	RRP5	3.533	4.89E-02
YDR129C	SAC6	2.555	8.61E-02
YFR040W	SAP155	2.207	8.94E-03
YMR263W	SAP30	2.459	1.30E-02
YER120W	SCS2	3.368	5.55E-03
YPL085W	SEC16	2.112	4.90E-02
YBR080C	SEC18	1.733	1.95E-02
YDR170C	SEC7	2.246	7.33E-6
YGR009C	SEC9	2.785	1.52E-02
YJL145W	SFH5	2.16	2.78E-5
YJR134C	SGM1	2.146	4.02E-03
YDR393W	SHE9	2.313	6.03E-02
YBR258C	SHG1	3.065	3.34E-03
YNL007C	SIS1	2.201	1.92E-02
YNL167C	SKO1	2.63	2.48E-02
YBL007C	SLA1	3.129	8.71E-02
YFL017W-A	SMX2	4.894	2.02E-02
YPR182W	SMX3	4.858	6.51E-03
YKL079W	SMY1	3.74	4.16E-02
YDR525W-A	SNA2	4.328	2.26E-02
YAL030W	SNC1	6.557	4.60E-02
YJR104C	SOD1	6.135	6.05E-02
YGL093W	SPC105	2.143	3.27E-02
YHR139C	SPS100	2.298	9.52E-5
YGR116W	SPT6	1.621	6.94E-02
YBR169C	SSE2	3.267	2.72E-02
YOR027W	STI1	3.884	3.30E-02
YLR150W	STM1	2.465	2.96E-02
YMR054W	STV1	2.15	7.40E-02
YDR172W	SUP35	3.079	1.30E-03
YPL016W	SWI1	4.407	7.28E-03
YJL052W	TDH1	3.061	8.20E-02
YGR186W	TFG1	2.193	8.67E-03
YGR181W	TIM13	2.338	1.35E-5
YER011W	TIR1	1.864	5.96E-02
YNL070W	TOM7	2.737	3.21E-5
YJL164C	TPK1	1.752	5.33E-03
YGL026C	TRP5	2.028	9.31E-02
YCR083W	TRX3	4.106	1.34E-03
YDR513W	TTR1	3.38	4.20E-02
YBR082C	UBC4	2.562	5.90E-02
YPL072W	UBP16	2.408	9.99E-02
YGR184C	UBR1	2.545	6.94E-02
YDL058W	USO1	2.36	3.16E-02
YHR039C-A	VMA10	6.915	2.19E-04
YGR020C	VMA7	1.859	7.09E-5
YEL051W	VMA8	2.568	9.03E-02
YLL040C	VPS13	4.182	1.05E-02
YOR132W	VPS17	3.846	7.90E-03
YKR020W	VPS51	1.982	8.56E-02
YER072W	VTC1	4.169	4.96E-03
YPL252C	YAH1	2.43	1.58E-02
YLR200W	YKE2	2.024	3.74E-02
YKL196C	YKT6	2.274	9.95E-5
YFR049W	YMR31	2.438	6.62E-02
YDL235C	YPD1	2.37	6.14E-5
YML001W	YPT7	3.513	1.57E-03

Table 4 - Microarrays analysis results of polysomal fractions of untreated and 30 min acetic acid treated cells. 368 genes were found down-regulated upon acetic acid treatment.

Probe ID	Gene symbol	Fold change	p-value
YGL177W	0	0.394	4,95E-01
YLL012W	0	0.597	4.84E-4
YCR064C	0	0.14	4,77E-01
YLR057W	0	0.693	4,76E-01
YFL068W	0	0.609	4,64E-01
YDR090C	0	0.423	4,56E-01
YGL146C	0	0.527	4,51E-01
YEL077C	0	0.368	4,51E-01
YLR161W	0	0.7	4,49E-01
YCR022C	0	0.35	4.36E-4
YPL264C	0	0.455	4,20E-01
YNL080C	0	0.612	4,15E-01
YNL337W	0	0.482	4,11E-01
YIL176C	0	0.666	4,09E-01
YDR492W	0	0.55	3,97E-01
YHR202W	0	0.592	3,90E-01
YGL114W	0	0.57	3,87E-01
YDR015C	0	0.418	3,74E-01
YHR199C	0	0.527	3,67E-01
YDR338C	0	0.506	3,63E-01
YOR084W	0	0.564	3.55E-4
YPL062W	0	0.275	3,38E-01
YOL155C	0	0.533	3.35E-4
YOR389W	0	0.443	3,33E-01
YDL023C	0	0.592	3,32E-01
YDR491C	0	0.265	3.29E-4
YKL223W	0	0.156	3,26E-01
YJL225C	0	0.391	3,25E-01
YOL124C	0	0.497	3,23E-01
YJR015W	0	0.547	3,21E-01
YPR123C	0	0.294	3,06E-01
YLL067C	0	0.372	3,06E-01
YDR455C	0	0.171	3.05E-4
YEL028W	0	0.403	3,02E-01
YIL177C	0	0.387	3,01E-01
YKL162C-A	0	0.5	3,01E-01
YHR033W	0	0.666	2,85E-01
YOR333C	0	0.176	2,79E-01
YLR125W	0	0.435	2.73E-4
YFL032W	0	0.239	2,67E-01
YLR124W	0	0.121	2.62E-4
YLR123C	0	0.299	2,61E-01
YOR378W	0	0.236	2.57E-4
YFL055W	0	0.384	2,54E-01
YBL096C	0	0.378	2,52E-01
YHL046C	0	0.688	2,51E-01
YOR298W	0	0.366	2,34E-01
YAR023C	0	0.449	2,21E-01
YDL187C	0	0.445	2,21E-01
YCR072C	0	0.592	2.18E-4
YAR053W	0	0.185	2,11E-01
YPR174C	0	0.52	2,10E-01
YBL044W	0	0.267	2,03E-01
YFR026C	0	0.393	1.98E-4
YEL067C	0	0.444	1,97E-01
YJL028W	0	0.244	1,90E-01
YBR209W	0	0.134	1,86E-01
YOR396W	0	0.357	1,85E-01
YDL033C	0	0.353	1,84E-01
YLL059C	0	0.519	1,79E-01
YLL064C	0	0.696	1,78E-01
YGR164W	0	0.127	1,71E-01
YLL066C	0	0.358	1,66E-01
YMR323W	0	0.38	1,65E-01
YLR162W	0	0.11	1,63E-01
YLR042C	0	0.558	1,61E-01

YIL054W	0	0.414	1,59E-01
YCL073C	0	0.407	1,57E-01
YGR266W	0	0.576	1,55E-01
YMR057C	0	0.303	1,47E-01
Q0010	0	0.096	1,46E-01
YKR043C	0	0.5	1,42E-01
YIL012W	0	0.205	1,42E-01
YKR011C	0	0.651	1,41E-01
YHR219W	0	0.348	1,38E-01
YPR204W	0	0.395	1,38E-01
YBR162C	0	0.344	1,38E-01
YKR005C	0	0.516	1,32E-01
YNR062C	0	0.409	1,32E-01
YPR170C	0	0.361	1,31E-01
YGL072C	0	0.495	1,28E-01
YNL227C	0	0.57	1,28E-01
YEL008W	0	0.152	1,21E-01
YML003W	0	0.441	1,19E-01
YML133C	0	0.37	1,17E-01
YIL152W	0	0.364	1,12E-01
YML018C	0	0.533	1,12E-01
YEL075W-A	0	0.428	1.09E-4
YDL032W	0	0.185	1,08E-01
YGR190C	0	0.3	1,06E-01
YFR055W	0	0.625	1,05E-01
YMR253C	0	0.49	1,05E-01
YBR124W	0	0.219	1,05E-01
YOR072W	0	0.335	1,01E-01
YPL017C	0	0.376	9,97E-02
YPR136C	0	0.214	9.85E-5
YNL087W	0	0.505	9.78E-5
YGL138C	0	0.268	9,67E-02
YIL174W	0	0.105	9,52E-02
YGR122C-A	0	0.495	9,31E-02
YDL034W	0	0.241	9,08E-02
YHR212C	0	0.565	9,00E-02
YPR157W	0	0.24	8,94E-02

YOL101C	0	0.362	8,71E-02
YFR056C	0	0.334	8,61E-02
YNL158W	0	0.463	8,39E-02
YLR317W	0	0.418	7,92E-02
YGR012W	0	0.655	7,81E-02
YJL213W	0	0.145	7.78E-5
YNL105W	0	0.183	7,67E-02
YDR526C	0	0.377	7,13E-02
YDL222C	0	0.648	7,01E-02
YNL176C	0	0.577	6,91E-02
YGL007W	0	0.226	6,77E-02
YOL159C-A	0	0.522	6,32E-02
YLR041W	0	0.603	6,11E-02
YMR290W-A	0	0.202	6,01E-02
YFL012W-A	0	0.064	5,84E-02
YEL068C	0	0.433	5,82E-02
YIL082W	0	0.391	5,78E-02
YLR122C	0	0.389	5,55E-02
YKL102C	0	0.404	5,15E-02
YPL162C	0	0.293	5,02E-02
YJR129C	0	0.458	4,57E-02
YJR013W	0	0.436	4,40E-02
YMR007W	0	0.301	4,21E-02
YJR071W	0	0.437	3,77E-02
YML034C-A	0	0.172	3,70E-02
YBR174C	0	0.24	3,69E-02
YIR040C	0	0.156	3,27E-02
YNR020C	0	0.594	3,06E-02
YBL083C	0	0.518	3,05E-02
YIR014W	0	0.307	3,02E-02
YBL109W	0	0.352	3,02E-02
YOL134C	0	0.09	2,61E-02
YBR012C	0	0.375	2,59E-02
YNR064C	0	0.418	2,50E-02
YOR343C	0	0.424	2,44E-02
YJL120W	0	0.138	2,26E-02
YMR252C	0	0.496	2,24E-02

YKR040C	0	0.369	2,21E-02
YEL074W	0	0.482	2,14E-02
YPL279C	0	0.469	2,09E-02
YIL032C	0	0.134	2,03E-02
YBR113W	0	0.365	1,80E-02
YER091C-A	0	0.166	1,41E-02
YIL175W	0	0.107	1,35E-02
YFL051C	0	0.239	1,31E-02
YLR463C	0	0.413	1,30E-02
YGR291C	0	0.071	1,25E-02
YKR106W	0	0.466	1,25E-02
YHR095W	0	0.095	1,24E-02
YPL277C	0	0.498	1,23E-02
YHL026C	0	0.43	1,20E-02
YOR364W	0	0.43	1,14E-02
YGR035C	0	0.471	1.14E-5
YNL095C	0	0.541	1.13E-5
YDR114C	0	0.158	1,03E-02
YKL030W	0	0.348	1,03E-02
YFR012W	0	0.126	9,15E-03
YPL114W	0	0.235	8,05E-03
YLL030C	0	0.095	7.82E-6
YML089C	0	0.258	7,37E-03
YGR287C	0	0.491	6,84E-03
YIL082W-A	0	0.527	6,50E-03
YBL108W	0	0.024	6,12E-03
YDL038C	0	0.209	5,90E-03
YBR232C	0	0.152	5.76E-6
YBR250W	0	0.303	5,53E-03
YOR314W-A	0	0.046	3,03E-03
YMR086C-A	0	0.399	2,97E-03
YGR259C	0	0.136	2.44E-6
YDR112W	0	0.201	1,79E-03
YJL119C	0	0.349	1,50E-03
YMR194C-A	0	0.18	1,34E-03
YDR053W	0	0.182	1,32E-03
YLR112W	0	0.231	1,28E-03

YPL182C	0	0.135	9.66E-7
YEL059W	0	0.368	5,71E-04
YMR122C	0	0.217	4,01E-04
YMR317W	0	0.22	2,17E-04
YBR178W	0	0.15	1,76E-04
YPL201C	0	0.232	9.46E-8
YDL096C	0	0.194	5,72E-05
YBL015W	ACH1	0.541	5.36E-5
YCR010C	ADY2	0.241	4.03E-4
YLR227C	ADY4	0.639	3,29E-01
YBR243C	ALG7	0.518	2,72E-02
YFL050C	ALR2	0.598	1,79E-01
YPR192W	AQY1	0.295	2,37E-02
YLL052C	AQY2	0.452	1,48E-01
YOL058W	ARG1	0.302	1.09E-4
YOL140W	ARG8	0.632	9,42E-02
YNL020C	ARK1	0.522	1,64E-01
YPR034W	ARP7	0.576	2,28E-02
YPR200C	ARR2	0.424	4,11E-01
YCR068W	ATG15	0.386	4,82E-01
YLL063C	AYT1	0.483	4,30E-01
YGR224W	AZR1	0.154	2,31E-02
YBL085W	BOI1	0.668	1,86E-01
YNR069C	BSC5	0.3	1,37E-01
YOL137W	BSC6	0.656	1,38E-01
YDR241W	BUD26	0.165	4,78E-01
YCR063W	BUD31	0.392	1.59E-4
YKR036C	CAF4	0.671	2,92E-01
YEL063C	CAN1	0.491	3,01E-01
YGR036C	CAX4	0.569	1,52E-01
YLR175W	CBF5	0.609	8,18E-02
YLR307W	CDA1	0.386	1,22E-01
YDL220C	CDC13	0.583	2,29E-01
YDL102W	CDC2	0.717	3,50E-01
YGL116W	CDC20	0.558	1,14E-01
YLR245C	CDD1	0.482	3,59E-01
YCR005C	CIT2	0.209	3,17E-04

YPR001W	CIT3	0.461	4,55E-01
YGL263W	COS12	0.363	4,12E-01
YLL018C-A	COX19	0.662	3,25E-01
YCR017C	CWH43	0.578	6,91E-02
YJR152W	DAL5	0.303	7,02E-03
YKL046C	DCW1	0.563	4,53E-02
YDL024C	DIA3	0.472	6.6E-6
YGR227W	DIE2	0.631	4,44E-01
YPL265W	DIP5	0.168	1,93E-03
YER088C	DOT6	0.598	1,17E-01
YDL101C	DUN1	0.598	3,35E-01
YHL016C	DUR3	0.297	6,08E-02
YHR068W	DYS1	0.537	2,20E-01
YDR446W	ECM11	0.268	2,04E-01
YHR021W-A	ECM12	0.239	2,53E-01
YBL043W	ECM13	0.294	3,53E-01
YMR128W	ECM16	0.539	1.26E-4
YPL021W	ECM23	0.142	1,09E-01
YBR078W	ECM33	0.505	5,45E-02
YHL043W	ECM34	0.248	1,29E-01
YKR004C	ECM9	0.473	1,97E-01
YDR261C	EXG2	0.739	4,23E-01
YMR246W	FAA4	0.486	3.12E-4
YLR377C	FBP1	0.273	4,43E-02
YCR028C	FEN2	0.504	4,39E-01
YMR058W	FET3	0.442	3,21E-02
YBR040W	FIG1	0.241	1.72E-7
YOR383C	FIT3	0.541	3,79E-01
YBL013W	FMT1	0.267	1,01E-02
YAL036C	FUN11	0.646	8,12E-02
YLR088W	GAA1	0.532	2,19E-01
YLR081W	GAL2	0.197	2,11E-01
YKR039W	GAP1	0.401	1,45E-02
YMR215W	GAS3	0.47	7,04E-02
YAL062W	GDH3	0.258	9,57E-02
YEL046C	GLY1	0.433	1.92E-4
YKR030W	GMH1	0.73	3,98E-01
YOR371C	GPB1	0.463	3,83E-01
YLL031C	GPI13	0.625	1,50E-01
YPL189W	GUP2	0.478	6,93E-02
YJL091C	GWT1	0.401	4,15E-01
YCL030C	HIS4	0.595	3,22E-01
YLR205C	HMX1	0.61	6,43E-02
YCR021C	HSP30	0.235	4,64E-02
YER039C	HVG1	0.585	3,48E-01
YFL011W	HXT10	0.282	6,55E-03
YOL156W	HXT11	0.138	2,24E-01
YIL170W	HXT12	0.148	2.66E-5
YIL171W	HXT12	0.311	1,16E-02
YMR011W	HXT2	0.477	3,19E-01
YJL214W	HXT8	0.431	4,42E-01
YJL077C	ICS3	0.382	5,00E-02
YMR195W	ICY1	0.372	1,35E-02
YOL103W	ITR2	0.536	1,73E-01
YLR347C	KAP95	0.593	2,03E-01
YHL003C	LAG1	0.539	3.45E-4
YJL062W	LAS21	0.396	2.16E-5
YNL268W	LYP1	0.389	4,15E-01
YKL029C	MAE1	0.425	1,68E-01
YGR289C	MAL11	0.258	3,26E-02
YBR298C	MAL31	0.221	4,33E-01
YER106W	MAM1	0.252	3,77E-03
YDL054C	MCH1	0.454	1,98E-01
YOL126C	MDH2	0.497	3,96E-01
YLR288C	MEC3	0.685	3,66E-01
YOR351C	MEK1	0.156	9.11E-6
YNL142W	MEP2	0.329	2,36E-03
YNL210W	MER1	0.301	3,35E-01
YLL061W	MMP1	0.27	5,14E-02
YJL186W	MNN5	0.568	8.66E-5
YHR120W	MSH1	0.62	4,90E-02
YFL003C	MSH4	0.426	4.97E-4
YMR023C	MSS1	0.716	3,09E-01
YGR257C	MTM1	0.507	2,80E-01

YIR019C	MUC1	0.315	1.03E-4
YHL036W	MUP3	0.458	6,00E-02
YJL116C	NCA3	0.422	2,80E-01
YBL024W	NCL1	0.533	2,17E-01
YOL104C	NDJ1	0.194	1,81E-01
YKR104W	NFT1	0.44	1,65E-01
YIL164C	NIT1	0.449	4,98E-01
YOR310C	NOP58	0.55	4,41E-01
YDR488C	PAC11	0.479	6,74E-02
YKR097W	PCK1	0.393	5,27E-02
YGR087C	PDC6	0.482	8,38E-02
YIL013C	PDR11	0.486	8,73E-02
YHR185C	PFS1	0.329	1.84E-4
YCL004W	PGS1	0.577	4,43E-02
YKL043W	PHD1	0.527	1,48E-02
YMR006C	PLB2	0.349	3,43E-02
YOL011W	PLB3	0.507	1,66E-01
YCR024C-A	PMP1	0.387	8,25E-02
YEL017C-A	PMP2	0.518	4,31E-01
YOR321W	PMT3	0.578	1,12E-01
YJR143C	PMT4	0.522	3,70E-01
YCR014C	POL4	0.582	3,33E-01
YIL037C	PRM2	0.441	1,73E-01
YDL039C	PRM7	0.381	1,71E-01
YGL120C	PRP43	0.509	3.03E-4
YKR013W	PRY2	0.487	4,90E-01
YDL055C	PSA1	0.57	1,70E-01
YMR137C	PSO2	0.659	4.31E-4
YGL063W	PUS2	0.305	8,12E-02
YOR380W	RDR1	0.509	6,70E-02
YHL024W	RIM4	0.371	1,48E-02
YLL046C	RNP1	0.373	2,35E-02
YNL330C	RPD3	0.595	2.03E-4
YMR127C	SAS2	0.628	1,43E-01
YER147C	SCC4	0.306	1,84E-02
YMR305C	SCW10	0.585	4.94E-4
YGL056C	SDS23	0.425	1,37E-02
YER081W	SER3	0.414	1,52E-01
YJL105W	Set-04	0.25	8.42E-6
YJR095W	SFC1	0.206	3,73E-03
YIL099W	SGA1	0.166	2,04E-02
YBL031W	SHE1	0.679	3,17E-01
YER118C	SHO1	0.613	1,74E-01
YIL123W	SIM1	0.384	1,26E-02
YOR307C	SLY41	0.604	3.6E-4
YDL123W	SNA4	0.578	2,68E-01
YMR017W	SPO20	0.262	2,42E-02
YCR018C	SRD1	0.542	3,48E-01
YOR247W	SRL1	0.388	6,34E-04
YMR101C	SRT1	0.548	8,79E-02
YDR082W	STN1	0.548	3,46E-01
YGL022W	STT3	0.624	3,65E-01
YLR092W	SUL2	0.546	1,45E-02
YNL066W	SUN4	0.56	2,85E-01
YAR042W	SWH1	0.381	4,32E-01
YIL047C	SYG1	0.486	1.2E-4
YDR058C	TGL2	0.572	7,77E-02
YBR240C	THI2	0.429	2,49E-01
YLR234W	TOP3	0.34	7,35E-02
YLL028W	TPO1	0.467	4,88E-03
YGR138C	TPO2	0.511	7,95E-03
YHR070W	TRM5	0.359	3,51E-02
YML085C	TUB1	0.463	3.84E-4
YKR042W	UTH1	0.348	1,52E-02
YDR398W	UTP5	0.63	6,19E-02
YGL225W	VRG4	0.461	4,81E-01
YNL283C	WSC2	0.638	6.59E-5
YDR259C	YAP6	0.643	3,58E-01
YCR059C	YIH1	0.65	2,75E-01
YMR106C	YKU80	0.62	3,56E-01
YDR545W	YRF1-1	0.343	1,54E-01
YER190W	YRF1-2	0.384	1,07E-01
YGR296W	YRF1-3	0.391	1,17E-01

Table 5 - Microarrays analysis results of polysomal fractions of 15 and 30 min acetic acid treated cells. 42 genes were found up-regulated (more than two fold) upon acetic acid treatment.

Probe ID	Gene symbol	Fold change	p-value
YOR343C	0	2.903	0.0020
YLR125W	0	2.191	2.98E-01
YDL089W	0	2.739	7.30E-01
YGR110W	0	2.163	6.45E-4
YDR003W	0	2.119	2.44E-4
YHL008C	0	2.724	0.0010
YNL217W	0	2.323	2.58E-03
YMR134W	0	2.029	5.95E-01
YBR284W	0	2.045	0.0080
YOR105W	0	2.671	3.36E-01
YDL027C	0	2.962	3.60E-01
YLR312C	0	3.596	0.0010
YIR014W	0	5.396	4.96E-4
YKL134C	40817	2.062	0.0030
Q0080	AAP1	12.234	6.74E-01
Q0050	AI1	6.807	0.0010
Q0055	AI2	7.842	0.0040
Q0085	ATP6	10.422	8.83E-01
YCL064C	CHA1	4.271	0.0030
Q0250	COX2	7.447	3.60E-01
Q0275	COX3	10.148	6.05E-01
YLR436C	ECM30	2.261	0.0020
YFL041W	FET5	2.476	0.0010
YKR067W	GPT2	2.608	4.44E-02
YOR267C	HRK1	2.154	0.0010
YMR081C	ISF1	2.329	0.0020
YOR336W	KRE5	2.665	9.64E-01
YDR062W	LCB2	2.849	9.94E-02

YNR008W	LRO1	2.341	7.87E-02
YOL060C	MAM3	2.69	7.07E-01
YDR194C	MSS116	2.412	0.0020
Q0130	OLI1	7.65	2.78E-01
YMR257C	PET111	2.105	3.74E-01
YCL004W	PGS1	2.424	1.55E-01
YOL084W	PHM7	2.475	0.0050
YOL011W	PLB3	2.968	1.02E-4
YIL147C	SLN1	2.163	4.37E-01
YHR139C	SPS100	10.534	1.74E-01
YJL093C	TOK1	2.161	3.84E-02
YLR121C	YPS3	2.428	0.0010
YMR089C	YTA12	2.485	0.0020
YDR285W	ZIP1	2.158	2.46E-01